ABSTRACT

Title of Dissertation: CHEMOENZYMATIC FC GLYCAN ENGINEERING FOR IMPROVING ANTIBODY IMMUNOTHERAPY

Chong Ou, Doctor of Philosophy, 2022

Dissertation directed by: Dr. Lai-Xi Wang, Professor
Department of Chemistry and Biochemistry

IgG antibodies contain a conserved *N*-glycan on the Fc domain. The structures of the glycan play an important role in modulating an antibody's effector functions. The Fc *N*-glycans also provide a suitable site for functionalization and conjugation of antibodies in a site-specific manner. The Wang lab have recently developed a general chemoenzymatic method for Fc glycan remodeling through endoglycosidase-based deglycosylation and reglycosylation. My thesis research focuses on three projects: Project 1, development of a site-selective conjugation method for synthesizing antibody-drug conjugates (ADCs); Project 2, application of the method for improving antibody's complement-dependent cytotoxicity (CDC); Project 3, exploration of a dual functionalization method for enhancing internalization and lysosomal delivery of antibodies.

Optimizing the synthesis for site-specific antibody conjugates using the glycan remodeling strategy is the first part of my thesis. We developed a facile synthetic strategy to functionalize glycan oxazolines from sialoglycan, which are the key donor substrates for enzymatic Fc glycan remodeling. An efficient chemoenzymatic method based on the EndoS2-D184M was also developed to functionalize therapeutical antibodies with different Clickable groups including

azide-, cyclopropene-, and norbornene-tags. Homogenous antibody-drug conjugates (ADCs), with drug-antibody ratio of 4 were successfully obtained through three different Click reactions on the tags introduced. Comparison experiments indicated that the ADCs generated by these three Click reactions showed potent cancer cell killing activity and excellent serum stability.

Complement-dependent cytotoxicity (CDC) is a major effector function for antibodies to deplete target cells. But for the IgG antibodies, which is the most widely used isotype for therapeutic antibodies, potent complement activation is restricted. With our optimized conjugation method, we constructed structurally well-defined antibody-αGal and antibody-rhamnose conjugates, which were designed to recruit natural anti-αGal and anti-rhamnose antibodies for enhancing CDC, using trastuzumab as a model antibody. Our preliminary *in vitro* study indicated that the antibody-rhamnose cluster conjugates could mediate potent CDC activity against targeted cancer cell with high selectivity.

Since the rate of receptor internalization is a key factor for the selection of druggable antigen, enhancing the internalization efficiency could improve the efficacy of the ADC and possibly broaden the druggable antigens for ADCs. At the same time, the lysosomal delivery of ADCs could enhance their pharmaceutical efficacy. Therefore, we introduced a pair of orthogonal Click groups on the sialo-complex type glycan (SCT), and we used one of the clickable groups to ligate the drug, while using another one to carry an internalizing factor. This platform provided great flexibility to test out different combinations of antibodies, cytotoxic drugs, and internalizing factors. To date, preliminary cell-based studies have indicated that could improve the toxicity of a cetuximab based ADC with mannose-6-phosphate as an auxiliary internalization factor.

CHEMOENZYMATIC FC GLYCAN ENGINEERING FOR IMPROVING ANTIBODY IMMUNOTHERAPY

by

Chong Ou

Dissertation submitted to the Faculty of the Graduate School of the
University of Maryland, College Park, in partial fulfillment
of the requirements for the degree of
Doctor of Philosophy
2022

Advisory Committee:

Professor Lai-Xi Wang, Chair
Professor Theodore Dayie
Professor Philip DeShong
Professor Lyle Isaacs
Professor Vincent Lee

Acknowledgements

Firstly, I would like to express my gratitude to my thesis advisor, Prof. Lai-Xi Wang for his guidance, mentoring, and giving me freedom and support when I learnt to design my own projects during all the years when I worked in Wang group.

I want to sincerely thank my family members for their understanding, support, and encouragement during all the years when I pursue higher education in the United States. I would never achieve anything without your support.

I would like to thank my committee members, Prof. Dayie, Prof. Deshong, Prof. Isaacs, and Prof. Lee for their constructive criticism. I also want to mention two of the committee members during my candidacy defense, Prof. Davis and Prof. Nemes. Thank you all for your input in my thesis research.

I want to appreciate the help from all the current and past members of Wang lab. I want to thank Dr. Qiang Yang for the training in biological techniques and providing constructive advice when I suffered from problems. I want to thank Dr. Hui Cai, Dr. Guanghui Zong, Dr. Xiao Zhang, Dr. Yuanwei Dai, Dr. Tiezheng Li and Dr. Miao Liu for helpful scientific discussions when I faced challenges. I also want to thank alumni, Roushu Zhang, Sunaina Prabhu, Xin Tong, and current graduate students, Grace Lunde, Thomas Donahue, Darnell Harris and Margaryta Gomozkova in Wang Lab. It is a great pleasure to work with all of you.

I also would like to thank all my collaborators, facility managers for NMR and MS instruments for their efforts to make this research possible.

Table of Contents

List of Schemes

List of Figures

Chapter 1: A Brief Overview of Antibody-Drug Conjugates

1.1 Mechanism of Action for Modern Antibody-Drug Conjugates

Antibody-drug conjugation was one of the most promising strategies for selective delivery of highly toxic drugs into malignant tumor cells, thanks to the high specificity of antibodies. [1] Proposed mechanism is shown in Figure 1-1a, which usually includes the following steps: 1) the antibody in ADC binds to cell surface cancer-related antigen; 2) the antigen-ADC complex gets internalized by endosome-lysosome pathway; 3) the linker gets cleaved; 4) the cytotoxic drug dissociates and circulates in cytoplasm; and 5) the drug acts on DNA or tubulin (depending on the nature of the drug), leading to apoptosis. [2, 3] As a result, ADCs can expand the therapeutic windows of traditional drugs by increasing local drug concentration and reducing the lowest effective dose. ADCs can also reduce systematic toxicity and increase maximum tolerated dose. [4, 5] Recently, this concept was also applied to the treatments of infection caused by bacteria. [6, 7] ADCs are typically constructed with the selection of four major components: the antibody, the linker, the conjugation chemistry, and the drug (toxin, Figure 1-1b). [2] All the four components are important for the efficacy of a given ADC. In this project, my research is to develop methods for site-specific antibody-drug conjugation through Fc glycan remodeling. My research focuses on design and evaluation of the ligation chemistry coupled with enzymatic Fc glycan remodeling of antibodies, using commercially available antibodies and drugs as the modeling systems.

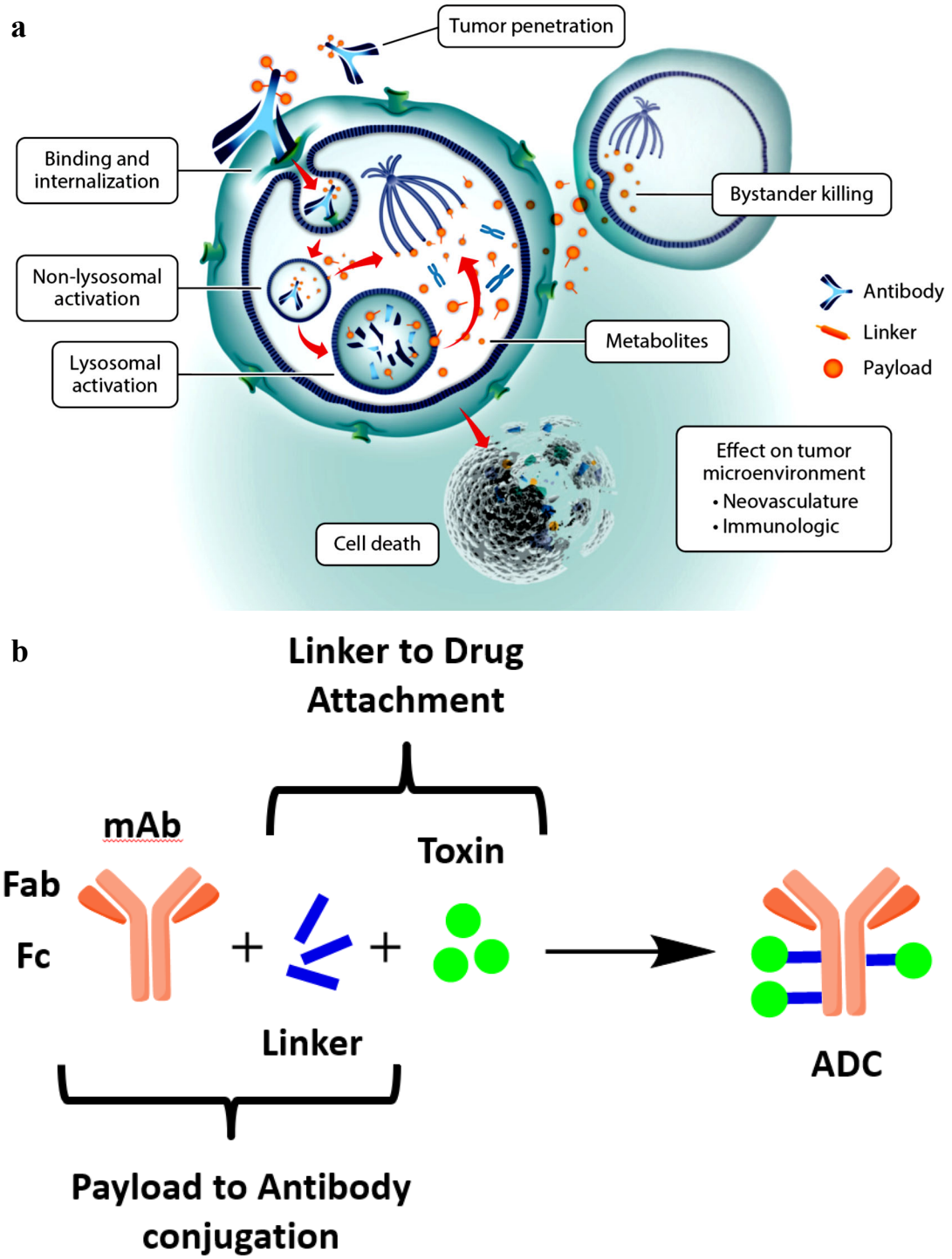

Figure 1-1. (*a*) Mechanism of action of ADCs with microtubule inhibitor as payloads [3]. (*b*) Typical components of ADCs.

1.2 Antibody-Drug Conjugates Currently Approved by FDA

So far 12 ADCs have been currently approved by FDA (Figure 1-2), and about 300 more ADCs are in pre-clinical or clinical development. These include: Gemtuzumab-Ozogamicin for treatment of acute myeloid leukemia, Inotuzumab-Ozogamicin for patients with mature B-cell acute lymphoblastic leukemia, Brentuximab-Vedotin targeting Hodgkin's lymphoma (HL) and anaplastic large cell lymphoma (ALCL). Gemtuzumab-Ozogamicin, developed by Wyeth (purchased by Pfizer in 2009), was the first ADC approved by FDA in 2000. However, this ADC was voluntarily withdrawn in 2010 for its lack of improvement over standard chemotherapy. Interestingly, it was approved by FDA again in September 2017 with modified dosage for the same use. This first-generation ADC contains an anti-CD33 monoclonal antibody (mAb), a cleavable hydrazine linker, and the calicheamicin as the cytotoxic drug, which was conjugated to the antibody through a random lysine coupling (Figure 1-2). [4, 8]

The second FDA-approved ADC was Brentuximab-Vedotin, developed by Seattle Genetics and Takeda in 2011. Brentuximab-Vedotin was recognized as a second-generation ADC, which consists of an anti-CD30 mAb, a protease-cleavable linker, and the MMAE (a microtubule inhibitor) as the payload which was conjugated to the antibody via cysteine alkylation with maleimide. The same payload was also used for three other ADCs: Polivy, Padcev, and Tivdak, targeting CD79b, Nectin4, and tissue actor respectively (Figure 1-2). [8, 9] The other second-generation ADC, Trastuzumab-Emtansine, which was developed by Genentech and Roche, got its approval in 2013. It consists of an anti-HER2 mAb, a non-cleavable thioether linker,

and the Mertansine (a microtubule inhibitor) as the warhead through random lysine ligation chemistry. [3, 4, 8]

In August 2017, FDA approved the fourth ADC, Inotuzumab Ozogamicin, which was developed by Pfizer with an anti-CD22 mAb using the same payload design (Figure 1-2). [3, 4, 8, 10]

In 2019, Enhertu, developed by Daichi Sankyo and AstraZeneca was approved by FDA for treatment of adult patients with unresectable or metastatic HER2+ breast cancer. In 2020, this ADC was further approved for treatment of patients with HER2-mutated non-small cell lung cancer. This ADC utilize an anti-HER2 antibody, the same as Brentuximab-Vedotin, but carrying 8 DXd molecules as the cytotoxic warhead via cysteine alkylation with maleimide (Figure 1-2). The Dxd is a topoisomerase I (TOP1) inhibitor, which is responsible for relaxing DNA supercoiling generated by transcription, replication. In 2020, Trodelvy developed by Immunomedics and Gilead Sciences was approved by FDA for treatment of patients with triple-negative breast cancer. This ADC consists of an anti-Trop2 antibody and on average 7.6 SN-38 molecules as the cytotoxic payloads via cysteine alkylation with maleimide (Figure 1-2). SN-38 is also a TOP1 inhibitor, which was conjugated to the antibody with an acid-sensitive hydrolysable linker for subsequent bystander effects. [4, 8, 9]

In 2020, FDA also approve another ADC, Blenrep, for the treatment of relapsed or refractory multiple myeloma. It was developed by GlaxoSmithKline that is composed of an afucosylated anti-B-cell maturation antigen (BCMA) antibody and about 4 MMAF molecules connected with non-cleavable linker. Like MMAE, MMAF

is also an inhibitor for microtubule polymerization. [9, 11] Due to the charge on the C-terminus phenylalanine, MMAF has much lower cell permeability than MMAE, which makes it suitable for the treatment of blood cancers, despite its higher IC_{50} values. [4, 8]

More recently, FDA approved Zynolonta for the treatment of relapsed or refractory large B-cell lymphoma in 2021. This ADC consists of an anti-CD19 antibody, on average 2.3 pyrrolobenzodiazepine (PBD) molecules as the cytotoxic payload, which selectively alkylates and crosslink the minor groove of DNA. The drug was conjugated to the antibody with a Val-Ala cleavable linker via cysteine alkylation with maleimide (Figure 1-2). [4, 8]

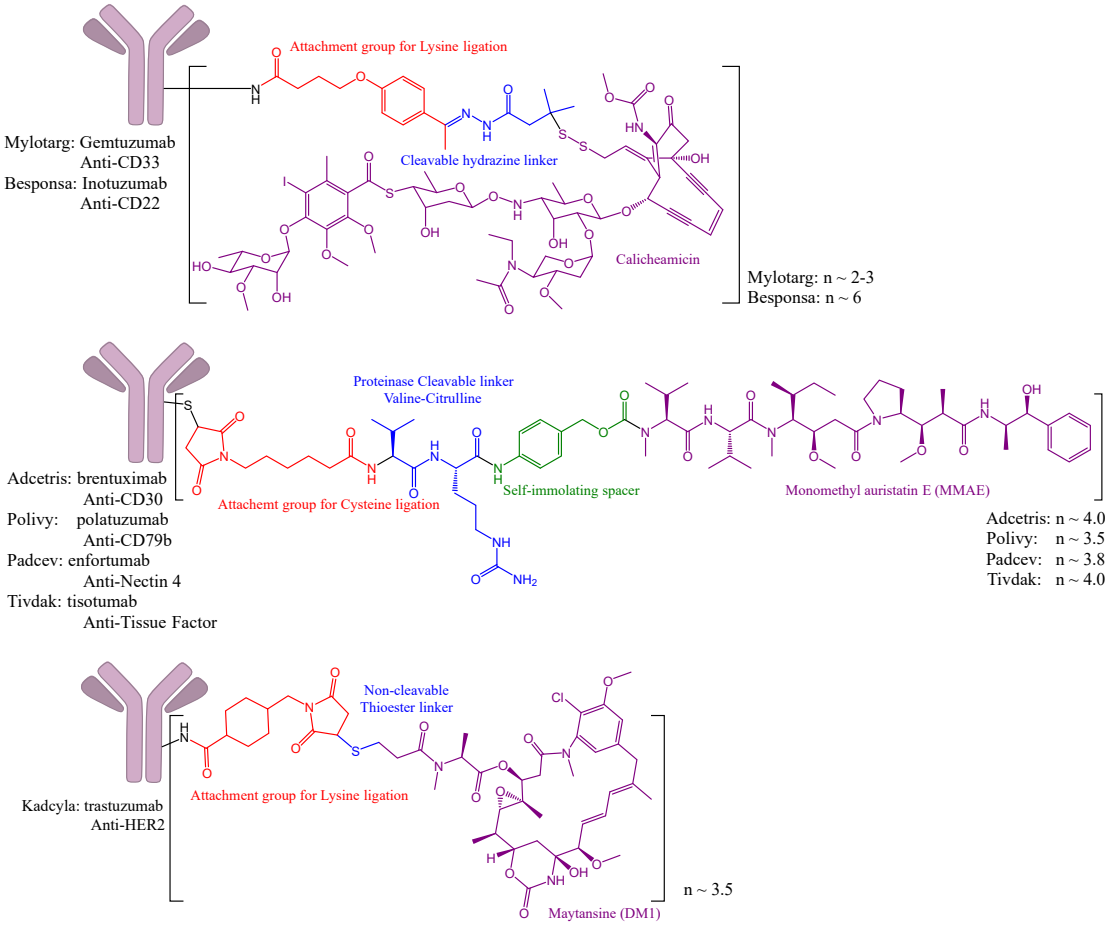

Figure 1-2. Structures of currently FDA approved ADCs.

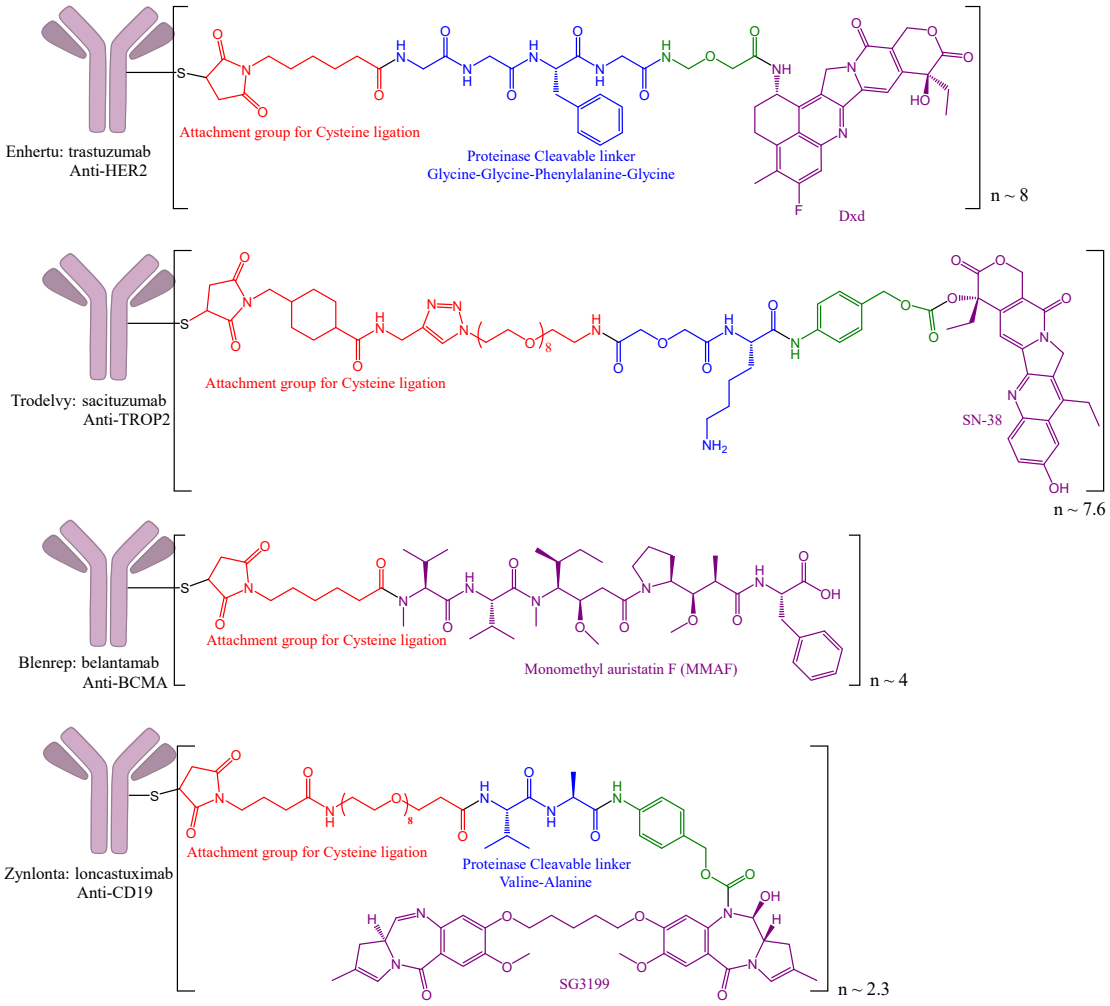

Figure 1-2. Structures of currently FDA approved ADCs. (Continued)

1.3 Site-specific ADCs based on Protein Engineering

Despite the impressive development in this field, all the FDA-approved ADCs and most of the ADCs in the pipeline have been made through nonspecific ligation chemistry such as random lysine ligation and cysteine ligation. [12] Take ADCs with random lysine ligation as an example, when the drug to antibody ratio (DAR) is four, there could be more than thousands of regioisomers, since the ligation could occur at any four sites from forty reactive lysine residues on IgGs. [12] Studies showed that the

heterogeneity of these regioisomers not only resulted in difference in efficacy and serum half-life, but also caused problems such as aggregation and varied antigen affinity. [1, 12-15] In addition to the problems in pharmacokinetics and therapeutic properties, the heterogeneity also raises concerns about consistency in production. [12] Therefore, it is of great interest to develop methods to generate site-specific linked antibody-drug conjugates.

Currently, a majority of the explorations and developments to achieve site-specific ADCs were based on protein engineering, such as engineered cysteines, enzyme-directed modification, and unnatural amino acid incorporation. [4, 12, 14] (Figure 1-3) The site-specific ADCs with two engineered reactive cysteine residues, named THIOMABs, was reported by Mallet and coworkers to have noticeable improved therapeutic index in animal models than second generation ADCs with higher DAR [15]. One particular drawback of THIOMABs was the conjugation chemistry used to generate the ADC: the thiosuccinimide bond formed between the thiols and alkyl maleimides is reversible, especially in physiological conditions, which results in measurable drug loss during circulation. [4]

A promising method to solve this problem was developed by Strop and coworkers in 2013. They genetically introduced a specific amino acid sequence, the glutamine tag, LL**Q**G, while the ligation of the payload was catalyzed by bacterial transglutaminases between glutamine side chains and primary amines. [16] The resulting ADC demonstrated similar performance as THIOMABs but the amide linkage was more stable than the thiol-maleimide linkage. [14, 16] Apart from the potential

immunogenicity of the sequence, this method often requires the removal of the Fc *N*-glycosylation for best ligation yield, which could influence the serum stability of the ADCs.[12]

Genetically encoded unnatural amino acid (UAA) incorporation was another method to construct site-specific ADCs, which was reported by Professor Peter G. Schultz in 2012. With their orthogonal amber suppressor tRNA/aaRS pair technology, they successfully introduced a p-acetylphenylalanine into different chosen sites on the surface of Anti-HER2 antibody. The resulting ADCs showed much improved cytotoxicity, pharmacokinetic and serum stability, when compared to second generation ADCs. [14, 17] The site-specific conjugates have been proved to be a valuable tool for researchers in many different fields. However, the effort required to initiate the stable expression of each of the UAA-containing mAbs was enormous compared to other methods. Besides, the biology of UAAs is not fully understood yet, and the unnatural amino acids could be immunogenic in humans. [12, 14]

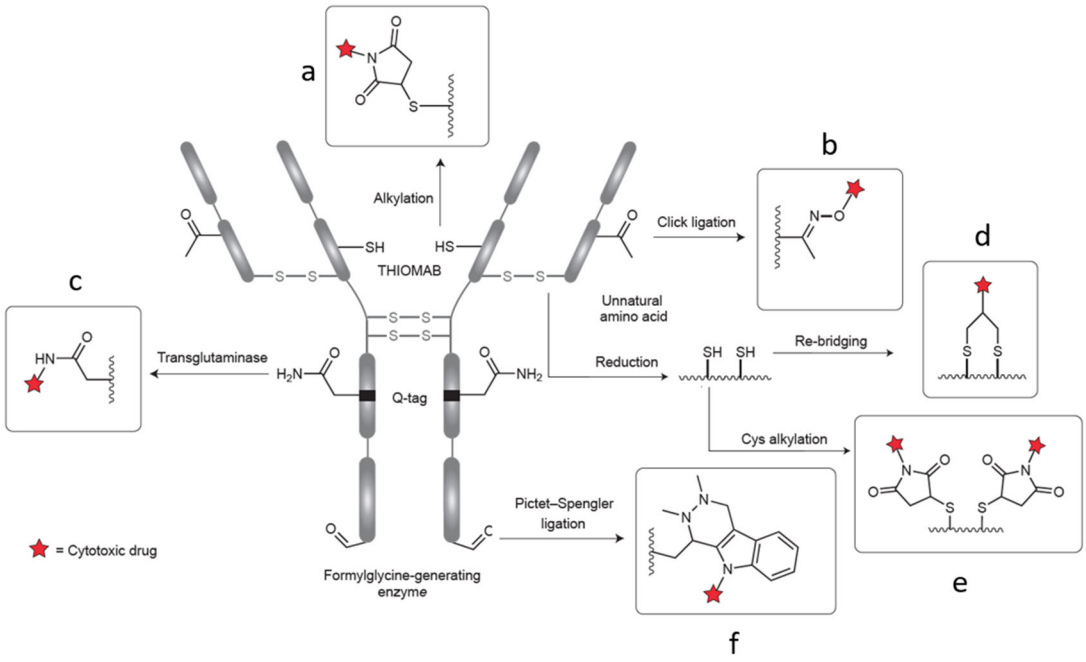

Figure 1-3. Site-specific ADCs based on protein modification. a) THIOMAB, Cysteine engineering, b) Unnatural Amino Acid incorporation, c) Glutamine-tag (Q-tag) insertion, d) Cys alkylation with functional disulfide rebridging, e) Cys alkylation with maleimide, f) C-termius sequence for enzymes.

1.4 Site-specific ADCs based on Glycoengineering

Glycoengineering is emerging as a promising general approach to generate site-specific ADCs. All human IgG antibodies possess a conserved *N*-glycosylation site at the N297 residue in the Fc domain, where antibodies bind to various receptors (Figure 1-4). [4, 12, 14, 18] The biosynthesis of the *N*-glycan of *N*-Glycoproteins starts in the endoplasmic reticulum (ER), where a dolichol-linked oligomannose precursor, $Glc_3Man_9GlcNAc_2$, is assembled in multiple steps by enzymes on ER membrane. This precursor is transferred by an oligosaccharyltransferase (OST) to the consensus sequence(Asn-X-Ser/Thr, where X can be any amino acid except Proline) on the conserved glycosylation site in the Fc of antibodies. When the antibody is correctly folded, the precursor is trimmed to $Man_8GlcNAc_2$. Then the antibody is translocated to

the Golgi apparatus, where the *N*-glycan is further processed into various glycoforms by a panel of glycosidases and glycosyltransferases to generate a mixture of glycoforms in most cases. [18, 19]

Periodate oxidation of the core fucose on the *N*-glycan reported by O'Shannessy and co-workers in 1984 was the first attempt to achieve site specific antibody conjugate. [12, 20] But the oxidant, $NaIO_4$, used to generate the aldehyde could also oxidize methionine on proteins and compromise protein functions. [12, 14] In 2013, Senter and coworkers reported constructing ADC through incorporated 6-thiofucose in antibody expression cell culture. [21] However, the fucose analogue was not incorporated in all antibodies, and the average DAR was about 1.3. [1, 21] Glycosyltransferase and sugar-nucleotides with bioorthogonal groups were also utilized by multiple groups to site-specifically functionalize the *N*-glycan by multiple groups. [22-25]

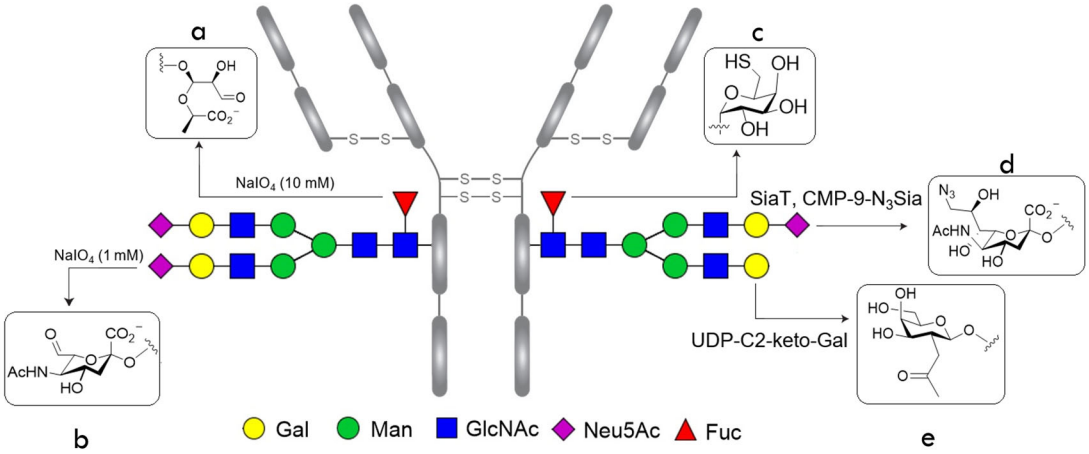

Figure 1-4. Site-specific ADCs based on Fc glycan modification. a) $NaIO_4$ oxidation of core fucose, b) $NaIO_4$ oxidation of sialic acid, c) NaIO4 oxidation of sialic acid, d) Enzymatic incorporation of C2-Keto-Gal, e) Enzymatic incorporation of C9-N_3-Sia.

In 2012, Wang group reported a novel method to produce homogenous antibody glycoforms by cleaving the heterogeneous glycans from commercially available

antibodies with wild-type endoglycosidase S (Endo-S), followed by transglycosylation reaction with Endo-S mutant and chemically synthesized glycan oxazolines. The same group also demonstrated that a fully synthesized Man_3-N_3, which was a truncated *N*-glycan with two azide handles, could be installed onto the antibody in a site-specific manner. [26] (Figure 1-5) Davis and coworkers applied this chemoenzymatic methodology to produce homogenous ADCs. Instead of using synthetic glycan, they used amine coupling reaction to install handles for click reaction onto the carboxylate groups on sialylated complex type glycan (SCT) obtained from natural sources. [27] This method was also utilized by multiple other groups across the world. [28-31]

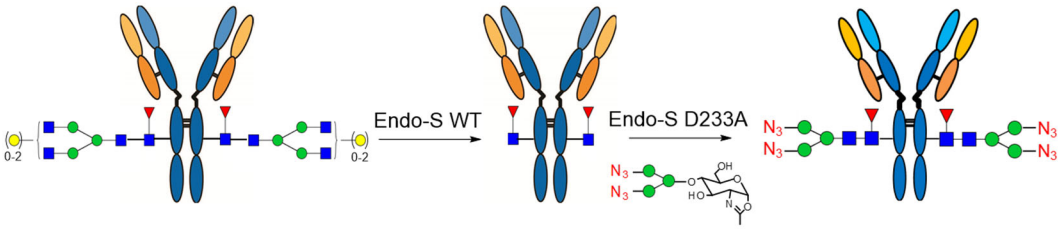

Figure 1-5. Site-specific antibody functionalization via chemo-enzymatic Fc glycan remodeling

1.5 Recent Development of Dual-functionalized Antibodies

Recently, significant amount of effort has been invested into the developments of homogeneous multi-functionalized ADCs for different purposes. Schultz and coworkers initiated the field in 2013 by genetically encoding a pair of orthogonally labeled UAAs simultaneously. UAAs with keto side chain and azido side chain had been coupled with oxime ligation and copper-free click reaction respectively, to obtain a homogenous fluorescence labeled ADC [32]. Several other groups also achieved similar results with their own methodologies [33, 34]. Bradley group took this concept one step further: they labeled the drug part and antibody part of the ADC with two types of

radioactive isotopes, and for the first time, studied the drug release process of ADC in animal models [35]. Due to the difference in drug sensitivities within heterogeneous tumor cell population, complementary drug combinations were administrated in almost all current cancer chemotherapies. Therefore, complementary drugs compacted in one ADC is also an area of hot pursuit. Huang and co-workers showcased their dual-drug ADCs with one kind of drug linked to the functionalized *N*-glycan with antibody glycan remodeling strategy, and another drug conjugated with non-specific lysine ligation.[28] In 2017, Senter and coworkers reported a homogenous dual-drug ADCs based on dual-cysteine multiplexing carrier, which demonstrated significant improvement in treatment [36]of drug resistant cancer cell lines in mouse model.[37] In 2018, Bruins and coworkers used a cyclopropanated trans-cyclooctene (cpTCO) based unnatural amino acid in the heavy chain and azide on the Fc *N*-glycan to achieve dual-functionalized antibody.[33] During the time we are working on this project, a similar study was published by Yamazaki and coworkers. They used azide and tetrazine functionalized linker and transglutaminase to conjugate it to an anti-HER2 antibody.[38]

1.6 Our Plan to Generate Site-Specific Dual-functionalized Antibody Conjugates

Site-specific ADCs have significant advantages in *in vivo* efficacy, tolerability and therapeutic index over commercially available ones based on random conjugation.[13, 15, 39] . My thesis research focuses on development of a site-selective conjugation method for synthesizing ADCs, utilizing this method for improving therapeutic antibody's CDC, and exploration for enhancing ADC internalization and lysosomal delivery with the dual functionalization method.

As a foundation of the thesis, an efficient method was developed to functionalize the SCT with different clickable groups including azide-, cyclopropene-, and norbornene-tags. Homogenous ADCs, with drug-antibody ratio of 4, were successfully obtained through three different click reactions on the tags introduced. A comparison cell-based study indicates that the ADCs generated by the three click reactions all showed potent cancer cell killing activity and excellent serum stability.

With this conjugation method, we also constructed structurally well-defined antibody-αGal and antibody-rhamnose conjugates, which were designed to recruit natural anti-αGal and anti-rhamnose antibodies for CDC, using trastuzumab as a model antibody. Our preliminary *in vitro* study indicates that the resulting conjugates could mediate potent CDC activity against targeted cancer cell with high selectivity.

In addition, by introducing a pair of orthogonal Click groups on the SCT, a highly homogenous dual-functionalized antibody could be obtained by the optimized Fc *N*-glycan remodeling method. Since the rate of receptor internalization is a key factor for the selection of druggable tumor antigen, enhancing the internalizing speed by a ligand could improve the efficacy of the ADC and possibly broaden the druggable antigens for ADCs.[36, 40-42] Therefore, we plan to use one of the Clickable groups to ligate the drug, while using another one to carry an internalizing factor. Also, this method that enables simultaneously delivery of complementary drugs could provide a platform to study the synergy of small molecule drugs in targeted therapies. This dual drug ADCs could be a valuable approach to overcoming drug resistance problems in treatments of tumors and other infectious diseases.

Chapter 2: One-Pot Conversion of Free Sialoglycans to Functionalized Glycan Oxazolines and Efficient Synthesis of Homogeneous Antibody-Drug Conjugates Through Site-Specific Chemoenzymatic Glycan Remodeling

Part of this work was published in in *Bioconjugate Chemistry* (**2021**, *36*, 1888-1897)

2.1 Introduction

Antibody–drug conjugates (ADCs) are a class of therapeutic agents that explore the specificity of antibodies to deliver highly toxic drugs to respective antigen-expressing cells to achieve targeted cell killing.[43, 44] So far twelve ADCs have been approved by US FDA for the treatment of cancers and many more are in the pipelines.[9, 45] Many factors contribute to the overall *in vivo* efficacy of an ADC. In addition to the choice of antibody, payload, and linker, the way how antibody is conjugated to the drug also plays an important role in dictating the therapeutic outcome of ADCs. The first generation ADCs have been produced through nonspecific conjugations at lysine and/or reduced cysteine residues, which usually result in heterogeneous mixtures of ADC entities that may differ in drug-to-antibody ratios (DARs), sites of attachment, stability, and pharmacokinetic properties.[4, 44] To overcome the issues of reproducibility, stability, and potential side effects associated with heterogeneous conjugations, the next generation of ADCs has been focused on site-specific conjugations that provide homogeneous conjugates with well-defined pharmacological properties and improved therapeutic index.[13, 15, 39] Significant progress has been made in recent years in the development of site-specific antibody-drug conjugation strategies[44] Some examples include: the introduction of unnatural amino acids or unpaired cysteines for subsequent

chemoselective ligation,[15, 17, 46-51] the selective C-/N-terminal modifications,[52, 53] the disulfide reduction/rebridging strategy,[54, 55] and the transglutamidase-mediated chemoenzymatic ligation.[56]

In addition to the site-selective modifications on amino acid residues of the protein domains, another approach is to conjugate drugs at the highly conserved *N*-glycans located at Asn-297 of the Fc domain [19, 57]. Since all IgG antibodies carry the conserved Fc *N*-glycans and they are spatially distant from the antigen-binding region, a unique advantage of the Fc glycan-mediated conjugation is that it does not modify the protein parts and the attachment of the drug to the Fc glycans usually will not interfere with the Fab-mediated antigen binding. Early attempt to functionalize the Fc glycans through oxidation of adjacent diols of terminal monosaccharides, have provided mixtures of conjugates due to the heterogeneity of the glycoforms and the oxidation at different sugar units.[58-60] The use of the galactosyltransferase mutants capable of accommodating modified UDP-galactose derivatives as the donor substrates has enabled the incorporation of a selected tag at the Fc glycans for subsequent site-specific conjugation with modified cytotoxic agents.[21, 25, 61, 62] Nevertheless, this approach usually requires the trimming of the heterogeneous Fc *N*-glycans to the terminal GlcNAc-glycan forms and, due to the moderate efficiency of the mutant enzyme on the unnatural sugar nucleotide substrate, a large excess of modified sugar nucleotide and enzyme as well as long incubation time are usually needed to drive the reaction, which often leads to incomplete reaction and thus heterogeneity of the products.

On the other hand, the endoglycosidase-catalyzed glycan remodeling strategy [63, 64], enabled by the discovery of the Endo-S and Endo-S2 glycosynthase mutants for efficient glycosylation without product hydrolysis,[65-67] has provided a promising method for generating homogenous glycoforms including ADCs.[19, 28, 57, 68-70] This method includes three key steps: the synthesis of selectively tagged glycan oxazoline as donor substrates, the enzymatic transfer of the tagged glycans to Fc-deglycosylated antibodies, and the Click drug conjugation. While this method has demonstrated promise for constructing ADCs, the synthesis of the selectively tagged glycan oxazolines remains to be improved,[69, 71] and the requirement of a large excess of glycan oxazolines and a relatively long incubation time to drive the reaction, partially due to the moderate activity of the Endo-S D233Q mutant,[65] leads to side reactions on the antibody that needs significant optimizations.[69, 70] In this paper, we report a facile one-pot synthesis of functionalized glycan oxazolines carrying azide-, cyclopropene-, and norbornene-tags, respectively, from free natural sialoglycans and their use for antibody glycan remodeling catalyzed by the Endo-S2 D184M mutant with minimized non-enzymatic side reactions.[66] The optimized chemoenzymatic method enabled a highly efficient synthesis of selectively tagged antibodies which are readily used for site-specific antibody-drug conjugation. We also performed a comparative study of three Click methods for conjugating the drug to make homogeneous antibody-drug conjugates (Figure 2-1) and evaluated the *in vitro* cytotoxicity of the resulting ADCs. The one-pot synthesis of functionalized glycan oxazolines, coupled with the efficient Endo-S2 D184M-catalyzed Fc glycan remodeling and Click drug conjugation, provides

a general and efficient approach to producing structurally well-defined, homogeneous antibody-drug conjugates.

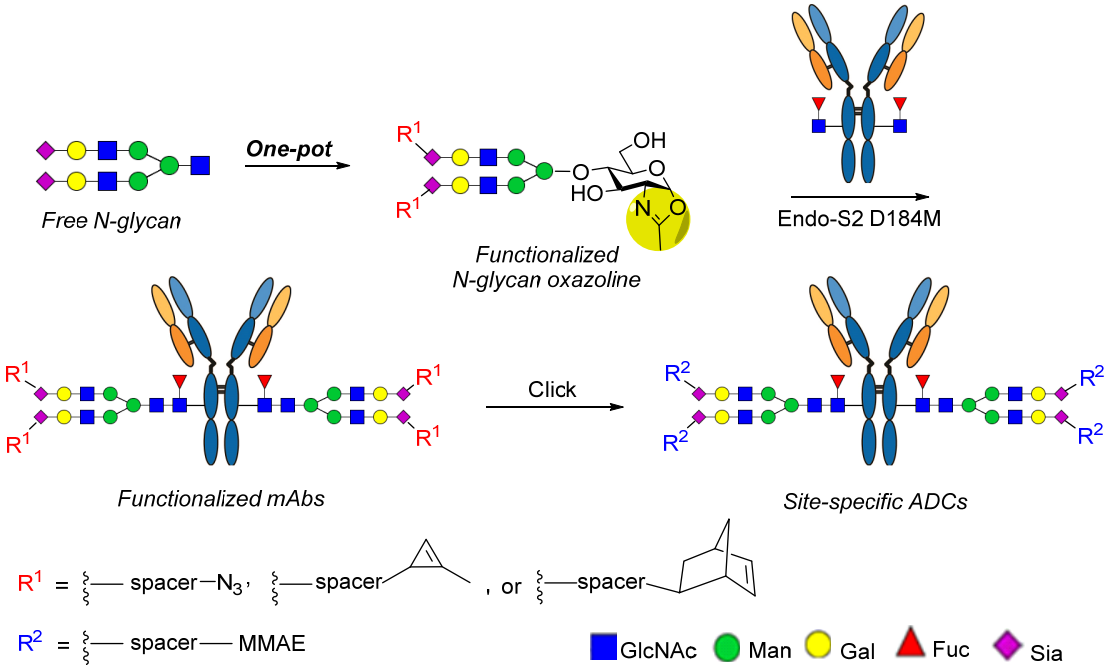

Figure 2-1. A general approach for the glycan-mediated site-specific antibody-drug conjugation via different Click reactions

2.2 Results and Discussion

Improved synthesis of azide-tagged sialylated *N*-glycans from free sialoglycans.

Davis and co-workers have previously reported that free sialylated *N*-glycan could be functionalized by amide coupling between the terminal sialic acids and a tagged amine using 4-(4,6-dimethoxy-1,3,5-triazin-2-yl)-4-methylmorpholinium chloride (DMTMM) as the coupling reagent. But a large excess of an azide-tagged amine (20 eq.) and DMTMM (40 eq.) at an elevated temperature should be applied to

give a moderate yield (72%).[69] We first repeated the coupling reaction using DMTMM and an azide-PEG-NH_2 under a similar condition. Unexpectedly, we found that the amide coupling was accompanied by the simultaneous formation of a glycoside derived from DMTMM, giving the 4,6-dimethoxy-1,3-5-triazin-2-yl α-glycoside (**2-2**) instead of the free reducing glycan (**2-3**) (Scheme 2-1). Glycoside **2-2** was purified by HPLC in excellent yield and its identity was verified by ESI-MS and NMR analysis. Indeed, Shoda and co-workers have previously reported that reducing sugars can be converted to 4,6-dimethoxy-1,3-5-triazin-2-yl α-glycoside using DMTMM in the presence of a base catalyst such as 2,6-lutidine in an aqueous solution.[72, 73] We speculated that the large excess of the azido-PEG-NH_2 might serve as the base to promote the formation of the glycoside. Interestingly, the α-glycoside (**2-2**) could be readily converted to the corresponding free reducing *N*-glycan by treatment with 0.1% TFA for 16 hours at rt. Recently, Manabe and co-workers have reported that coupling of the *N*-glycan (**2-1**) and amine NH_2-$(CH_2CH_2O)_3CH_2CH_2$-N_3 using DMTMM as the dehydrating agent under the previously described conditions failed to give the expected coupling product, but the use of a phosphonium salt-based reagent, (benzotriazol-1-yloxy) tris(pyrrolidino)-phosphonium hexafluorophosphate (PyBOP), provided the desired sialic acid and amine coupling product in 57% yield.[71] The resulting azide-tagged antibody has been successfully used for making antibody-drug conjugates.[74]

To optimize the amide coupling reaction without the α-glycoside formation, we reasoned that the pH of the reaction, the reaction temperature, and the quantity of the azido-PEG-NH_2 and DMTMM might be important factors to modulate the outcome. A searching of the reaction conditions, including varying the pH (pH 5-10), the amount

of the azido-PEG-NH_2 (3-20 equiv.), and the temperature (30-60 ºC), we found that the pH was critical, and a basic condition led to significant formation of the by-product, the 4.6-dimethoxy-1,3-5-triazin-2-yl α-glycoside (**2-2**). We observed that keeping a slightly acidic condition (pH = 5.5), combined with the use of a significantly reduced amount of azido-PEG-NH_2 and DMTMM and an elevated temperature, gave the best coupling yield of the tagged glycan (**2-3**) without formation of the α-glycoside (**2-2**). Thus, treatment of the sialoglycan (**2-1**) with 3 equivalents of azido-PEG-NH_2 and a total of 10 equivalents of DMTMM (added in two portions) in an aqueous buffer (pH 5.5) at 50 ºC for 6 h gave the desired amide product (**2-3**) in a 92% yield after G15 gel filtration (Scheme 2-1). The functionalized glycans were readily converted to the corresponding glycan oxazolines in water by using 2-chloro-1,3-dimethylimidazolinium chloride (DMC) as the dehydrating reagent, following the previously reported procedures.[72]

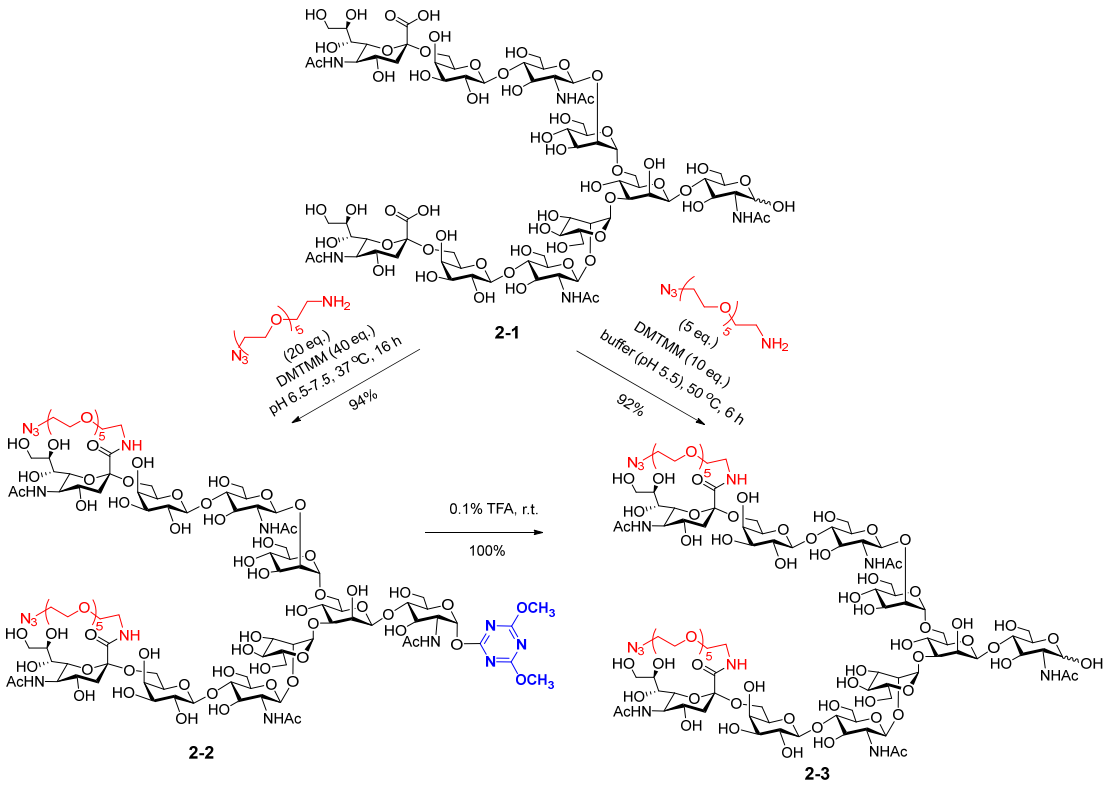

Scheme 2-1. Synthesis of functionalized *N*-glycans using DMTMM coupling.

A "one-pot" and optimized synthesis of the functionalized *N*-glycan oxazolines.

The chemoenzymatic Fc glycan-specific conjugation requires the synthesis of the functionalized glycan oxazolines as the key donor substrate [57]. As the DMTMM-catalyzed amine coupling under the above-described conditions gave almost quantitative transformation to the azide-tagged *N*-glycan, we attempted to develop a strategy to directly synthesize the azide-tagged glycan oxazoline from the corresponding sialylated *N*-glycans in a "one-pot" manner, which are key donor substrates for the endo-glycosynthase mutant-catalyzed glycan remodeling and conjugation of antibodies [19, 57, 65, 66]. We sought to combine the *N*-glycan functionalization and oxazoline formation in a one-pot manner by tuning the reaction conditions, including the pH, temperature, and reagents (Scheme 2-2). The DMTMM

catalyzed amide formation reaction was carried out first under a slight acidic condition (pH 5.5) at 50 ºC, and the reaction was monitored by HPLC until its completion within 6 h. Then, the reaction mixture was cooled on ice, and TEA (70 equiv.) and DMC (30 equiv.) were added. The formation of the corresponding sugar oxazoline product was complete within 30 min at 0 ºC. The oxazoline was purified with P2 size exclusion chromatography to remove all other smaller molecules, affording the pure azide-tagged glycan oxazoline (**2-4a**) in 86% isolated yield. Compared with the previous method, this facile one-pot functionalization-oxazoline formation procedure significantly simplified the protocol, resulting in a much-enhanced overall yield (Scheme 2-2). An attempt to use DMC/TEA under either acidic or basic conditions failed to provide the amine coupling product (data not shown). Thus, DMTMM appeared to be an appropriate dehydrating reagent to enable the "one-pot" conversions. Similarly, the cyclopropene- and norbornene-modified *N*-glycan oxazolines, **2-4b** and **2-4c** were synthesized in a one-pot" manner in excellent yields, which are two different partners for chemo-selective Click reactions (Scheme 2-2).

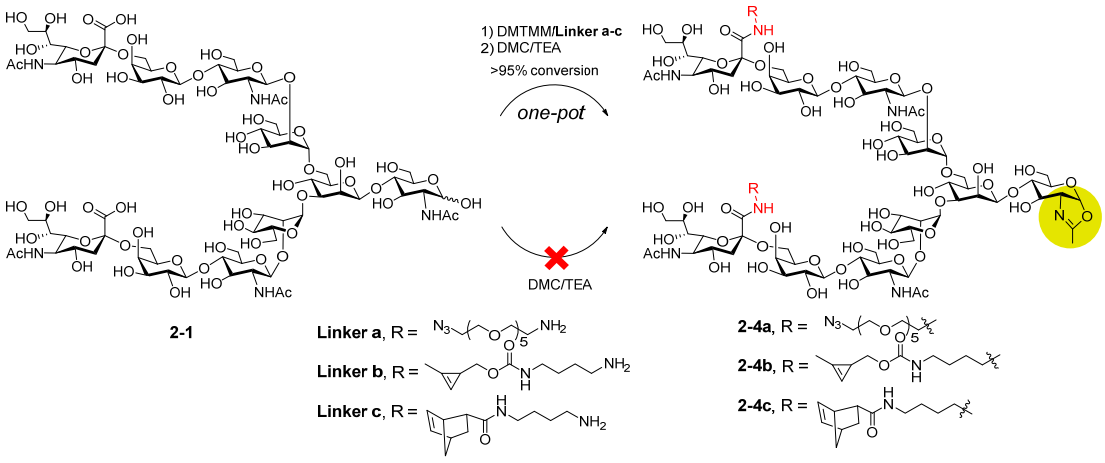

Scheme 2-2. One-pot transformation of free sialoglycans into functionalized glycan oxazolines.

Site-specific Fc glycan remodeling with the functionalized glycan oxazolines using Endo-S2/Endo-S2 mutants.

We have previously reported the generation and use of Endo-S mutants for site-specific Fc glycan remodeling of intact antibodies with natural and azide-modified *N*-glycan oxazolines [65]. The Endo-S D233Q mutant has been used for glycan remodeling followed by Click reactions to produce antibody-drug conjugates [28, 68, 69, 74]. Since the Endo-S D233Q catalyzed enzymatic glycan transfer is relatively slow, the reaction condition should be optimized to minimize non-enzymatic side reactions [69, 74]. On the other hand, we have reported that the glycosynthase mutant (D184M) derived from Endo-S2, another antibody-specific endoglycosidase from *Streptococcus pyogenes* of serotype M49 demonstrates significantly enhanced glycosylation efficiency and much reduced reaction time without detectable side reactions for antibody Fc-glycan remodeling [66, 67, 75]. Thus, we examined the feasibility of Endo-S2 D184M mutant to transform antibody with the functionalized glycan oxazolines, using trastuzumab (Herceptin), an anti-epidermal growth factor receptor 2 (HER-2) therapeutic monoclonal antibody, as a model for testing the Fc glycan remodeling and antibody-drug conjugation. Thus, recombinant trastuzumab was treated with an immobilized wild-type Endo-S2 to give the deglycosylated antibody (Fucα1,6GlcNAc-trastuzumab, **2-6**). The wild-type enzyme was readily removed by simple centrifugation after reaction. It should be mentioned that since Endo-S2 is such an efficient endoglycosidase for Fc deglycosylation, the use of immobilized Endo-S2 for deglycosylation is important, as any trace amount contamination of Endo-S2, e.g., from trace Fc-associated co-purification in the protein A purification steps, could result in

slow hydrolysis of the final product during transglycosylation and/or in storage [67]. The Fucα1,6GlcNAc-trastuzumab (**2-6**) was purified by affinity chromatography on a protein A column, the identity of which was verified by LC-ESI-MS analysis (Figure 2-2).

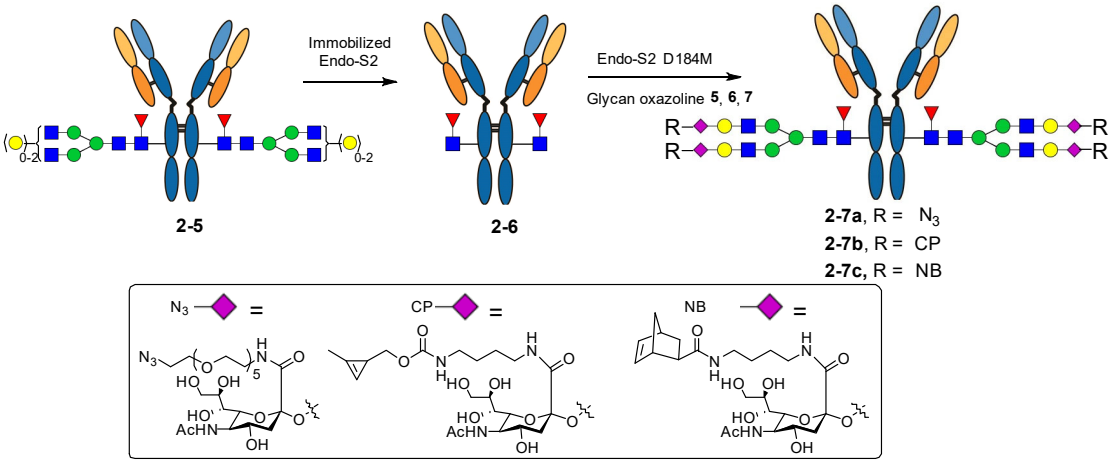

Scheme 2-3. Chemoenzymatic glycan remodeling using the Endo-S2/Endo-S2 D184M enzyme pair for site-specific introduction of functional tags in the antibody.

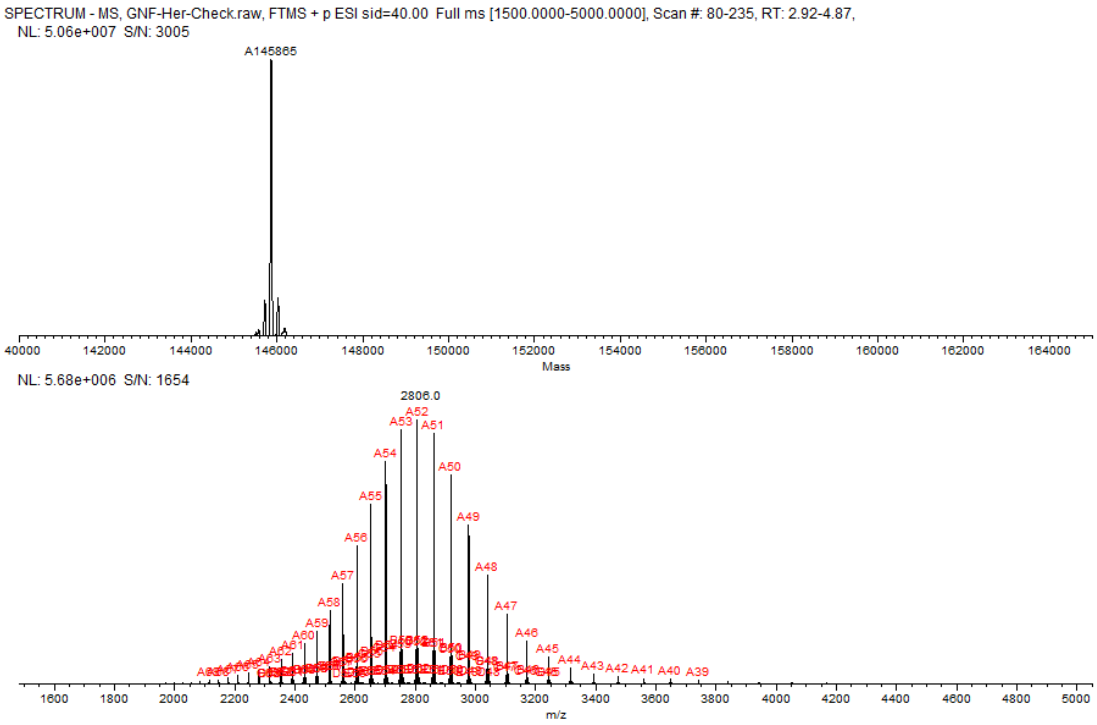

Figure2-2. LC-MS analysis of the deglycosylated trastuzumab (Fucα1,6GlcNAc-trastuzumab, (**2-6**).

The Endo-S2 D184M catalyzed transglycosylation of Fucα1,6GlcNAc-trastuzumab (**2-6**) with the respective functionalized glycan oxazoline (**2-4a**-**c**) was performed in a Tris buffer (100 mM pH 7.2) at 30 °C, and the reaction was monitored by LC-ESI-MS analysis of intact antibodies. We found that under the above conditions, only 20 molar equivalents of the azide-glycan oxazoline (**2-4a**) per antibody and less than 0.5% (by weight) of the Endo-S2 mutant would be sufficient for achieving essentially quantitative glycosylation within 20 min to give the azide-tagged antibody (**2-7a**) (Scheme 2-3). The enzymatic reaction was equally efficient for the cyclopropene- and norbornene-modified glycan oxazolines (**2-4b** and **2-4c**) to provide the cyclopropene- and norbornene-tagged antibodies (**2-7b** and **2-7c**), respectively (Scheme 2-3). The final products were purified by affinity chromatography on a protein

A column in an excellent isolated yield. The identity and homogeneity of the tagged antibodies (**2-7a**, **2-7b** and **2-7c**) were confirmed by LC-ESI-MS analysis (Figure 2-3A-C) of both the intact antibodies and the Fc domains released by IdeS treatment (Figure 2-3D-F). The observed molecular mass (deconvolution data) of **2-7a**, **2-7b**, and **2-7c** was 151025 Da, 150587 Da, and 150630 Da, which matched well with their calculated value of 151022 Da, 150589 Da, and 150629 Da, respectively. In addition to the intact antibody analysis, LC-ESI-MS analysis of the monomeric Fc domain of **2-7a**, **2-7b** and **2-7c** released from IdeS treatment further confirmed the site-selectivity and homogeneity of the final products (Figure 2-3). The raw LC-ESI-MS data were shown in Figure 2-4, Figure 2-5. Notably, previous studies have reported that in the case of the Endo-S D233Q catalyzed glycosylation of the GlcNAc(α1,6Fuc)-antibody (**2-6**), a relatively large excess of the glycan oxazolines (up to 100 equivalents in multiple additions) and large amount of the enzyme (up to 20% by weight) are required to drive the relatively slow reaction to completion, which leads to accumulation of non-enzymatically modified antibody products without optimization of the reaction conditions.[69, 74, 76]

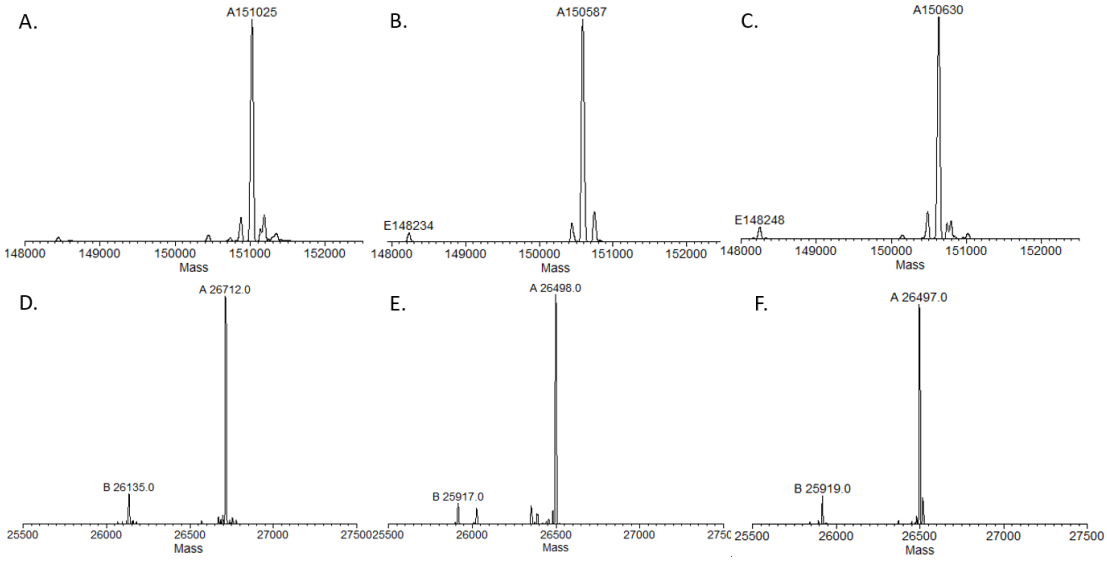

Figure 2-3. LC-ESI-MS analysis of the functionalized intact antibodies (**2-7a**,**2-7b** and **2-7c**) and the Fc domains released by IdeS treatment. A) the deconvoluted mass of intact antibody **2-7a**; B) the deconvoluted mass of intact anibody **2-7b**; C) the deconvoluted mass of intact antibody **2-7c**. D) the deconvoluted mass of the Fc domain of antibody **2-7a**; E) the deconvoluted mass of the Fc domain of antibody **2-7b**; F) the deconvoluted mass of the Fc domain of antibody **2-7c**.

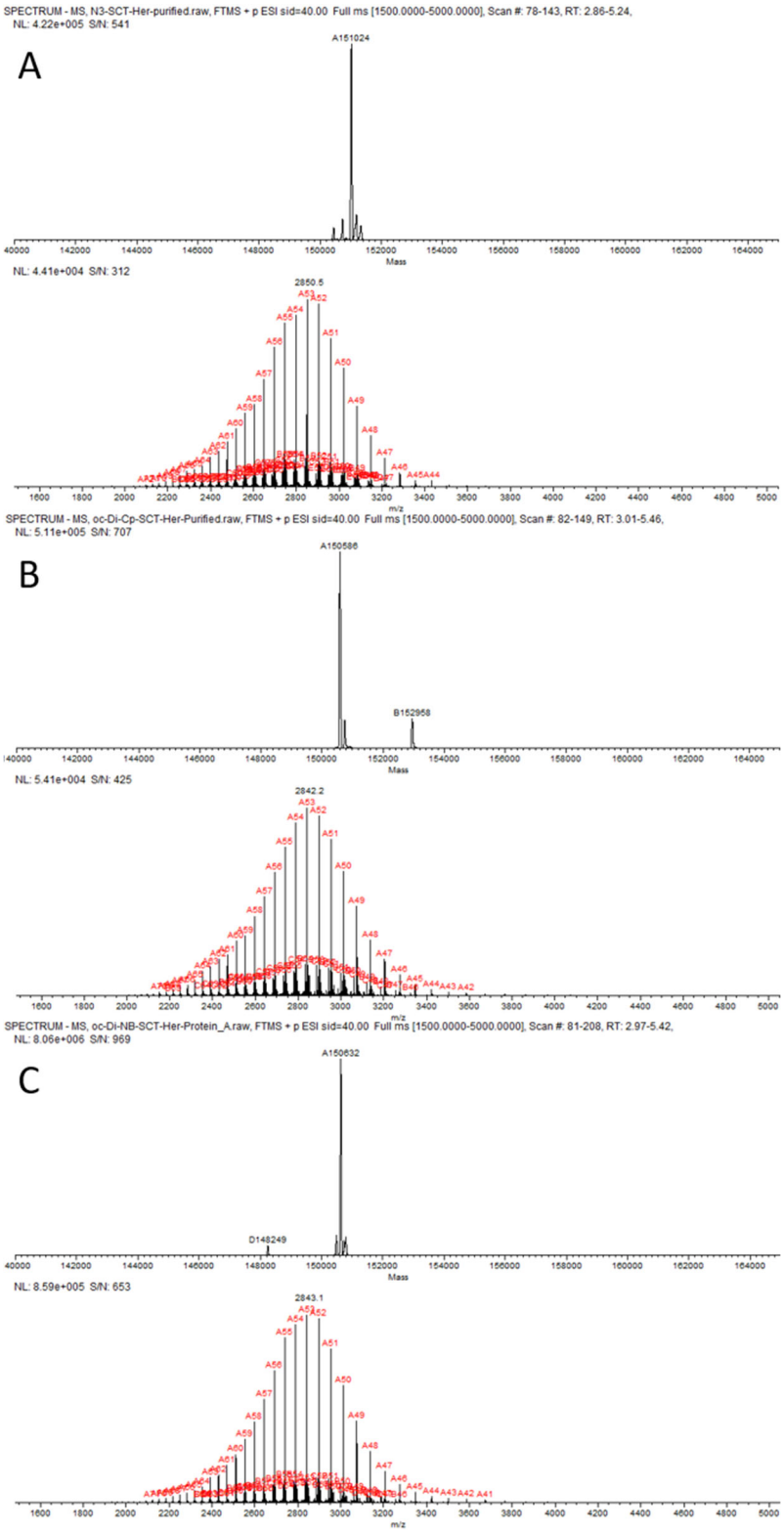

Figure 2-4. LC-ESI-MS analysis of the intact functionalized antibodies A) deconvoluted mass and raw data of intact **2-7a**; B) deconvoluted mass and raw data of intact **2-7b**; C) deconvoluted mass and raw data of intact **2-7c**.

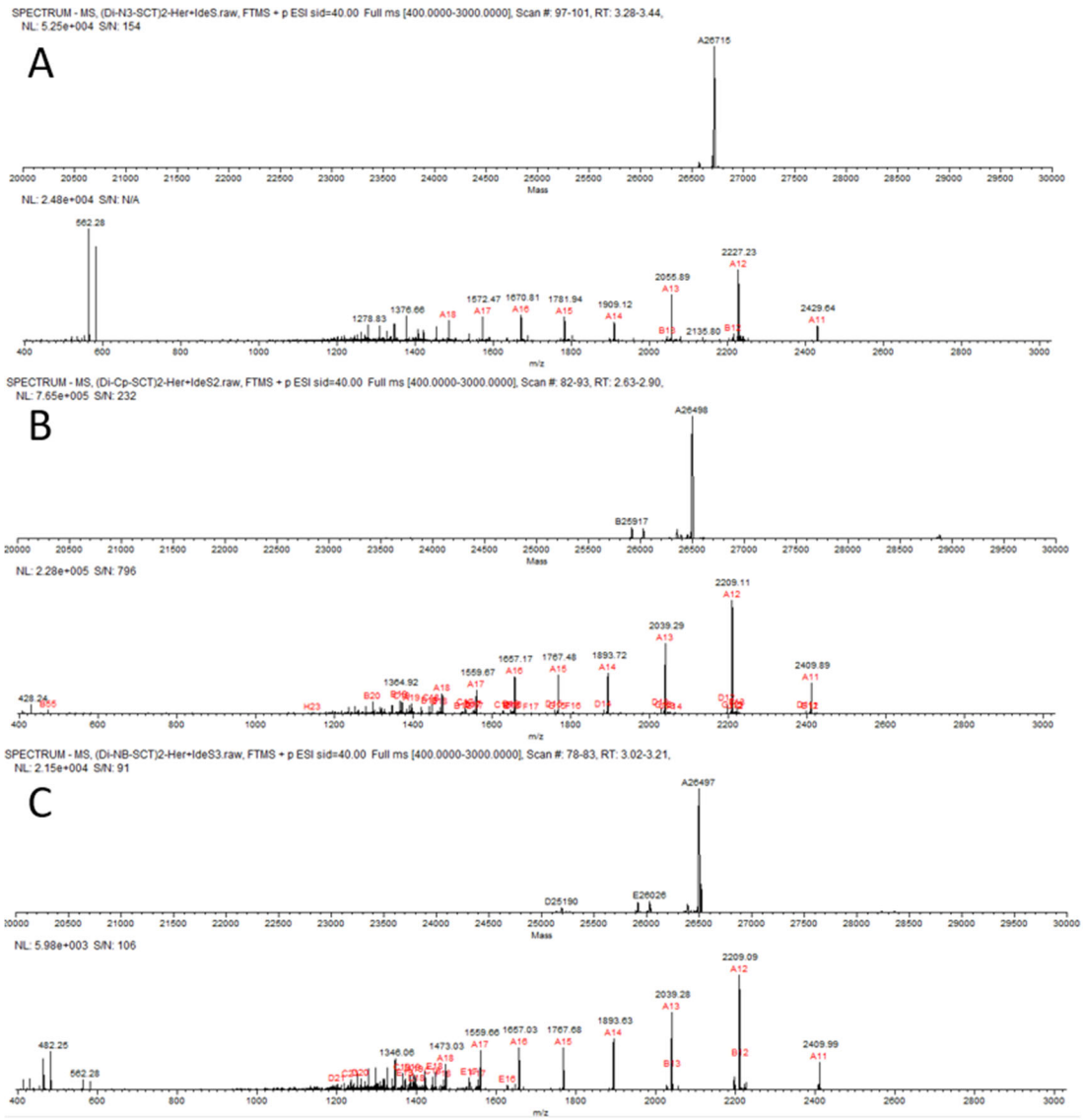

Figure 2-5. LC-ESI-MS analysis of the Fc domains released by IdeS treatment of the functionalized antibodies A) deconvoluted mass and raw data for Fc domains of **2-7a**; B) deconvoluted mass and raw data for Fc domains of **2-7b**; C) deconvoluted mass and raw data for Fc domains of **2-7c**.

To verify the difference in efficiency of the Endo-S D233Q and Endo-S2 D184M catalyzed glycosylations with the selectively modified glycan oxazolines, we performed a side-by-side comparative analysis of the enzymatic glycosylation using the azide-modified glycan oxazoline (**2-4a**) as the donor substrate. We found that under

an optimized condition (molar ratio of glycan oxazoline **2-4a** to antibody **2-6**, 20:1; antibody concentration 25 mg/mL; Tris buffer, pH 7.2; incubation at 30 ºC), the Endo-S2 D184M catalyzed reaction gave essentially quantitative conversion to the expected glycosylated antibody product (**2-7a**) (M = 151024, Figure 2-6B) within 20 min without any side reactions, while the Endo-S D233Q catalyzed reaction required 80 min for completion. Interestingly, even in the case of Endo-S D233Q mutant, we detected only trace amount of non-enzymatic glycation, with an addition of an extra glycan moiety (M = 153601, Figure 2-6F). This result was contradictory to the previously reported relatively slow reactions with Endo-S D233Q mutant and the side reactions when large amount of glycan oxazolines, longer reaction time, and higher pH were applied. [69, 74, 76] taken together, these results indicate the high efficiency of the Endo-S2 D184M-catalyzed glycosylation for introducing the functionalized glycans into intact antibodies.

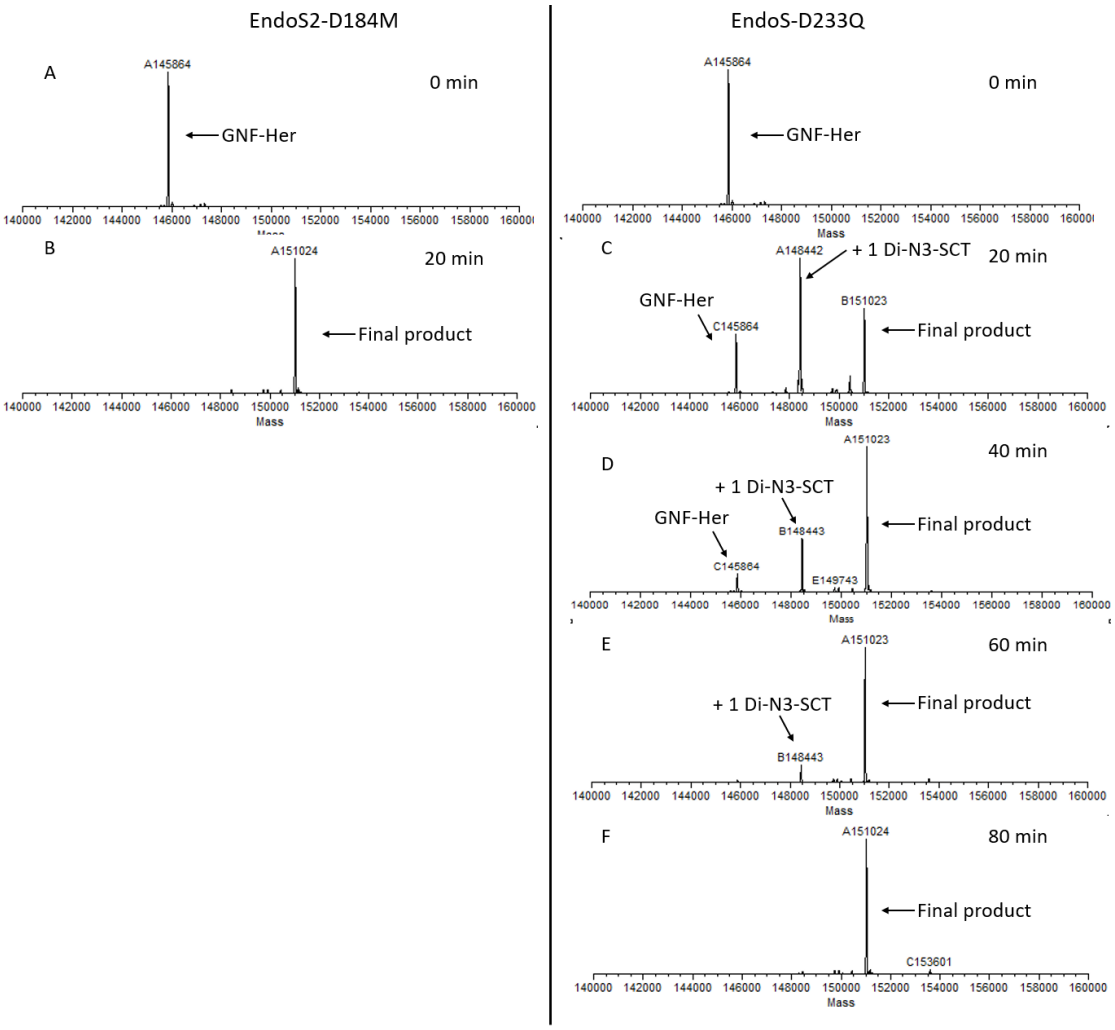

Figure 2-6. The progress of the transglycosylation reactions catalyzed by EndoS2-D184M and EndoS-D233Q. 1mg **2-6**, 25 mg/mL, 20 eq. **2-4a**, 100 mg/mL, final enzyme concentration 0.1 mg/mL. LC-ESI-MS intact antibody analysis of the reaction mixtures at 20 minutes intervals. A) the deconvoluted mass of **2-6**; B) the deconvoluted mass of the reaction mixture catalyzed by EndoS2-D184M at 20 min; C) the deconvoluted mass of the reaction mixture catalyzed by EndoS-D233Q at 20 min; D) the deconvoluted mass of the reaction mixture catalyzed by EndoS-D233Q at 40 min; E) the deconvoluted mass of the reaction mixture catalyzed by EndoS-D233Q at 60 min; F) the deconvoluted mass of the reaction mixture catalyzed by EndoS-D233Q at 80 min.

Synthesis of homogeneous antibody-drug conjugates via Click reactions.

In this study, we selected monomethyl auristatin E (MMAE) as the payload for making the antibody-drug conjugates (ADCs). MMAE, coupled with the valine-citrulline cleavable linker, has been used as the payload in four FDA-approved ADCs [44, 45]. Also, ADCs based on auristatin and trastuzumab have been tested effective against T-DM1 resistant cell lines [77]. The Click reactions between azide-tagged antibody and dibenzylcyclooctyne (DBCO) have been widely used to generate ADCs [28, 62, 74, 78]. Recently, the inverse electron demand Diels–Alder (iEDDA) reaction has also been applied to synthesize site-specific ADCs[79, 80]. Despite the impressive progress, a side-by-side comparison of these different Click reactions in ADCs have not been performed. It is of high interest to see if the distinct Click linkages will make difference in cancer cell killing performance of the resulting ADCs. To construct the antibody-drug conjugates with the three distinct Click conjugations, we synthesized two functionalized MMAE derivatives, the DBCO-modified MMAE (**2-8**) and the tetrazine-modified MMAE (**2-9**) as distinct Click partners for the strain-promoted alkyne-azide cycloaddition reaction and the inverse electron demand Diels-Alder reaction, respectively. A cathepsin B cleavable valine-citrulline linker was introduced in the construct with a self-immolation spacer [60, 81]. Then the DBCO or the tetrazine moiety was linked to MMAE to give the DBCO- and tetrazine-modified MMAE (**2-8** and **2-9**), respectively.

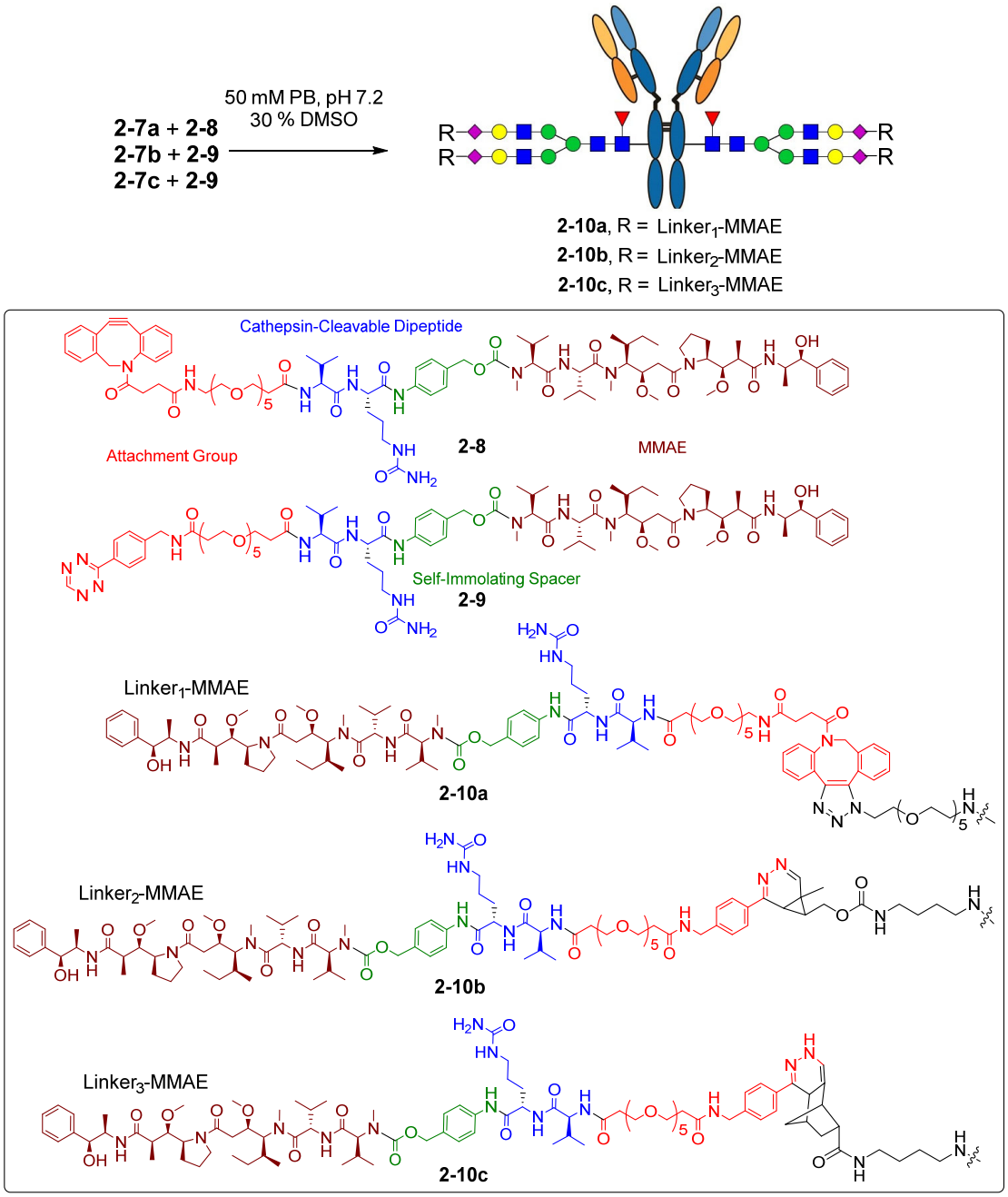

Scheme 2-4. Synthesis of homogeneous ADCs through Click reactions.

The conjugation between the azide-tagged antibody (**2-7a**) and the DBCO-modified MMAE (**2-8**) was carried out in 30% DMSO at r.t. with a final concentration of the antibody at 2 mg/mL and 20 molar equivalents of the payload per Click handle

being used (Scheme 2-4). The reaction was monitored by LC-ESI-MS, which indicated the completion of conjugation with 8 h to give ADC **2-10a**. The conjugation between the cyclopropene- or norbornene-tagged antibody (**2-7b** or **2-7c**) and the tetrazine-modified MMAE (**2-9**) was performed under the same conditions as described for the preparation of ADC **2-10a**. We found that the reaction between the cyclopropene-antibody (**2-7b**) and the tetrazine-modified MMAE (**2-9**) went very fast, which took less than 4 h for completion to give the ADC (**2-10b**). This result was consistent with previous observations [79]. On the other hand, the Click reaction between the norbornene-tagged antibody (**2-7c**) and the tetrazine-modified MMAE (**2-9**) was relatively slow, which required 16 h to go to completion to give the conjugate (**2-10c**) (Scheme 4). The final products (**2-10a**, **2-10b**, and **2-10c**) were purified by protein A affinity chromatography and their identity was confirmed by LC-ESI-MS analysis (Figure 2-7). The ESI-MS analysis of the intact ADCs (Figures 2-7 A-C) showed that the observed deconvolution data matched well with the expected mass of the intact ADC and that each ADC carried 4 payloads, giving a drug-to-antibody ratio (DAR) of 4. The ESI-MS analysis of the monomeric Fc domain released by IdeS treatment of the intact ADCs (Figures 2-7 D-F) further confirmed that the MMAE was site-specifically attached to the Fc domain of the antibody. The original data on the ESI-MS analysis of the intact antibodies and the Fc domains of ADCs **2-10a, 2-10b** and **2-10c** were shown in Figures 2-8 and 2-9. It should be mentioned that a minor peak corresponding to a loss of 762 Da from the intact antibody or the Fc domain was observed in the ESI-MS spectra (Figure 2-7). This species was presumably generated by fragmentation at the aminobenzyl carbamate moiety in the linker of the ADCs. Similar fragments have been

observed in the ESI-MS analysis of ADCs with the same moiety in the linkers in a previous report [50].

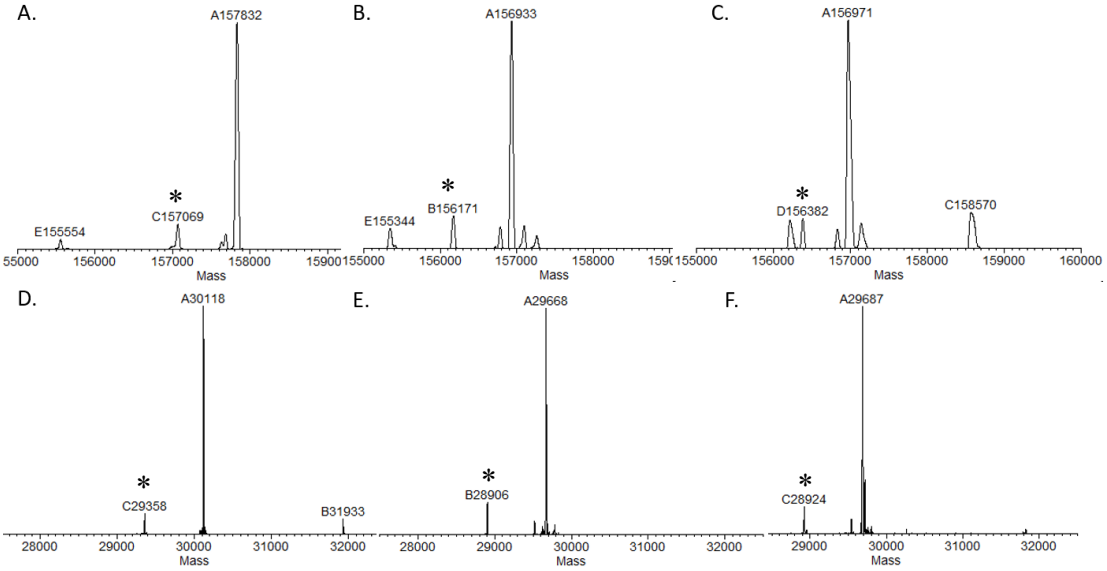

Figure 2-7. LC-ESI-MS analysis of the intact antibody-drug conjugates (**2-10a**, **2-10b** and **2-10c**) and the Fc domains released by IdeS treatment. A) the deconvoluted mass of intact ADC **2-10a**; B) the the deconvoluted mass of intact ADC **2-10b**; C) the deconvoluted mass of intact ADC **2-10c**. D) the deconvoluted mass of the Fc domain of **2-10a**; E) the deconvoluted mass of the Fc domain of **2-10b**; F) the deconvoluted mass of the Fc domain of **2-10c**. Asterisked peaks indicate the ion fragments derived from the intact antibody or its Fc domain, which corresponds to a loss of 762 Da.

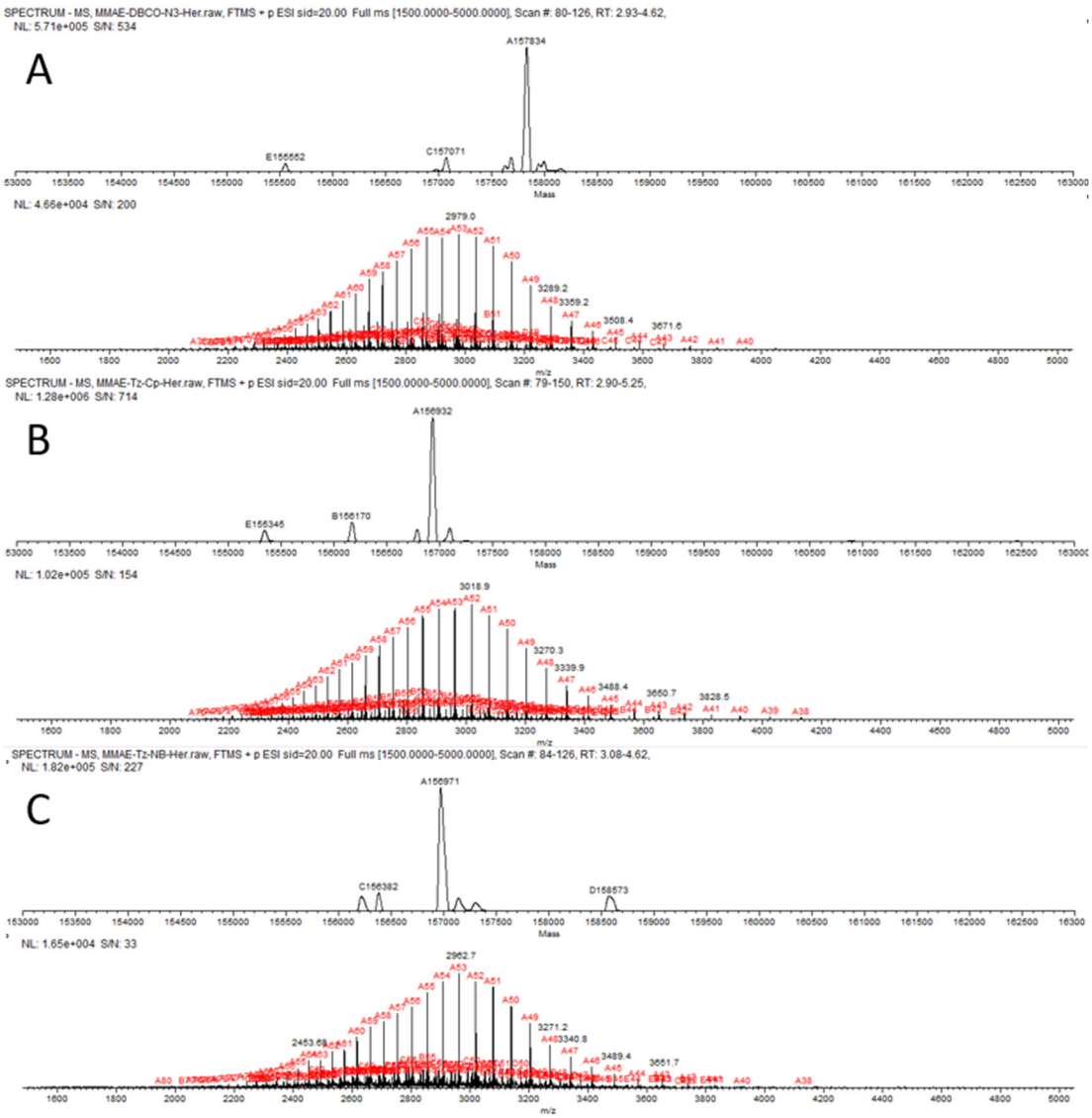

Figure 2-8. LC-ESI-MS analysis of the intact antibody conjugates A) deconvoluted mass and raw data of intact antibody **2-10a**; B) deconvoluted mass and raw data of intact antibody **2-10b**; C) deconvoluted mass and raw data of intact antibody **2-10c**.

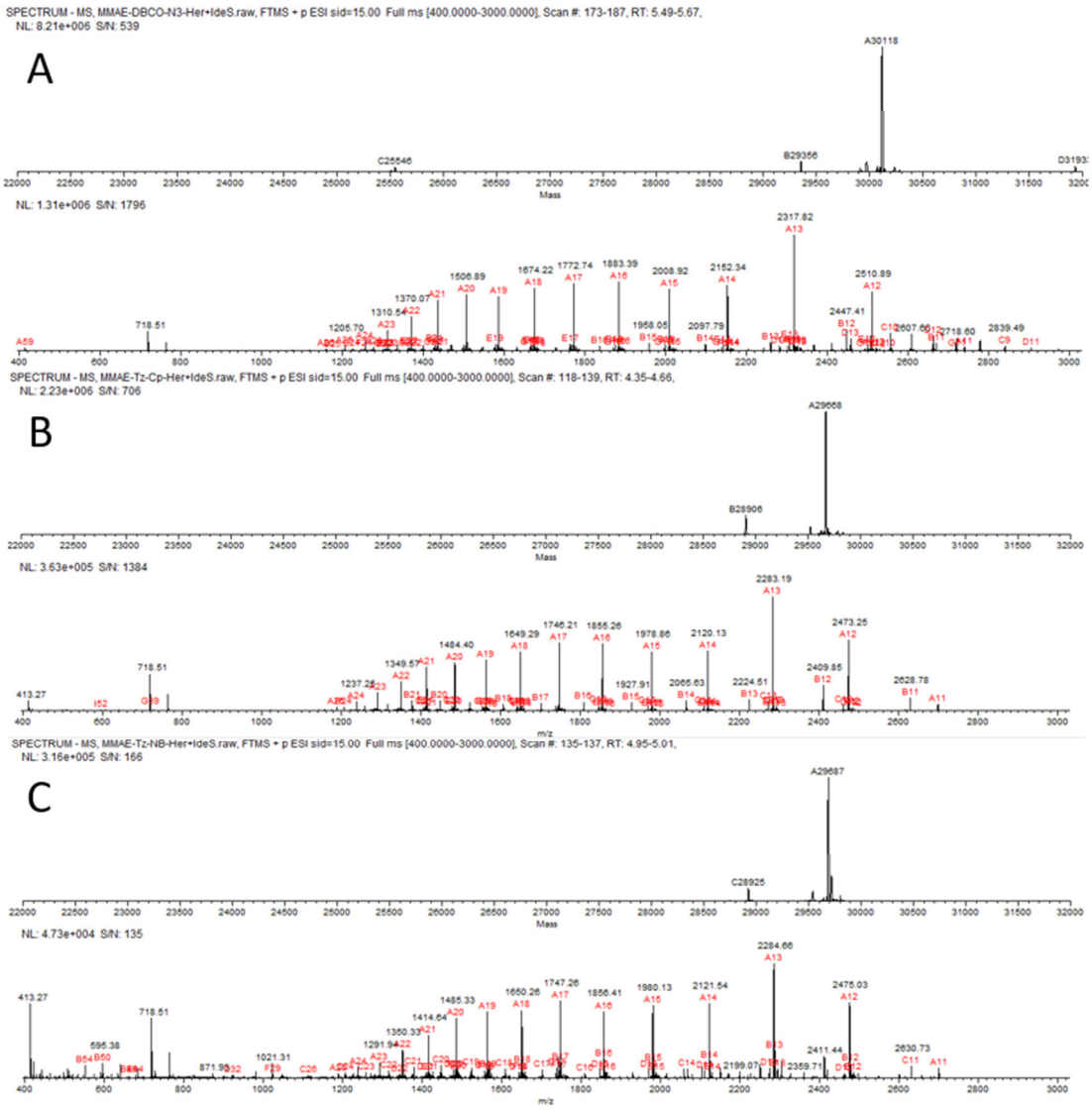

Figure 2-9. LC-ESI-MS analysis of the Fc domains released by IdeS treatment of the antibody-drug conjugates A) deconvoluted mass and raw data for Fc domains of **2-10a**; B) deconvoluted mass and raw data for Fc domains of **2-10b**; C) deconvoluted mass and raw data for Fc domains of **2-10c**.

Finally, ESI-MS analysis of the protein backbone of the intact antibody and the Fc domain after PNGase F treatment to remove the modified Fc *N*-glycans further confirmed that there were no additional modifications of the protein backbone except the MMAE attachment to the Fc glycans (Figures 2-10, Supporting Information). To verify if there was any aggregation of the synthetic antibody-drug conjugates, we

performed size exclusion chromatography of the three ADCs (**2-10a, 2-10b, and 2-10c**). We found that ADC **2-10a** did not have any aggregation, while ADCs **2-10b** and **2-10c** generated by the tetrazine-based Click reaction showed about 8% aggregation product (Figure 2-11), indicating some difference in the stability of the respective conjugates. We also examined the serum stability of the three ADCs (**2-10a, 2-10b, and 2-10c**) using rat serum as a model system. We found that after incubation of the synthetic ADCs with the rat serum at 37 ^{o}C for 3 days, there was no payload coming off from the antibody conjugates as indicated by the LC-ESI-MS analysis of the antibodies and the conjugates (Figure 2-12). These results suggested that the antibody-drug conjugates constructed by the present method had a reasonable serum stability.

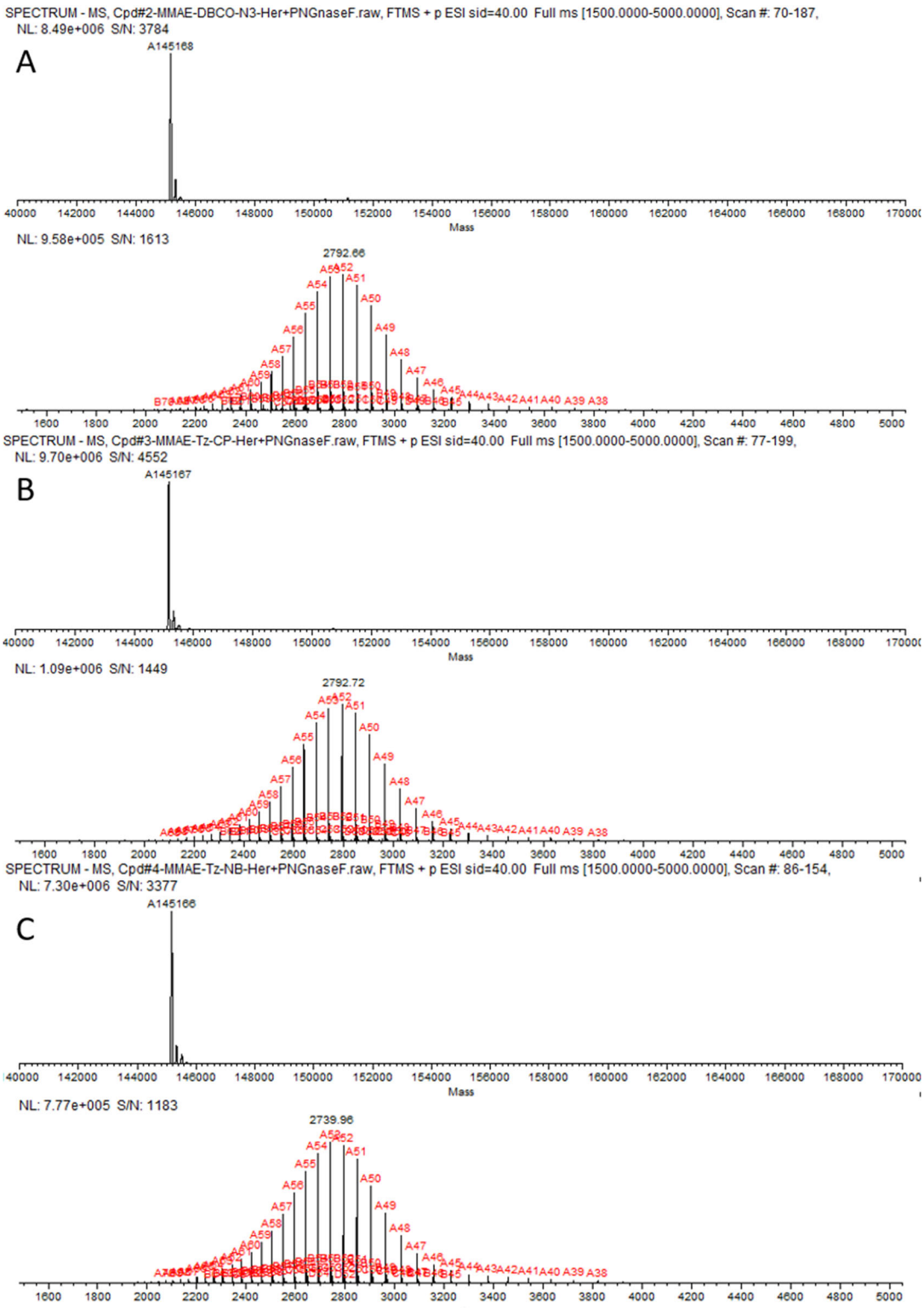

Figure 2-10. LC-ESI-MS analysis of the intact antibody backbones after PNGase F treatment of the antibody-drug conjugates. A) deconvoluted mass and raw data of intact antibody **2-10a**; B) deconvoluted mass and raw data of intact antibody **2-10b**; C) deconvoluted mass and raw data of intact antibody **2-10c**.

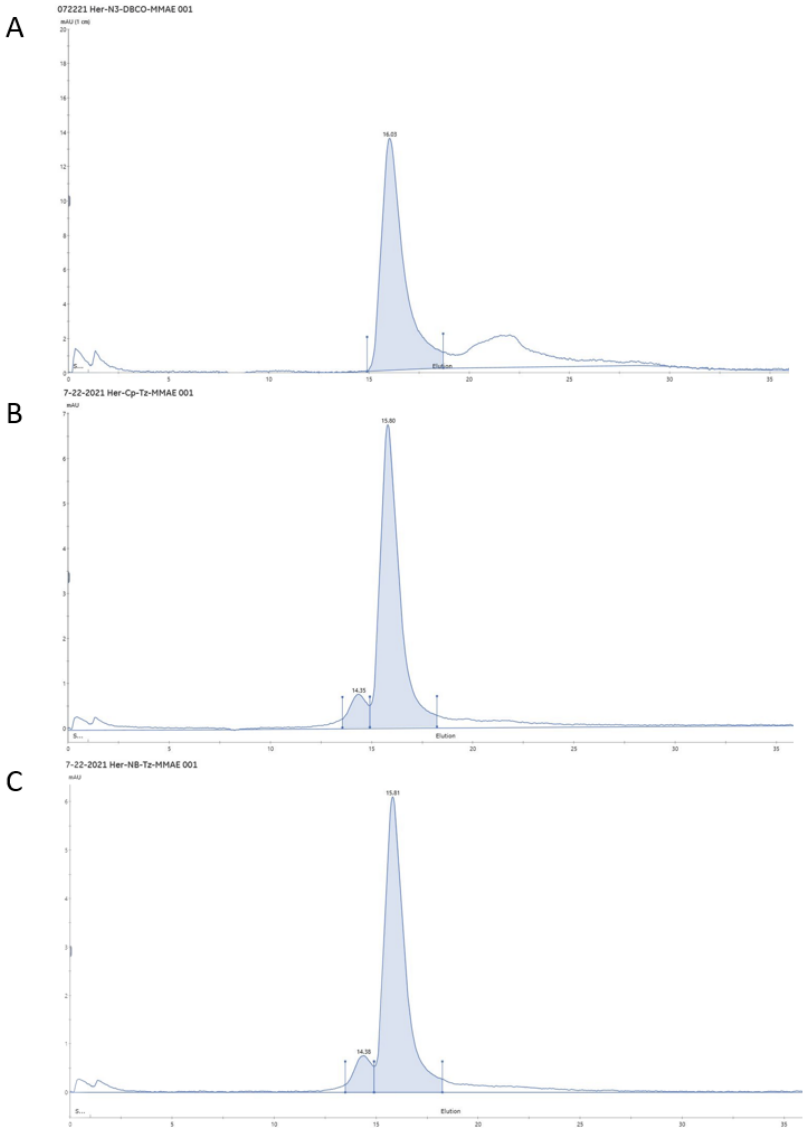

Figure 2-11. Size exclusion chromatography for the ADCs (**2-10a**, **2-10b** and **2-10c**). A) size exclusion chromatography for **2-10a**; B) size exclusion chromatography for **2-10b**; C) size exclusion chromatography for **2-10c**.

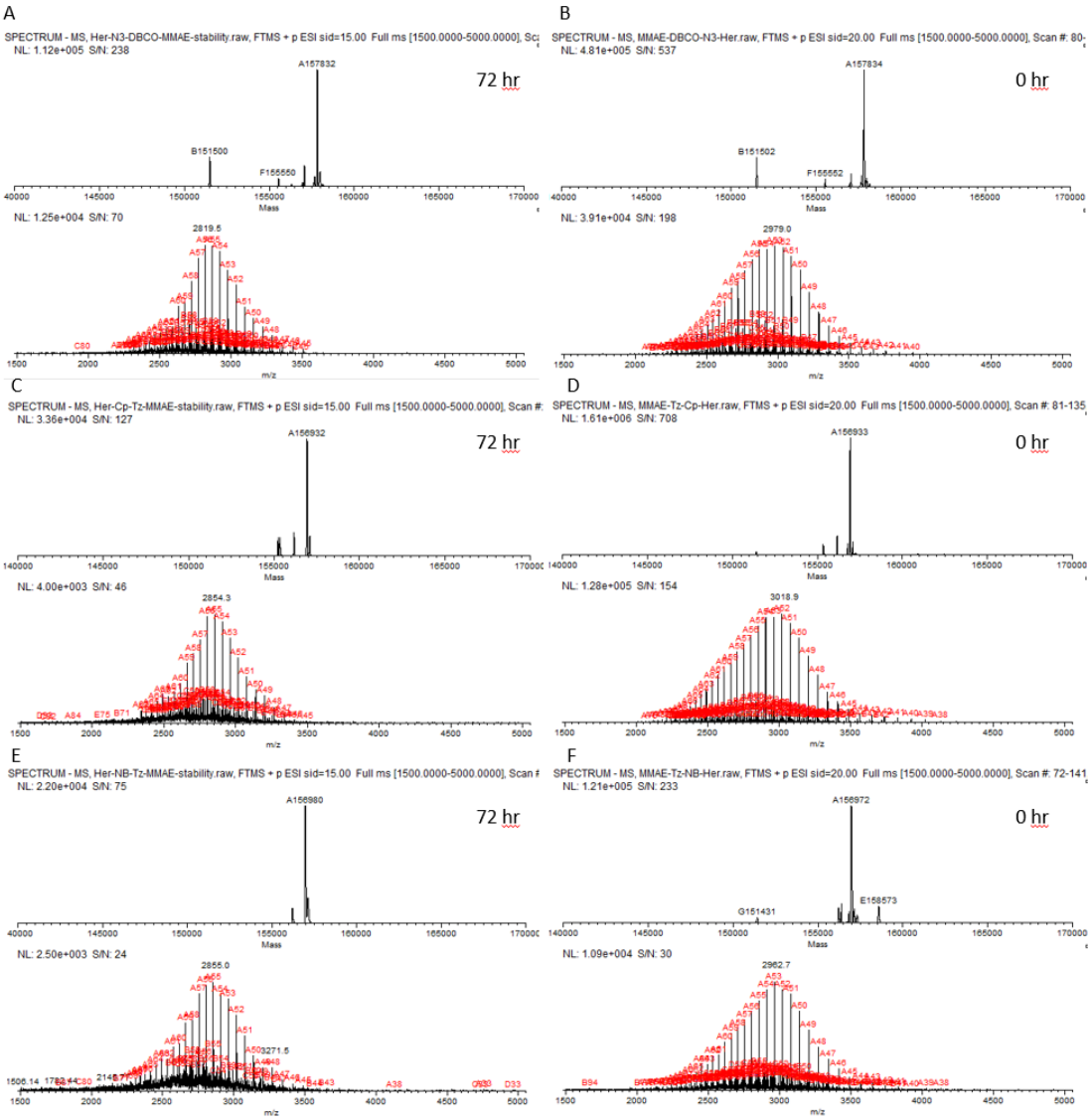

Figure 2-12. Serum stability results. A) the deconvoluted mass of **2-10a** incubated in rat serum for 72 hours; B) the deconvoluted mass of **2-10a** at 0 hour; C) the deconvoluted mass of **2-10b** incubated in rat serum for 72 hours; D) the deconvoluted mass of **2-10b** at 0 hour; E) the deconvoluted mass of **2-10c** incubated in rat serum for 72 hours; F) the deconvoluted mass of **2-10c** at 0 hour.

Evaluation of the in vitro cytotoxicity of the ADCs.

To compare the potency of the ADCs synthesized with different Click reactions, we studied the *in vitro* cytotoxicity of ADCs with SK-BR-3 (high HER-2 expressing) and T47D (low HER-2 expressing) cells. For the SK-BR-3 cell line, our ADCs

demonstrated a dose-dependent killing of the antigen-positive cells (Figure 2-13A). Meanwhile, the low HER-2 expressing T47D cells were insensitive to the ADCs up to 1 μg/mL (Figure 2-13B). These results suggest the antibody retains its high specificity on HER2 after all the modifications. The IC_{50} of the antibody-drug conjugates (**2-10a**, **2-10b**, and **2-10c**) against SK-BR-3 cells were measured as 13.9 ng/mL, 15.4 ng/mL, and 21.8 ng/mL, respectively, (corresponding to 88 pM, 162 pM, and 138 pM, respectively). The data indicated that the azide-alkyne MMAE conjugate (**2-10a**) was a slightly better than the cyclopropene- or norbornene-tetrazine MMAE conjugates (**2-10b** and **2-10c**) for cell killing. However, the IC_{50} data (100-200 pM) are quite comparable to those MMAE-based ADCs with similar DARs [60, 74, 77, 79]. The results from the present side-by-side comparison study suggest that the ADCs generated by the two different types of Click reactions (SPAAC vs. iEDDA reactions) are equally efficient for target cell killing. Taken together, the results suggest that the one-pot synthesis of functionalized glycan oxazolines coupled with the efficient Endo-S2 D184M-catalyzed Fc glycan remodeling and Click drug conjugation provides a general and efficient approach to producing structurally well-defined, homogeneous antibody-drug conjugates with high potency.

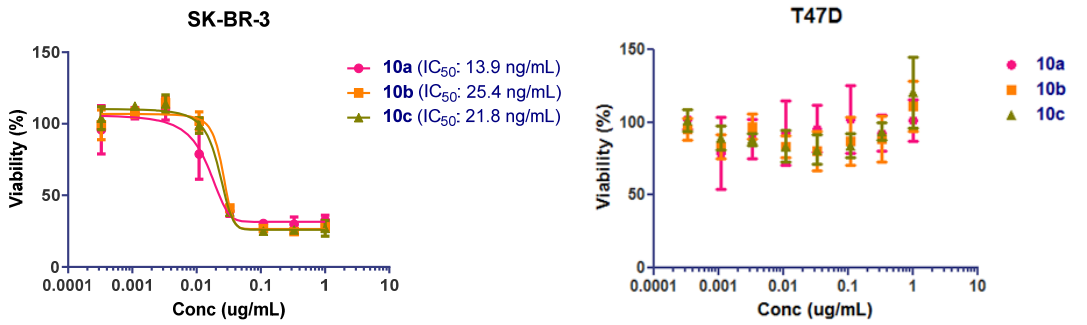

Figure 2-13. Cytotoxicity assays of the antibody-drug conjugates with the SK-BR-3 (HER2 overexpression) and the T47D (HER2 low expression) cancer cell lines. All assays were performed in triplicate.

2.3 Conclusion

An efficient, Fc glycan-mediated chemoenzymatic method for site-specific antibody-drug conjugation is described. This improved approach is enabled by the optimized synthesis of selectively modified glycan oxazolines from free sialoglycans in a one-pot manner and the use of the highly efficient endoglycosidase mutant (Endo-S2 D184M) for transferring the tagged glycans to provide the selectively tagged antibodies ready for Click drug conjugation. The enhanced enzymatic activity of the Endo-S2 D184M mutant over the previously used Endo-S D233Q mutant for transferring the selectively modified glycans permits the use of much less amount of glycan oxazolines with much shorter reaction time to complete the enzymatic reaction, thus minimizing the potential non-enzymatic side reactions. The homogeneous ADCs constructed by the present method showed excellent serum stability and demonstrated potent and selective cytotoxicity against HER2-overexpressing cancer cells. This improved method is also quite flexible for introducing different tags into an antibody, allowing site-specific payload conjugation with different Click reactions to construct

homogeneous antibody-drug conjugates. This research was published in *Bioconjugate Chemistry* in 2021.[82]

2.4 Experimental Procedures

Materials and Methods.

Chemicals, reagents, and solvents were purchased from Sigma−Aldrich and/or TCI, and used as received unless otherwise specified. Monoclonal antibody Hercptin was purchased from Premium Health Services Inc. (Columbia, MD). All moisture sensitive reactions were carried out under argon atmosphere, using standard Schlenk techniques. All anhydrous solvents were prepared and stored according to standard procedures. Thin-layer chromatography was performed on silica gel 60-F_{254} on glass plates (Merck) and revealed with *p*-anisaldehyde stain. Silica gel (200−425 mesh) used in flash chromatography for large-scale reactions was purchased from Sigma-Aldrich. Columns for flash chromatography for small-scale reactions were performed on Isolera One system with ZIP KP-Sil columns (Biotage) with elution condition specified for each target compound. Solvent gradients were given refer to stepped gradients and concentrations are reported as % v/v. Preparative HPLC was performed with Waters 1525 Binary HPLC pump coupled with 2489 UV/Vis Detector under UV 214 nm and 280 nm with a Waters Symmetry C18 column (7 μm, 19 × 300 mm) using water containing 0.1% trifluoracetic acid as phase A, MeCN containing 0.1% trifluoracetic acid as phase B. Semi-preparative HPLC for the toxic payloads was performed on the same instrument with an Aglient Eclipse XDB-C18 column (5 μm, 9.4× 250 mm) using water containing 0.1% formic acid as phase A, MeCN containing 0.1% formic acid as phase B .

Purification of sialoglycans and proteins using AKTA prime plus FPLC system.

The FPLC system (GE Healthcare) was used for purification of the SCT, mono-functionalized SCT equipped with HiTrap Q XL 2 × 5 mL (GE Heatlthcare), antibodies with HiTrap Protein A HP 1 mL (GE Heatlthcare), and Endo-S2 WT with Histrap HP histindine-tagged protein purification columns 5 mL (GE Healthcare). Concentration of antibodies and enzymes was determined by NanoDrap 200c (Thermo Scientific).

LC-ESI-MS analysis of glycans and MMAE derivatives

LC-MS for glycans, glycopeptides and payload derivatives were performed on HPLC-SQ2 detector (Waters) with a Waters XBridge C18 column (3.5 μm, 2.1× 50 mm) using water containing 0.1% formic acid as phase A, MeCN containing 0.1% formic acid as phase B. Analytical HPLC for modified *N*-glycans was performed on the same instrument equipped with a Waters XBridge BEH130 C18 column (3.5 μm, 4.6 × 250 mm) for modified glycans with a linear gradient of acetonitrile (0−60%, v/v) with water containing FA (0.1%) over 30 min at a flow rate of 0.5 mL/min under UV 214 nm. The analytical HPLC for payload derivatives was analyzed with an Aglient Eclipse SDB-C18 column (5 μm, 3.0× 250 mm) under UV 214 nm and 280 nm with methods specialized for each compound.

LC-ESI-MS analysis of intact antibody derivatives.

LC-ESI-MS analysis of intact tagged antibodies and antibody-drug conjugates was performed with Exactive Plus Orbitrap Mass Spectrometer (Thermo Scientific) equipped with a Waters XBridge BEH300 C-4 column (3.5 μm, 2.1 × 50 mm) with gradient elution of water containing 0.1% formic acid as phase A, MeCN containing 0.1% formic acid as phase B. Mass spectra were deconvoluted using MagTran (ver 1.03 b2). For the antibody Fc analysis, the antibody samples in PBS were incubated with Ide-S at 37 °C for 2 hours. The samples were analyzed by with Exactive Plus Orbitrap Mass Spectrometer (Thermo Scientific) equipped with an Agilent Poroshell 300SB C8 column (5 μm, 1.0 × 75 mm) with gradient elution of water containing 0.1% formic acid as phase A, MeCN containing 0.1% formic acid as phase B. Mass spectra were deconvoluted using MagTran (ver 1.03 b2).

LC-ESI-MS analysis of Fc domains released by IdeS treatment.

The antibody samples in PBS were incubated with IdeS at 37 °C for 2 h. The samples were analyzed by with Exactive Plus Orbitrap Mass Spectrometer (Thermo Scientific) equipped with an Agilent Poroshell 300SB C8 column (5 μm, 1.0 × 75 mm) with gradient elution of water containing 0.1% formic acid as phase A, MeCN containing 0.1% formic acid as phase B. Mass spectra were deconvoluted using MagTran (ver 1.03 b2).

NMR analysis.

^{1}H, ^{13}C, and $^{1}H-^{1}H$ COSY NMR spectra were recorded on 400 MHz or 600 MHz spectrometer (Bruker) with $CDCl_3$, MeOD-d_4, D_2O or DMSO-d_6 as the solvent (solvent residue peak 7.26, 3.31, 4.79, 2.50 ppm). All ^{13}C NMR spectra were performed with proton decoupling, and all chemical shifts are reported in part per million (ppm) and referenced to residual solvent. ^{1}H-NMR chemical shifts were recorded relative to the solvent residual peak ($CDCl_3$ at 7.26 ppm, MeOD-d_4 at 3.31ppm, D_2O at 4.79 ppm, DMSO-d_6 at 2.50 ppm). ^{13}C NMR chemical shifts are reported relative to the solvent residual peak ($CDCl_3$ at 77.00 ppm, MeOD-d_4 at 49.00 ppm, DMSO-d_6 at 39.51 ppm). The number of protons (n) corresponding to a resonance signal was indicated by nH and spin-spin coupling constants (J value) recorded in Hz.

Preparation of free sialoglycan (SCT) from the sialoglycopeptide (SGP) isolated from chicken egg yolks.

Isolation of the sialoglycopeptide (SGP) from chicken egg yolks. SGP was isolated from chicken egg yolk powder according to the previously reported procedure.[83] ESI-MS: $[M + 2H]^{2+}$ calcd. for $C_{112}H_{191}N_{15}O_{70}^{2+}$, 1433.59 (100%); found (*m/z*), 1433.81.

Enzymatic cleavage of SGP to produce the sialoglycan (2-1). SGP (150 mg) was dissolved in 3 mL pH 7.4 PBS buffer, 500 μg of Endo-S2 wild type was added to

the solution (substrate to enzyme ratio, 300 to 1). The reaction mixture was incubated at 37 °C for 16 hours, the digestion can be checked with LC-SQ2. After the digestion was complete, the reaction mixture was purified by G-15 column to remove salts and most of the peptide. The elutes were concentrated and loaded to a HiTrap Q XL 2 × 5 mL column. The column was eluted with a linear gradient of 200 mM NaCl (0−40%, v/v) with water over 60 min. The fractions were checked with *p*-anisaldehyde stain, the glycan containing fractions were collect and lyophilized. The solid was dissolved in 1 mL water and desalt with G-10 column. The fractions containing the free glycans were pooled and lyophilized to give the *N*-glycan (**2-1**) as a white powder (86 mg, 81 % yield). ESI-MS: $[M + 2H]^{2+}$ calcd for $C_{76}H_{127}N_5O_{57}^{2+}$, 1010.86; found (*m/z*), 1011.03,.

Endo-S2 overexpression, purification and immobilization

Endo-S2 WT overexpression. Endo-S2 with His10-tag was overexpressed and purified following the previously reported procedure. [84] From 800 mL of cell culture, 32 mg of the Endo-S2 WT was isolated. The purity was checked by SDS-PAGE. The activity was tested with SGP cleavage reaction.

Immobilization of Endo-S2 WT on agarose resin. The immobilization was carried out following the manufacturer's instructions. A mixture of NHS-activated agarose resin (150 mg) and Endo-S2 WT (2.5 mL, 14 mg) was incubated at r.t. in a column for 2 h. Then the column was washed and the flow-through was collected to measure the free enzyme that was not immobilized, which was used to determine the

loading ratio with Bradford protein assay. The resin was washed with 3 mL PBS buffer twice. And then 3 mL of the Quenching Buffer (1 M Tris) was added. The mixture was mixed end-over-end for 20 min at room temperature. The resin was washed with 3 mL PBS buffer, and stored in pH 7.4 PBS buffer with 0.5% NaN_3 at 4 °C. About 7 mg of the enzyme was immobilized, and the suspension was aliquoted into 7 tubes. The activity of the immobilized enzyme was determined by an enzymatic deglycosylation reaction of IVIG, with 100:1 substrate to enzyme ratio.

Synthesis of the functionalized SCT and cytotoxic payloads

Synthesis of alkene-based linkers

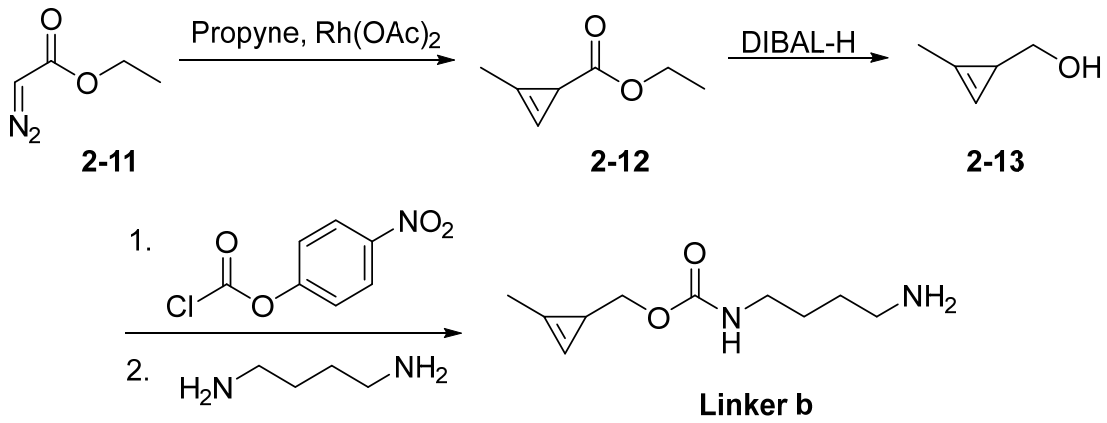

Scheme 2-5. Synthesis of the cyclopropene-functionalized amine.

Synthesis of ethyl-2-methylcycloprop-2-ene-1-carboxylate (2-12) [85]. A 100 mL 2-neck round bottom flask with $Rh(OAc)_2$ (442 mg, 1.00 mmol, 5 mol %) powder

was fitted with a dry ice condenser and exchanged to argon. Dry CH_2Cl_2 was added to the flask, then the cold trap was cooled by dry ice/acetone. Propyne (about 10 mL) was condensed into the flask. The round bottom flask was then lowered into a water bath (20 °C). Ethyl diazoactate (2.4 mL, 23 mmol) was added to the mixture dropwise over 1 hour with rapid stirring. The reaction was stirred at r.t. for another hour, and TLC analysis suggested the reaction was completed. The product was purified by flash silica gel column chromatography by pentane with a linear gradient of diethyl ether (0-15%, v/v) over 15 column volumes (CV). After careful evaporation, compound **2-12** was isolated as a colorless oil (2.3 g, 79%). ^{1}H NMR ($CDCl_3$, 600 MHz) δ = 1.24 (3H, t, J = 7.1 Hz, CH_2CH_3), 2.11 (1H, s, C*H*CO), 2.16 (3H, s, CH_3C=), 4.12–4.14 (2H, m, CH_2CH_3), 6.34 (1H, d, J = 0.6 Hz, C*H*=C). ^{13}C NMR (150 MHz, $CDCl_3$) δ = 9.98, 13.88, 19.58, 59.66, 94.22, 111.16, 175.97. DART-TOF: $[M + H]^+$ calcd for $C_7H_{11}O_2^+$, 127.08; found (*m/z*), 127.05.

Synthesis of (2-methylcycloprop-2-en-1-yl) methanol (2-13). In a 250 mL 2-neck round bottom flask, **2-12** (3.8 g, 30 mmol, 1 eq) was dissolved in 40 mL CH_2Cl_2 under argon. With fast stirring, DIBAL-H (45 mL of 1M solution in CH_2Cl_2, 45 mmol, 1.5 eq) was added dropwise to the above solution over 30 min at -10 °C. The mixture was stirred for another 30 min at -10 °C when the TLC showed the reaction was complete. Then the reaction mixture was quenched carefully by H_2O (2 mL), NaOH (2 mL, 1 M solution in H_2O), and H_2O (4.6 mL). The mixture was stirred for a further 2 hours at room temperature before it was diluted with 400 mL CH_2Cl_2 and dried over $MgSO_4$. The organic solution was carefully concentrated to 10 mL then purified by

flash silica gel column chromatography with pentane with a linear gradient of diethyl ether (0-40%, v/v) over 15 CV. The desired cyclopropene alcohol **2-13** was isolated as a colorless oil (1.5 g, 56%). ^{1}H NMR ($CDCl_3$, 600 MHz) δ = 1.67 (1H, td, C*H*CO), 2.15 (3H, s, C*H*$_3$C=), 3.47–3.58 (2H, m, C*H*$_2$CH$_3$), 6.63 (1H, s, C*H*=C). DART-TOF: $[M + H]^+$ calcd for $C_5H_9O^+$, 85.06; found (*m/z*), 85.02.

Synthesis of (2-methylcycloprop-2-en-1-yl)methyl (4-aminobutyl)carbamate (Linker b). To the solution of **2-13 (**1.50 g, 17.8 mmol, 1 eq) in 40 mL CH_2Cl_2, DIPEA (13.8 g, 110 mmol, 6 eq) was added, followed by the addition of 4-nitrophenyl chloroformate (10.7 g, 53.1 mmol, 3 eq) at room temperature. After the reaction was stirred for 8 hours, TLC shows the complete consumption of **2-3**. The mixture was added dropwise to a solution of 1,4-diaminobutane (4.7 g, 54 mmol, 3 eq) in 100 mL CH_2Cl_2 over 30 min at 0 °C. The reaction was completed after stirred at room temperature for 6 hours. After TLC confirmed the complete consumption of the starting material, the reaction mixture was washed with brine (50 mL) three times. Then it was concentrated purified by flash silica gel column chromatography by ethyl acetate and methanol (6:1 – 3:1, v/v, with 1% TEA). The product **Linker b** was isolated as a slightly yellow oil (1.5 g, 42% over two steps). ^{1}H NMR (MeOD-*d*$_4$, 600 MHz) δ = 1.51-1.53 (4H, m, NH_2CH_2C*H*$_2$C*H*$_2$), 1.63 (1H, td, C*H*CH_2O), 2.15 (3H, s, C*H*$_3$C=), 2.68 (2H, t, *J* = 6.6 Hz, NH_2C*H*$_2$), 3.12 (2H, t, *J* = 6.6 Hz, CPNHC*H*$_2$), 3.80–3.97 (2H, m, C*H*$_2$CH$_3$), 6.65 (1H, s, C*H*=C). ^{13}C NMR (150 MHz, MeOD-*d*$_4$) δ = 11.59, 18.36, 28.32, 30.53, 41.44, 42.07, 73.02, 102.90, 122.24, 159.44. HR-ESI-MS: $[M + H]^+$ calcd for $C_{10}H_{19}N_2O_2^+$, 199.1441; found (*m/z*), 199.1436 $[M + H]^+$.

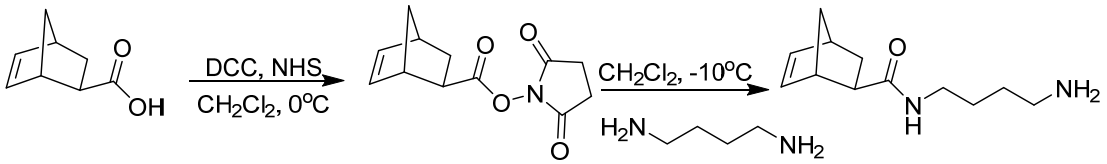

Scheme 2-6. Synthesis of the norbornene functionalized amine.

Synthesis of norbornenyl *N*-hydroxysuccinimidyl ester (2-15). To the solution of **2-14 (**1.26 g, 10.1 mmol, 1 eq) and *N*-hydroxysuccinimide (1.15 g, 10.0 mmol, 1.1 eq) in 20 mL CH_2Cl_2, EDC (2.10 g, 10.9 mmol, 1.2 eq) was added at 0 °C. The reaction was stirred at room temperature for 3 hours before TLC confirmed its completion. The reaction mixture was washed with brine (50 mL) three times and dried over $MgSO_4$. Then the product was concentrated and used without further purification. The ^{1}H NMR spectra agreed with the reported data. ^{1}H NMR ($CDCl_3$, 400 MHz) δ = 1.43-1.45 (2H, m), 1.52-1.55 (1H, m), 2.05 (1H, m), 2.49 (1H, m,), 2.83 (4H, s, COC*H*$_2$), 3.00 (1H, s, =CHC*H*), 3.12 (1H, s, =CHC*H*), 3.80–3.97 (2H, m, C*H*$_2$CH$_3$), 6.12-6.21 (2H, m, C*H*=C).

Synthesis of norbornenyl-amine (Linker c). The solution of **2-15** (1 eq) in CH_2Cl_2 (40 mL) was added dropwise to a solution of 1,4-diaminobutane (2.4 g, 27 mmol, 3 eq) and DIPEA (3.5 g, 27 mmol, 3 eq) over 30 min at 0 °C. The reaction was completed after stirred at room temperature for 6 hours. After TLC confirmed the complete consumption of the starting material, the reaction mixture was washed with brine (50 mL) three times. Then it was concentrated purified by flash silica gel column chromatography by ethyl acetate and methanol (6:1 – 3:1, v/v, with 1% TEA). The

product **Linker c** was isolated as a slightly yellow oil (835 mg, 44% over two steps). ^{1}H NMR (MeOD-d_4, 600 MHz) δ = 1.28 (2H, m), 1.55 (4H, m, $NH_2CH_2CH_2CH_2$), 1.69 (1H, m), 1.84 (1H, m), 2.10 (1H, m), 2.76 (2H, t, J = 6.6 Hz, NH_2CH_2), 2.78 (1H, s, =CHC*H*), 2.84 (1H, s, =CHC*H*), 3.19 (2H, t, NBNHCH_2), 6.14 (2H, s, C*H*=C). ^{13}C NMR (150 MHz, MeOD-d_4) δ = 27.77, 29.09, 31.23, 39.99, 41.48, 42.76, 45.24, 47.08, 137.31, 139.00, 178.45. HR-ESI-MS: $[M + H]^+$ calcd for $C_{10}H_{19}N_2O_2^+$, 199.1441; found (*m/z*), 199.1436.

Synthesis of the azide-, cyclopropene- and norbornene-modified *N*-glycans and *N*-glycan oxazolines

Synthesis of the Di-N_3-SCT-DMT (2-2). To a mixture of **2-1** (10 mg, 20 mg/mL) and N3-linker-NH2 (30 mg, 20 eq), DMTMM (55 mg, 40 eq) was added into a buffer (PBS, pH7.4). The reaction mixture was incubated at 37 ºC for 16 h and monitored with LC-MS. After the completion of reaction, the product was purified with size-exclusion column (G15, Bio-Rad) to give white power (12.6 mg, 93%). ^{1}H NMR (D_2O, 400 MHz) δ = 1.77 (2H, m, H3f$_{ax}$, H3f'$_{ax}$), 1.92, 1.94, 1.95 (15H, 3s, 5 × CH_3), 2.602 (2H, dd, H3f$_{eq}$, H3f'$_{eq}$), 3.37–3.47 (12H, m, H4c, H4c', H2e, H2e', 2 × CH_2NH, 2 × CH_2N_3), 3.48–3.63 (59H, m, H4a, H5a(β), H5b, H5c', H6c, H6c', H4d, H4d', H5d, H5d', H3e, H3e', H6e, H6e', H4f, H4f', H7f, H7f', H9f, H9f', 10 × CH_2OCH_2), 3.61–3.75 (10H, m, H3a, H6a, H3b, H5c, H2d, H2d', H3d, H3d', H6f, H6f'), 3.76–3.89 (25H, m, H2a, H6'a, H4b, H6b, H6'b, H3c, H3c', H6'c, H6'c', H6d, H6d', H6'd, H6'd', H4e, H4e', H5e, H5e', H6'e, H6'e', H5f, H5f', H8f, H8f', H9'f, H9'f'), 4.03

(1H, br s, H2c'), 4.11 (1H, br s, H2c), 3.90 (6H, s, 2 × OCH_3 on DMT), 4.18 (1H, br s, H2b), 4.34 (2H, d, $J_{1,2}$ = 8.0 Hz, H1e, H1e'), 4.50 (2H, br s, H1d, H1d'),, 4.70 (1H, d, H1b), 4.86 (1H, s, H1c'), 5.05 (1H, s, H1c), 6.41 (1H, d, $J_{1,2}$ = 3.2 Hz, H1a(α)). ^{13}C NMR (100 MHz, D_2O) δ =21.62, 21.98, 37.77, 38.30, 46.22, 49.71, 49.73, 51.26, 54.17, 55.42, 59.74, 61.19, 62.21, 62.59, 66.56, 67.38, 67.90, 68.05, 68.70, 68.77, 69.11, 69.15, 70.23, 70.64, 72.03, 73.07, 73.94, 80.03, 80.37, 98.95, 103.21, 168.66, 172.86, 174.25, 174.56. ESI-MS: $[M + 2H]^{2+}$ calcd for $C_{105}H_{180}N_{16}O_{67}^{2+}$, 1369.0596; found (*m/z*), 1369.0471.

Synthesis of the Di-N_3-SCT (2-3). SCT **2-1** (58.2 mg, 28.8 μmol, 1 eq) was dissolved in 200 μL 50mM Phosphate Buffer in a 1 mL glass vial with a stirring bar. N_3-PEG_5-NH_2 (**Linker a**, 26.4 mg, 86.4 μmol, 3 eq) was added to the solution, and the pH was adjusted to 5 by adding 2 M HCl solution. DMTMM (39.7 mg, 144 μmol, 5 eq) was added. The reaction was stirred at 50 °C for 3 hours. Another portion of DMTMM (39.7 mg, 144 μmol, 5 eq) was added, and the reaction was heated for another 3 hours. HPLC was used to confirm the completion of the reaction. If there is still some DMT remains, TFA solution was added, the solution was stirred at room temperature for 3 hours. Once its completed, the mixture was centrifuged at 14000 rpm for 5 min, the supernatant was purified by G-15 size exclusion column. The glycan containing fractions were collected and lyophilized to afford **2-2** (70.6 mg, 92 %). ^1H NMR (D_2O, 600 MHz) δ = 1.76 (2H, dd, J = 12.3 Hz, $H3f_{ax}$, $H3f'_{ax}$), 1.90, 1.95, 1.97 (15H, 3s, 5 × CH_3), 2.62 (2H, t, J = 12.7 Hz, $H3f_{eq}$, $H3f'_{eq}$), 3.39–3.47 (12H, m, H4c, H4c', H2e, H2e', 2 × CH_2NH, 2 × CH_2N_3), 3.48–3.63 (59H, m, H4a, H5a(β), H5b, H5c', H6c,

H6c', H4d, H4d', H5d, H5d', H3e, H3e', H6e, H6e', H4f, H4f', H7f, H7f', H9f, H9f', 10 × CH_2OCH_2), 3.61–3.75 (10H, m, H3a, H6a, H3b, H5c, H2d, H2d', H3d, H3d', H6f, H6f'), 3.76–3.93 (25H, m, H2a, H6'a, H4b, H6b, H6'b, H3c, H3c', H6'c, H6'c', H6d, H6d', H6'd, H6'd', H4e, H4e', H5e, H5e', H6'e, H6'e', H5f, H5f', H8f, H8f', H9'f, H9'f'), 4.03 (1H, br s, H2c'), 4.11 (1H, br s, H2c), 4.18 (1H, br s, H2b), 4.36 (2H, d, $J_{1,2}$ = 7.8 Hz, H1e, H1e'), 4.51 (2H, d, $J_{1,2}$ = 6.3 Hz, H1d, H1d'), 4.53 (0.3H, d, H1a(β)), 4.70 (1H, d, H1b), 4.86 (1H, s, H1c'), 5.05 (1H, s, H1c), 5.13 (0.7H, d, $J_{1,2}$ = 2.7 Hz, H1a(α)). ^{13}C NMR (150 MHz, D_2O) δ = 21.85, 21.97, 37.76, 38.29, 49.71, 51.25, 53.13, 54.17, 55.61, 59.60, 59.72, 59.92, 61.18, 61.25, 62.20, 62.59, 65.21, 65.28, 65.50, 66.54, 66.85, 66.90, 67.37, 67.88, 68.03, 68.67, 68.76, 69.08, 69.10, 69.14, 69.45, 69.80, 70.21, 70.63, 71.25, 71.61, 71.68,71.90, 72.01, 72.42, 73.06, 73.92, 74.00, 75.81, 75.98, 79.39, 79.76, 80.03, 80.29, 80.37, 90.04, 94.46, 96.53, 98.84, 98.92, 98.95, 99.09, 99.99, 103.19, 168.63, 174.05, 174,15, 174.30, 174.53. ESI-MS: $[M + 2H]^{2+}$ calcd for $C_{100}H_{175}N_{13}O_{65}^{2+}$, 1299.5405; found (*m/z*), 1299.

One-Pot Synthesis of Azide Functionalized SCT-oxazoline (2-4a). SCT **2-1** (60.0 mg, 29.7 μmol, 1 eq) was dissolved in 200 μL 50 mM Phosphate Buffer in a 1 mL glass vial with a stirring bar. N_3-PEG_5-NH_2 (**Linker a**, 27.4 mg, 89.1 μmol, 3 eq) was added to the solution, and the pH was adjusted to 5 by adding 2 M HCl solution. DMTMM (40.1 mg, 148 μmol, dry powder, 5 eq) was added. The reaction was stirred at 50 °C for 3 hours. Another portion of DMTMM (40.1 mg, 148 μmol) was added, and the reaction was heated for another 3 hours. HPLC was used to confirm the completion of the reaction. If there is still some DMT remains on the reducing end,

TFA solution was added, the solution was stirred at room temperature for 3 hours. The reaction mixture was neutralized cooled on ice for 30 min. Triethyalamine (TEA, 212 mg, 2.08 mmol, 70 eq) was added to the solution, followed by 2-chloro-1,3-dimethylimidazolinium chloride (DMC, 150 mg, 0.891 mmol, 30 eq). The mixture was allowed to react on ice for 30 min. The mixture was centrifuged at 14000 rpm for 3 min before it was purified by P-2 size exclusion column with 0.1% TEA as the eluent. The glycan containing fractions were lyophilized with addition of 5 µL 1M NaOH to yield **2-4a** as a white powder (62.6 mg, 82%). ^{1}H NMR (D_2O, 600 MHz) δ = 1.76 (2H, t, J = 12.3 Hz, H3f$_{ax}$, H3f'$_{ax}$), 1.90, 1.95, 1.97 (15H, 3 s, 5 × CH_3), 2.62 (2H, t, J = 12.7 Hz, H3f$_{eq}$, H3f'$_{eq}$), 3.39–3.47 (12H, m, H4c, H4c', H2e, H2e', 2 × CH_2NH, 2 × CH_2N_3), 3.48-3.63 (59H, m, H4a, H5a(β), H5b, H5c', H6c, H6c', H4d, H4d', H5d, H5d', H3e, H3e', H6e, H6e', H4f, H4f', H7f, H7f', H9f, H9f', 10 x CH_2OCH_2), 3.61–3.75 (10H, m, H3a, H6a, H3b, H5c, H2d, H2d', H3d, H3d', H6f, H6f'), 3.76–3.93 (25H, m, H2a, H6'a, H4b, H6b, H6'b, H3c, H3c', H6'c, H6'c', H6d, H6d', H6'd, H6'd', H4e, H4e', H5e, H5e', H6'e, H6'e', H5f, H5f', H8f, H8f', H9'f, H9'f'), 4.03 (1H, br s, H2c'), 4.11 (1H, br s, H2c), 4.18 (1H, br s, H2b), 4.36 (2H, d, $J_{1,2}$ = 7.8 Hz, H1e, H1e'), 4.51 (2H, d, $J_{1,2}$ = 6.3 Hz, H1d, H1d'), 4.70 (1H, s, H1b), 4.86 (1H, s, H1c'), 5.05 (1H, s, H1c), 6.00 (1H, d, $J_{1,2}$ = 7.2 Hz, H1a). ^{13}C NMR (150 MHz, D_2O) δ = 12.53, 21.62, 21.97, 37.77, 38.30, 49.71, 51.26, 54.16, 59.73, 61.19, 62.20, 62.59, 64.78, 65.30, 65.38, 66.53, 66.86, 67.38, 67.88, 68.03, 68.68, 68.76, 68.96, 69.09, 69.14, 69.81, 70.21 70.44, 70.63, 71.62, 71.67, 72.01, 72.42, 73.05, 73.84, 73.93, 75.62, 76.01, 77.46, 80.00, 80.37, 96.13, 98.77, 98.93, 99.01, 99.52, 100.88, 103.20, 168.08, 168.63, 174.17,

174.54. HR-ESI-MS: $[M + 2H]^{2+}$ calcd for $C_{100}H_{173}N_{13}O_{64}^{2+}$, 1290.5352; found (*m/z*), 1290.5300.

One-pot synthesis of cyclopropene functionalized SCT-oxa (2-4b). SCT **2-1** (20.0 mg, 9.9 μmol, 1 eq) was dissolved in 50 μL water and 30 μL THF in a 1 mL glass vial with a stirring bar. CP-NH_2 (**Liner b**, 9.8 mg, 49.6 μmol, 5 eq), and the pH was adjusted to 5 by adding 2 M HCl solution. DMTMM (13.7 mg, 49.6 μmol, dry powder, 5 eq) was added. The reaction was stirred at 50 °C for 3 hours. Another portion of DMTMM (13.7 mg, 49.6 μmol, 5 eq) was added, and the reaction was heated for another 3 hours. If there is still some DMT remains on the reducing end, TFA solution was added, the solution was stirred at room temperature for 3 hours. The reaction mixture was neutralized cooled on ice for 30 min Triethyalamine (TEA, 70.7 mg, 0.69 mmol, 70 eq) was added to the solution, followed by 2-chloro-1,3-dimethylimidazolinium chloride (DMC, 50.2 mg, 0.297 mmol, 30 eq). The mixture was allowed to react on ice for 30 min. The mixture was centrifuged at 14000 rpm for 3 min before it was purified by P-2 size exclusion column with 0.1% TEA as the eluent. The glycan containing fractions were lyophilized with addition of 2 μL 1M NaOH to give the Di-CP-SCT-oxa (**2-4b**) as a white solid (17.8 mg, 76%). ^{1}H NMR (D_2O, 600 MHz) δ 1.52–1.55 (8H, m, 4 × $NHCH_2CH_2$), 1.61 (2H, s, 4 × OCH2CH), 1.82 (2H, dd, J = 12.3 Hz, $H3f_{ax}$, $H3f'_{ax}$), 2.03, 2.05, 2.06 (15H, 3s, 5 × CH_3), 2.11 (6H, s, 2 × CH3 on CP) 2.70 (2H, t, J = 12.7 Hz, $H3f_{eq}$, $H3f'_{eq}$), 2.98–3.12 (8H, m, 2 × CH_2 NH-NB, 2 × CH_2NH-SCT), 3.39–3.47 (4H, m, H4c, H4c', H2e, H2e'), 3.48–3.63 (19H, m, H4a, H5a(β), H5b, H5c', H6c, H6c', H4d, H4d', H5d, H5d', H3e, H3e', H6e, H6e', H4f,

H4f', H7f, H7f', H9f, H9f'), 3.61–3.75 (10H, m, H3a, H6a, H3b, H5c, H2d, H2d', H3d, H3d', H6f, H6f'), 3.76–3.93 (29H, m, H2a, H6'a, H4b, H6b, H6'b, H3c, H3c', H6'c, H6'c', H6d, H6d', H6'd, H6'd', H4e, H4e', H5e, H5e', H6'e, H6'e', H5f, H5f', H8f, H8f', H9'f, H9'f', 2 × CHCH_2O), 4.15 (2H, br s), 4.19 (2H, br s, H2c, H2c'), 4.39 (1H, br s, H2b), 4.43 (2H, d, $J_{1,2}$ = 7.8 Hz, H1e, H1e'), 4.63 (2H, d, $J_{1,2}$ = 6.3 Hz, H1d, H1d'), 4.74 (1H, d, H1b), 4.94 (1H, s, H1c'), 5.12 (1H, s, H1c), 6.10 (1H, d, $J_{1,2}$ = 7.2 Hz, H1a), 6.64 (2H, m, 2 × C*H*=C). ^{13}C NMR (150 MHz, D_2O) δ = 10.35, 12.53, 16.13, 21.65, 21.98, 25.13, 26.15, 33.48, 37.67, 38.75, 39.51, 48.64, 51.34, 54.20, 59.75, 61.19, 62.61, 64.81, 65.31, 65.40, 66.50, 66.88, 67.32, 67.85, 68.84, 68.97, 69.14, 69.82, 70.23, 70.45, 70.68, 71.63, 71.68, 72.01, 72.44, 73.05, 73.86, 73.96, 75.65, 76.04, 77.47, 79.99, 80.30, 96.14, 98.80, 98.95, 99.01, 99.54, 100.73, 100.89, 103.16, 120.08, 158.51, 168.08, 168.25, 174.13, 174.58. HR-ESI-MS: $[M + 2H]^{2+}$ calcd for $C_{96}H_{157}N_9O_{58}^{2+}$, 1182.4818; found (*m/z*), 1182.4755.

One-pot synthesis of norbornene-modified glycan oxazoline Di-NB-SCT-oxa (2-4c). The oxazoline **2-4c** was synthesized starting with SCT (20 mg) in the same way as described for the synthesis of **2-4b**. The product was purified by gel filtration as described above to give **2-4c** as a white solid (16.5 mg, 70%). ^{1}H NMR (D_2O, 600 MHz) δ = 1.22–1.35 (4H, m, Hs on NB), 1.42–1.52 (8H, m, 4 × $NHCH_2CH_2$), 1.64–1.67 (4H, m, Hs on NB), 1.76 (2H, dd, J = 12.3 Hz, $H3f_{ax}$, $H3f'_{ax}$), 1.90, 1.95, 1.97 (15H, 3s, 5 × CH_3), 2.10–2.12 (2H, m, Hs on NB), 2.62 (2H, t, J = 12.7 Hz, $H3f_{eq}$, $H3f'_{eq}$), 2.87 (4H, m, 2 × CH_2 NH-NB), 3.39–3.47 (8H, m, H4c, H4c', H2e, H2e', 2 × CH_2NH-SCT), 3.48–3.63 (19H, m, H4a, H5a(β), H5b, H5c', H6c, H6c', H4d, H4d',

H5d, H5d', H3e, H3e', H6e, H6e', H4f, H4f', H7f, H7f', H9f, H9f'), 3.61–3.75 (10H, m, H3a, H6a, H3b, H5c, H2d, H2d', H3d, H3d', H6f, H6f'), 3.76–3.93 (25H, m, H2a, H6'a, H4b, H6b, H6'b, H3c, H3c', H6'c, H6'c', H6d, H6d', H6'd, H6'd', H4e, H4e', H5e, H5e', H6'e, H6'e', H5f, H5f', H8f, H8f', H9'f, H9'f'), 4.03 (1H, br s, H2c'), 4.11 (1H, br s, H2c), 4.18 (1H, br s, H2b), 4.36 (2H, d, $J_{1,2}$ = 7.8 Hz, H1e, H1e'), 4.51 (2H, d, $J_{1,2}$ = 6.3 Hz, H1d, H1d'), 4.70 (1H, d, H1b), 4.86 (1H, s, H1c'), 5.05 (1H, s, H1c), 6.00 (1H, d, $J_{1,2}$ = 7.2 Hz, H1a), 6.13 (4H, m, 4 × C*H*=CH). ^{13}C NMR (150 MHz, D_2O) δ = 12.54, 21.65, 21.99, 25.26, 25.74, 29.70, 37.68, 38.42, 38.78, 40.87, 43.63, 45.57, 45.87, 51.33, 54.18, 59.74, 61.19, 62.16, 62.63, 64.80, 65.31, 65.40, 66.49, 66.88, 67.33, 67.84, 68.83, 68.96, 69.13, 69.82, 70.22, 70.45, 70.68, 71.63, 71.68, 72.01, 72.43, 73.06, 73.85, 73.95, 75.64, 76.05, 77.47, 79.98, 80.30, 96.14, 98.80, 98.95, 99.02, 99.54, 100.88, 103.17, 135.79, 137.83, 168.08, 168.24, 174.14, 174.58, 178.68. HR-ESI-MS: $[M + 2H]^{2+}$ calcd for $C_{100}H_{161}N_9O_{56}^{2+}$, 1192.5025; found (*m/z*), 1192.4965.

Synthesis of the cytotoxic payloads

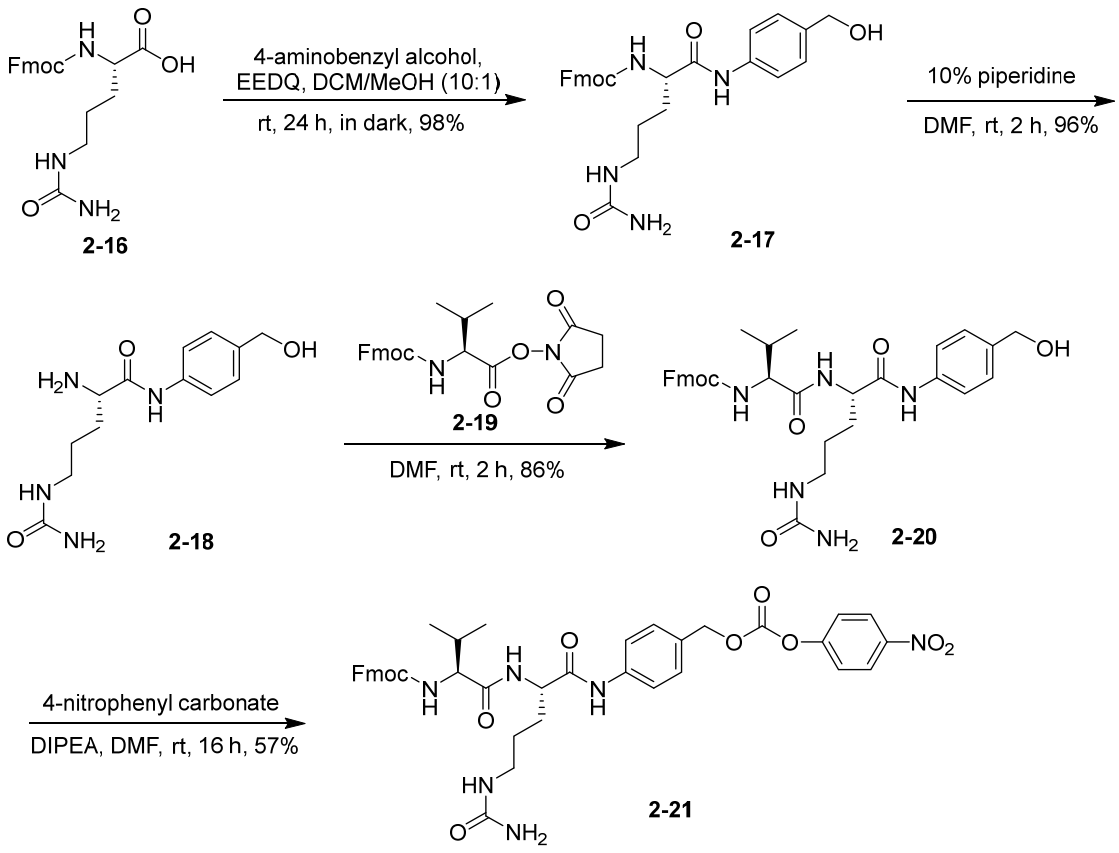

Scheme 2-7. Synthesis of the activated dipeptide linker **2-21**.

Synthesis of Fmoc-Cit-PABOH (2-17). To a stirred solution of compound **2-16** (2.40 g, 6.04 mmol, 1 eq) and 4-aminobenzyl alcohol (1.12 g, 9.06 mmol, 1.5 eq) in DCM/MeOH (40 mL, 10:1, v/v) was added EEDQ (2.98 g, 12.1 mmol, 2 eq) at 25 °C. The mixture was stirred at the same temperature for 24 hours in dark under argon atmosphere. Then, the solvents were removed in vacuo and the solid was filtered, washed with ethyl ether (30 mL) three times. The filter cake was collected and dried

over oil pump to afford **2-17** (2.98 g, 98%) as a white solid, which was used in the next step without further purification. ^{1}H NMR (400 MHz, $CDCl_3$) δ = 1.32– 1.79 (4H, m), 2.90– 3.12 (2H, m), 3.18 (3H, d, J = 4.9 Hz), 4.10 – 4.16 (1H, m), 4.23 (4H, m), 4.44 (2H, d, J = 5.2 Hz), 5.13 (1H, t, J = 5.6 Hz), 5.45 (2H, s), 6.02 (1H, t, J = 5.4 Hz), 7.30 (4H, m), 7.41 (2H, t, J = 7.4 Hz), 7.57 (2H, d, J = 8.3 Hz), 7.71– 7.79 (m, 2H), 7.88 (2H, d, J = 7.5 Hz), 9.99 (1H, br).

Synthesis of Cit-PABOH (2-18). To a stirred solution of **2-17**（2.0 g, 3.98 mmol, 1 eq）in DMF (16 mL) was added piperidine (1.7 mL, 17.2 mmol, 4.3 eq) dropwise at 25 °C. The mixture was stirred at 25 °C for another 2 hours. The reaction was concentrated in vacuo and the residue was washed with ethyl ether (40 mL) twice and dried over oil pump to afford **2-18** (1.07 g, 96%). The crude product was used directly in the following step.

Synthesis of Fmoc-Val-Cit-PABOH (2-20). Fmoc-L-valine *N*-hydroxysuccinimide ester **2-19** (2.1 g, 4.78 mmol, 1.25 eq) in DMF (10 mL) was added to a solution of **2-18** (1.07 g, 3.82 mmol, 1 eq) in DMF (10 mL) was at 25 °C. The solution was stirred for another 2 hours under argon atmosphere. TLC showed **2-18** was fully consumed. The reaction mixture was concentrated to dryness, filtered and washed with MeOH (20 mL) and ethyl ether (50 mL). The filter cake was collected to afford the dipeptide **2-20** (2.06 g, 86%) as a white solid. ^{1}H NMR (400 MHz, DMSO-d_6) δ = 0.87 (6H, dd), 1.28 – 1.53 (2H, m), 1.53 – 1.80 (2H, m), 1.87– 2.10 (1H, m), 2.86– 3.11 (2H, m), 3.94 (1H, t, J = 7.8 Hz), 4.15– 4.35 (3H, m), 4.44 (3H, m), 5.12

(1H, br), 5.42 (2H, br), 5.99 (1H, br), 7.24 (2H, d, J = 8.1 Hz), 7.49 – 7.28 (5H, m), 7.55 (2H, d, J = 8.1 Hz), 7.74 (2H, t, J = 7.9 Hz), 7.88 (2H, d, J = 7.3 Hz), 8.12 (1H, d, J = 7.3 Hz), 9.99 (1H, s). ^{13}C NMR (101 MHz, DMSO-d_6) δ = 17.76, 18.72, 24.71, 26.28, 29.04, 29.95, 46.19, 52.57, 59.62, 62.10, 65.19, 118.39, 119.59, 124.85, 126.43, 126.57, 127.14, 136.95, 137.01, 140.21, 143.27, 143.41, 155.63, 158.41, 169.89, 170.75, 172.40. ESI-MS: $[M + H]^+$ calcd for $C_{33}H_{40}N_5O_6^+$, 602.30; found (*m/z*), 602.50.

Synthesis of Fmoc-Val-Cit-PABC-PNP (2-21). To a stirred solution of **2-20** (60 mg, 0.1 mmol, 1.0 eq) and 4-nitrophenyl carbonate in anhydrous DMF (5 mL) was added DIPEA (69 µL, 0.4 mmol, 4 eq) dropwise at 25 °C. The mixture was stirred at room temperature for 16 hours. The reaction was quenched by adding 15% citric acid (30 mL), extracted with ethyl acetate (50 mL) twice. The organic phase was combined and washed with brine. The solvents were concentrated in vacuo and the residue was purified by prep-HPLC to afford **2-21** (44 mg, 57%) as a white solid. ^{1}H NMR (600 MHz, DMSO-d_6) δ = 0.87 (6H, dd), 1.34 – 1.49 (2H, m), 1.57 – 1.80 (2H, m), 1.95 – 2.05 (1H, m), 2.90 – 3.08 (2H, m), 3.94 (1H, dd), 4.20– 4.35 (1H, m), 4.44 (1H, m), 5.24 (2H, br), 5.42 (2H, br), 5.99 (1H, br), 7.32 (2H, d, J = 8.1 Hz), 7.39 – 7.45 (5H, m), 7.55 (2H, m), 7.64 (2H, d), 7.72-7.77 (2H, dd), 7.88 (2H, d, J = 7.3 Hz), 8.12 (1H, d, J = 7.3 Hz),8.30-8.33 (2H, m), 10.14 (1H, s). ^{13}C NMR (150 MHz, DMSO) δ = 18.21, 19.16, 26.72, 29.38, 30.40, 46.66, 53.09, 60.03, 65.64, 70.21, 119.03, 120.03, 122.55, 125.30, 125.34, 127.58, 129.41, 139.32, 140.66, 143.73, 143.86, 145.15, 151.90, 155.26, 156.06, 158.85, 170.67, 171.23. ESI-MS: $[M + H]^+$ calcd for $C_{40}H_{43}N_6O_{10}^+$, 767.30; found (*m/z*), 767.58.

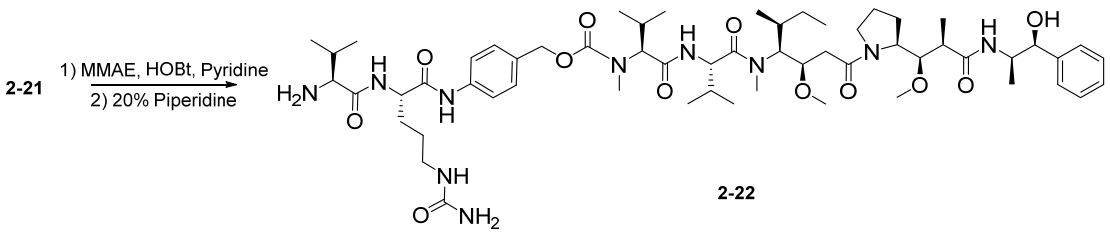

Scheme 2-8. Synthesis of dipeptide-MMAE (**2-22**)

Synthesis of Val-Cit-PABC-MMAE (2-22) [86]. In a 1.5 mL centrifuge tube, **2-21** (20 mg, 26 μmol, 1.3 eq), MMAE (14.4 mg, 20 μmol, 1.0 eq), and HOBt (3.5 mg, 26 μmol, 1.3 eq) was dissolved in dry DMF (400 μL) and pyridine (200 μL). The mixture reacted at room temperature under argon for 9 hours before HPLC-SQ2 analysis showed complete consumption of the reactant. Then the reaction mixture was quenched by sat. $NaHCO_3$ (25 mL), the product was collected as a white solid after high-speed centrifugation. Without further purification, the solid was dissolved in ACN and THF (v/v, 1/1, 4 mL). After high-speed centrifugation, piperidine (1 mL) was added to the supernatant at room temperature. The HPLC-SQ2 confirmed the reaction was finished after 30 min, the mixture was diluted with water (5 mL) and then concentrated in vacuo and the residue was purified by semi prep-HPLC to afford **2-22** (12.6 mg, 56% over two steps) as a white solid. ^{1}H NMR (600 MHz, DMSO + 5% D_2O) δ = 0.68 – 1.07 (31H, m), 1.26 (1H, s), 1.34 – 1.84 (10H, m), 1.87 – 1.98 (1H, m), 2.00 – 2.12 (3H, m), 2.20 – 2.29 (1H, m), 2.37 (1H, d), 2.79 –2.89 (3H, m), 2.91 –3.32 (14H, m), 3.52 (1H, m), 3.73 (1H, d), 3.90 – 4.02 (2H, m), 4.21 (1H, m), 4.39 (1H, d), 4.43 – 4.50 (3H, m), 4.97 –5.10 (2H, m), 7.10 – 7.18 (1H, m), 7.20-7.37 (6H, m), 7.54 (2H, br). ESI-MS: $[M + H]^+$ calcd for $C_{58}H_{95}N_{10}O_{12}^+$, 1123.71; found (*m/z*), 1123.85.

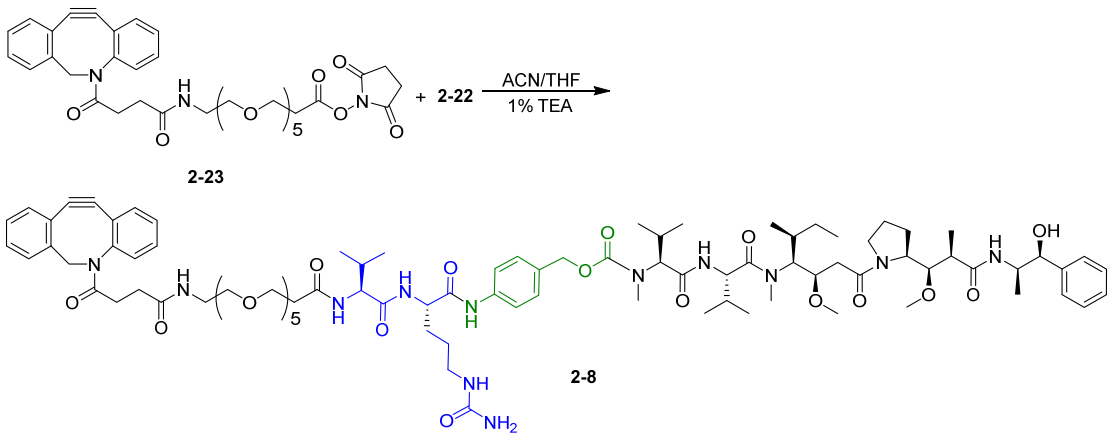

Scheme 2-9. Synthesis of the DBCO-tagged MMAE (**2-8).**

Synthesis of DBCO-PEG-Val-Cit-PABC-MMAE (2-8) [86]**.** In a 1.5 mL centrifuge tube, **2-23** (1.4 mg, 1.65 µmol, 1.5 eq) and **2-22** (1.2 mg, 1.1 µmol) were dissolved in ACN and THF (v/v, 1/1, 300 µL) with TEA (3 µL) at room temperature. The reaction was finished after 4 hours, confirmed by HPLC-SQ2. The mixture was diluted with 50% ACN with 0.1% TFA (2 mL) and into semi prep-HPLC directly to afford **2-8** (1.5 mg, 80%) as a white powder. HR-ESI-MS: $[M + H]^+$ calcd for $C_{90}H_{133}N_{12}O_{20}^+$, 1701.9754; found (*m/z*), 1701.9694.

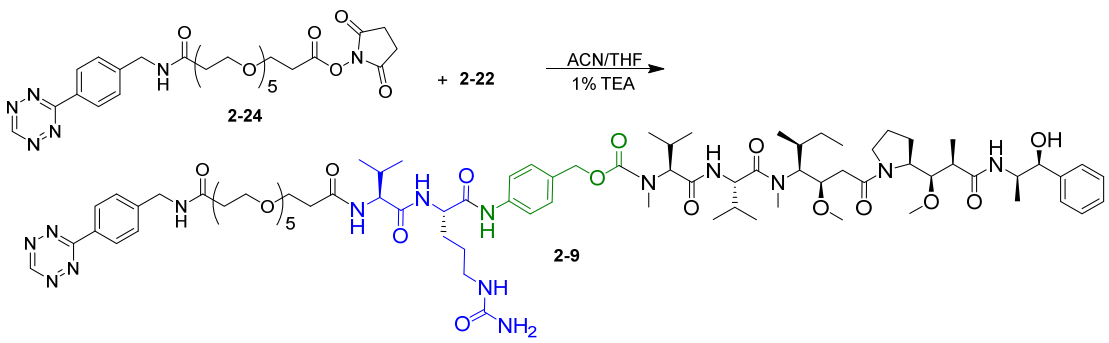

Scheme 2-10. Synthesis of the tetrazine-tagged MMAE (**2-9**).

Synthesis of the Tz-PEG-Val-Cit-PABC-MMAE (2-9). In a 1.5 mL centrifuge tube, **2-24** (2.9 mg, 4.8 μmol, 1.5 eq) and **2-22** (3.6 mg, 3.2 μmol) were dissolved in ACN and THF (v/v, 1/1, 800 μL) with TEA (8 μL) at room temperature. The reaction completed within 4 hours, confirmed by HPLC-SQ2. The mixture was diluted with 50% ACN with 0.1% TFA (3 mL) and into semi prep-HPLC directly to afford **2-9** (4.3 mg, 84%) as a pink powder. HR-ESI-MS: $[M + H]^+$calcd for $C_{81}H_{126}N_{15}O_{19}^+$, M = 1612.9349; found (*m/z*), 1612.9407.

Chemoenzymatic synthesis of the azide-, cyclopropene- and norbornene-tagged antibodies.

Preparation of GNF-Her (2-6) with immobilized Endo-S2 WT. The suspension of the immobilized Endo-S2 WT (100 μL, 2 mg/mL) was centrifuged at 14000 rpm for 5 min, the supernatant was removed and discarded. Intact Herceptin **2-5** solution (4 mL, 5.5 mg/mL) was added to the resin, and mixed end to end at 30 °C. The progress was

checked by LC-MS and compared with reported data. The cleavage reaction was completed within 3 hours, then the mixture was centrifuged at 14000 rpm for 5 min. The immobilized enzyme was recovered and resuspend in 1 x PBS buffer with 0.5% NaN_3. The GNF-Her **2-6** in the solution was purified with protein A chromatography, exchanged to Tris buffer (100 mM, pH 7.2) and concentrated to 25 mg/mL with a spin filter to yield deglycosylated Herceptin **2-6** (20 mg, 91%). ESI-MS: calcd for GNF-Her, M = 145865 Da; found (*m/z*), 2702.16 $[M + 54H]^{54+}$, 2753.11 $[M + 53H]^{53+}$, 2806.10 $[M + 52H]^{52+}$,2861.00 $[M + 51H]^{51+}$, 2977.90 $[M + 49H]^{49+}$, deconvolution of the ESI-MS, M = 145865 Da.

General Procedure for transglycosylation reactions. To the solution of **2-6** (25 mg/ml in 100 mM Tris buffer), glycan oxazoline **2-4a**, **2-4b**, **2-4c** (30 eq, 100 mg/mL in 100 mM Tris buffer) was added. After adjusting the pH to 7.4, Endo-S2 D184M mutant (9.1 mg/mL) was added to the solution. The final enzyme concentration was 0.1 mg/mL. The reaction was carried out at 30 °C for 40 min before the reacting mixture was analyzed by LC-MS, and typically reactions reached completion in 40 min. The functionalized Herceptin **2-7a**, **2-7b**, **2-7c** were purified by protein A chromatography with standard procedures. With a 10k cut-off centrifugal filters, the buffer was exchanged to phosphate buffer (50 mM pH 7.2), and the product was concentrated to 5 mg/mL.

Synthesis of compound 2-7a. Prepared from **2-6** (6.5 mg, 45 nmol, 1 eq) and **2-5** (3.4 mg, 1.4 μmol, 30 eq) with General Procedure B to yield azide functionalized

Herceptin **2-7a** (6 mg, 92%). ESI-MS: calcd for Her-(Di-N_3-SCT)$_2$, M = 151022 Da; found (*m/z*), 2797.64 $[M + 54H]^{54+}$, 2850.5 $[M + 53H]^{53+}$, 2905.20 $[M + 52H]^{52+}$,2962.20 $[M + 51H]^{51+}$, 3021.40 $[M + 50H]^{50+}$, 3083.00 $[M + 49H]^{49+}$, deconvolution of the ESI-MS, M = 151024 Da.

Synthesis of compound 2-7b Prepared from **2-6** (5.0 mg, 35 nmol, 1 eq) and **2-4b** (2.4 mg, 1.0 μmol, 30 eq) with General Procedure B to yield cyclopropene functionalized Herceptin **2-7b** (5.0 mg, 96%). ESI-MS: calcd for Her-(Di-Cp-SCT)$_2$, M = 150589 Da; found (*m/z*), 2789.61 $[M + 54H]^{54+}$, 2842.21 $[M + 53H]^{53+}$, 2953.64 $[M + 51H]^{51+}$, 3012.69 $[M + 50H]^{50+}$, deconvolution of the ESI-MS, M = 150586 Da.

Synthesis of compound 2-7c. Prepared from **2-6** (8.0 mg, 55 nmol, 1 eq) and **2-4c** (4.0 mg, 1.6 μmol, 30 eq) with General Procedure B to yield cyclopropene functionalized Herceptin **2-7c** (6.5 mg, 81%). ESI-MS: calcd for Her-(Di-NB-SCT)$_2$, M = 150629 Da; found (*m/z*), 2739.82 $[M + 55H]^{55+}$, 2843.07 $[M + 53H]^{53+}$, 2954.55 $[M + 51H]^{51+}$, 3013.63 $[M + 50H]^{50+}$, deconvolution of the ESI-MS, M = 150632 Da.

Comparison of the transglycosylation reactions catalyzed by EndoS2-D184M and EndoS-D233Q. To the solution of **2-6** (1mg, 6.7 nmol, 40 uL, 25 mg/mL in 100 mM Tris) **2-4a** (0.35 mg, 133 nmol, 3.5 μL, 100 mg/mL) was added. The pH of the mixture was confirmed within 7.0 to 7.4 by pH paper. EndoS2-D184M (4.4 ug, 0.34 μL, 13 mg/mL) or EndoS-D233Q (4.4 μg, 0.34 μL, 13 μg/mL) was added to each reaction vessel, so the final enzyme concentration was 0.1 mg/mL. The reaction

mixtures were incubated at 30 °C. A sample was taken every 20 minutes from each vessel until the reaction was completed. (Figure S2') The EndoS2-D184M catalyzed reaction was complete within 20 minutes. On the other hand, the EndoS-D233Q required more than 60 minutes.

Preparation of antibody-drug conjugates by Click reactions.

Preparation of 2-10 a. A solution of azide-tagged antibody **2-7a** (2 mg, 13 nmol) and the DBCO-modified MMAE (**2-8**) (459 µg, 0.27 µmol, 20 eq) in a phosphate buffer (50 mM, pH 7.2) containing 30% dimethyl sulfoxide (DMSO) (final volume, 1 mL) was incubated at ambient temperature (23 ºC). The reaction mixture was shielded from light and gently vortexed. The reaction was monitored by LC-ESI-MS analysis. After 8 h, the Click reaction was complete as indicated by LC-ESI-MS. The mixture was then diluted with phosphate buffer (5 mL, 50 mM, pH 7.2) and filtered by 0.22 µm syringe filter. The conjugate product in the filtrate was purified by protein A chromatography to give **2-10a** (1.7 mg, 83%). ESI-MS of **2-10a**: calcd. M = 157830 Da; found (*m/z*), 2870.74 $[M + 55H]^{55+}$, 2923.86 $[M + 54H]^{54+}$, 2978.93 $[M + 53H]^{53+}$, 3036.20 $[M + 52H]^{52+}$, 3095.80 $[M + 51H]^{51+}$, deconvolution of the ESI-MS, M = 157834 Da. Fc analysis: calcd, M = 30118 Da; found (m/z), 1772.74 $[M + 17H]^{17+}$, 1883.39 $[M + 16H]^{16+}$, 2008.92 $[M + 15H]^{15+}$, deconvolution data, M = 30118 Da.

Preparation of 2-10b. The Click reaction between the cyclopropene-modified antibody (**2-7b**) (2.0 mg, 13 nmol, 1 eq) and the tetrazine-modified MMAE (**2-9**) (419

μg, 0.26 μmol, 20 eq) was performed in the same way as described for the synthesis of **2-10a**. The reaction was complete within 4 h and subsequent affinity column purification gave **2-10b** (1.7 mg, 83%). ESI-MS of **2-10b**: calcd M = 157129 Da; found (*m/z*), 2854.21 $[M + 55H]^{55+}$, 2907.16 $[M + 54H]^{54+}$, 2961.90 $[M + 53H]^{53+}$, 3018.84 $[M + 52H]^{52+}$, 3078.08 $[M + 51H]^{51+}$, deconvolution of the ESI-MS, M = 157132 Da. Fc analysis: calcd M = 29697 Da; found (m/z), 1746.21 $[M + 17H]^{17+}$, 1855.26 $[M + 16H]^{16+}$, 1978.86 $[M + 15H]^{15+}$, deconvolution of the ESI-MS, M = 29698 Da.

Preparation of 2-10c. The Click reaction between the norbornene-modified antibody (**2-7c**) (2.0 mg, 13 nmol, 1 eq) and the tetrazine-modified MMAE (**2-9**) (430 μg, 0.27 μmol, 20 eq) was performed in the same way as described for the synthesis of **2-10b**. The reaction was complete within 16 h and subsequent affinity column purification gave **2-10c** (1.4 mg, 68%). ESI-MS of **2-10c**: calcd M = 156969 Da; found (*m/z*), 2854.90 $[M + 55H]^{55+}$, 2907.88 $[M + 54H]^{54+}$, 2962.64 $[M + 53H]^{53+}$, 3019.60 $[M + 52H]^{52+}$, 3078.71 $[M + 51H]^{51+}$, deconvolution of the ESI-MS, M = 156971 Da. Fc analysis: calcd M = 29688 Da; found (m/z), 1747.26 $[M + 17H]^{17+}$, 1856.41 $[M + 16H]^{16+}$, 1980.13 $[M + 15H]^{15+}$, deconvolution of the ESI-MS, M = 29687 Da.

In Vitro Assays

***In Vitro* cytotoxicity.** T47D and SKBR3 (ATCC) cells were cultured in DMEM supplemented with 10% FBS, 50 U/ml penicillin, and 50 μg/mL streptomycin (ThermoFisher) and seeded at 200,000 cells/mL into a 96 well plate (20,000 cells/well)

and grown for 24 hours until 60% confluent. Cells were then washed with PBS and incubated with fresh media containing the ADCs starting at a concentration of 1 μg/mL and serially diluted 1:2. Each compound was assessed in duplicate wells, and cells without compound served as control. Plates were incubated for 72 hours and cell viability was analyzed by CellTiter-Glo Luminescent Cell Viability Assay (Promega) as per manufacturer's instructions. Briefly, equal volume kit reagent to media was added to each well. Cells were then lysed and incubated for 10 mins before luminescence was recorded.

Size Exclusion Chromatography. The size exclusion chromatography was carried out by a ÄKTA pure system (Cytiva), equipped with a Superdex® 200 Increase 10/300 GL column (Cytiva). PBS was used as the mobile phase. The flow rate was 0.75 mL/min, over 48 min. 50 μg of the conjugates **2-10a-c** was injected. (Figure S17) There was no aggregation found for **2-10a**; while there were 8-9% aggregation for **2-10b** and **2-10c**.

Serum Stability Assay (2019-ACIE-Hckenberger) In a 1.5 mL centrifuge tube, 200 μlLrat serum (Sigma Aldrich, United States) were mixed with 50 μl ADCs **2-10a-c** (2.0 mg/ml), then filtered with UFC30GV0S centrifugal filter units (Merck, Germany) and incubated at 37°C for 3 days. The conjugates were enriched by 50 μL anti-human-IgG (Fc-Specific) agarose slurry (Sigma Aldrich, United States) according to reported procedures. The concentration of the conjugates was measured, then analyzed by LC-MS.

2.5 Supporting Information

NMR spectra

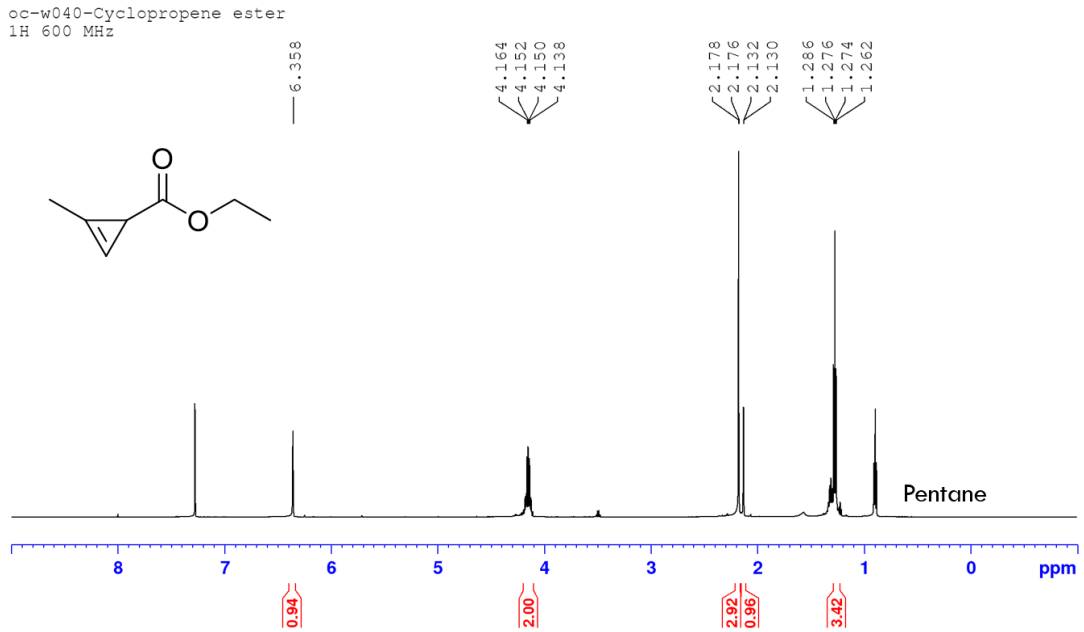

^{1}H NMR (600MHz, $CDCl_3$): compound **2-12**

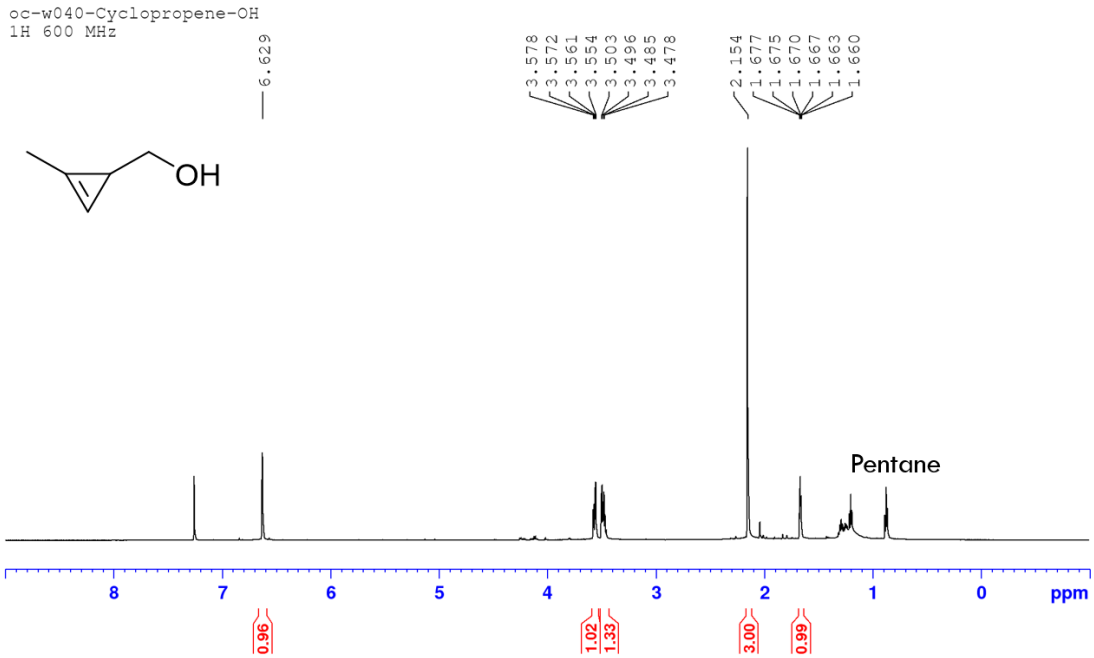

^{1}H NMR (600MHz, $CDCl_3$): compound **2-13**

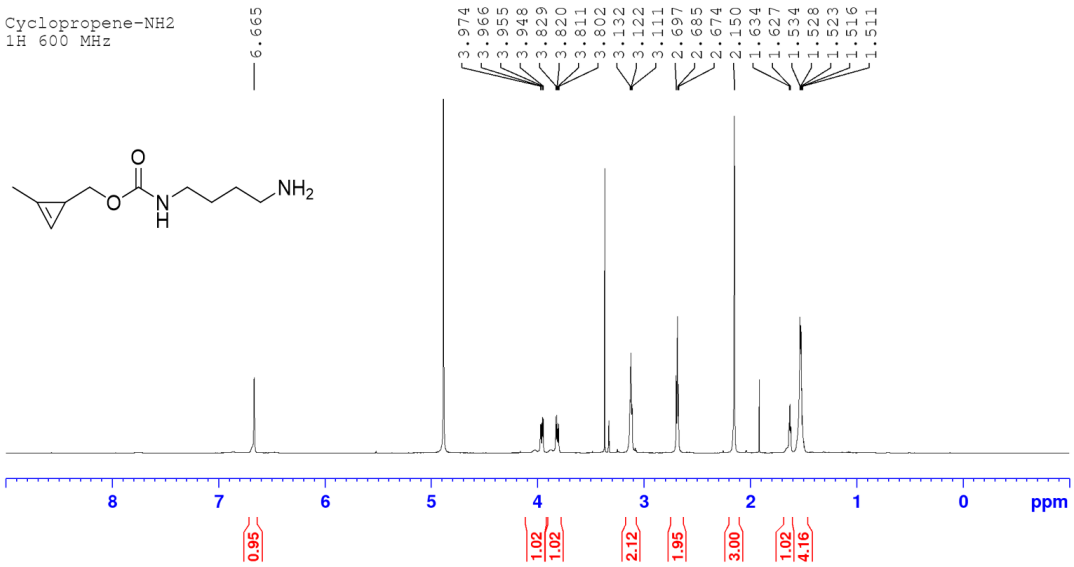

^{1}H NMR (600MHz, $CDCl_3$): compound **Linker b**

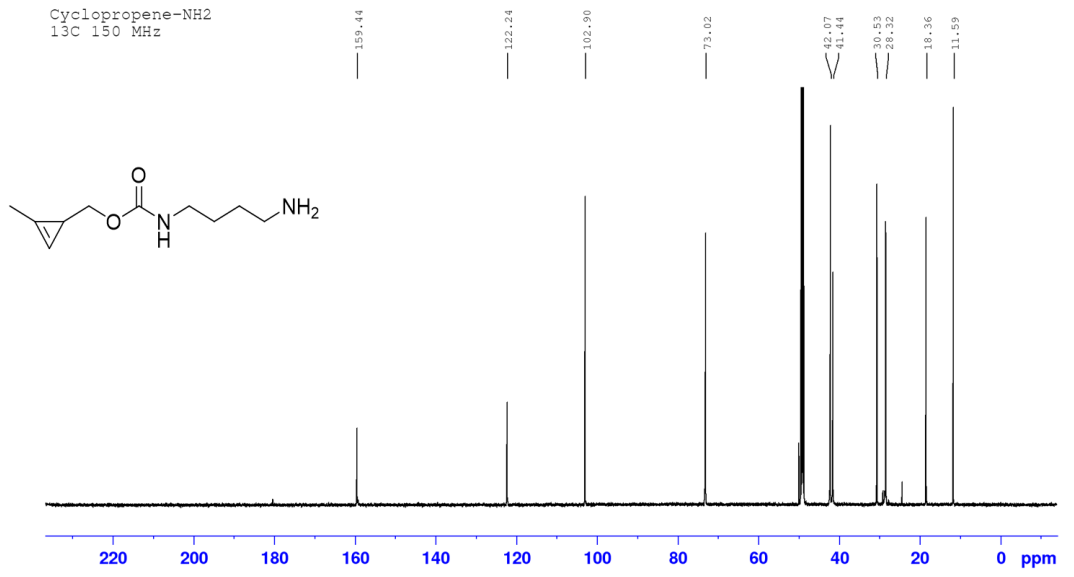

^{13}C NMR (150MHz, $CDCl_3$): compound **Linker b**

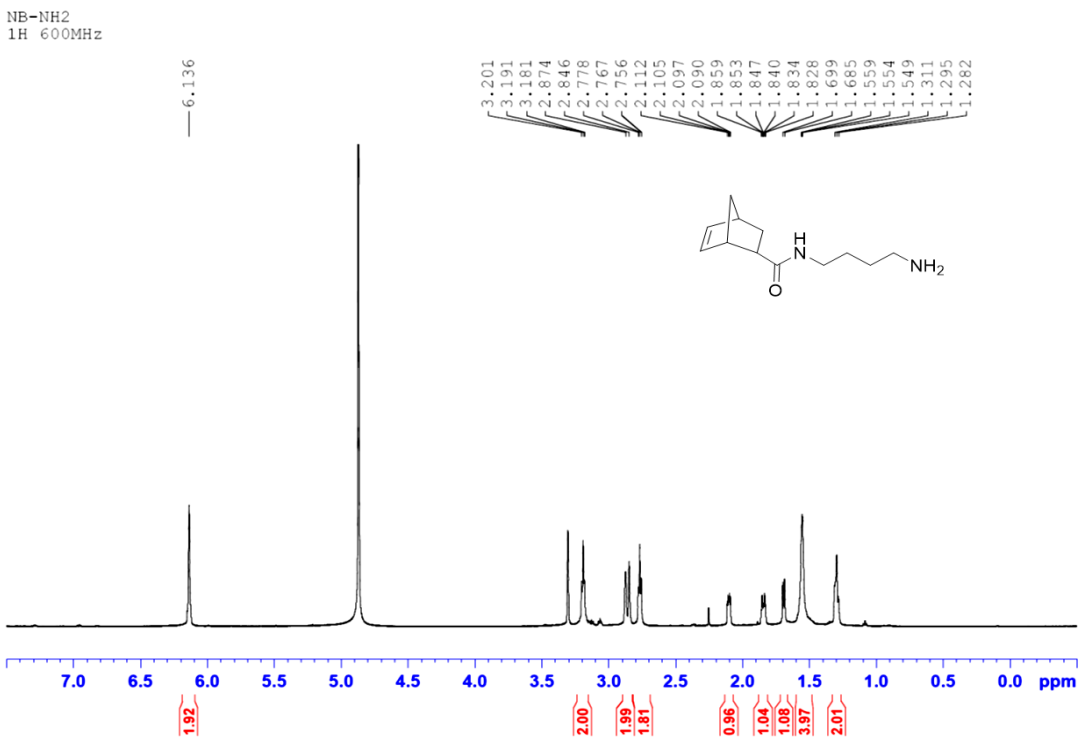

^{1}H NMR (600MHz, $CDCl_3$): compound **Linker c**

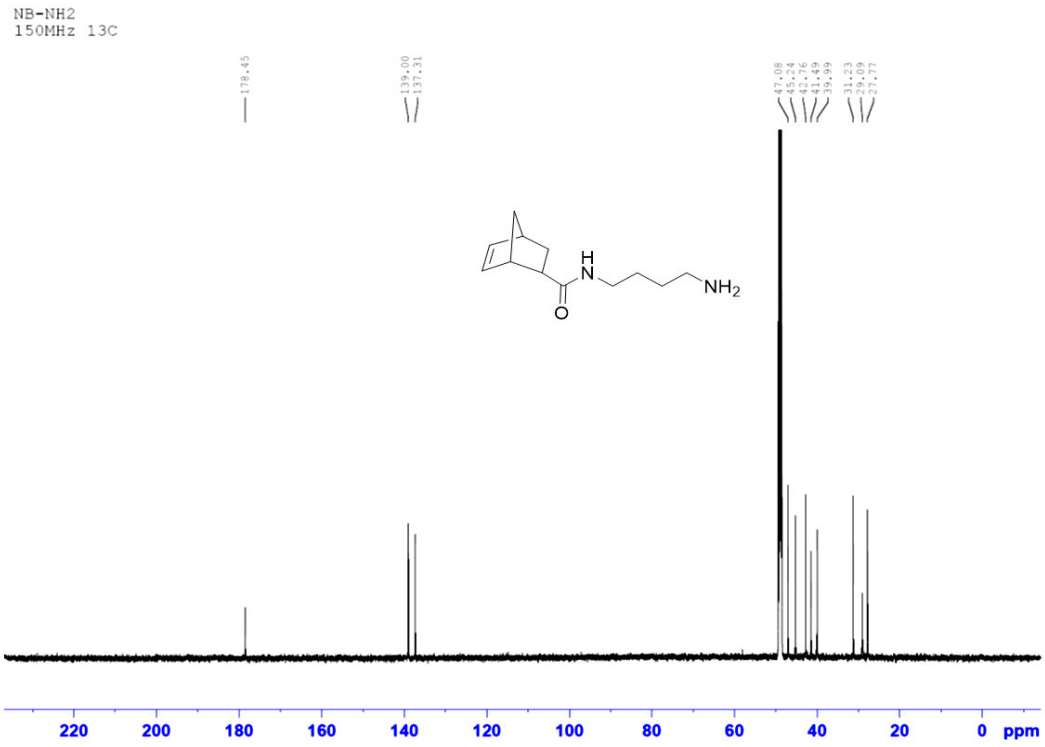

^{13}C NMR (150MHz, $CDCl_3$): compound **Linker c**

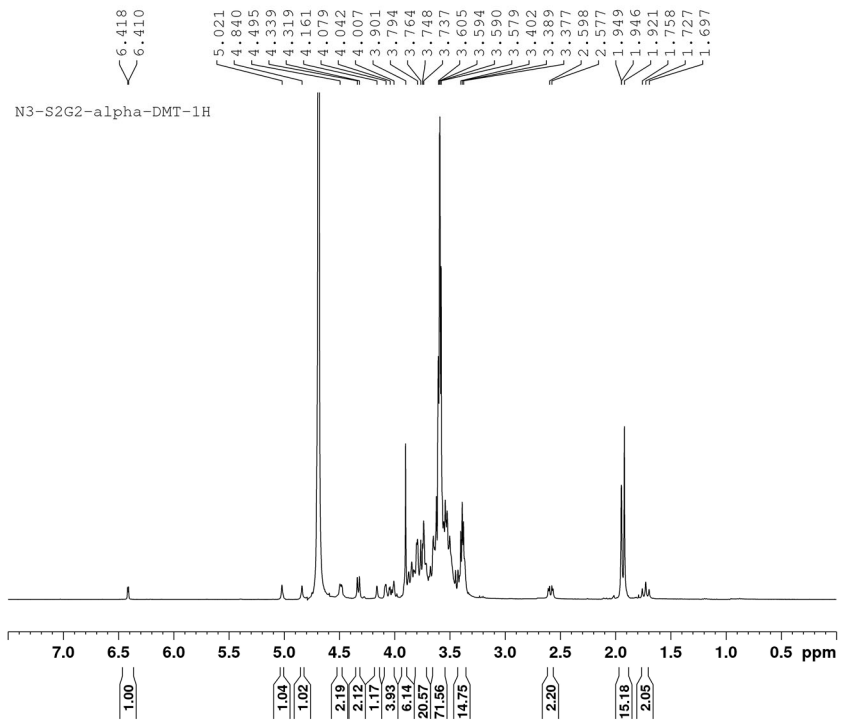

^{1}H NMR (400MHz, D_2O): compound **2-2**

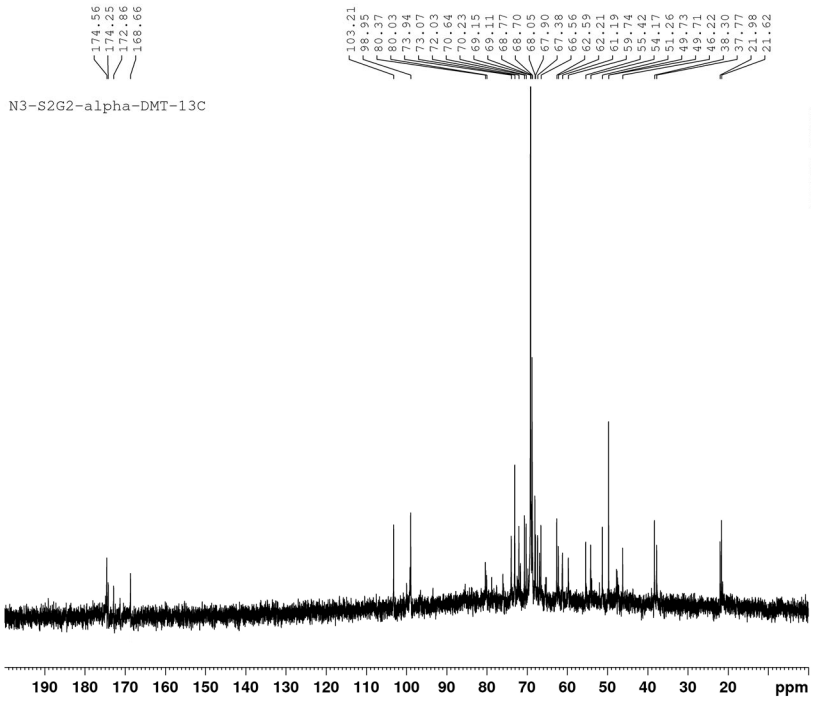

^{13}C NMR (100MHz, $CDCl_3$): compound **2-2**

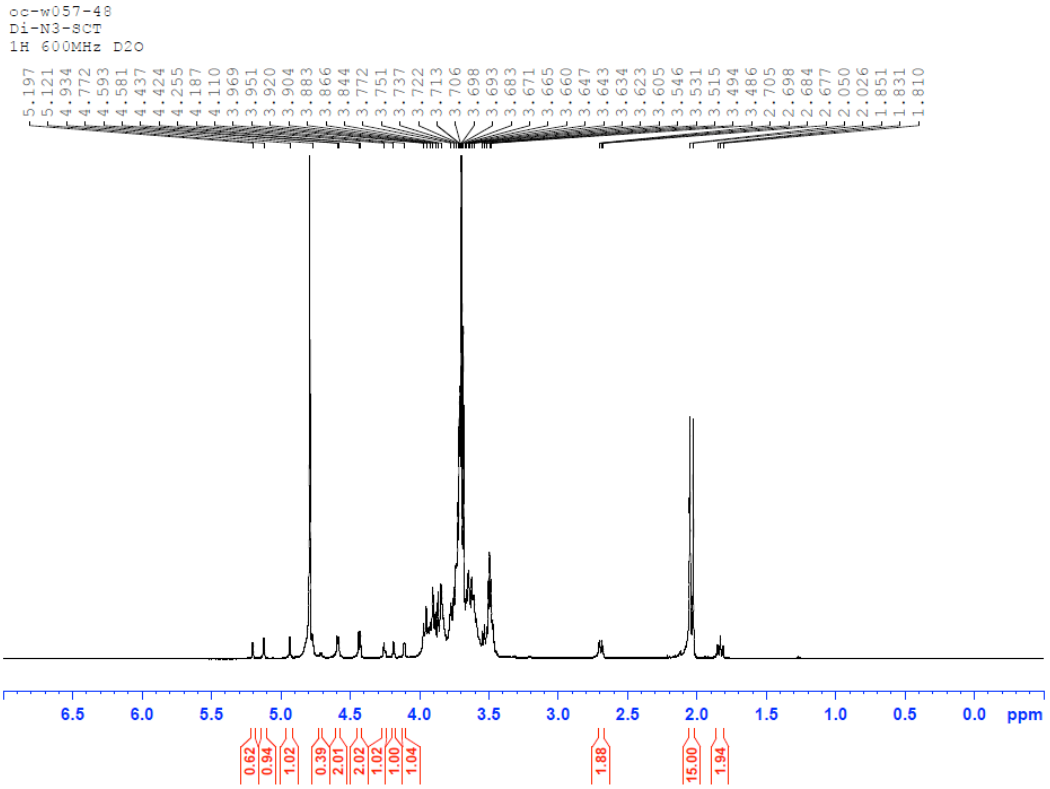

^{1}H NMR (600MHz, D_2O): compound **2-3**

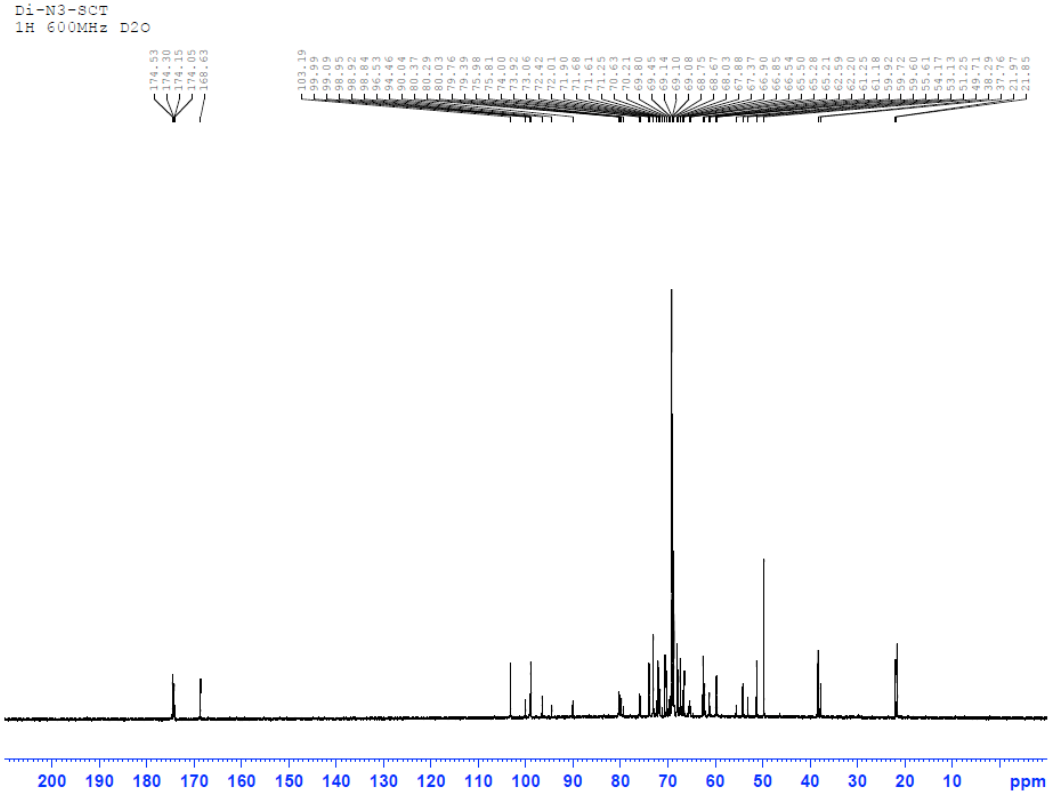

^{13}C NMR spectrum (150 MHz, D_2O): compound **2-3**

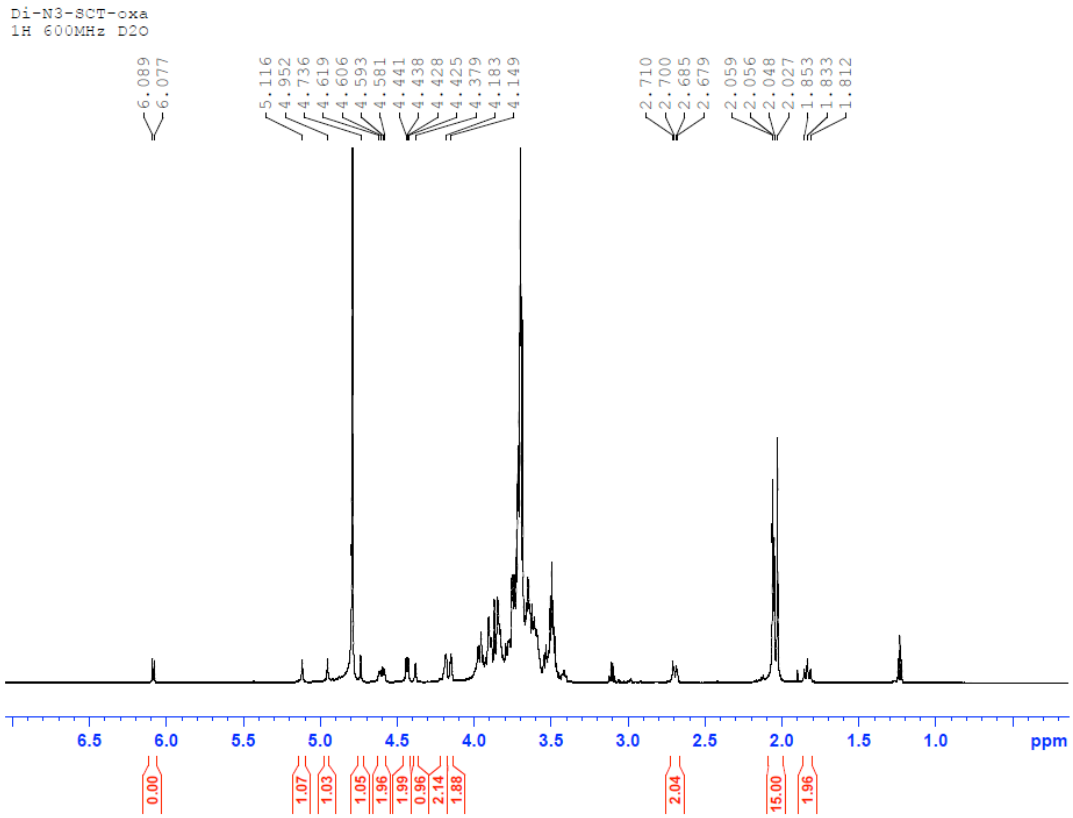

^{1}H NMR spectrum (600 MHz, D_2O): compound **2-4a**

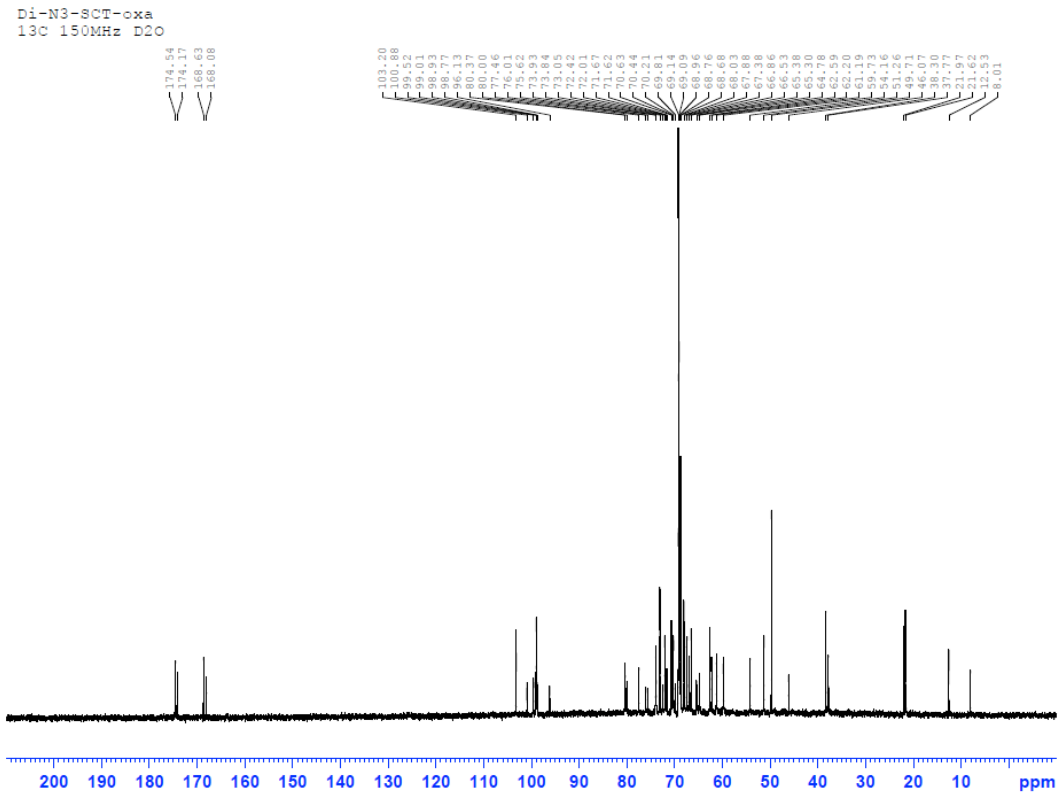

^{13}C NMR spectrum (150 MHz, D_2O): compound **2-4a**

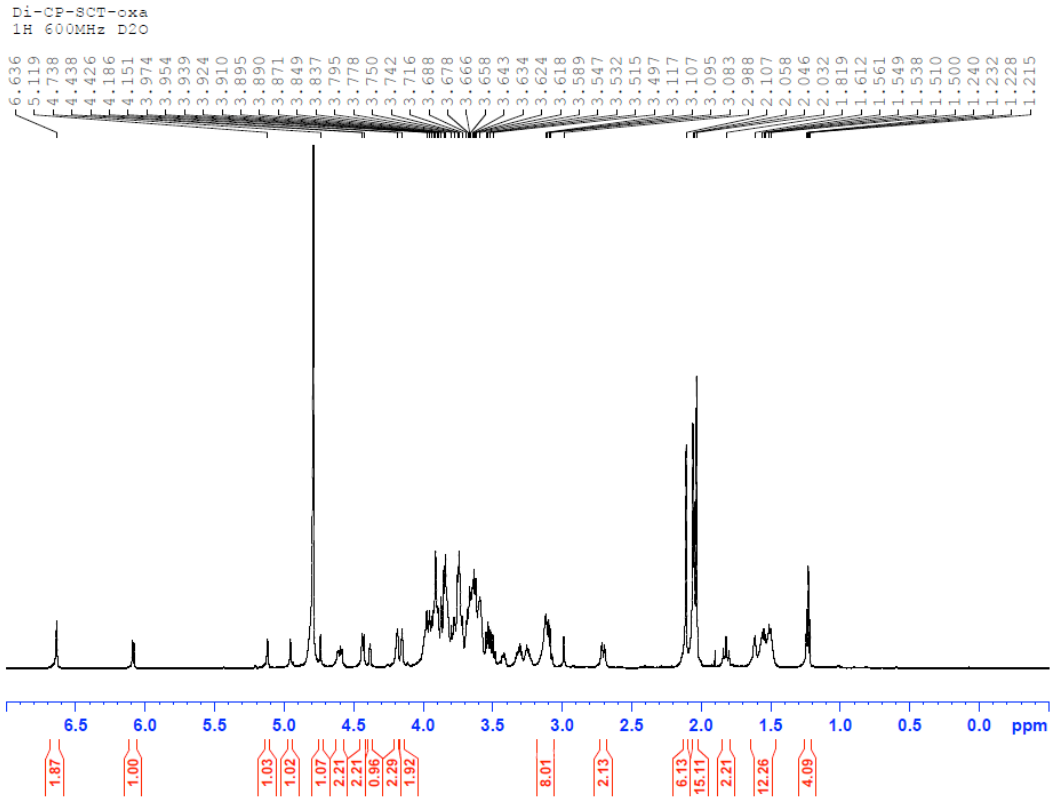

^{1}H NMR spectrum (600 MHz, D_2O): compound **2-4b**

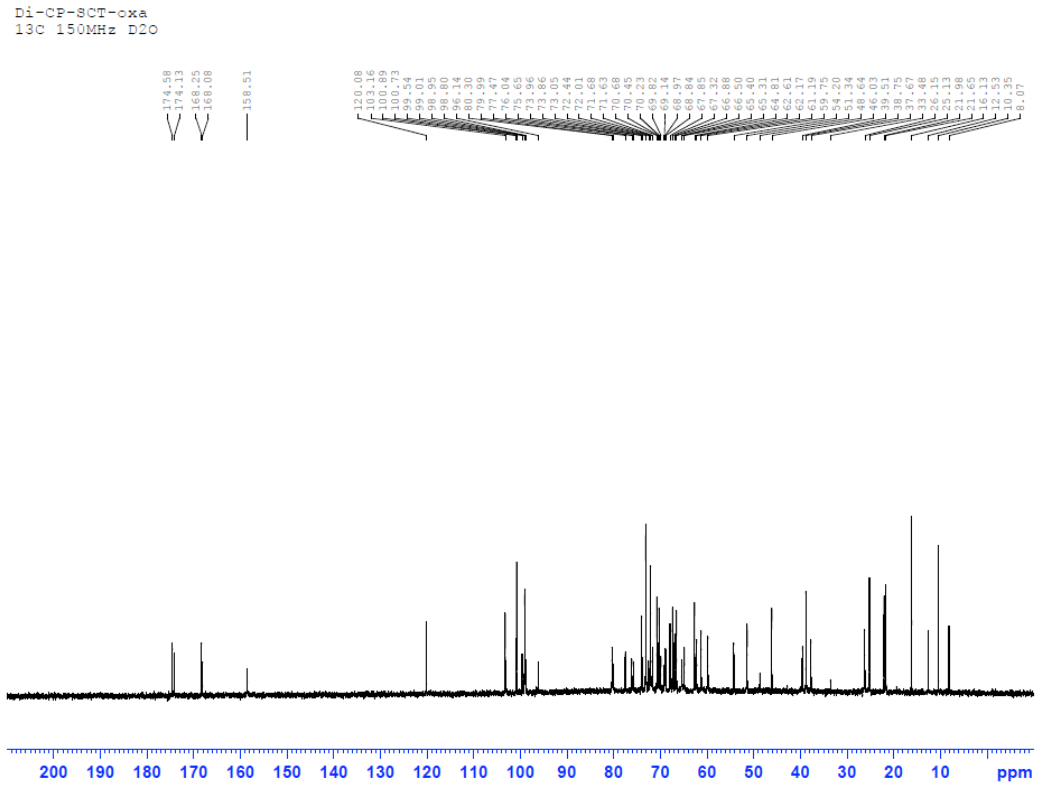

^{13}C NMR spectrum (150 MHz, D_2O): compound **2-4b**

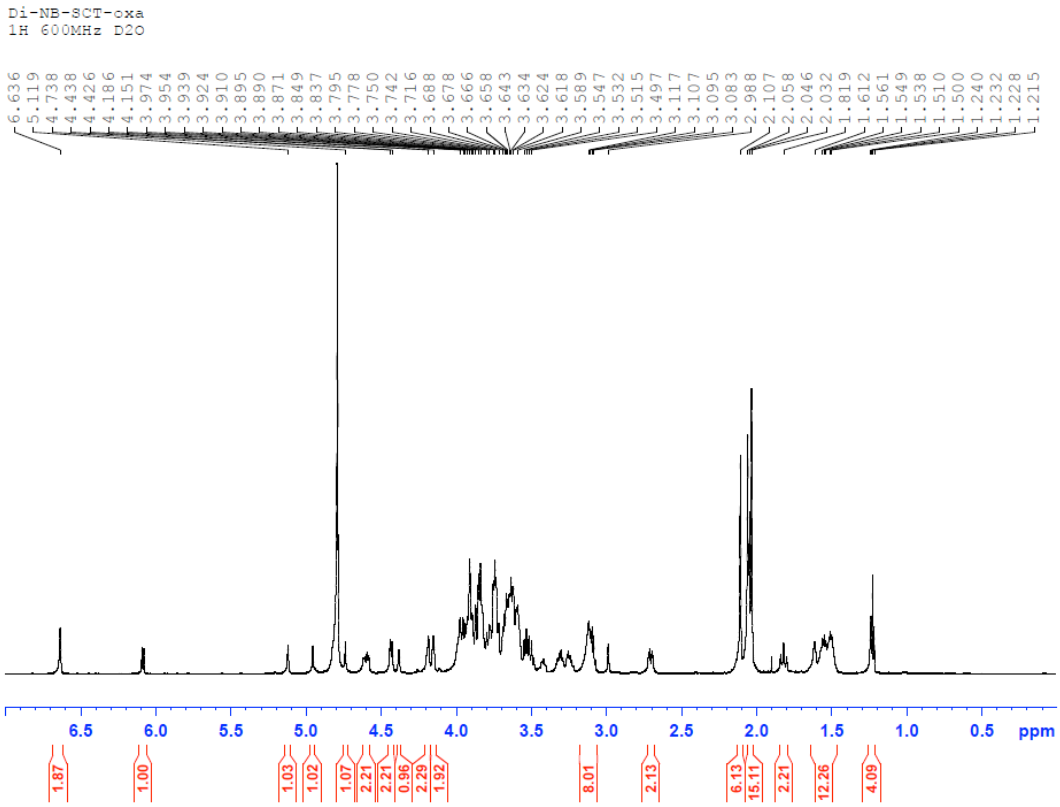

^{1}H NMR spectrum (600 MHz, D_2O): compound **2-4c**

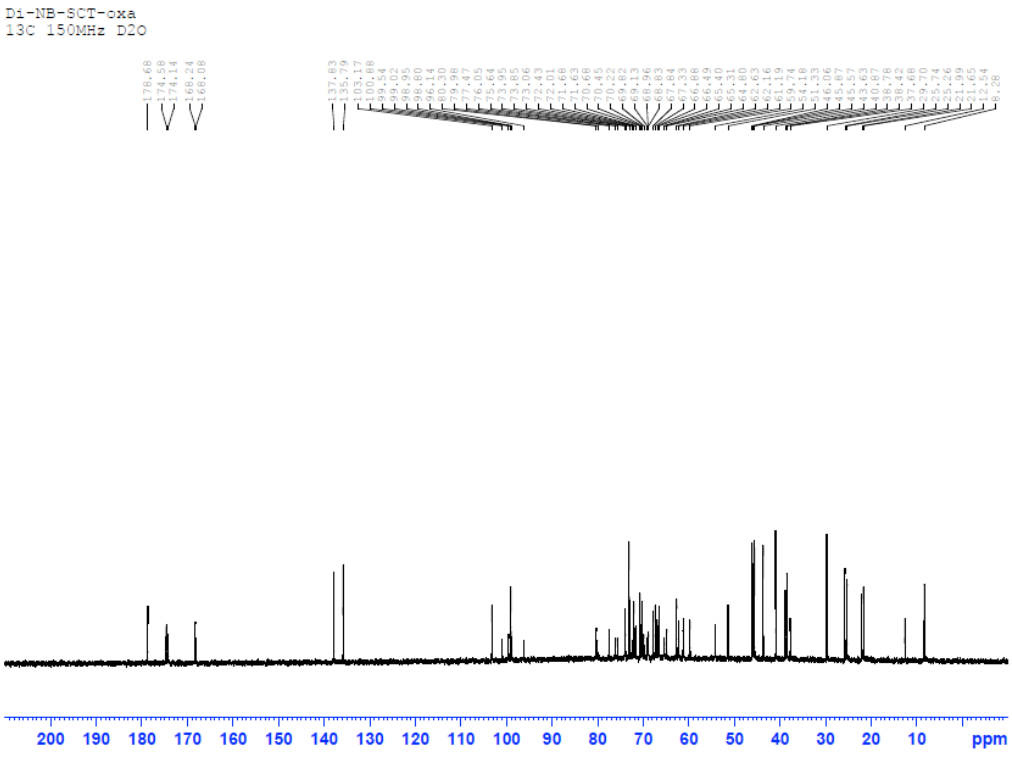

^{1}C NMR (150MHz, D_2O): compound **2-4c**

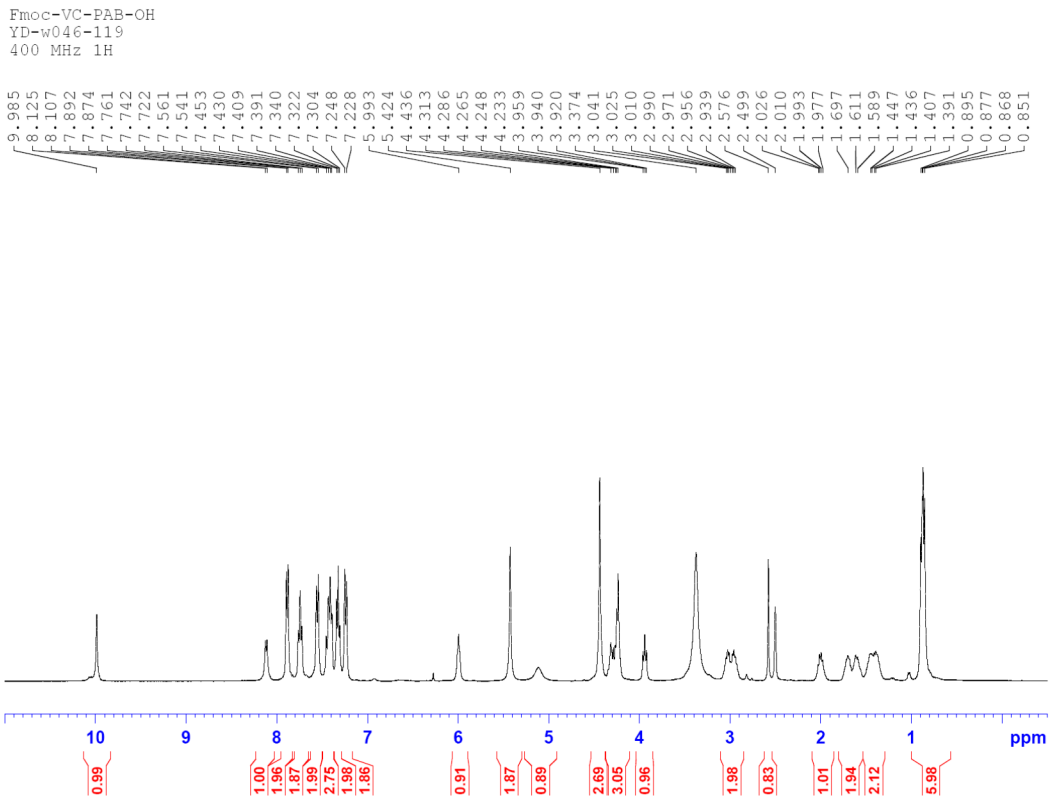

^{1}H NMR spectrum (400 MHz, DMSO-*d*6): compound **2-20**

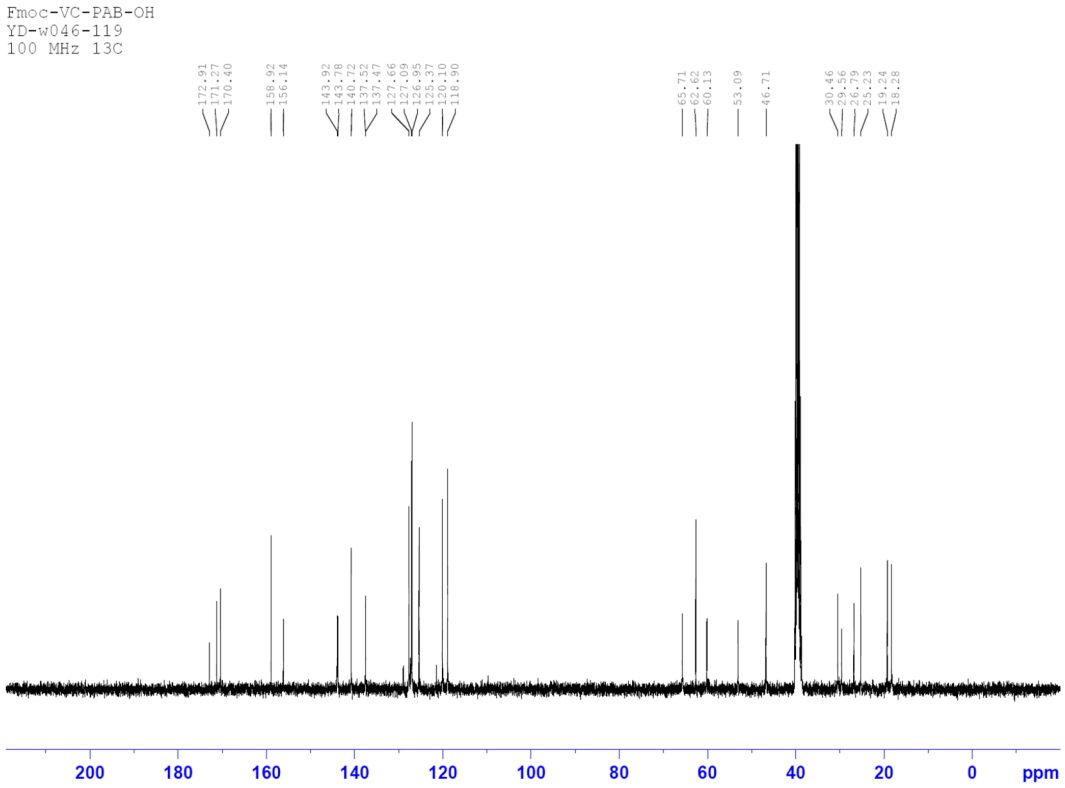

^{13}C NMR spectrum (100 MHz, DMSO-*d*6): compound **2-20**

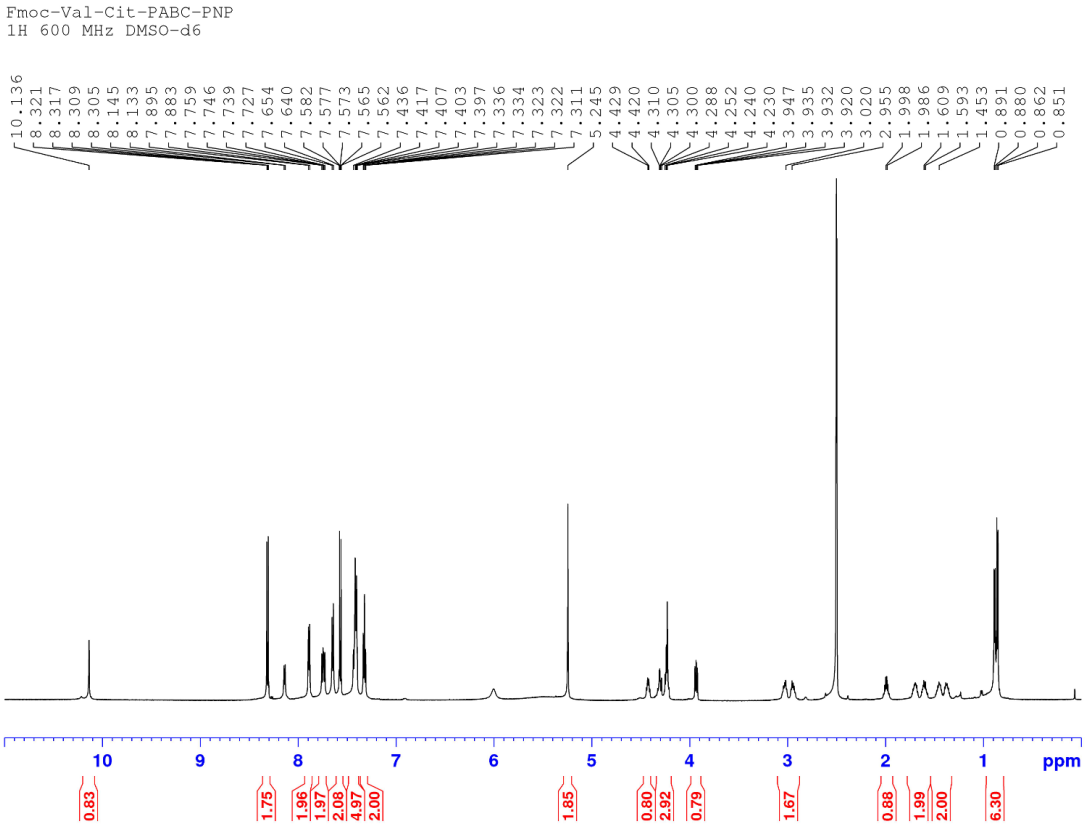

^{1}H NMR spectrum (600 MHz, DMSO-*d*6): compound **2-21**

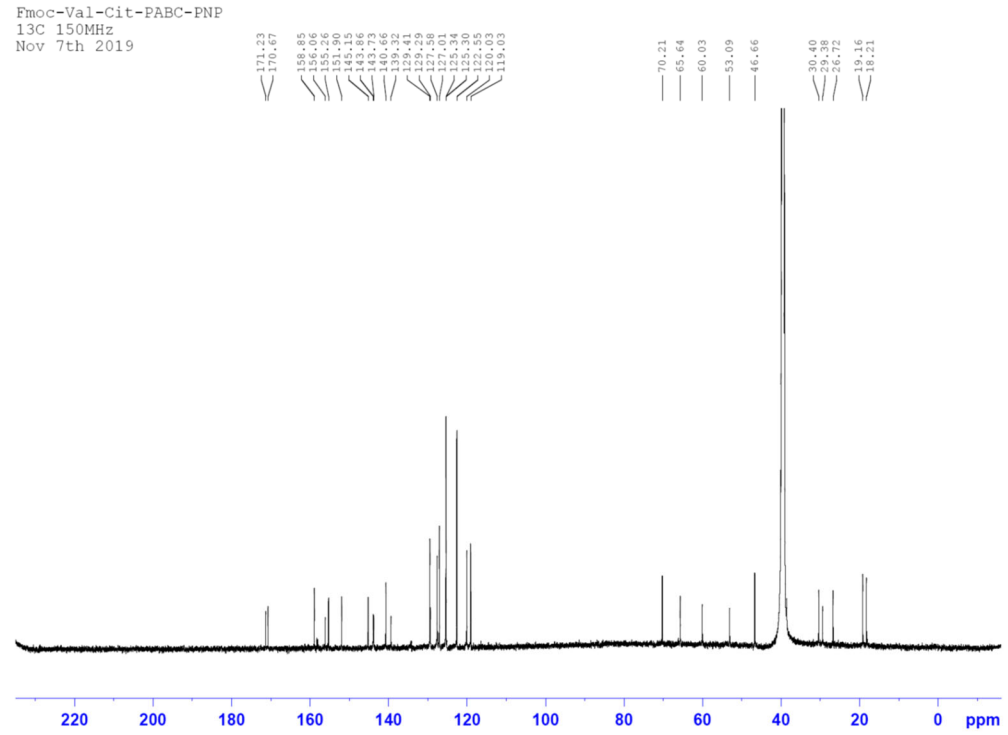

^{13}C NMR spectrum (150 MHz, DMSO-*d*6): compound **2-21**

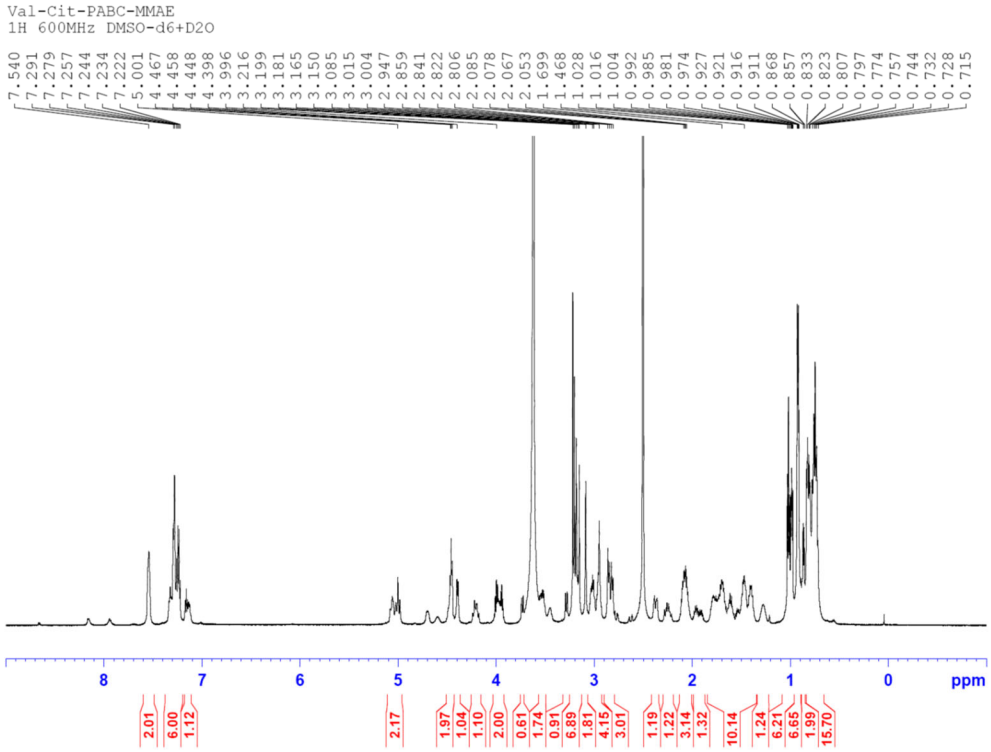

^{1}H NMR spectrum (600 MHz, DMSO-d6): compound **2-22** (Commercial product).

Chapter 3: Synthetic antibody-rhamnose cluster conjugates show potent complement-dependent cell killing by recruiting natural antibodies

Part of this work was published in *Chemistry-A European Journal* (**2022**, *28*, e202200146)

3.1 Introduction

Complement-dependent cytotoxicity (CDC) is one of the major mechanisms for antibody-mediated killing of target cells.[87] Nevertheless, many therapeutic antibodies are limited by their low potency in stimulating a strong complement-dependent cytotoxicity. One strategy to achieve complement-dependent targeted cell killing is to explore novel bi-functional molecules consisting of a target-binding motif and a specific antigenic structure to recruit naturally abundant antibodies, such as the anti-αGal and anti-rhamnose (anti-Rha) antibodies to the target cells.[88-92] The α-Gal epitope, Gala1-3Galb1-4GlcNAc-R, is expressed abundantly on glycolipids and glycoproteins in non-human primates and New World monkeys, but it is not present on human cells. As a result, humans produce large quantities of anti-αGal antibodies in circulation: up to 1-2% of total serum IgG and 3-8% of total IgM natural antibodies are anti-αGal antibodies.[93-95] The interaction between αGal and anti-αGal antibodies are largely responsible for the rejection of the transplanted tissues following xenotransplantation, mainly due to activation of the complement systems.[96] On the other hand, anti-Rha antibodies are also abundant in human sera, which have been found even at higher concentrations than the anti-αGal antibodies in human serum samples.[89, 97, 98] Moreover, the majority of anti-Rha antibodies are of IgM type, while most of the anti-

αGal antibodies are of IgG type.[89, 99-101] It has been shown that the IgM type antibody is much more efficient than the monomeric IgG type antibody to initiate complement-dependent cytotoxicity, as the IgMs is inherently a pentamer that can efficiently bind to the multi-subunit C1q complement protein in a multivalent fashion to trigger the downstream effects, while the IgG antibody must form hexamer complex to engage an efficient multivalent interactions with the multi-subunit C1q complement protein.[102-104]

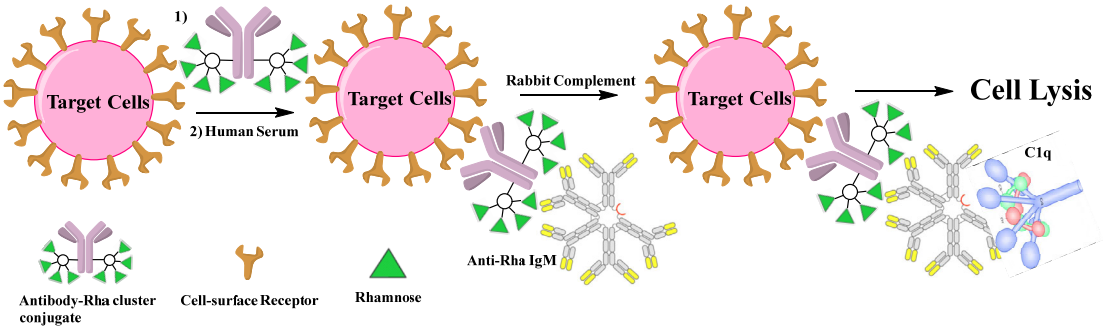

Figure 3-1. Homogenous antibody conjugates that recruit serum antibodies and initiate CDC.

To explore the potential of natural anti-αGal or anti-Rha antibodies for targeting cancer, bacterial and/or virus-infected cells, several groups have previously designed and synthesized bi-functional small molecules, by conjugating a target-binding ligand to an αGal oligosaccharide or a rhamnose moiety, to recruit natural anti-αGal or anti-Rha antibodies for complement-dependent cell killing.[88-92] For example, Kiessling and co-workers have reported the synthesis of αGal-integrin ligand conjugates for targeting cancer;[88, 89] Yi and co-workers have assembled bi-functional liposomes incorporating rhamnose and folic acid to recruit anti-Rha antibodies to target folate receptor-overexpressing tumor cells.[92] Recently, Fukase and co-workers have reported the first

synthesis of αGal oligosaccharide-antibody conjugates, and the cell-based assays have shown that the presentation of multiple copies of the αGal epitopes (multi-valency) was important for an efficient cancer cell killing.[70] While this study provides proof-of-concept data indicating the feasibility of using antibody-αGal conjugates for targeted cancer cell killing, the lysine-based antibody-αGal conjugation and the reduction of antibodies into monomeric antibodies for thiol-maleimide ligation both lead to mixtures of heterogeneous conjugates. We report in this paper a highly efficient chemoenzymatic synthesis and comparative study of structurally well-defined, homogeneous conjugates of an antibody with rhamnose and αGal oligosaccharide clusters, respectively. Trastuzumab, a therapeutic antibody targeting HER2 over-expressing cancer cells, was selected as a model antibody, and the carbohydrate antigens were introduced specifically at the Fc glycosylation site by a chemoenzymatic Fc glycan remodeling approach. The resulting glycoengineered antibodies carrying the rhamnose and αGal oligosaccharide clusters were designed to recruit natural anti-Rha and anti-αGal antibodies, respectively, for targeted cell killing (Figure 3-1). It was found that the antibody-rhamnose cluster conjugates were much more efficient than the antibody-αGal cluster conjugate for the complement-dependent cell killing. During the submission of this manuscript, Wu and co-workers have reported rituximab-rhamnose conjugates by reaction of partially reduced rituximab with a maleimide-functionalized rhamnose derivative, and the resulting antibody-rhamnose conjugates demonstrate antitumor efficacy in a xenograft model.[105] This work was published in Chemistry-A European Journal in 2022.[106]

3.2 Results and Discussion

Chemical synthesis of the dibenzocyclooctyne (DBCO)-functionalized rhamnose and αGal clusters

As a general synthetic design, we sought to introduce azide tags into the antibody through the chemoenzymatic Fc glycan remodeling method that we have recently described,[82] and then to Click the synthetic oligosaccharide antigens to the antibody to construct the conjugates. For this purpose, we first synthesized the DBCO-functionalized rhamnose and rhamnose clusters (Scheme 3-1). The synthesis of DBCO-tagged rhamnose (**3-3**) was achieved by reaction of rhamnose derivative **3-1** with the NHS-active ester (**3-2**) (Scheme 3-1a). For constructing a tetravalent rhamnose cluster, we chose a tri-lysine core as the scaffold. The synthesis of the tri-lysine core (**3-7**) was shown in Scheme 3-1b. At the C-terminus of **3-4**, a short N-methyl ethylenediamine spacer with an Fmoc protecting group was introduced to provide a handle for further functionalization. The N-methyl spacer (**3-5**) was specifically chosen to provide linker stability without premature release.[107, 108] For the synthesis of the tetravalent rhamnose cluster (**3-13**), the tri-lysine core (**3-7**) was reacted with NHS-activated rhamnose derivative (**3-10**) to give the rhamnose cluster (**3-11**). After de-O-acetylation followed by removal of the Fmoc group, the resulting compound (**3-12**) was reacted with the NHS activated ester (**3-2**) to give the DBCO-tagged rhamnose cluster (**3-13**) after LH20 size exclusion chromatography (Scheme 3-1c).

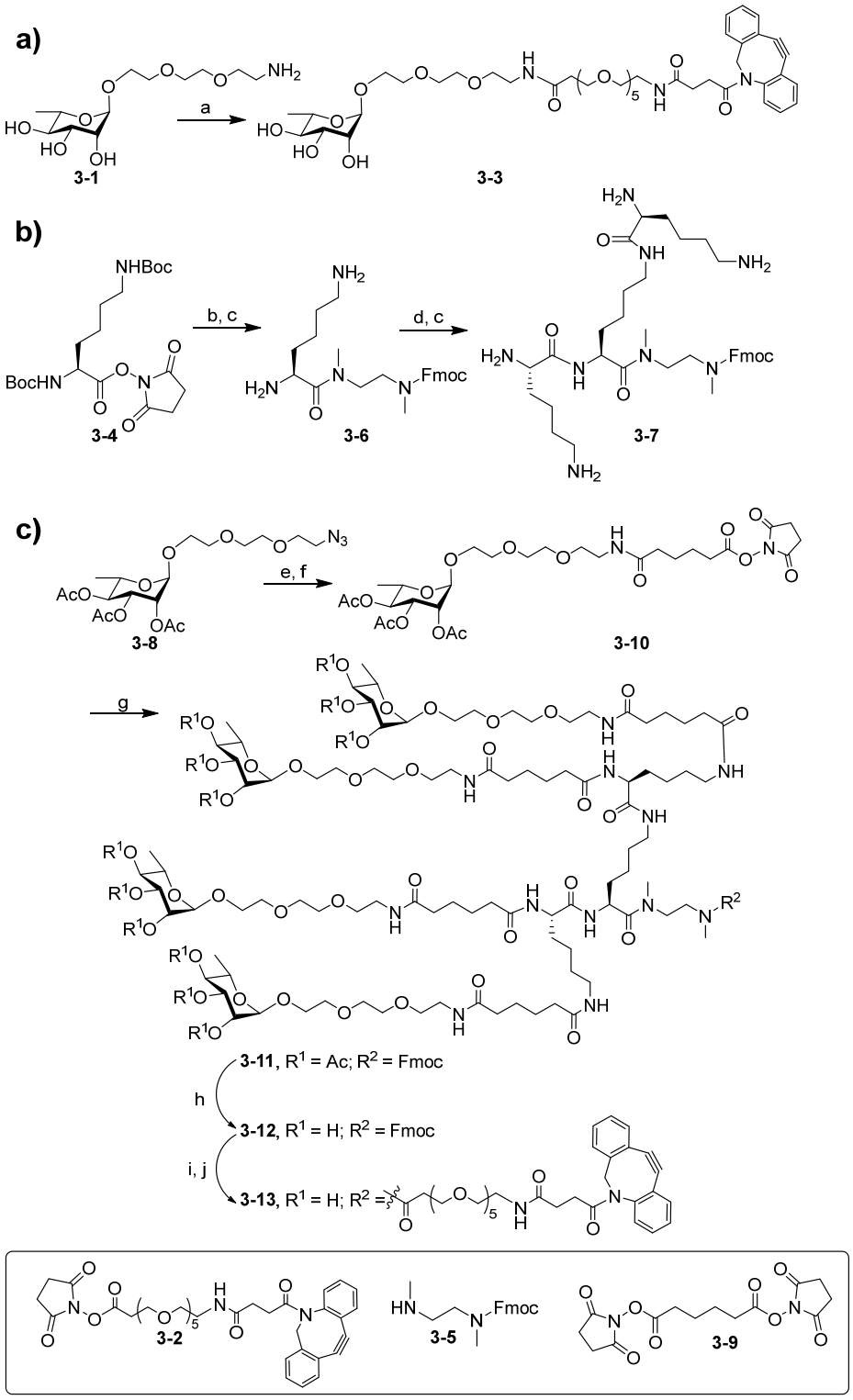

Scheme 3-1. Chemical synthesis of the monovalent and multivalent rhamnose-based antibody recruiting molecules. a) **3-2**, DMSO, Et_3N, r.t., 60%; b) **3-5**, CH_2Cl_2, Et_3N, r.t.; c) TFA/ CH_2Cl_2, (1:1, v/v) 0ºC; d) **3-4**, CH_2Cl_2, Et_3N, r.t.; e) Pd/C, H_2, MeOH; f) **3-9**, CH_2Cl_2, Et_3N, r.t., 79% over two steps; g) 7, DMSO, Et3N, r.t.; h) hydrazine, H_2O, r.t.; i) 20% piperidine, r.t.; j) **3-2**, DMSO, Et_3N, r.t., 73% over four steps.

To construct the DBCO-functionalized αGal trisaccharide and its cluster, we first synthesized the αGal trisaccharide following a previously published procedure.[109] Then the amine-functionalized αGal was reacted with **3-2** to give the DBCO-functionalized αGal trisaccharide (**3-15**) (Scheme 3-2a). To synthesize a cluster of α-Gal trisaccharide, **3-14** was activated as an NHS ester, then it was reacted with the tri-lysine core (**3-7**) to give the tetravalent α-Gal oligosaccharide (**3-17**). Finally, deprotection of **3-17** followed by reaction with **3-2** gave the desired DBCO-functionalized α-Gal trisaccharide cluster (**3-18**) (Scheme 3-2b).

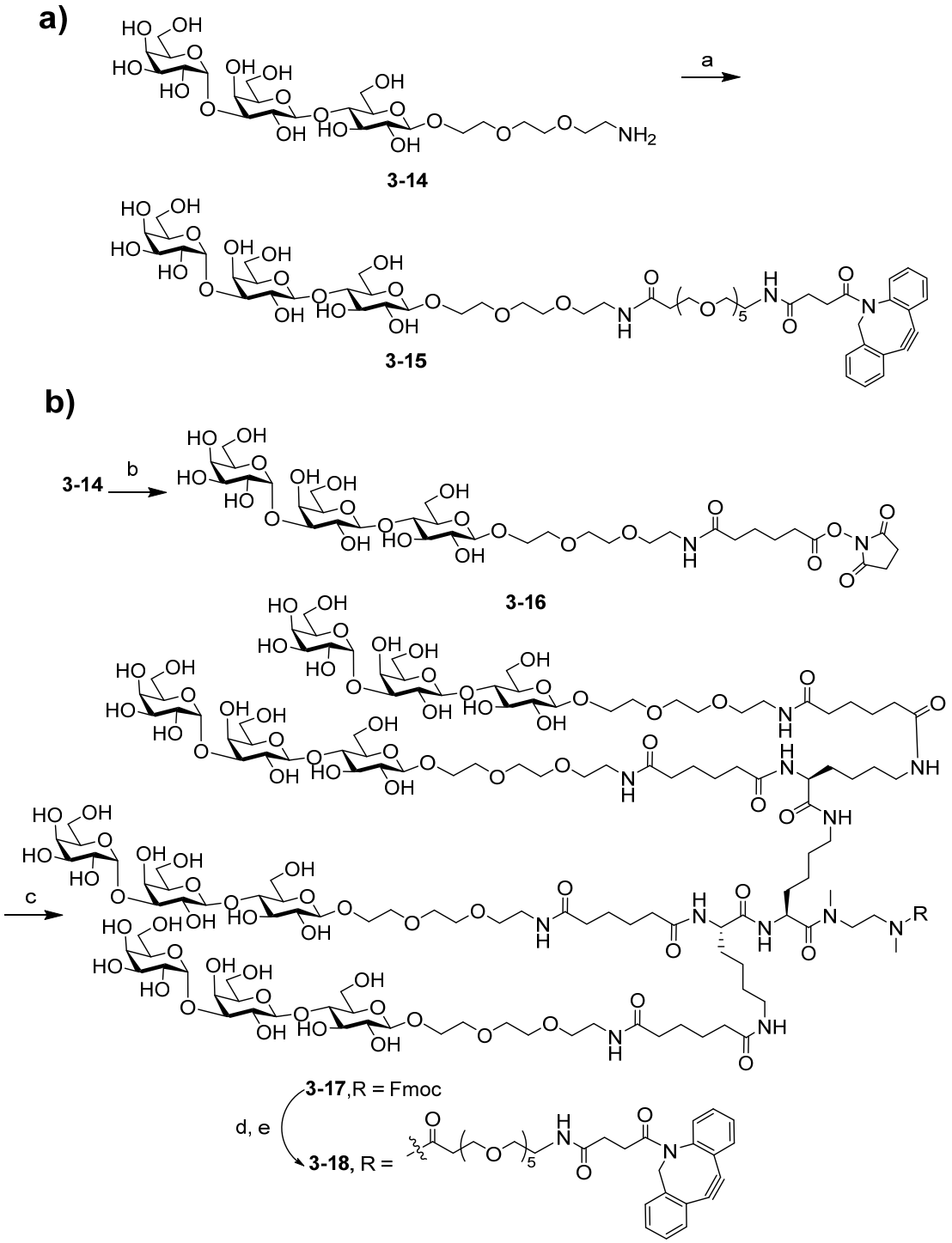

Scheme 3-2. Chemical synthesis of the monovalent and multivalent α-Gal-based antibody recruiting molecules. a) **3-2**, DMSO, Et_3N, r.t., 58%; b) **3-9**, DMSO, Et_3N, r.t., 67%; c) **3-7**, DMSO, Et_3N, r.t.; d) piperidine, r.t.; e) **3-2**, DMSO, Et_3N, r.t., 65% over three steps.

Chemoenzymatic synthesis of the antibody-rhamnose and αGal cluster conjugates

With the successful synthesis of DBCO-functionalized αGal and rhamnose clusters, we sought to construct the antibody conjugates utilizing the Fc glycan-mediated chemoenzymatic modification approach, which is validated to achieve antibody conjugates with high homogeneity and great efficiency.[28, 65, 69, 74, 82] Thus, trastuzumab was trimmed with immobilized Endo-S2, followed by efficient Fc modification with glycosynthase EndoS2-D184M and the di-N_3-SCT-oxazoline to yield the azide functionalized antibody (**3-20**).[82] Then, the homogenous antibody-rhamnose (**3-21** and **3-22**) and antibody-αGal-conjugates (**3-23** and **3-24**) were generated by incubating **3-20** at 5 mg/mL with the DBCO derivatives (**3-3**, **3-13**, **3-15**, and **3-18**, respectively, 12 molar equivalents per antibody) at room temperature (Scheme 3-3).

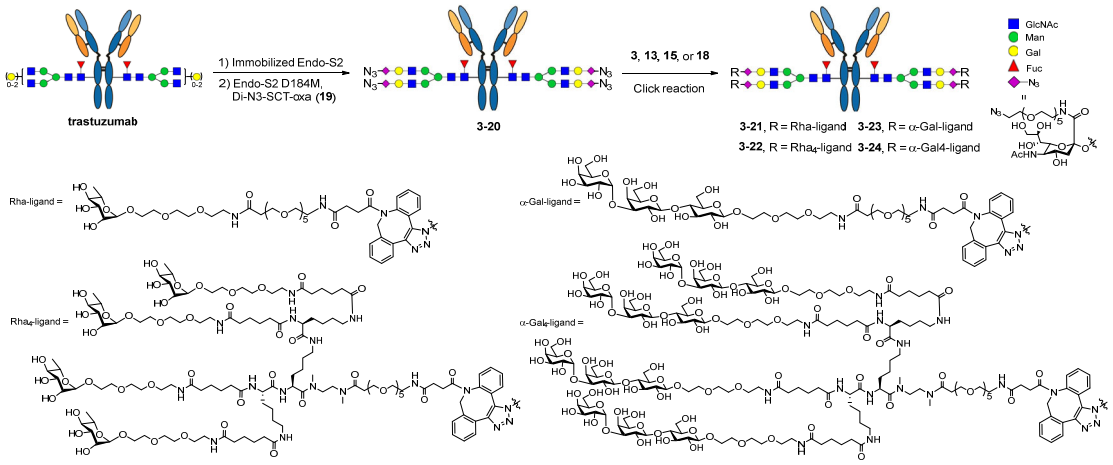

Scheme 3-3. Synthesis of the antibody conjugates via chemoenzymatic Fc glycan remodeling followed by Click reaction

The reactions were monitored by LC-MS analysis. It was found that the Click reaction with DBCO derivatives (**3-3** and **3-15**) were completed within 10 h, while the

reactions of DBCO derivatives **3-13** and **3-18** took a much longer time, which required about 24 h to complete, probably due to the bulkiness of the Clickable oligosaccharide clusters. The final products were purified by affinity chromatography on a protein A column in an excellent isolated yield. The identity and homogeneity were confirmed by LC-ESI-MS analysis of both the intact antibodies (Figures 3-2a-d) and the Fc domains after IdeS treatment (Figures 3-2e-h). The observed molecular mass (deconvolution data) of **3-21**, **3-22**, **3-23** and **3-24** was 154521 Da, 161718 Da, 155882 Da and 167156 Da, which matched well with their calculated value of 154518 Da, 161714 Da, 155879 Da and 167159 Da, respectively. In addition to the intact antibody analysis, LC-ESI-MS analysis of the monomeric Fc domain of **3-21**, **3-22**, **3-23** and **3-24** released from the IdeS treatment of the antibody conjugates further confirmed the site-selectivity and homogeneity of the final products (Figures 3-2e-h). The raw LC-ESI-MS data were shown in Figure 3-3 and Figure 3-4.

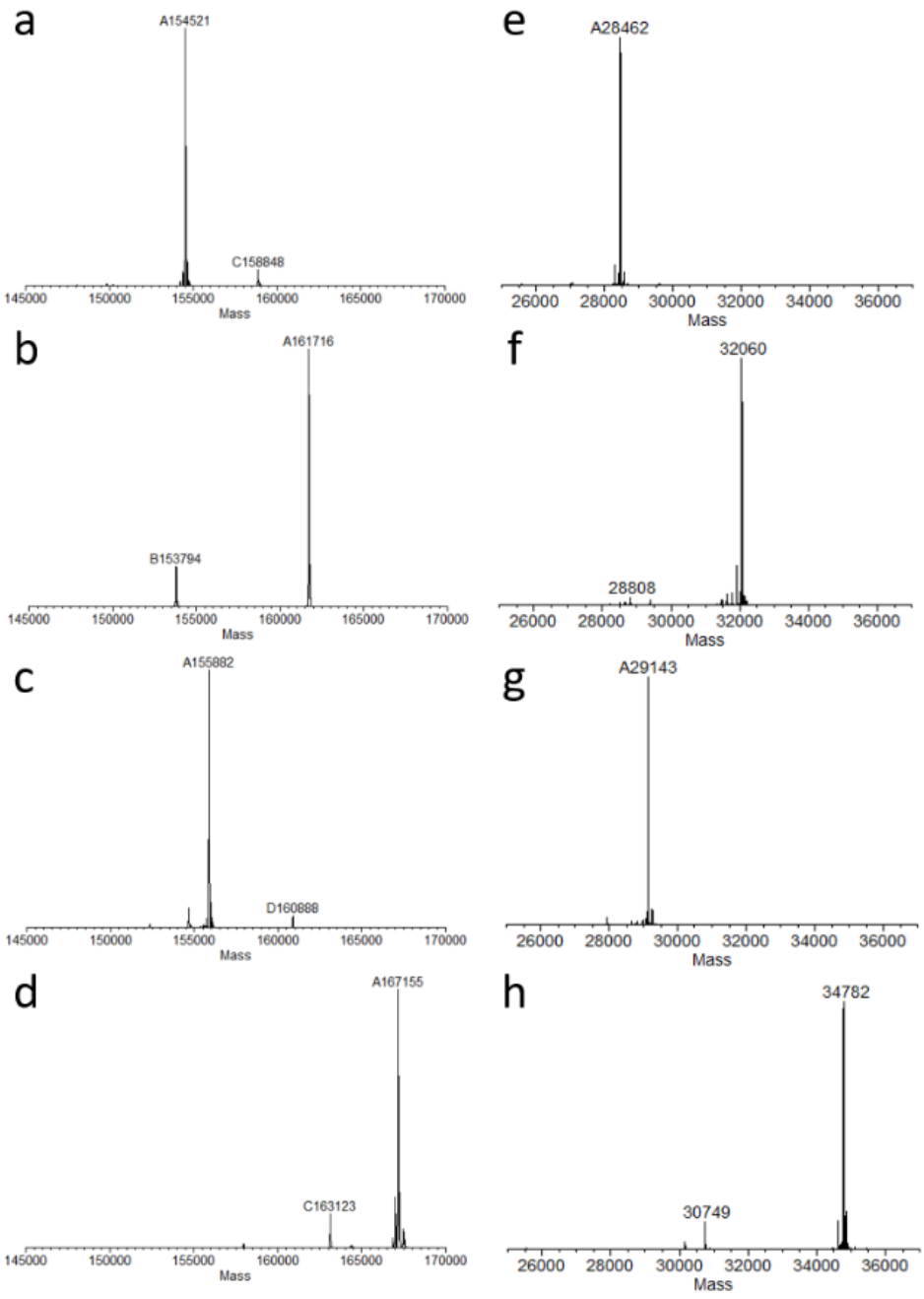

Figure 3-2. LC-ESI-MS analysis of the intact conjugates (**3-21**, **3-22**, **3-23** and **3-24**) and the Fc domains released by IdeS treatment. a) the deconvoluted mass of intact rhamnose conjugate (**3-21**); b) the deconvoluted mass of intact rhamnose cluster conjugate (**3-22**); c) the deconvoluted mass of intact α-Gal conjugate (**3-23**); d) the deconvoluted mass of intact α-Gal cluster conjugate (**3-24**)**;** e) the deconvoluted mass of the Fc domain of rhamnose conjugate (**3-21**); f) the deconvoluted mass of the Fc domain of rhamnose cluster conjugate (**3-22**); g) the deconvoluted mass of the Fc domain of α-Gal conjugate (**3-23**); h) the deconvoluted mass of the Fc domain of α-Gal cluster conjugate (**3-24**).

The use of the selectively azide-tagged biantennary *N*-glycan for Fc glycan remodeling and subsequent conjugation has several advantages, including the site-specific conjugation and the preservation of the natural Fc *N*-glycan core after remodeling, which could be important for maintaining antibody stability and favorable pharmacokinetic property. Our previous studies have demonstrated that glycosynthase EndoS2-D184M possesses quite relaxed substrate specificity in transferring different natural and selectively modified glycan oxazolines,[66, 75, 82, 110] Recently, we have shown that both the wild type and the EndoS2-D184M mutant of Endo-S2 can efficiently transfer selectively azide-functionalized Manb1,4-GlcNAc oxazoline to the deglycosylated antibody for constructing homogeneous antibody-drug conjugates.[110] This method could provide an alternative approach for making the antibody-rhamnose or aGal cluster conjugates.

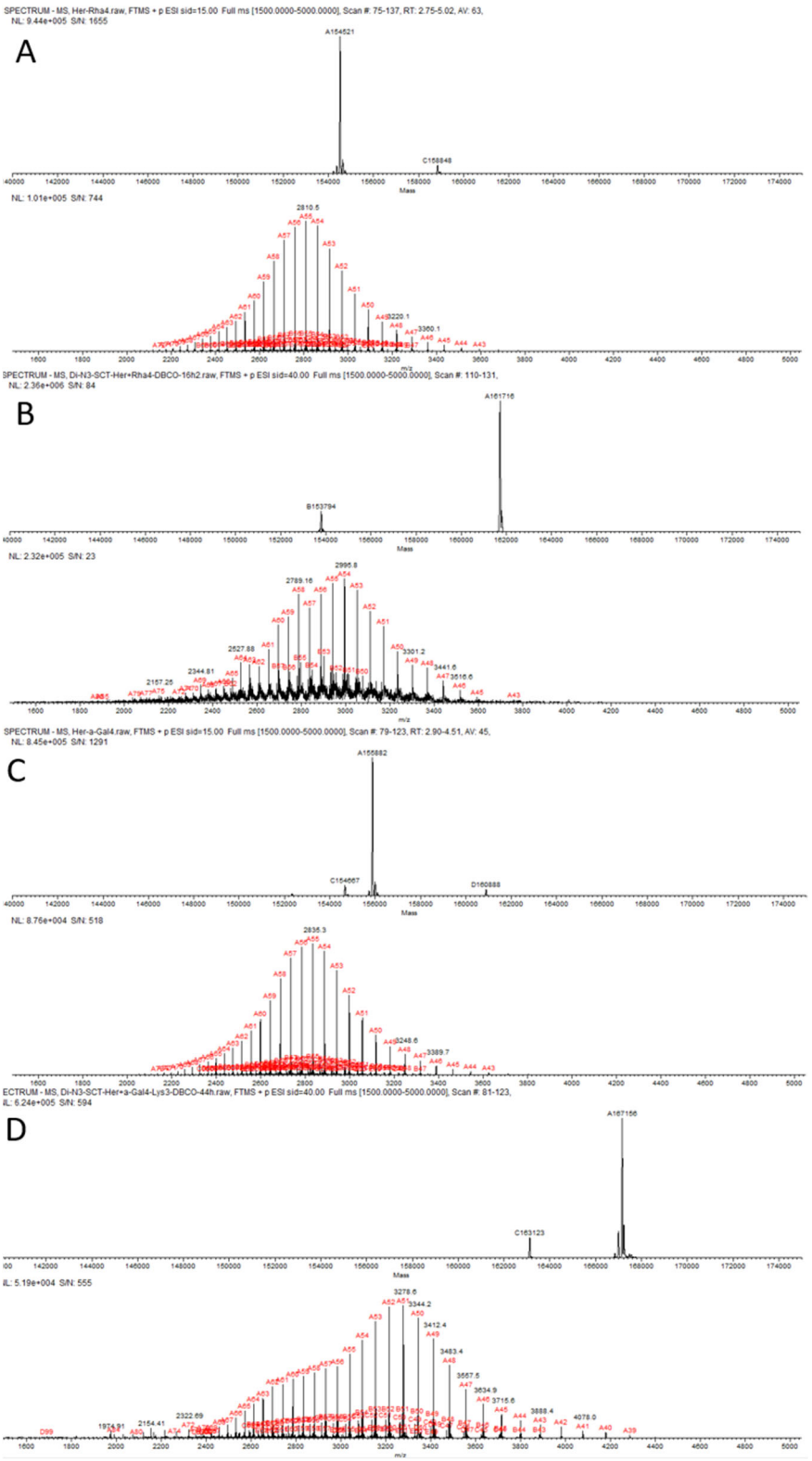

Figure 3-3. LC-ESI-MS analysis of the intact antibody conjugates. A) deconvoluted mass and raw data of intact antibody **3-21**; B) deconvoluted mass and raw data of intact antibody **3-22**; C) deconvoluted mass and raw data of intact antibody **3-23**; D) deconvoluted mass and raw data of intact antibody **3-24**.

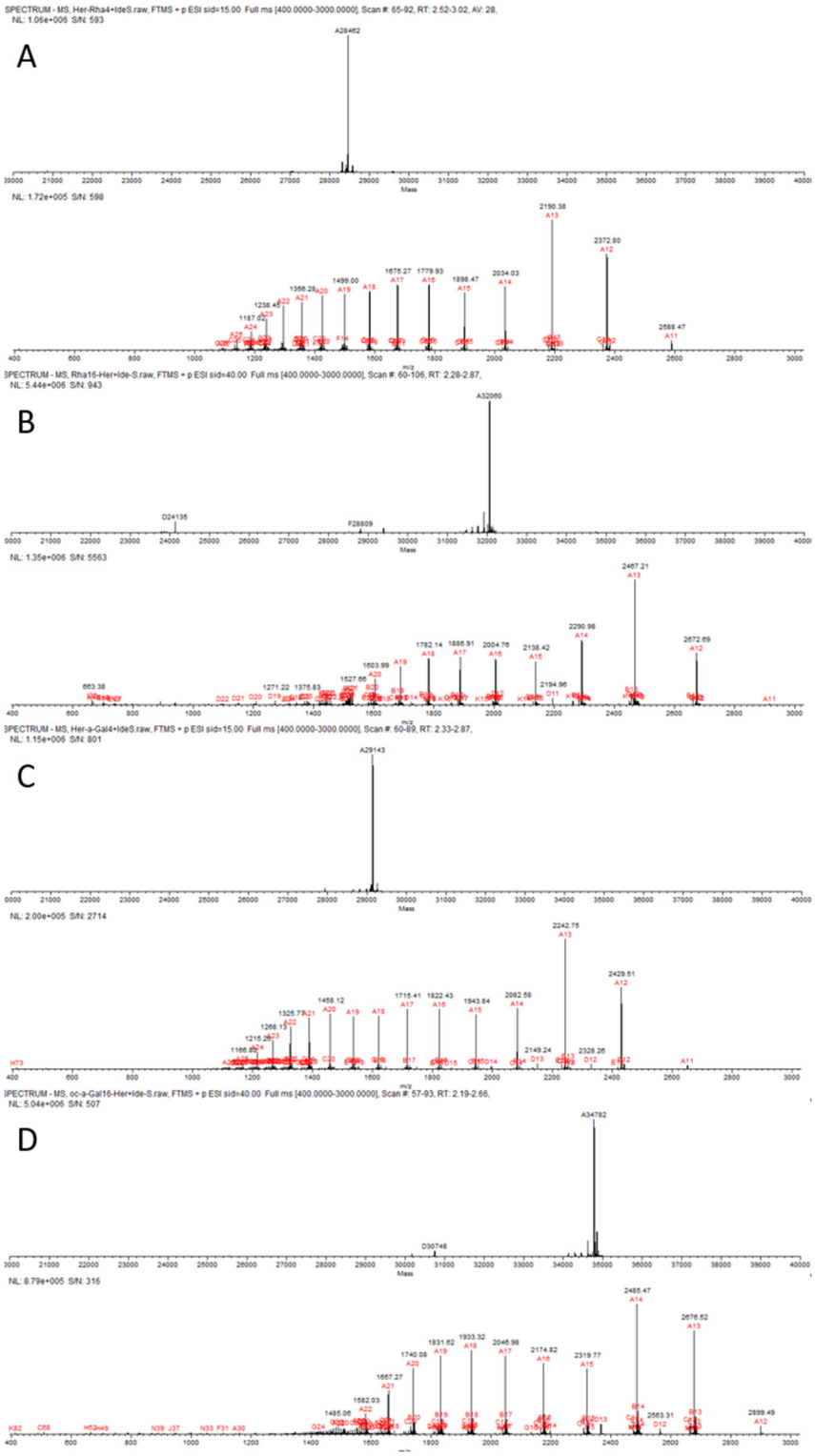

Figure 3-4. LC-ESI-MS analysis of the Fc domains released by IdeS treatment of the antibody conjugates A) deconvoluted mass and raw data for Fc domains of **3-21**; B) deconvoluted mass and raw data for Fc domains of **3-22**; C) deconvoluted mass and raw data for Fc domains of **3-23;** D) deconvoluted mass and raw data for Fc domains of **3-24**.

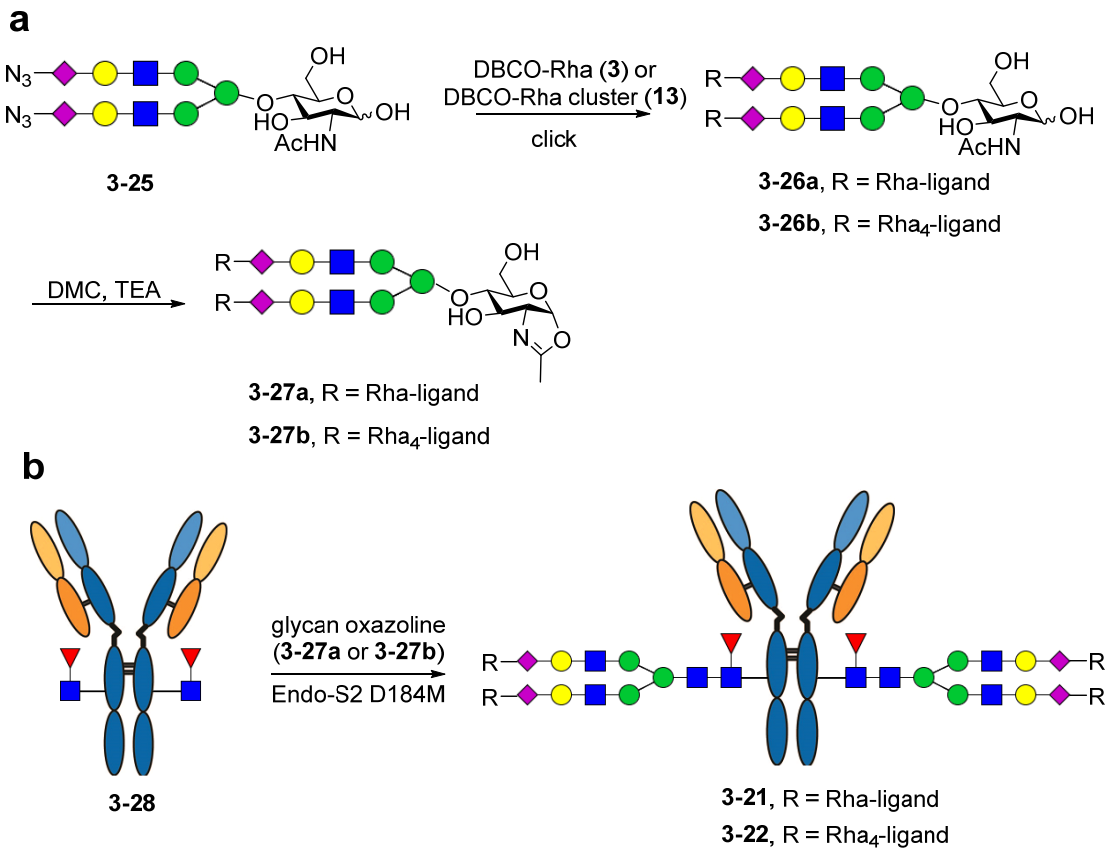

Scheme 3-4. Direct enzymatic transfer of Rha ligand-loaded glycans to antibodies using the Endo-S2 D184M

Given the broad substrate specificity of the Endo-S2 mutant, we reasoned that the enzyme might be able to transfer ligand-preloaded glycan oxazolines to make the final antibody conjugates in a single step. To test this hypothesis, we first conjugated the monomeric and tetrameric rhamnose to the azide-functionalized *N*-glycan using the ring-strain-promoted cycloaddition reaction to give **3-26a** and **3-26b**, respectively. The ligand-functionalized sialylated glycan was then converted to oxazolines **3-27a** and **3-27b** using the single-step glyan oxazoline formation reaction with dehydrating agent 3-chloro-1,3-dimethylimidazolinium chloride (DMC) in water.[111, 112] We found that EndoS2-D184M could tolerate the rhamnose modification on the glycan oxazoline and

could smoothly transfer the antigen-loaded glycan to the deglycosylated trastuzumab (**3-28**) to give the corresponding antibody conjugate (**3-21**). Using 30 equivalents of the glycan oxazoline (**3-27a**), the reaction completed within 40 min (Figure 3-5). However, we found that the larger Rha cluster-containing glycan oxazoline (**3-27b**) was transferred much more slowly than the simpler Rha-loaded glycan oxazoline (**3-27a**). (Scheme 3-5) Interestingly, the major product was a monosubstituted antibody when the reaction was carried out for 60 min (Figure 3-6). The results suggest that the Endo-S2 mutant could tolerate the modifications on the glycan oxazolines, but a modification with a larger moiety such as the Rha clusters slows down the transglycosylation reaction, which would require optimization of the conditions to drive the reaction to completion.

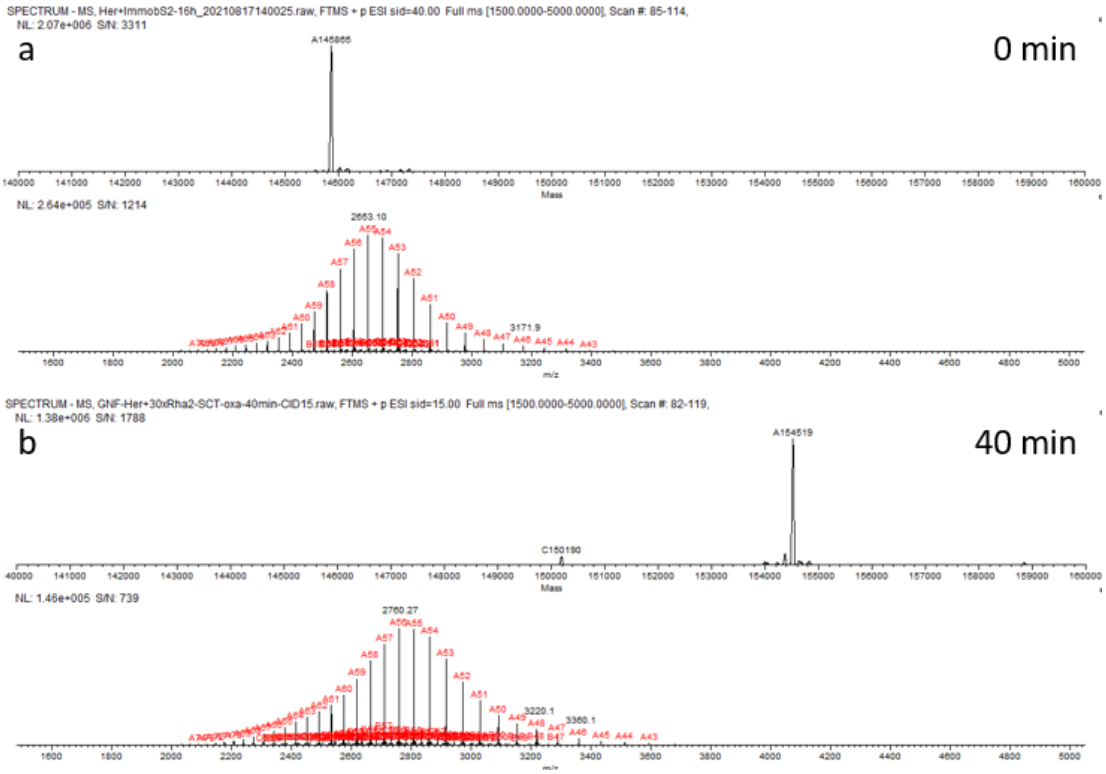

Figure 3-5. The LC-ESI-MS monitoring of the glycosylation reactions between azide-glycan oxazoline **3-27a** and antibody **3-28** catalyzed by Endo-S2 D184M. A mixture of the deglycosylated antibody **3-28** (0.5 mg, 3.3 nmol, 25 mg/mL), glycan oxazoline **3-27a** (0.44 mg, 100 nmol, 30 *mol. equiv.* of the antibody), and the mutant enzyme (0.1 mg/mL) in a Tris buffer (100 mM, pH 7.2) was incubated at 30 °C and the reaction was monitored by LC-ESI-MS analysis of the intact antibodies at 20 min intervals. a) the deconvoluted mass of **3-28**; b) the deconvoluted mass of the reaction mixture catalyzed by Endo-S2 D184M at 40 min.

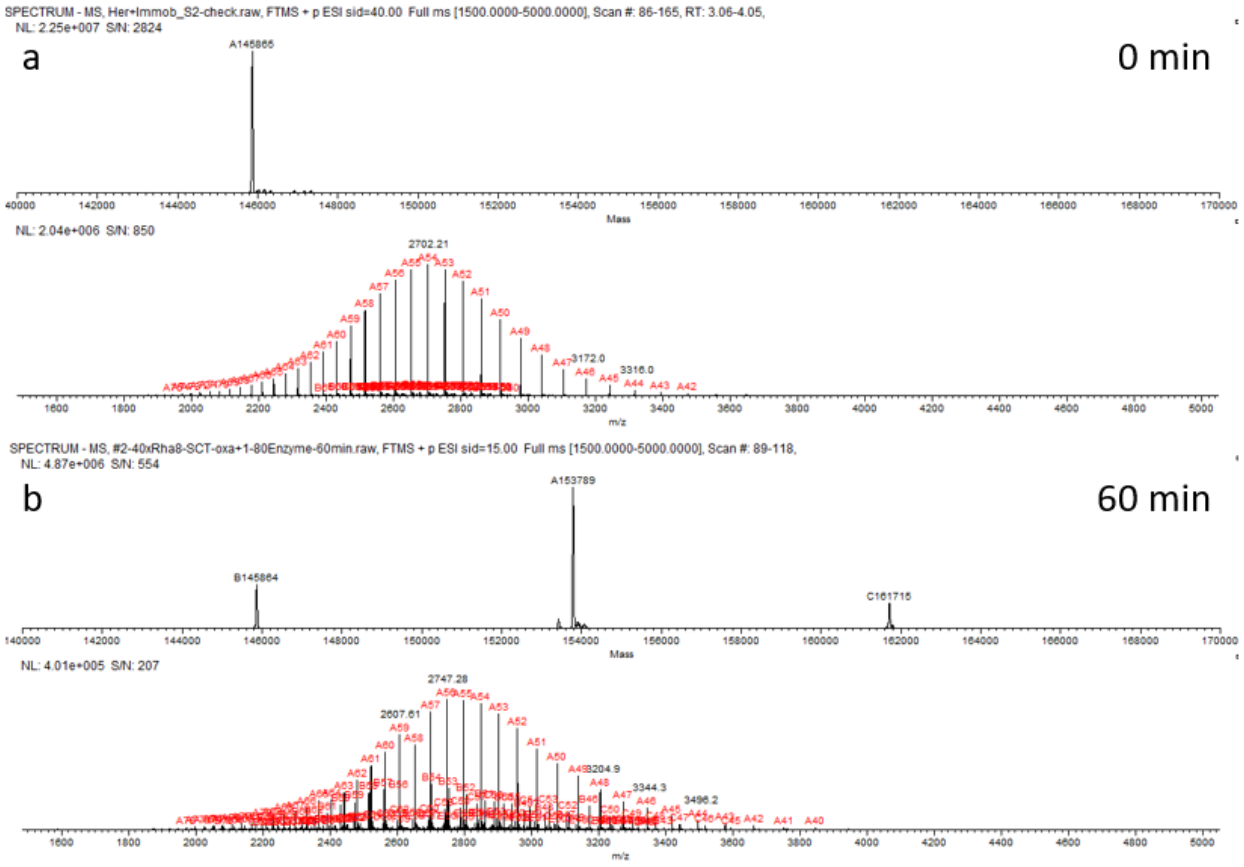

Figure 3-6. The LC-ESI-MS monitoring of the glycosylation reactions between azide-glycan oxazoline **3-27b** and antibody **3-28** catalyzed by Endo-S2 D184M. A mixture of the deglycosylated antibody **3-28** (0.1 mg, 3.3 nmol, 25 mg/mL), glycan oxazoline **3-27b** (0.44 mg, 100 nmol, 40 *mol. equiv.* of the antibody), and the mutant enzyme (0.4 mg/mL) in a Tris buffer (100 mM, pH 7.2) was incubated at 30 ºC and the reaction was monitored by LC-ESI-MS analysis of the intact antibodies at 20 min intervals. a) the deconvoluted mass of **3-28**; b) the deconvoluted mass of the reaction mixture catalyzed by Endo-S2 D184M at 60 min.

Cell-based assay of the complement-dependent cytotoxicity of the antibody conjugates.

To compare the potency of the conjugates **3-21**, **3-22**, **3-23** and **3-24** we studied the *in vitro* cytotoxicity of the antibody conjugates with BT474 (high HER-2 expressing) and T47D (low HER-2 expressing) cells. In this assay, the anti-aGal and anti-rhamnose antibodies were provided by commercially available human serum.

Serum-free RPMI media was used to carry out the assays to avoid the possible αGal contamination from the FBS. The complement required to lyse the cells was provided by standard rabbit complement. Since rabbit complement itself could lysate cells even at relatively low concentration, we screened for the best combination amount of human serum and rabbit complement to minimize the effect of non-specific CDC. We found that 10 μL of human serum (Millipore Sigma) and 4 μL of rabbit complement (Cedarlane Laboratories) per well gave the best balance between non-specific killing caused by the complement (about 10-15%) and the efficacy of the conjugates. Under this condition, we found that conjugate **3-22**, with sixteen rhamnose antigen, was the most potent antibody conjugate, which killed more than 70% of the HER2 high-expression cancer cells within 2 h (Figure 3-5a). The calculated EC50 value for **3-22** was 0.57 nM (92 ng/mL). To our amazement, the conjugate **3-21**, with only four rhamnose antigen, could also lyse up to 50% of BT474 cells in relatively short period of time (Figure 3-7a). The reason that the best antibody-rhamnose conjugates did not reach to 100% target cell killings may be due to the varied levels of HER2 expression of BT474 and/or the unstable nature of the complements during the incubation of the assays. It is expected that these results could be more efficient when the complement is persistent as in the case of *in vivo* situation. In contrast, the killing of the αGal conjugates (**3-23** and **3-24)** were much weaker than the antibody-rhamnose cluster conjugates (**3-21** and **3-22**). It was found that conjugate **3-24**, with sixteen αGal epitope managed to lyse up to 20% of the BT474, while conjugate **3-23**, with four αGal epitope could lyse only about 10% of the BT474 at 25 μg/mL. (Figure 3-7b) To eliminate the possibility that the difference between the rhamnose conjugates and the

αGal conjugates was caused by the specific batch of the human serum that was used for the assay, the cytotoxicity assay was also carried out by using the human serum obtained from a different source (Cosmo Bio USA). The results were almost identical (Figure 3-8). Given the fact that the average anti-rhamnose antibodies in human blood is usually higher than the anti-aGal antibodies,[89, 97] with a higher percentage of the anti-rhamnose antibodies being of the IgM type,[89, 99, 101] These results suggest that recruiting the more potent anti-Rha IgM antibodies could be a more efficient strategy than targeting the anti-aGal antibodies. For the HER-2 low-expressing cell line, none of these four antibody conjugates showed cytotoxicity in a dose-dependent manner up to 50 μg/mL (Figure 3-7c, 3-7d). This study demonstrates that the antibody-rhamnose cluster conjugates are a promising construct for augmenting potent complement-dependent cytotoxicity for targeted cell killing.

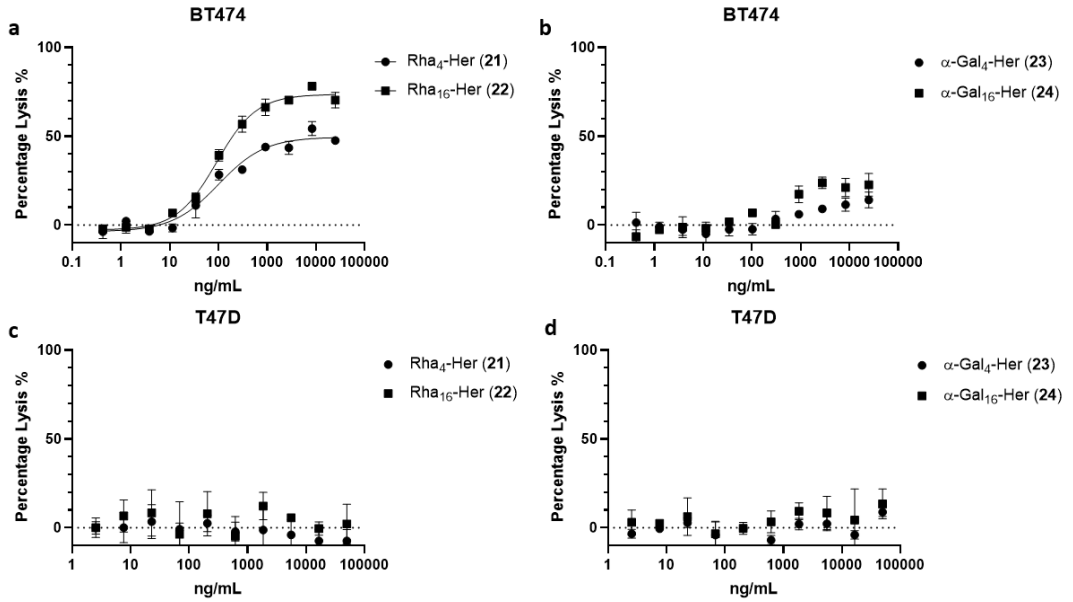

Figure 3-7. Cell killing assays for breast cancer cell lines a) rhamnose conjugates with BT-474 (HER2 overexpression); b) α-Gal conjugates with BT-474 (HER2 overexpression); c) rhamnose conjugates with T47D (HER2 low expression); d) α-Gal conjugates with T47D (HER2 low expression). All assays were performed in triplicate.

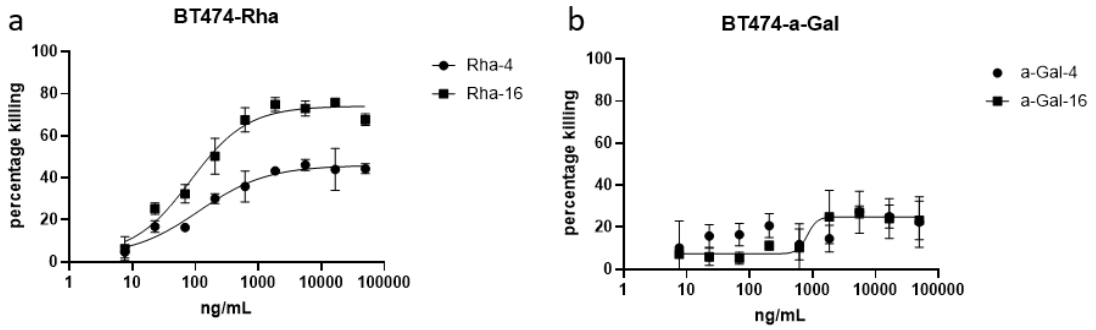

Figure 3-8. Cell killing assays for breast cancer cell lines a) Rhamnose conjugates with BT-474 (HER2 overexpression); b) α-Gal conjugates with BT-474 (HER2 overexpression). The human serum was purchesed from Cosmo Bio USA. All assays were performed in triplicate.

3.3 Conclusion

A highly efficient chemoenzymatic synthesis of homogeneous antibody-rhamnose cluster and antibody-αGal cluster conjugates is described. The construction of the antibody conjugates was achieved by site-specific chemoenzymatic Fc glycan remodeling followed by a Click reaction. Alternatively, the antibody-rhamnose conjugate could also be achieved by direct Fc glycan remodeling with a rhamnose-preloaded glycan oxazoline. A comparative study reveals that the antibody-rhamnose cluster conjugates are more potent than the corresponding antibody-αGal oligosaccharide conjugates in recruiting natural antibodies for targeted cancer cell killing. These results suggest that antibody-rhamnose conjugates represent a promising strategy for augmenting complement-dependent targeted cell killing by recruiting the more effective natural anti-Rha IgM antibodies. Future studies should be directed to evaluation of the cytotoxicity of the antibody conjugates in animal models.

3.4 Experimental Section

Materials and Methods

Chemicals, reagents, and solvents were purchased from Sigma−Aldrich and/or TCI and used as received unless otherwise specified. Monoclonal antibody Hercptin was purchased from Premium Health Services Inc. (Columbia, MD). All moisture sensitive reactions were carried out under argon atmosphere, using standard Schlenk techniques. All dry solvents were prepared according to standard procedures. Thin-layer chromatography was performed on silica gel 60-F_{254} on glass plates (Merck) and revealed with *p*-anisaldehyde stain. Silica gel (200−425 mesh) used in flash chromatography for large-scale reactions was purchased from Sigma-Aldrich. Columns for flash chromatography for small-scale reactions were performed on Isolera One system with ZIP KP-Sil columns (Biotage) with elution condition specified for each target compound. Solvent gradients were given refer to stepped gradients and concentrations are reported as % v/v. Preparative HPLC was performed with Waters 1525 Binary HPLC pump coupled with 2489 UV/Vis Detector under UV 214 nm and 280 nm with a Waters Symmetry C18 column (7 μm, 19 × 300 mm) using water containing 0.1% trifluoracetic acid as phase A, MeCN containing 0.1% trifluoracetic acid as phase B. Semi-preparative HPLC for the toxic payloads was performed on the same instrument with an Aglient Eclipse XDB-C18 column (5 μm, 9.4× 250 mm) using water containing 0.1% formic acid as phase A, MeCN containing 0.1% formic acid as phase B.

Purification of antibody and antibody conjugates using AKTA prime plus FPLC system.

The FPLC system (GE Healthcare) was used for purification of the functionalized antibodies equipped with 1mL HiTrap protein A column (GE Heatlthcare). Concentration of antibodies was determined by NanoDrap 200c (Thermo Scientific).

LC-ESI-MS analysis of antigen-DBCO payloads

LC-MS for glycans, glycopeptides and payload derivatives were performed on HPLC-SQ2 detector (Waters) with a Waters XBridge C18 column (3.5 μm, 2.1× 50 mm) using water containing 0.1% formic acid as phase A, MeCN containing 0.1% formic acid as phase B. The analytical HPLC for payload derivatives was analyzed with an Aglient Eclipse SDB-C18 column (5 μm, 3.0× 250 mm) under UV 214 nm and 280 nm with methods specialized for each compound. HR-ESI-MS was performed with Exactive Plus Orbitrap Mass Spectrometer (Thermo Scientific) equipped with a Waters XBridge C18 column (3.5 μm, 2.1× 50 mm).

LC-ESI-MS analysis of intact antibody derivatives.

LC-ESI-MS analysis of intact tagged antibodies and antibody-drug conjugates was performed with Exactive Plus Orbitrap Mass Spectrometer (Thermo Scientific) equipped with a Waters XBridge BEH300 C-4 column (3.5 μm, 2.1 × 50 mm) with gradient elution of water containing 0.1% formic acid as phase A, MeCN containing

0.1% formic acid as phase B. Mass spectra were deconvoluted using MagTran (ver 1.03 b2).

LC-ESI-MS analysis of Fc domains released by IdeS treatment.

The antibody samples in PBS were incubated with IdeS at 37 °C for 2 h. The samples were analyzed by with Exactive Plus Orbitrap Mass Spectrometer (Thermo Scientific) equipped with an Agilent Poroshell 300SB C8 column (5 μm, 1.0 × 75 mm) with gradient elution of water containing 0.1% formic acid as phase A, MeCN containing 0.1% formic acid as phase B. Mass spectra were deconvoluted using MagTran (ver 1.03 b2).

NMR analysis.

^{1}H, ^{13}C, and COSY NMR spectra were recorded on 400 MHz or 600 MHz spectrometer (Bruker) with $CDCl_3$, MeOD-d_4, D_2O or DMSO-d_6 as the solvent (solvent residue peak 7.26, 3.31, 4.79, 2.50 ppm). All ^{13}C NMR spectra were performed with proton decoupling, and all chemical shifts are reported in parts per million (ppm) and referenced to residual solvent. ^{1}H-NMR chemical shifts were recorded relative to the solvent residual peak ($CDCl_3$ at 7.26 ppm, MeOD-d_4 at 3.31ppm, D_2O at 4.79 ppm, DMSO-d_6 at 2.50 ppm). ^{13}C NMR chemical shifts are reported relative to the solvent residual peak ($CDCl_3$ at 77.00 ppm, MeOD-d_4 at 49.00 ppm, DMSO-d_6 at 39.51 ppm). The number of protons (*n*) corresponding to a resonance signal was indicated by *n*H and spin-spin coupling constants (*J* value) recorded in Hz.

Synthesis of the Antibody recruiting molecules

Synthesis of Rhamnose-PEG-DBCO (3-3). The rhamnose-PEG-NH_2 **3-1** (3.5 mg, 12 μmol) was weighed into a 1.5 mL centrifuge tube. A solution of the DBCO-PEG-NHS (**3-2**) (8 mg, 11.5 μmol, 50 mg/mL) was added, followed by 1 μL of TEA. The mixture reacted at room temperature for 2 hours before HPLC-SQ2 analysis showed completion of the reaction. The mixture was diluted with water and purified by semi prep-HPLC to afford **3-3** (6 mg, 60%). HR-ESI-MS: $[M+H]^+$ calcd for $C_{44}H_{64}N_3O_{15}^+$, 874.4332; found (m/z), 874.4304. HPLC (0.4 mL/min, 25-60%B, 30min, t_R = 14.2 min, Figure 3-9)

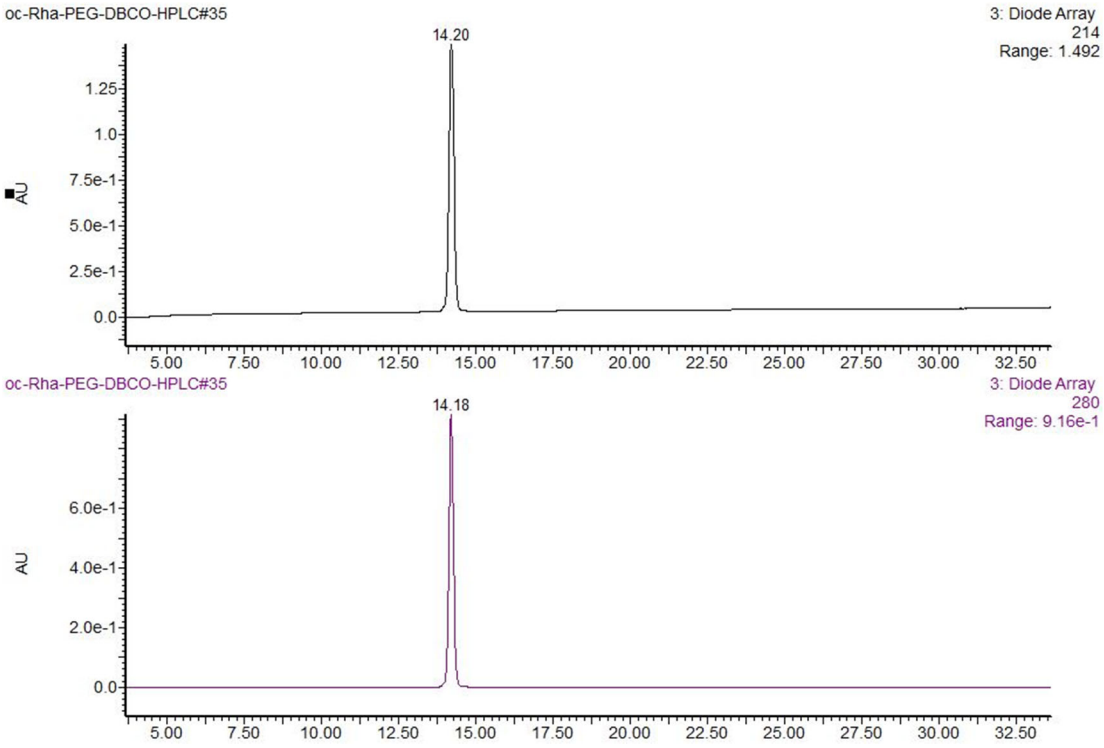

Figure 3-9. HPLC profile for **3-3**, 0.4 mL/min, 25-60%B, 30 min

Synthesis of compound 3-6. To a solution of **3-4** (857 mg, 1.5 mmol) and **3-5** (400 mg, 1.3 mmol) in DCM (10 mL), TEA (303 mg, 3 mmol) was added at room

temperature. After the mixture was stirred at room temperature for 16 hours, the solvent was removed in vacuo and the intermediate was purified by flash silica gel column chromatography by hexane and acetone (9:1 to 2:1, v/v). After it was concentrated under vacuo, the intermediate was treated with TFA/DCM (1:1, v/v) on ice for 30 minutes. The product in TFA salt form was concentrated and used without further purification (700 mg).

Synthesis of compound 3-7. In a 25 mL round-bottom flask, **3-4** (350 mg, 0.52 mmol) and **6** (850 mg, 1.92 mmol) were dissolved in DCM (10 mL). The mixture was stirred for 3 hours after TEA (255 mg, 2.5 mmol) was added. The solvent was removed *in vacuo* and the intermediate was purified by flash silica gel column chromatography by hexane and acetone (9:1 to 1:1, v/v). After it was concentrated under vacuo, the intermediate was treated with TFA/DCM (1:1, v/v) on ice for 30 minutes. The product as a TFA salt was concentrated and used without further purification (614 mg).

Synthesis of compound 3-10. 2-(2-(2-azido)ethoxy)ethyl-2,3,4-tri-O-acetyl-α-L-Rhamnose [113] (1.7 g, 3.8 mmol) was dissolved in MeOH (20 mL) with 1M HCl (200 μL). The solution was stirred with 5% Pd/C (78 mg) under H_2 atmosphere at room temperature for 1 hour. After filtration and concentration under vacuo, the resulting amine was used for next step without further purification. To a solution of **3-9** (700 mg, 2.05 mmol) in DCM (20 mL), a solution of pre-OAc-Rha amine (290 mg, 0.688 mmol) in DCM (10 mL) was added dropwise. The reaction mixture was stirred for another 2 hours at room temperature before the solvent was removed *in vacuo* and the intermediate was purified by flash silica gel column chromatography by hexane and

EtOAc (9:1 to 1:1 with 0.5% AcOH, v/v). The product was isolated as a colorless oil (284 mg, 79%, over two steps). ^{1}H NMR (400 MHz, DMSO-*d*6): δ = 1.12 (3H, d, *J* = 6.2 Hz), 1.57 (4H, m), 1.93 (3H, s), 2.03 (3H, s), 2.10 (5H, m), 2.66 (2H, t, *J* = 6.6 Hz), 2.81 (4H, br), 3.18 (2H, m), 3.40 (2H, t, *J* = 5.9 Hz), 3.45-3.65 (8H, m), 3.70 (1H, m), 3.86 (1H, m), 4.82 (1H, d, *J* = 1.2 Hz), 4.88 (1H, t, *J* = 9.9 Hz), 5.05-5.10 (2H, m), 7.87 (1H, m). ^{13}C NMR (100 MHz, DMSO-*d*6): δ = 17.68, 20.91, 20.95, 21.07, 24.26, 24.78, 25.90, 30.37, 35.09, 38.90, 33.15, 66.94, 69.10, 69.43, 69.65, 69.74, 70.02, 70.21, 70.54, 97.06, 169.37, 170.18, 170.72, 172.23. ESI-MS: $[M + H]^+$ calcd for $C_{28}H_{43}N_2O_{15}^+$, 647.2658; found (m/z), 647.4511.

Synthesis of Rha$_4$-dendrimer-DBCO (3-13). To a solution of **3-7** (6.5 mg, 7.7 μmol) in DMSO (100 μL), a solution of **3-10** (30 mg, 46.4 μmol) in DMSO (300 μL) was added followed by TEA (1.17 mg, 11.4 μmol) at room temperature. After HPLC-SQ2 analysis suggested the reaction was completed, the reaction mixture was diluted with 2 mL water. Hydrazine was added so the final hydrazine concentration was 3%. The mixture was left at room temperature for 16 hours before piperidine (200 μL) was added to the mixture to remove the Fmoc protection group at room temperature. Fmoc removal was completed within 30 minutes. The mixture was lyophilized and purified by LH-20 size exclusion chromatography. A solution of **3-2** (6.9 mg, 10 μmol) in DMSO (140 μL) was added to the intermediate. The mixture reacted at room temperature for 6 hours before HPLC-SQ2 analysis showed completion of the reaction. The mixture was diluted with water and purified by semi prep-HPLC to afford **3-13** (15 mg, 73%, over four steps). HR-ESI-MS: $[M + H]^+$ calcd for $C_{126}H_{211}N_{14}O_{47}^+$,

2673.4549 (100%); found (m/z), 2673.4546. HPLC (0.4 mL/min, 10-50%B, 30min, t_R = 20.8 min, Figure 3-10)

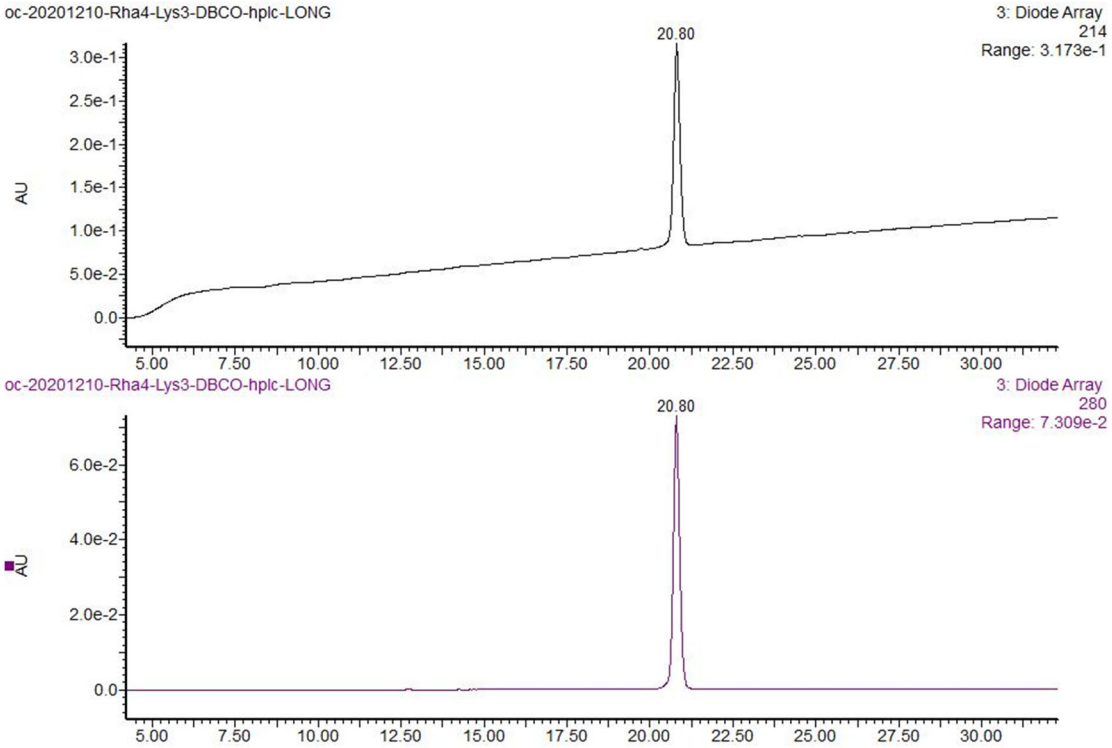

Figure 3-10. HPLC profile for **3-13**, 0.4 mL/min, 10-50%B, 30 min

Synthesis of compound α-Gal-PEG-DBCO (3-15). To a solution of **3-14** [90] (2 mg, 3.15 μmol) in DMSO (100 μL), the DBCO-PEG-NHS (**3-2**) (4 mg, 5.8 μmol) in DMSO (80 μL) was added, followed by 0.5 μL of TEA. The mixture reacted at room temperature for 2 hours before HPLC-SQ2 analysis showed completion of the reaction. The mixture was diluted with water and purified by semi prep-HPLC to afford **3-15** (2.2 mg, 58%). ESI-MS: $[M + H]^+$ calcd for $C_{56}H_{84}N_3O_{26}^+$, 1214.5338; found (m/z), 1214.8262. HPLC (0.4 mL/min, 10-50%B, 30min, t_R = 21.6 min, Figure 3-11)

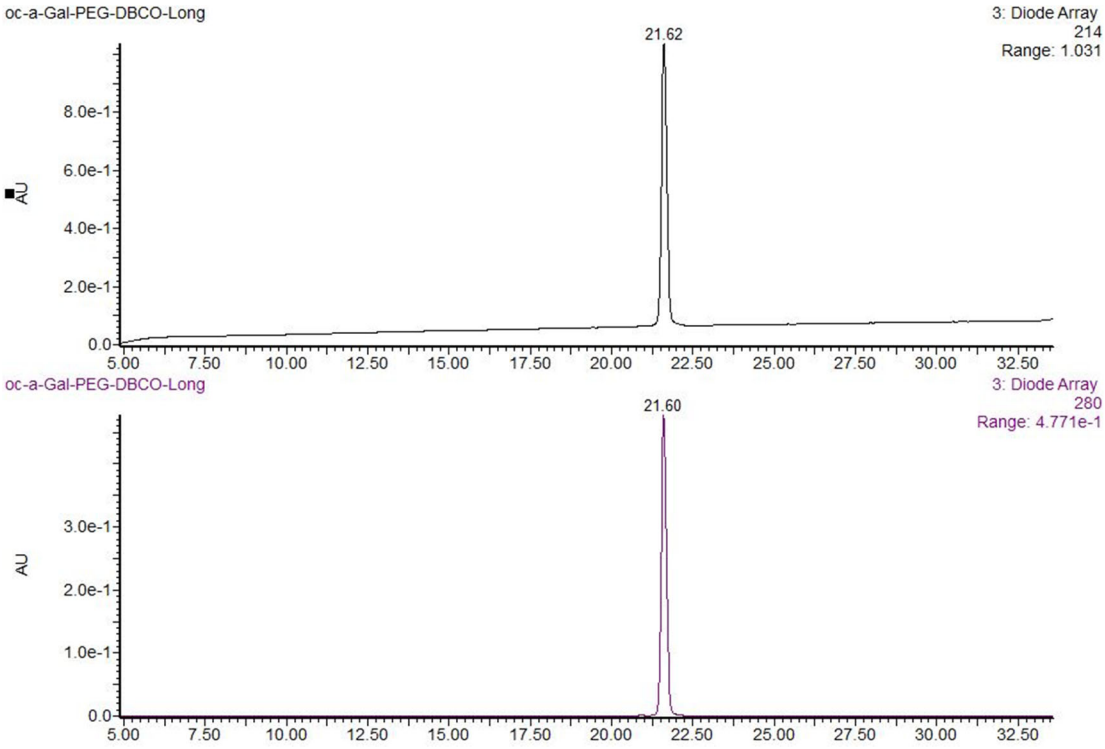

Figure 3-11. HPLC profile for **3-15**, 0.4 mL/min, 10-50%B, 30 min

Synthesis of compound 3-16. To a stirring solution of **3-9** (21.4 mg, 63 μmol) in DMSO (0.6 mL) the solution of **3-14** (10 mg, 15.7 μmol) was added dropwise over 30 minutes at room temperature. The reaction was stirred at room temperature for another 2 hours before HPLC-SQ2 analysis showed completion of the reaction. The mixture was diluted with water, lyophilized, and then purified by semi-prep HPLC to afford **3-16** (8.5 mg, 67%) as a white powder. ^{1}H NMR (600 MHz, D_2O): δ = 1.69 (4H, m), 2.28 (2H, t, J = 7.0 Hz), 2.72 (2H, t, J = 7.0 Hz), 2.91 (4H, br), 3.32 (1H, m), 3.36 (2H, t, J = 5.3 Hz), 3.60-3.85 (21H, m), 3.92 (1H, m), 3.95 (1H, m), 3.99 (1H, d, J = 2.9 Hz), 4.03 (1H, m), 4.14-4.18 (2H, m), 4.49 (2H, dd, J_1 = 8.0 Hz J_2 = 2.2 Hz), 5.11 (1H, d, J = 3.8 Hz). ^{13}C NMR (150 MHz, D_2O): δ = 22.74, 23.99, 24.67, 25.02, 29.57, 34.69, 38.39, 59.67, 60.42, 60.48, 64.31, 67.71, 68.24, 68.37, 68.63, 68.80, 68.87, 69.08, 69.14, 69.19, 70.34, 72.29, 73.90, 74.26, 74.56, 76.71, 78.17, 94.94, 101.61,

102.38, 170.09, 172.92, 175.99. HR-ESI-MS: $[M + H]^+$ calcd for $C_{34}H_{57}N_2O_{23}^+$, 861.3347; found (m/z), 861.3313.

Synthesis of DBCO functionalized α-Gal dendrimer (3-18). To a solution of **3-7** (1.0 mg, 1.1 μmol) in DMSO (100 μL), a solution of **3-16** (4.8 mg, 5.7 μmol) in DMSO (100 μL) was added followed by TEA (1.17 mg, 11.4 μmol) at room temperature. After HPLC-SQ2 analysis suggested the reaction was completed, the reaction mixture was diluted with 1 mL water. Piperidine (120 μL) was added to the mixture to remove the Fmoc protection group at room temperature. Deprotection was completed within 30 minutes. The mixture was lyophilized, before a solution of **3-2** (1.0 mg, 1.4 μmol) in DMSO (100 μL) was added. The mixture reacted at room temperature for 6 hours before HPLC-SQ2 analysis showed completion of the reaction. The mixture was diluted with water and purified by semi prep-HPLC to afford **3-18** (3.1 mg, 65%, over three steps). HR-ESI-MS: $[M + 2H]^{2+}$ calcd for $C_{174}H_{292}N_{14}O_{91}^{2+}$, 2017.4337 (100%); found (m/z), 2017.3817. HPLC (0.4 mL/min, 10-50%B, 30min, t_R = 16.5 min, Figure 3-12)

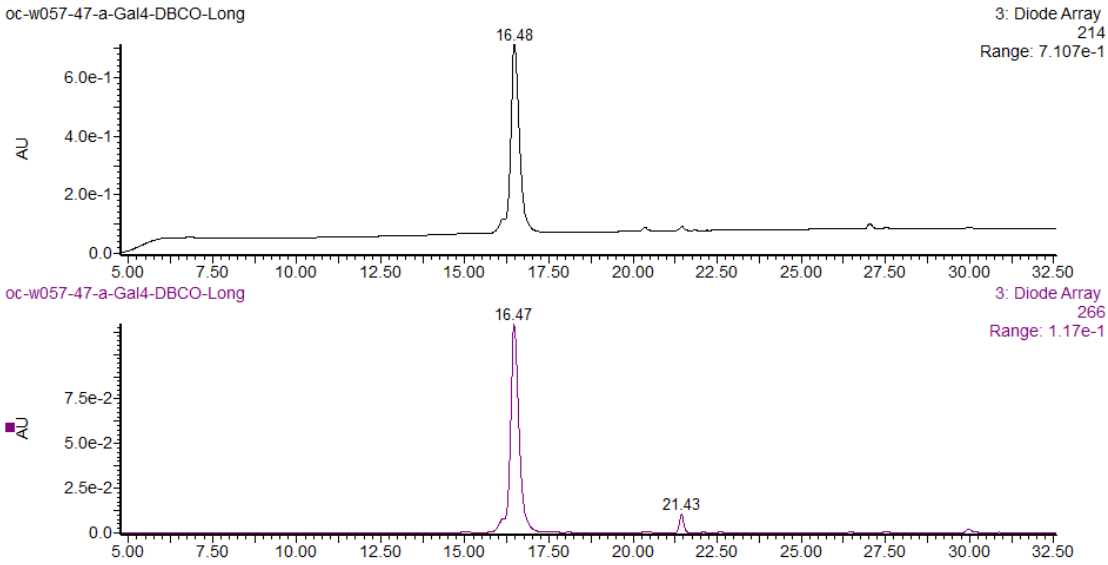

Figure 3-12. HPLC profile for **3-18**, 0.4 mL/min, 10-50%B, 30 min

Synthesis of Rhamose functionalized SCT-oxa (3-27a). A solution of Di-N3-SCT (**3-25**) (5.0 mg, 1.9 µmol) and **3-3** (4.2 mg, 4.8 µmol) in DI water (400 µL) was incubated at room temperature for 4 h when LC-MS indicated the completion of the reaction. The solution was then cooled on ice, and TEA (11.7 mg, 115 µmol) and 2-chloro-1,3-dimethylimidazolinium chloride (DMC) (8.1 mg, 45.5 µmol) were added, following the previously described procedure.[111, 112] The reaction mixture was kept on ice for 45 min, then it was diluted with 0.1 % ammonium hydroxide, and the glycan oxaozline was purified by semi-prep HPLC with gradient elution (10%-70%B, 40min) of water containing 0.1% ammonium hydroxide as phase A, MeCN containing 0.1% ammonium hydroxide as phase B. **3-27a** was isolated as a white powder after lyophilization (6 mg, 72%, over two steps). ^{1}H NMR (600 MHz, D_2O): δ = 7.92 – 7.83 (m, 1H), 7.82 – 7.74 (m, 1H), 7.72 – 7.65 (m, 2H), 7.64 –7.49 (m, 4H), 7.44 – 7.21 (m, 8H), 6.04 (d, J = 7.2 Hz, H-1-GlcNAc-Ox), 5.91 – 5.80 (m, 3H), 5.61 – 5.53 (m, 2H), 5.18 – 5.16 (m, 1H), 5.12 – 5.00 (m, 3H), 4.95 – 4.86 (m, 4H), 4.78 – 3.02 (m, 183H),

2.71 – 2.60 (m, 4H), 2.51 – 2.38 (m, 8H), 2.05 – 1.97 (m, 15H), 1.85 – 1.75 (m, 3H), 1.71 – 1.54 (m, 4H), 1.28 – 1.21 (m, 6H). HR-ESI-MS $[M + 2H]^{2+}$ calcd for $C_{188}H_{299}N_{19}O_{94}^{2+}$, 2164.4628 (100%); found (m/z), 2164.4403.

Synthesis of rhamose cluster functionalized SCT-oxa (3-27b). A solution of Di-N3-SCT (**3-25**) (1 mg, 0.385 μmol) and **3-13** (2.5 mg, 0.962 μmol) in DI water (200 μL) was incubated at room temperature for 4 h. Then, the solution was cooled at 0°C, and TEA (2.6 mg, 25 μmol) and DMC (1.6 mg, 9.62 μmol) were added, and the reaction mixture was incubated at 0 °C for 45 min. The glycan oxazoline was purified by semi-prep HPLC with gradient elution (10%-70%B, 40min) of water containing 0.1% ammonium hydroxide as phase A, MeCN containing 0.1% ammonium hydroxide as phase B. **3-27b** was isolated as a white powder after lyophilization (1.8 mg, 59%, over two steps). ^{1}H NMR (600 MHz, D_2O): δ = 7.90 – 7.85 (m, 1H), 7.82 – 7.74 (m, 1H), 7.72 – 7.65 (m, 4H), 7.64 –7.49 (m, 4H), 7.42 – 7.25 (m, 8H), 6.04 (d, J = 7.3 Hz, H-1-GlcNAc-Ox), 5.91 – 5.80 (m, 3H), 5.61 – 5.53 (m, 2H), 5.18 – 5.16 (m, 1H), 5.12 – 5.00 (m, 3H). 4.94 – 4.88 (m, 2H), 1.28 – 1.21 (m, 24H). HR-ESI-MS $[M + 4H]^{4+}$ calcd for $C_{352}H_{595}N_{41}O_{158}^{4+}$, 1981.9966 (100%); found (m/z), 1981.9896.

Preparation of Antibody Conjugates

Synthesis of Rha_4-Herceptin conjugate (3-21). A solution of azide-tagged antibody **3-20** (2 mg, 13 nmol) and the Rha-PEG-DBCO (**3-3**) (113 μg, 0.13 μmol, 10 eq) in a phosphate buffer (50 mM, pH 7.2) (final volume, 500 μL) was incubated at ambient temperature (23 °C). The reaction mixture was shielded from light and gently vortexed. The reaction was monitored by LC-ESI-MS analysis. After 8 h, the Click reaction was

complete as indicated by LC-ESI-MS. The mixture was then diluted with phosphate buffer (5 mL, 50 mM, pH 7.2) and filtered by 0.22 μm syringe filter. The conjugate product in the filtrate was purified by protein A chromatography to give **3-21** (1.8 mg, 87%). ESI-MS of **3-21**: calcd. M = 154518 Da; found (*m/z*), 2810.50 $[M + 55H]^{55+}$, 2862.53 $[M + 54H]^{54+}$, 2916.46 $[M + 53H]^{53+}$, 2972.55 $[M + 52H]^{52+}$, deconvolution of the ESI-MS, M = 154521 Da. Fc analysis: calcd, M = 28463 Da; found (m/z), 2034.03 $[M + 14H]^{14+}$, 2090.38 $[M + 13H]^{13+}$, 2372.80 $[M + 12H]^{12+}$, deconvolution data, M = 28462 Da.

Synthesis of Rha_{16}-Herceptin conjugate (3-22). A solution of azide-tagged antibody **3-20** (2 mg, 13 nmol) and the Rha_4-PEG-DBCO (**3-13**) (721 μg, 0.27 μmol, 20 eq) in a phosphate buffer (50 mM, pH 7.2) (final volume, 500 μL) was incubated at ambient temperature (23 ºC). The reaction mixture was shielded from light and gently vortexed. The reaction was monitored by LC-ESI-MS analysis. After 16 h, the Click reaction was complete as indicated by LC-ESI-MS. The mixture was then diluted with phosphate buffer (5 mL, 50 mM, pH 7.2) and filtered by 0.22 μm syringe filter. The conjugate product in the filtrate was purified by protein A chromatography to give **3-22** (1.9 mg, 88%). ESI-MS of **3-22**: calcd. M = 161714 Da; found (*m/z*), 2941.30 $[M + 55H]^{55+}$, 3052.25 $[M + 53H]^{53+}$, 3110.84 $[M + 52H]^{52+}$, 3171.81 $[M + 51H]^{51+}$, deconvolution of the ESI-MS, M = 161718 Da. Fc analysis: calcd, M = 32061 Da; found (m/z), 2291.05 $[M + 14H]^{14+}$, 2467.16 $[M + 13H]^{13+}$, 2672.64 $[M + 12H]^{12+}$, deconvolution data, M = 32060 Da.

Synthesis of α-Gal$_4$-Herceptin conjugate (3-23). A solution of azide-tagged antibody **3-20** (2 mg, 13 nmol) and the α-Gal-PEG-DBCO (**3-15**) (157 μg, 0.13 μmol, 10 eq) in a phosphate buffer (50 mM, pH 7.2) (final volume, 500 μL) was incubated at ambient temperature (23 ºC). The reaction mixture was shielded from light and gently vortexed. The reaction was monitored by LC-ESI-MS analysis. After 8 h, the Click reaction was complete as indicated by LC-ESI-MS. The mixture was then diluted with phosphate buffer (5 mL, 50 mM, pH 7.2) and filtered by 0.22 μm syringe filter. The conjugate product in the filtrate was purified by protein A chromatography to give **3-23** (1.9 mg, 87%). ESI-MS of **3-23**: calcd. M = 155879 Da; found (*m/z*), 2835.26 [M + 55H]$^{55+}$, 2887.68 [M + 54H]$^{54+}$, 2942.18 [M + 53H]$^{53+}$, 2998.70 [M + 52H]$^{52+}$, deconvolution of the ESI-MS, M = 155882 Da. Fc analysis: calcd, M = 29143 Da; found (m/z), 2082.71 [M + 14H]$^{14+}$, 2242.71 [M + 13H]$^{13+}$, 2429.57 [M + 12H]$^{12+}$, deconvolution data, M = 29143 Da.

Synthesis of α-Gal$_{16}$-Herceptin conjugate (3-24). A solution of azide-tagged antibody **3-20** (2 mg, 13 nmol) and the α-Gal-PEG-DBCO (**3-15**) (1.09 mg, 0.27 μmol, 20 eq) in a phosphate buffer (50 mM, pH 7.2) (final volume, 500 μL) was incubated at ambient temperature (23 ºC). The reaction mixture was shielded from light and gently vortexed. The reaction was monitored by LC-ESI-MS analysis. After 40 h, the Click reaction was complete as indicated by LC-ESI-MS. The mixture was then diluted with phosphate buffer (5 mL, 50 mM, pH 7.2) and filtered by 0.22 μm syringe filter. The conjugate product in the filtrate was purified by protein A chromatography to give **3-24** (2.0 mg, 90%). ESI-MS of **3-24**: calcd. M = 167159 Da; found (*m/z*), 3040.18 [M + 55H]$^{55+}$, 3096.46 [M + 54H]$^{54+}$, 3154.81 [M + 53H]$^{53+}$, 3215.53 [M + 52H]$^{52+}$,

deconvolution of the ESI-MS, M = 167158 Da. Fc analysis: calcd, M = 34783 Da; found (m/z), 2319.77 $[M + 15H]^{15+}$, 2485.47 $[M + 14H]^{14+}$, 2676.52 $[M + 13H]^{13+}$, deconvolution data, M = 34782 Da.

Synthesis of Rha_4-Herceptin conjugate (3-21) via transglycosylation. To the solution of **3-28** (500 μg, 25 mg/ml in 100 mM Tris buffer), glycan oxazoline **3-27a** (941 μg, 30 eq, 100 mg/mL in 100 mM Tris buffer) was added. After adjusting the pH to 7.4, Endo-S2 D184M mutant (13 mg/mL) was added to the solution. The final enzyme concentration was 0.1 mg/mL. The reaction was carried out at 30 °C and monitored by LC-MS every 20 minutes. The reaction reached completion in 60 min. The product was purified by protein A chromatography to yield **3-21** (420 μg, 82%). ESI-MS of **3-21**: calcd. M = 154518 Da; found (*m/z*), 2810.48 $[M + 55H]^{55+}$, 2862.51 $[M + 54H]^{54+}$, 2916.44 $[M + 53H]^{53+}$, 2972.53 $[M + 52H]^{52+}$, deconvolution of the ESI-MS, M = 154519 Da.

Synthesis of Rha_{16}-Herceptin conjugate (3-22) via transglycosylation. To the solution of **3-28** (105 μg, 35 mg/ml in 100 mM Tris buffer), glycan oxazoline **3-27b** (220 μg, 40 eq, 100 mg/mL in 100 mM Tris buffer) was added. After adjusting the pH to 7.4, Endo-S2 D184M mutant (13 mg/mL) was added to the solution. The final enzyme concentration was 0.4 mg/mL. The reaction was carried out at 30 °C and monitored by LC-MS every 20 minutes.

***In Vitro* Cytotoxicity Assay**

BT474 cells (ATCC HTB-20) were cultured in HybriCare medium (ATCC 46-X) supplemented with 10% fetal bovine serum (FBS), 100 U/mL penicillin, and 100

μg/mL streptomycin in T-75 flasks (CELLTREAT). T47D cells (ATCC HTB-133) were maintained in RPMI-1640 medium (ATCC 30- 2001) containing FBS, 4 mg/L insulin, 100 U/mL penicillin, and 100 μg/mL streptomycin in T-75 flasks (CELLTREAT).

For the cytotoxicity assays, cells were seeded into 96-well plates with 25,000 cells per well and grown for 24 hours at 37 °C and 5% CO_2. The FBS containing media was removed. The serum free RPMI media with the antibody conjugates (starting at a concentration of 25 μg/mL for BT474 and 50 μg/mL for T47D and serially diluted 1:3) was added. Each compound was assessed in triplicate wells, the cells without compound served as control. After incubation for 2 hours, the antibody conjugates solution was removed. 70μL serum free RPMI and 10 μL human serum was added to each well and incubated for 15 minutes. Then 20 μL of 20% rabbit complement diluted by serum free RPMI was added to each well and incubated for 2 hours. The cells were then washed with PBS before the incubation with RPMI media containing 10% Cell Counting Kit-8 (Dojindo). The absorbance of formazan released by viable cells was measured at 450 nm using a spectrophotometer after incubation for 2−3 h at 37 °C and 5% CO_2. Finally, the cell viability curve and the EC50 values were calculated using GraphPad Prism software.

3.5 Supporting Information

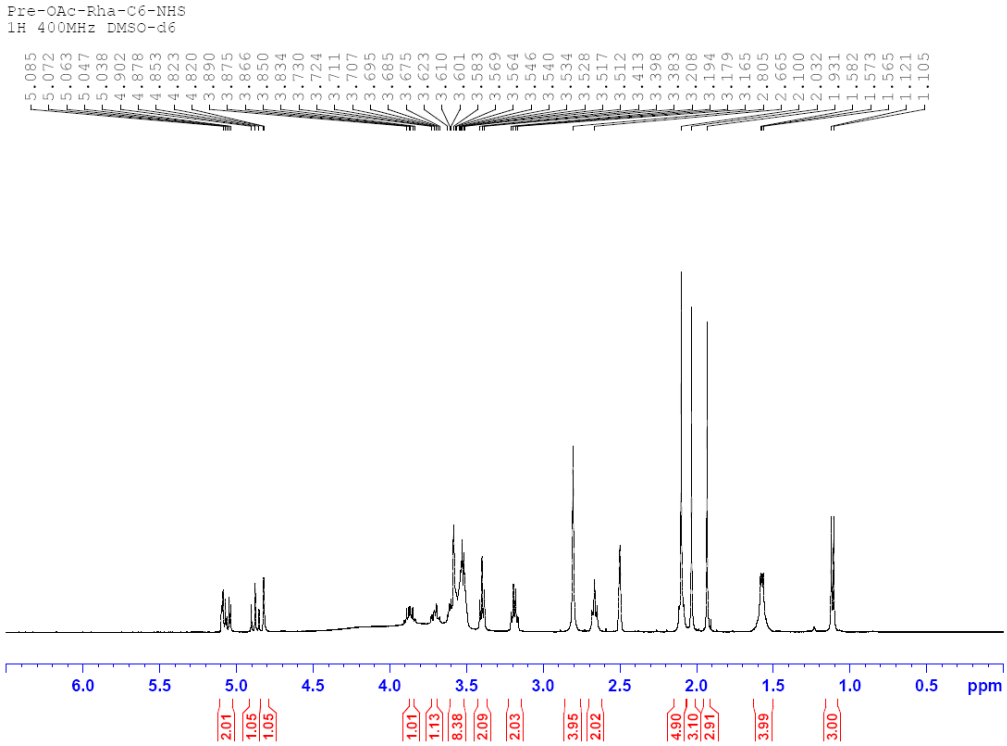

^{1}H NMR spectrum (400 MHz, DMSO-*d*6): compound **3-10**

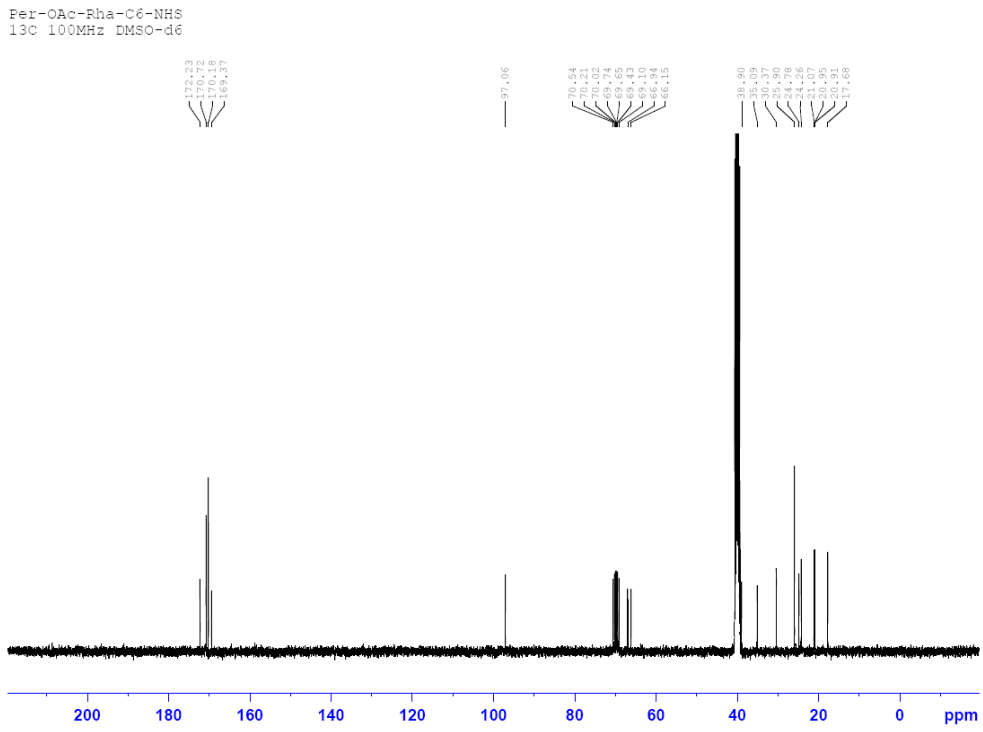

^{13}C NMR spectrum (100 MHz, DMSO-*d*6): compound **3-10**

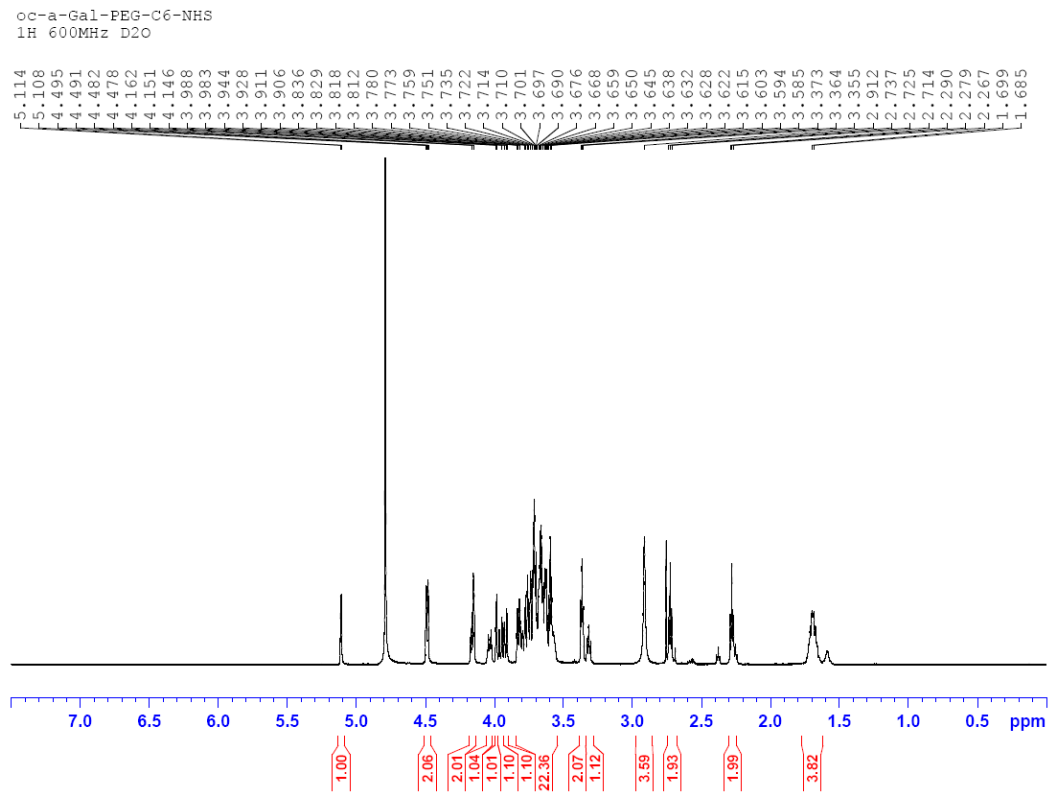

^{1}H NMR spectrum (600 MHz, D_2O): compound **3-16**

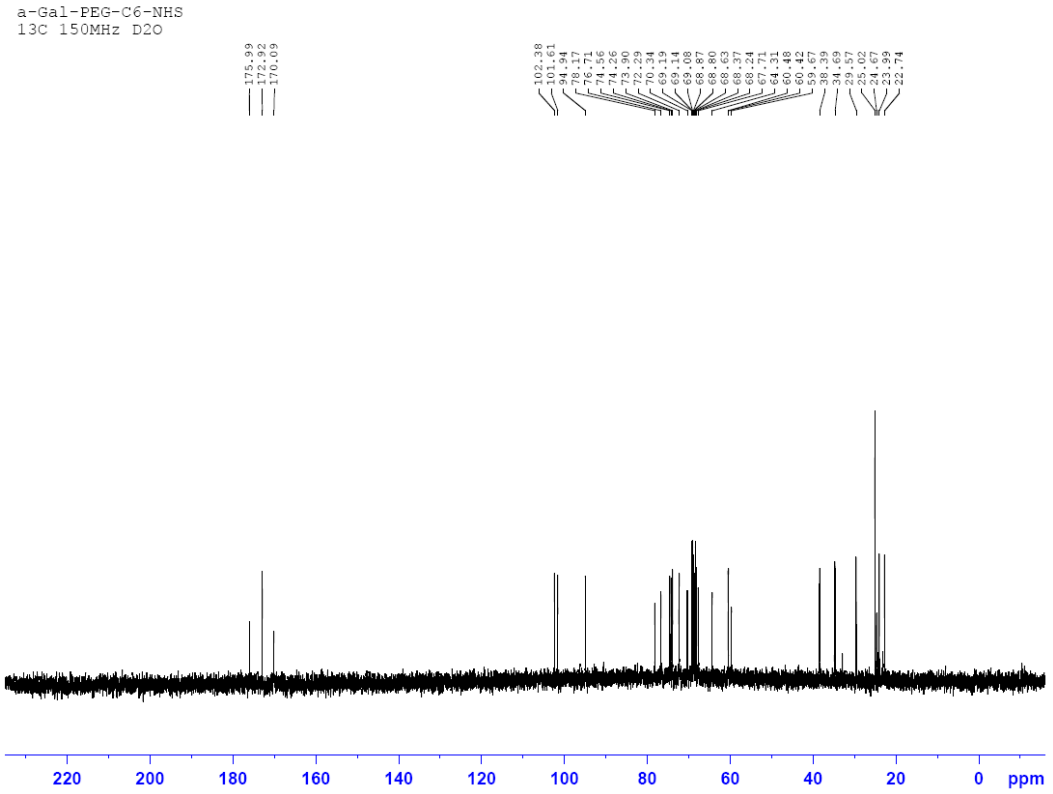

^{13}C NMR spectrum (150 MHz, D_2O): compound **3-16**

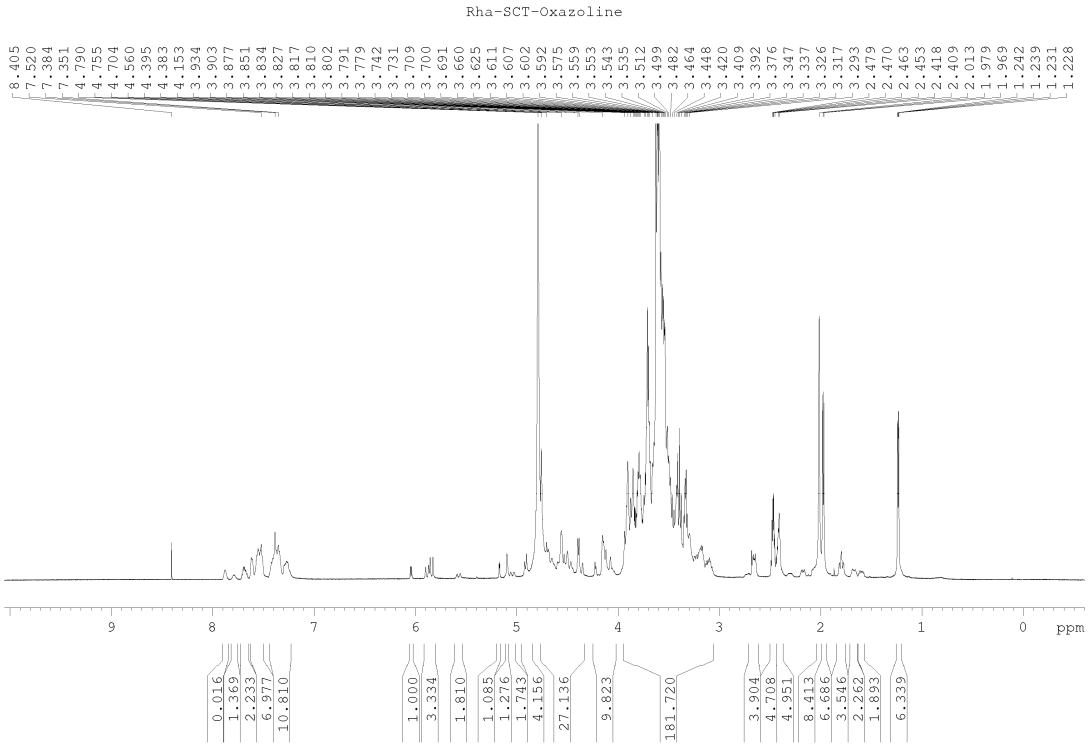

^{1}H NMR spectrum (600 MHz, D_2O): compound **3-26a**

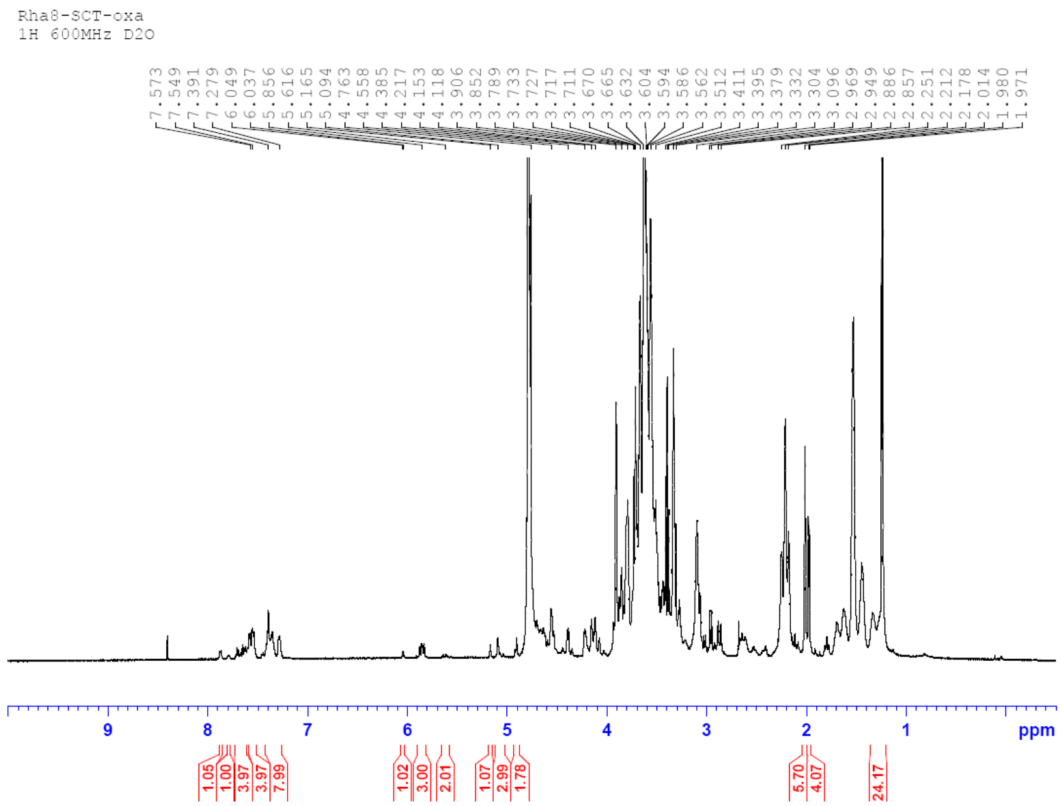

^{1}H NMR spectrum (600 MHz, D_2O): compound **3-26b**

Chapter 4: Antibody-Drug Conjugates with Dual Functional Ligands for Enhanced Internalization and Lysosomal Delivery

4.1 Introduction

As discussed in Chapter 1, to achieve both high selectivity and toxicity, modern antibody-drug conjugates deliver potent drugs into their targeted cells through internalization and lysosomal trafficking. Previous studies suggest that enhancing the lysosomal delivery of the ADCs, their potency and therapeutic efficacy could be improved significantly. [36, 41, 42] Besides, due to this requirement the tumor-specific antigens suitable for ADCs are severely limited.[9, 114] The conjugation of an internalizing factor to an antibody-drug conjugate could possibly broaden the scope of druggable tumor antigens. Herein, we proposed a flexible method to generate functionalized ADCs based on Fc glycan engineering with dual-functionalized *N*-glycans followed by stepwise Click reactions.

The ability to achieve double functionalized antibody is always highly desirable due to the inherent and acquired drug resistance observed in current ADC therapies. Recent research indicated some drug resistance could be overcome by using another drug with the same antibody. [77, 115, 116] Therefore, it is of high interest to develop ADCs carrying two drugs with high homogeneity. Currently, several groups have reported their research of generating dual-drug antibody-drug conjugates, but many of these attempts did not produce homogenous ADCs. [28, 34, 78, 80] Nowadays, achieving the

synthesis of ADCs with high homogeneity is still challenging: in 2017, Levengood and coworkers reported successful generation of homogeneous dual-drug ADCs by orthogonal cysteine protection[37]; in 2018, Bruins and coworkers used a cpTCO based unnatural amino acid in the heavy chain and azide on the Fc *N*-glycan to achieve dual-functionalized antibody. [33]

To achieve the synthesis of the dual-functionalized antibody through orthogonal Click reactions, the selection of the bioorthogonal ligation reactions is also crucial. The strain-promoted azide-alkyne cycloaddition (SPAAC) developed by Bertozzi and coworkers was our first choice since it is one of the most widely used Click reactions for functionalization of antibodies.[12, 117] Among other bioorthogonal reactions, inverse electron demand Diels-Alder reaction (IEDDA) pioneered by Dr. Fox and Dr. Hilderbrand was the most ideal, because it has been used for antibody conjugations recently and it has been used orthogonally to the SPAAC in other applications.[33, 80, 118-122] Due to the potential problem of cross-reactivity between the ligands of these two Click reactions, we decided to introduce azide and cyclopropane groups together onto the antibody according to previous research.[119, 122, 123] During the time we are working on this project, a similar study was published by Yamazaki and coworkers. They used azide and tetrazine functionalized linker and transglutaminase to conjugate it to an anti-HER2 antibody.[38]

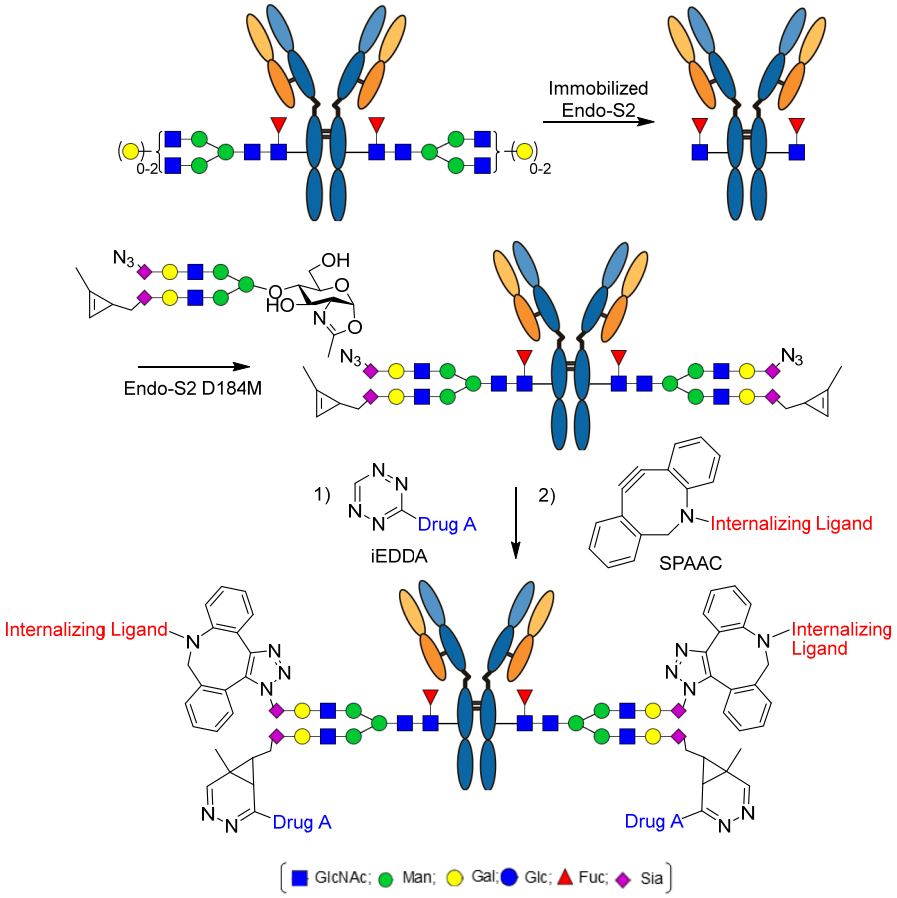

Figure 4-1. Fc glycan remodeling of Herceptin to generate dual-drug ADC

The cation-independent mannose 6-phosphorate receptor (CI-MPR) has been used to transport extracellular proteins into the lysosome. The enzyme replacement therapy was based on targeting recombinant lysosomal enzyme with M6P-containing high mannose oligosaccharide signals to treat Pompe diseases, a lysosomal storage disease. [124, 125] In recent years, M6P ligand was also used as a lysosome-targeting chimaeras (LYTACs) to selectively achieve lysosomal degradation of membrane proteins of interest.[126, 127] Therefore, the M6P ligands could be used as an internalization factor for ADCs. Due to the fact that the expression of the CI-MPR is found on most of heathy cells, the ADCs functionalized with M6P was used as a model

compound for a proof of concept for the overall platform. Further studies are being carried out with tumor specific internalizing ligands, such as folic acid.

4.2 Results and Discussion

Chemical synthesis of the dual-functionalized antibodies with Fc glycan engineering

As we optimized the *N*-glycan functionalization using DMTMM in Chapter 2, 3 equivalents of **Linker a** was required to complete the reaction for Di-N_3-SCT (**2-2**). Using the same conditions, with 1 equivalent of **Linker a**, the mono-N_3-SCT (**4-2**) could be obtained with very good overall conversion yield (70-80%) according to HPLC. The compound could be purified by either anion exchange or preparative HPLC. The **Linker b** could be installed to the other sialic acid by the same reaction with 61% isolated yield. And the dual-functionalized oxazoline could be obtained by the previous described method. (Scheme 4-1)

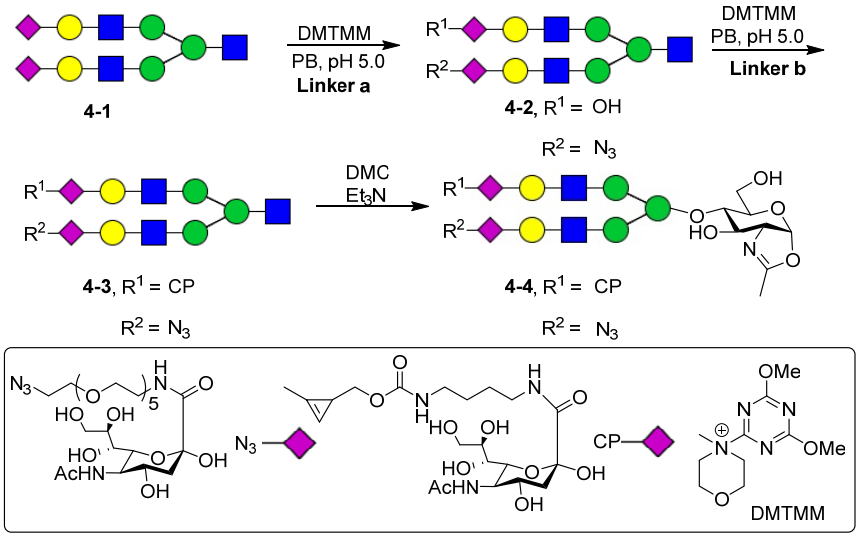

Scheme 4-1. Synthesis of dual-functionalized SCT-oxazoline

Two types of antibodies were used in this work: trastuzumab (Herceptin), an anti-human epidermal growth factor receptor 2 (HER-2) therapeutic monoclonal antibody; and Cetuximab, an anti-epidermal growth factor receptor. HER-2 was the target for two of the FDA approved ADCs against solid tumors, which could be efficiently internalized when cross-linked by antibodies.[9] This antibody conjugate was used to study the binding to CI-M6P receptor and the evaluation of antigen positive and negative cell lines. On the other hand, the EGFR is also a tumor specific antigen and target for therapeutic antibody, but due to its slow internalization after antibody binding, it was not a great target for antibody drug conjugates. In 2016, Sellmann and coworkers reported their ADC with enhanced the internalizing rate of EGFR receptor by generating a bispecific antibody. The researchers claimed their ADC possesses higher potency while retaining selectivity.[40] So we conducted our study with this antibody and tested if we could improve the efficacy of ADC by M6P as an internalizing ligand. The glycan remodeling was carried out as reported in our previous chapters, the Fc glycan on the commercially available antibodies were trimmed by immobilized Endo-S2, then the dual-functionalized glycan oxazoline was transferred to the antibody with Endo-S2 D184M. (Scheme 4-2) The glycoengineered Herceptin (**4-7a**) was characterized by LC-ESI-MS analysis of intact antibody, while the functionalized Cetuximab (**4-7b**) was characterized by LC-ESI-MS analysis of the Fc domain, because there are Fab glycan in the Cetuximab, which makes the intact antibody analysis too complex.[128] (Figure 4-2)

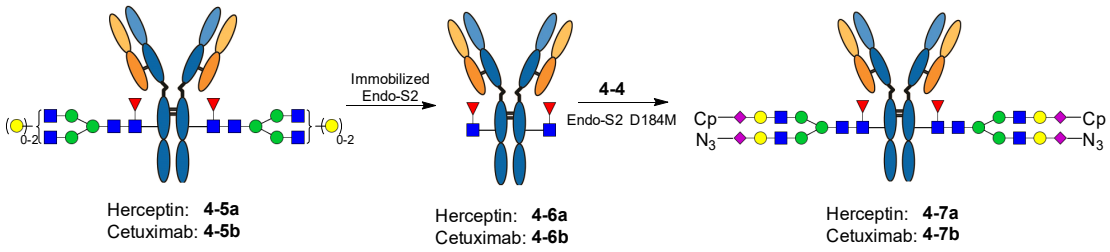

Scheme 4-2. Chemoenzymatic synthesis of dual functionalized antibodies.

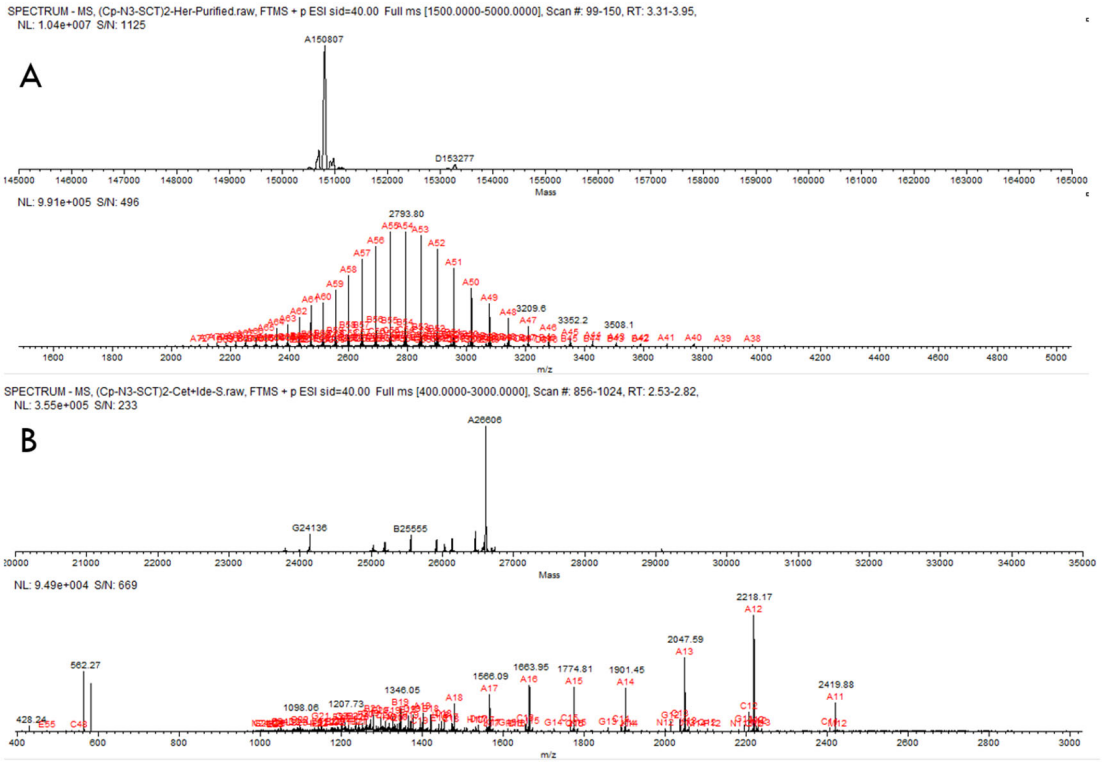

Figure 4-2. LC-ESI-MS analysis of the dual functionalized antibody. A) the deconvoluted mass of intact antibody **4-7a**; B) the deconvoluted mass of Fc domain of antibody **4-7b**

Minimal structure for the CI-MPR ligand

Wang lab has been working in studying the structure-function relationship for the mannose-6-phosphate glycan ligands. In 2016, we confirmed that a single M6P moiety on the α-1,3-branch of the high mannose glycan is sufficient for efficient

binding to CI-MPR, while a M6P moiety on the α-1,6-branch of the same glycoforms did not provide meaningful binding.[129] More recently, Dr. Zhang in our lab further optimized the structure of M6P containing *N*-Glycans, and kindly provided the M6P containing antibody and M6P ligands used in this project. The results revealed that the penta-saccharide containing the Man6P-α-1,2-Man disaccharide as an crucial motif to achieve high affinity binding to the CI-MPR.[130] Also, the same minimal tetra-saccharide was used for the Fc glycan engineering. The resulting antibody (**4-8**) could bind to the CI-MPR at high affinity (K_D = 30.2 nM). (Figure 4-3) And the glycan engineered antibody could efficiently internalize and trigger lysosomal degradation of its target.[127]

To generate an internalizing ligand for ADC, a smaller M6P glycan structure is desirable. And based on previous studies, the Man6P-α-1,2-Man structure is essential for high-affinity binding toward the CI-MPR. Therefore, we generated an antibody conjugate with a M6P disaccharide (**4-9**). Also, we synthesized the M6P monosaccharide conjugate (**4-10**) to compare the binding affinity against CI-MPR. Indeed, the conjugate with two Man6P-α-1,2-Man ligands (**4-9**) bind to the receptor with similar affinity (K_D = 42.6 nM) compared to the antibody M6P glycoforms (**4-8**). On the other hand, the M6P monosaccharide did not show any meaningful binding. (Figure 4-3) Therefore, the M6P disaccharide was selected as the internalizing ligand for this project.

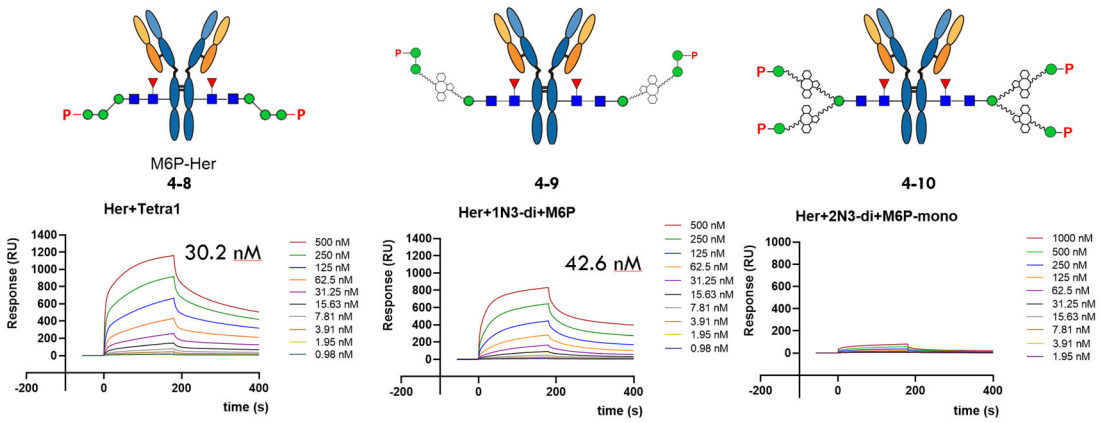

Figure 4-3 SPR binding experiments of CI-MPR with M6P containing antibodies. The antibody analytes were flowed over the immobilized CI-MPR with 2-fold serial dilution from the highest concentration of 500 nM.

Synthesis of M6P functionalized ADCs with MMAE payload

The M6P-functionalized ADCs were synthesized with a stepwise maner: the MMAE-Tetrazing (**2-9**) was Clicked to the dual-functionalized Herceptin **4-7a** or Cetuximab **4-7b** with method reported in Chapter 2. The intermediates were purified with protein A affinity chromatography and their identity was confirmed by LC-ESI-MS analysis (Figure 4-4). **4-12a** and **4-12b** were also used as comparison for the *in vitro* assays to study the efficacy of the internalizing factors. Then the disaccharide M6P ligands were Clicked onto the antibody with reported method in Chapter 3. (Scheme 4-3) There was no observed cross reactivity issue in this synthetic route. The final products were purified by buffer exchange and characterized by LC-ESI-MS analysis (Figure 4-4). Since we already confirmed that the serum stability were similar between the bonds formed by these two bioorthogonal reactions, we believe the M6P functionalized ADCs also had great overall serum stability.

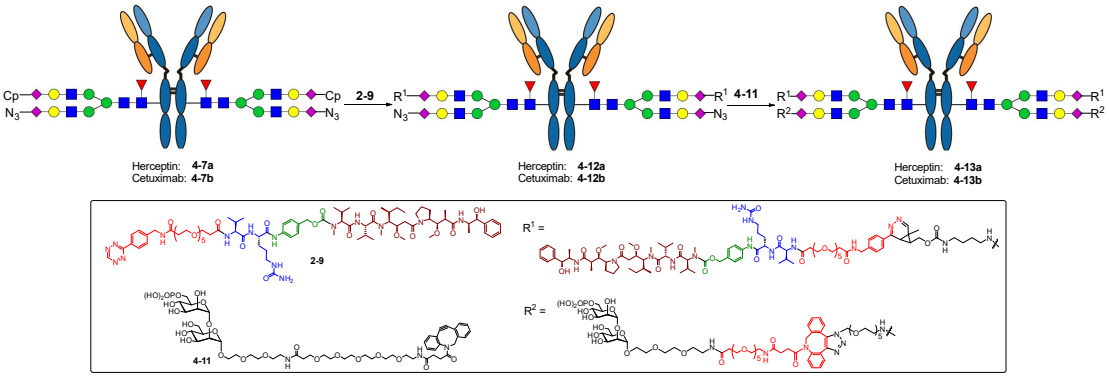

Scheme 4-3. Stepwise synthesis of the M6P functionalized ADC

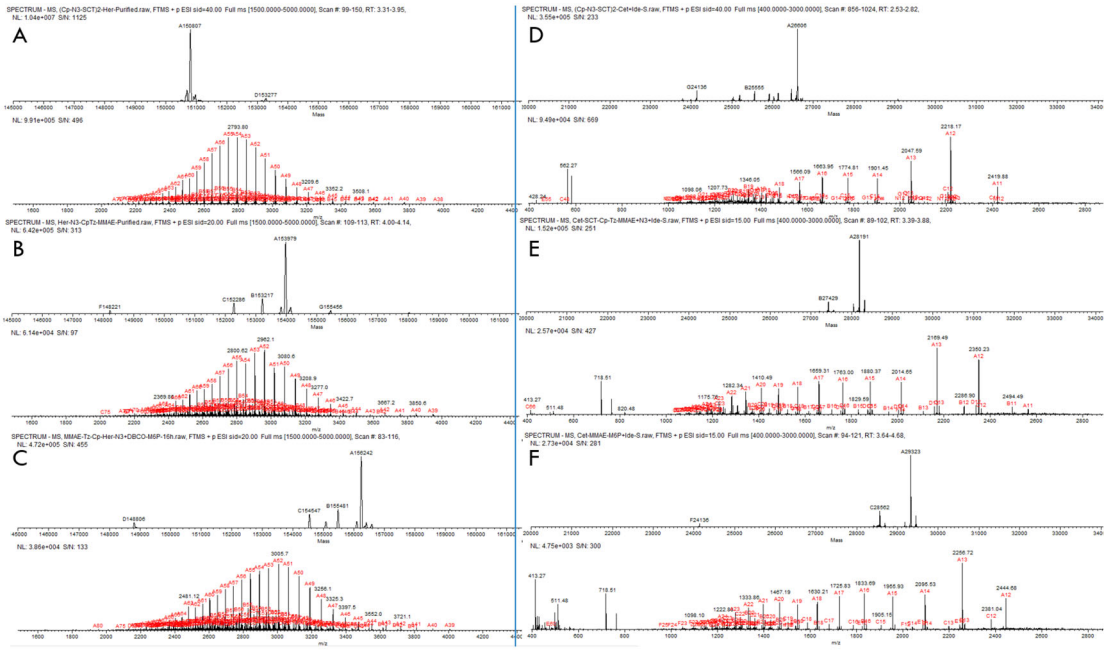

Figure 4-4. LC-ESI-MS analysis of the dual functionalized antibody. A) the deconvoluted mass of intact antibody **4-7a**; B) the deconvoluted mass of intact antibody **4-12a;** C) the deconvoluted mass of intact antibody **4-13a**; D) the deconvoluted mass of Fc domain of antibody **4-7b;** E) the deconvoluted mass of Fc domain of antibody **4-12b** F) the deconvoluted mass of Fc domain of antibody **4-13b**

To confirm the M6P functionalized ADC still binds to the CI-MPR, we did another SPR experiment. To our surprise, the affinity of our ADC-M6P bindings to the CI-MPR (K_D = 4.79 nM) was more than 8-fold stronger than the antibody conjugate **4-9**. (Figure 4-5) One possibility is that the SCT-based ADC construct provided more

flexibility and longer linker compared to the disaccharide-based antibody conjugates (**4-9**), so the two M6P ligands could reach the binding sites on the same receptor simultaneously.

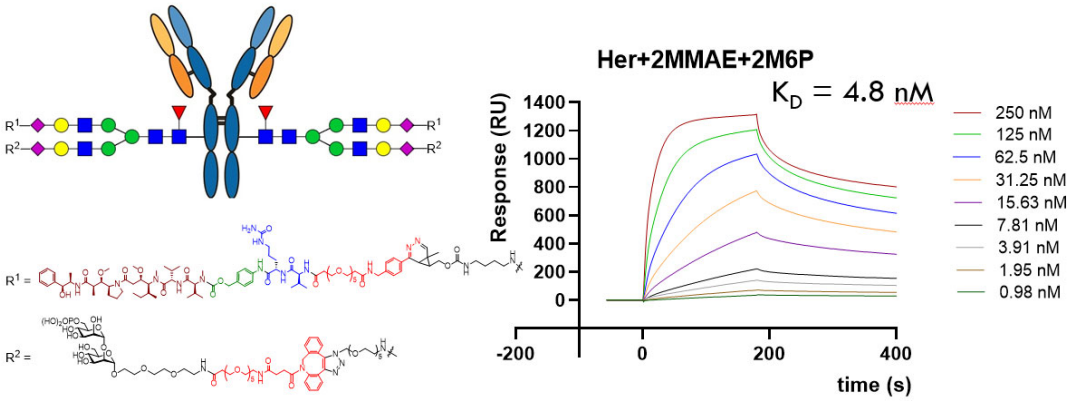

Figure 4-5. SPR binding experiments of CI-MPR with M6P functionalized ADC. The antibody analytes were flowed over the immobilized CI-MPR with 2-fold serial dilution from the highest concentration of 250 nM.

Cell-based assay of the cytotoxicity of the ADC with M6P internalizing factor

To compare the potency of the M6P functionalized ADCs, BT474 (HER-2 overexpressing) and T47D (low HER-2 expressing) cells were used. For the BT474 cell line, the Herceptin based ADCs with the M6P ligand demonstrated about the same dose-dependent killing of the antigen-positive cells (Figure 4-6A). As the HER2 is a fast-internalizing receptor, it is understandable the M6P ligands do not show significant benefit. Meanwhile, the low HER-2 expressing T47D cells were insensitive to the ADCs up to 10 μg/mL (Figure 4-6B). These results suggest the antibodies retain high specificity on HER2 after all the modifications.

On the other hand, for the slow-internalizing EGFR, BT474 (EGFR expressing) and SKBR3 (EGFR expressing) cells were used. In this case, there was noticeable differences between **4-12b** and **4-13b**. With the BT474 cell line, the M6P-functionalized Cetuximab **4-13b** showed about 3-fold increase in cytotoxicity (Figure 4-6C). While with the BT474 cell line, the M6P-functionalized Cetuximab **4-13b** showed about 2-fold increase in cytotoxicity (Figure 4-6D). These results suggested that the M6P disaccharide functionalized antibody drug conjugates could increase the cytotoxicity profile for antibodies targeting slow-internalizing receptors, therefore possibly broaden the druggable tumor-specific antigens. Also, this study provides a general and efficient approach to produce structurally well-defined, homogeneous dual-functionalized antibody conjugates via double Click reactions.

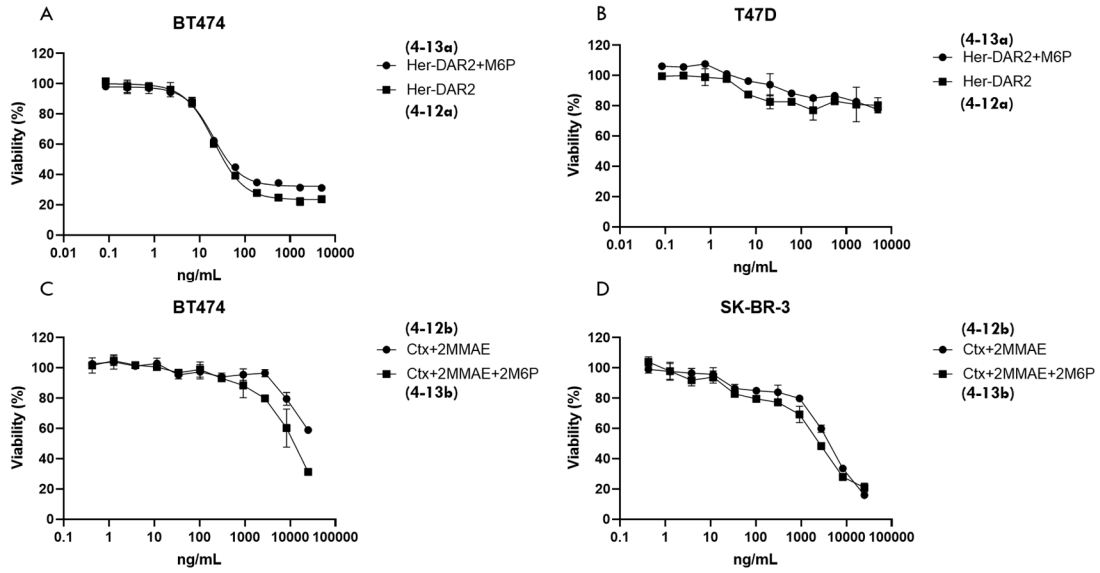

Figure 4-6. Cell killing assays for breast cancer cell lines with A) BT-474 (HER2 overexpression) with Herceptin based antibody conjugates **4-12a** and **4-13a**; B) T47D (HER2 low expressing) with Herceptin based antibody conjugates **4-12a** and **4-13a**; C) BT-474 (EGFR positive) with Cetuximab based antibody conjugates **4-12b** and **4-13b**; D) SK-BR-3 (EGFR positive) with Cetuximab based antibody conjugates **4-12b** and **4-13b**. All assays were performed in triplicate.

4.3 Conclusion

In this chapter, we discussed the strategy to generate homogenous dual-functionalized antibody conjugates with Fc glycan engineering. With the orthogonal Click reactions, we generated antibody-drug conjugates with M6P ligands. The resulting antibody conjugates showed strong binding to the CI-MPR. And cellular experiments suggested for the slow-internalizing receptors, such as EGFR, the antibody conjugates with M6P ligands demonstrated 2-3 folds benefit in cytotoxicity compared to the conjugates with no M6P. While for the fast-internalizing receptors, like HER2, there was no significant difference. On the other hand, for the antigen negative cell line (T47D), non-specific toxicity was not observed up to 10 ug/mL, which suggests the antibody conjugates remained their specificity. As we discussed, this work is a proof of concept that the ADCs with internalizing factors could improve its cytotoxicity profile *in vitro*. In the next stage of this project, we are working on synthesis of folate based internalizing factors, which is also a cancer specific antigen.

4.4 Experimental

Materials and Methods

Chemicals, reagents, and solvents were purchased from Sigma−Aldrich and/or TCI and used as received unless otherwise specified. Monoclonal antibody Hercptin was purchased from Premium Health Services Inc. (Columbia, MD). All moisture sensitive reactions were carried out under argon atmosphere, using standard Schlenk techniques. All dry solvents were prepared according to standard procedures. Thin-layer chromatography was performed on silica gel 60-F_{254} on glass plates (Merck) and revealed with *p*-anisaldehyde stain. Silica gel (200−425 mesh) used in flash chromatography for large-scale reactions was purchased from Sigma-Aldrich. Columns for flash chromatography for small-scale reactions were performed on Isolera One system with ZIP KP-Sil columns (Biotage) with elution condition specified for each target compound. Solvent gradients were given refer to stepped gradients and concentrations are reported as % v/v. Preparative HPLC was performed with Waters 1525 Binary HPLC pump coupled with 2489 UV/Vis Detector under UV 214 nm and 280 nm with a Waters Symmetry C18 column (7 μm, 19 × 300 mm) using water containing 0.1% trifluoracetic acid as phase A, MeCN containing 0.1% trifluoracetic acid as phase B. Semi-preparative HPLC for the toxic payloads was performed on the same instrument with an Aglient Eclipse XDB-C18 column (5 μm, 9.4× 250 mm) using water containing 0.1% formic acid as phase A, MeCN containing 0.1% formic acid as phase B.

Purification of antibody and antibody conjugates using AKTA prime plus FPLC system.

The FPLC system (GE Healthcare) was used for purification of the functionalized antibodies equipped with 1mL HiTrap protein A column (GE Heatlthcare) with standard procedures. Concentration of antibodies was determined by NanoDrap 200c (Thermo Scientific).

LC-ESI-MS analysis of antigen-DBCO payloads

LC-MS for glycans, glycopeptides and payload derivatives were performed on HPLC-SQ2 detector (Waters) with a Waters XBridge C18 column (3.5 μm, 2.1× 50 mm) using water containing 0.1% formic acid as phase A, MeCN containing 0.1% formic acid as phase B. The analytical HPLC for payload derivatives was analyzed with an Aglient Eclipse SDB-C18 column (5 μm, 3.0× 250 mm) under UV 214 nm and 280 nm with methods specialized for each compound. HR-ESI-MS was performed with Exactive Plus Orbitrap Mass Spectrometer (Thermo Scientific) equipped with a Waters XBridge C18 column (3.5 μm, 2.1× 50 mm).

LC-ESI-MS analysis of intact antibody derivatives.

LC-ESI-MS analysis of intact tagged antibodies and antibody-drug conjugates was performed with Exactive Plus Orbitrap Mass Spectrometer (Thermo Scientific)

equipped with a Waters XBridge BEH300 C-4 column (3.5 μm, 2.1 × 50 mm) with gradient elution of water containing 0.1% formic acid as phase A, MeCN containing 0.1% formic acid as phase B. Mass spectra were deconvoluted using MagTran (ver 1.03 b2).

LC-ESI-MS analysis of Fc domains released by IdeS treatment.

The antibody samples in PBS were incubated with IdeS at 37 °C for 2 h. The samples were analyzed by with Exactive Plus Orbitrap Mass Spectrometer (Thermo Scientific) equipped with an Agilent Poroshell 300SB C8 column (5 μm, 1.0 × 75 mm) with gradient elution of water containing 0.1% formic acid as phase A, MeCN containing 0.1% formic acid as phase B. Mass spectra were deconvoluted using MagTran (ver 1.03 b2).

NMR analysis.

^{1}H, ^{13}C, and COSY NMR spectra were recorded on 400 MHz or 600 MHz spectrometer (Bruker) with $CDCl_3$, MeOD-d_4, D_2O or DMSO-d_6 as the solvent (solvent residue peak 7.26, 3.31, 4.79, 2.50 ppm). All ^{13}C NMR spectra were performed with proton decoupling, and all chemical shifts are reported in part per million (ppm) and referenced to residual solvent. ^{1}H-NMR chemical shifts were recorded relative to the solvent residual peak ($CDCl_3$ at 7.26 ppm, MeOD-d_4 at 3.31ppm, D_2O at 4.79 ppm, DMSO-d_6 at 2.50 ppm). ^{13}C NMR chemical shifts are reported relative to the solvent

residual peak ($CDCl_3$ at 77.00 ppm, MeOD-d_4 at 49.00 ppm, DMSO-d_6 at 39.51 ppm). The number of protons (*n*) corresponding to a resonance signal was indicated by *n*H and spin-spin coupling constants (*J* value) recorded in Hz.

Surface Plasmon Resonance (SPR) Measurements.

SPR measurements were performed on a Biacore T200 instrument (GE Healthcare) at 25°C. Approximately 2000 resonance units (RU) of asialofetuin, fibronectin, β-1-integrin, BSA, MUC-1 and CD147were immobilized on a CM5 sensor chip in a sodium acetate buffer (50 μg/mL, pH 4.0), using the amine coupling kit provided by the manufacturer. A reference channel was immobilized with ethanolamine. Binding analyses were performed by injecting a solution of Drgal1 over four cells at 2-fold increasing concentration in HBS-P running buffer (10 mM HEPES, 150 mM NaCl, P20 surfactant 0.05% v/v, pH 7.4) containing 10 mM 2ME at a flow rate of 20 μL/min for 2 min and allowed to dissociate for another 5 min. The surface was regenerated after each cycle by injecting a 2 M $MgCl_2$ (aq) solution for 3 min at a flow rate of 30 μL/min. Kinetic analyses were performed by global fitting of the binding data to a 1:1 Langmuir binding model using BIAcore T200 evaluation software.

Synthesis of dual-functionalized SCT-oxa

Synthesis of the Mono-N_3-SCT (4-2). To a 1 mL glass vial with a stirring bar, SCT (61.8 mg, 30.6 μmol, 1 eq) was dissolved in 200 μL water. **Linker a** (9.4 mg, 8 μL, 30.6 μmol, 1 eq) was added to the solution, and the pH was adjusted to 6.0 – 6.5 by 10 μL 2 M HCl solution. DMTMM (42.2 mg, 153 μmol, 5 eq) was weighed and added as dry powder. The reaction was stirred at 50 °C for 3 hours. Another portion of DMTMM (52.2 mg, 153 μmol, 5 eq) was added, and the reaction was heated for another 3 hours. After using HPLC to confirm the completion of the reaction, 0.5% TFA (750 μL) was added to the vial, the mixture was stirred 16 hours at room temperature. The mixture was centrifuged at 14000 rpm for 5 min, the supernatant was purified by G-15 size exclusion column. The glycan containing fractions were collected and purified by HiTrap Q XL 2 × 5 mL column, and eluted with a linear gradient of 200 mM NaCl (0−40%, v/v) with water over 60 min. The corresponding fractions were collected and concentrated under vacuum, then desalted by G-10 size exclusion column. The glycan containing fractions were combined and lyophilized to afford **4-2** (50.2 mg, 71 %). ^{1}H NMR (D_2O, 600 MHz) δ = 1.76 (2H, dt, H3f$_{ax}$, H3f'$_{ax}$), 1.90, 1.95, 1.97 (15H, 3 s, 5 × CH_3), 2.62 (2H, 2 t, H3f$_{eq}$, H3f'$_{eq}$), 3.39–3.47 (8H, m, H4c, H4c', H2e, H2e', 1 × CH_2NH, 1 × CH_2N_3), 3.48–3.63 (39H, m, H4a, H5a(β), H5b, H5c', H6c, H6c', H4d, H4d', H5d, H5d', H3e, H3e', H6e, H6e', H4f, H4f', H7f, H7f', H9f, H9f', 5 × CH_2OCH_2), 3.61–3.75 (10H, m, H3a, H6a, H3b, H5c, H2d, H2d', H3d, H3d', H6f, H6f'), 3.76–3.93 (25H, m, H2a, H6'a, H4b, H6b, H6'b, H3c, H3c', H6'c, H6'c', H6d, H6d', H6'd, H6'd', H4e, H4e', H5e, H5e', H6'e, H6'e', H5f, H5f', H8f, H8f', H9'f,

H9'f'), 4.03 (1H, br s, H2c'), 4.11 (1H, br s, H2c), 4.18 (1H, br s, H2b), 4.36 (2H, d, $J_{1,2}$ = 7.8 Hz, H1e, H1e'), 4.51 (2H, d, $J_{1,2}$ = 6.3 Hz, H1d, H1d'), 4.53 (0.3H, d, H1a(β)), 4.70 (1H, d, H1b), 4.86 (1H, s, H1c'), 5.05 (1H, s, H1c), 5.13 (0.7H, d, $J_{1,2}$ = 2.7 Hz, H1a(α)). ESI-MS: $[M + 2H]^{2+}$ calcd for $C_{88}H_{151}N_9O_{61}^{2+}$, 1154.95 (100%); found (*m/z*), 1155.23.

Synthesis of the CP-N$_3$-SCT (4-3). To a 1 mL glass vial with a stirring bar, **4-2** (40.8 mg, 30.6 μmol, 1 eq) was dissolved in 150 μL water. CP-NH_2 (19.4 mg, 92 μmol, 3 eq) was added to the solution, and the pH was adjusted to 6.0 – 6.5 by 20 μL 2 M HCl solution. DMTMM (42.2 mg, 153 μmol, 5 eq) was weighed and added as dry powder. The reaction was stirred at 50 °C for 3 hours. Another portion of DMTMM (52.2 mg, 153 μmol, 5 eq) was added, and the reaction was heated for another 3 hours. After using HPLC to confirm the completion of the reaction, 0.5% TFA (750 μL) was added to the vial, the mixture was stirred for 16 hours at room temperature. The mixture was centrifuged at 14000 rpm for 5 min, the supernatant was purified by preparative HPLC. The corresponding fractions were combined and lyophilized to afford **4-3** (27.1 mg, 61%). ^{1}H NMR (D_2O, 600 MHz) δ = 1.50–1.60 (4H, m, 2 × $NHCH_2CH_2$), 1.64 (1H, t, C*H*CH=), 1.83 (2H, dd, $H3f_{ax}$, $H3f'_{ax}$), 2.05–2.15 (18H, m, 5 × CH_3, CH_3C=), 2.69–2.76 (2H, dd, $H3f_{eq}$, $H3f'_{eq}$), 3.16 (2H, m, CH_2NH-CP), 3.16-3.27 (4H, m, CH_2 NH-Cp, CH_2NH-SCT), 3.46–3.54 (8H, m, H4c, H4c', H2e, H2e', CH_2NH-SCT, 1 × CH_2N_3), 3.55–3.69 (39H, m, H4a, H5a(β), H5b, H5c', H6c, H6c', H4d, H4d', H5d, H5d', H3e, H3e', H6e, H6e', H4f, H4f', H7f, H7f', H9f, H9f', 5 × CH_2OCH_2), 3.69–3.82 (10H, m, H3a, H6a, H3b, H5c, H2d, H2d', H3d, H3d', H6f, H6f'), 3.83–4.00

(25H, m, H2a, H6'a, H4b, H6b, H6'b, H3c, H3c', H6'c, H6'c', H6d, H6d', H6'd, H6'd', H4e, H4e', H5e, H5e', H6'e, H6'e', H5f, H5f', H8f, H8f', H9'f, H9'f'), 4.14 (1H, br s, H2c'), 4.21 (1H, br s, H2c), 4.28 (1H, br s, H2b), 4.45 (2H, d, $J_{1,2}$ = 5.3 Hz, H1e, H1e'), 4.61 (2H, d, $J_{1,2}$ = 6.6 Hz, H1d, H1d'), 4.76 (0.3H, d, H1a(β)), 4.96 (1H, s, H1c'), 5.15 (1H, s, H1c), 5.23 (0.7H, d, $J_{1,2}$ = 3.4 Hz, H1a(α)), 6.66 (1H, m, C*H*=C). HR-ESI-MS: $[M + H]^+$ calcd for $C_{98}H_{166}N_{11}O_{61}^+$, 2490.0203 (100%); found (*m/z*), 2490.0364.

Synthesis of CP-N_3-SCT-oxa (4-4). Compound **4-4** was synthesized with the method reported in Chapter 3 (5.2 mg, 90%). ^{1}H NMR (D_2O, 600 MHz) δ = 1.50–1.60 (4H, m, 2 × $NHCH_2CH_2$), 1.64 (1H, t, C*H*CH=), 1.83 (2H, dd, H3f$_{ax}$, H3f'$_{ax}$), 2.05–2.15 (18H, m, 5 × CH_3, CH_3C=), 2.69–2.76 (2H, dd, H3f$_{eq}$, H3f'$_{eq}$), 3.16 (2H, m, CH_2NH-CP), 3.16-3.27 (4H, m, CH_2 NH-Cp, CH_2NH-SCT), 3.46–3.54 (8H, m, H4c, H4c', H2e, H2e', CH_2NH-SCT, 1 × CH_2N_3), 3.55–3.69 (39H, m, H4a, H5a(β), H5b, H5c', H6c, H6c', H4d, H4d', H5d, H5d', H3e, H3e', H6e, H6e', H4f, H4f', H7f, H7f', H9f, H9f', 5 × CH_2OCH_2), 3.69–3.82 (10H, m, H3a, H6a, H3b, H5c, H2d, H2d', H3d, H3d', H6f, H6f'), 3.83–4.00 (25H, m, H2a, H6'a, H4b, H6b, H6'b, H3c, H3c', H6'c, H6'c', H6d, H6d', H6'd, H6'd', H4e, H4e', H5e, H5e', H6'e, H6'e', H5f, H5f', H8f, H8f', H9'f, H9'f'), 4.14 (1H, br s, H2c'), 4.21 (1H, br s, H2c), 4.28 (1H, br s, H2b), 4.45 (2H, d, $J_{1,2}$ = 5.3 Hz, H1e, H1e'), 4.61 (2H, d, $J_{1,2}$ = 6.6 Hz, H1d, H1d'), 4.96 (1H, s, H1c'), 5.15 (1H, s, H1c), 6.11 (1H, d, $J_{1,2}$ = 7.2 Hz, H1a), 6.66 (1H, m, C*H*=C). HR-ESI-MS: $[M + H]^+$ calcd for $C_{98}H_{164}N_{11}O_{61}^+$, 2472.0097 (100%); found (*m/z*), 2472.0254.

Synthesis of dual-functionalized antibody conjugates

Synthesis of compound 4-7a. Prepared from **4-6a** (3 mg, 21 nmol, 1eq) and **4-4** (1.5 mg, 0.62 μmol, 30eq) with the General Procedure B in Chapter 2 to yield antibody **4-7a** (2.9 mg, 93%). ESI-MS of intact **4-7a**: calcd. M = 150809 Da; found (m/z), 2793.71 $[M + 54H]^{54+}$, 2846.39 $[M + 53H]^{53+}$, 2901.14 $[M + 52H]^{52+}$, deconvolution of the ESI-MS, M = 150807 Da

Synthesis of compound 4-7b. Prepared from **4-6b** (3 mg, 21 nmol, 1eq) and **4-4** (1.5 mg, 0.62 μmol, 30eq) with the General Procedure B in Chapter 2 to yield antibody **4-7a** (2.8 mg, 90%). ESI-MS of Fc of **4-7b**: calcd. M = 26606 Da; found (m/z),1774.81 $[M + 15H]^{15+}$, 1901.45 $[M + 14H]^{14+}$, 2047.59 $[M + 13H]^{13+}$, 2218.17 $[M + 12H]^{12+}$, deconvolution of the ESI-MS, M = 26606 Da

Synthesis of ADC 4-12a. Prepared from **4-7a** (2.5 mg, 16 nmol, 1eq) and **2-9** (0.27 mg, 0.16 μmol, 10eq) with the method reported in Chapter 2 to yield antibody conjugate **4-12a** (2.0 mg, 78%). ESI-MS of intact **4-12a**: calcd. M = 153977 Da; found (m/z), 2852.39 $[M + 53H]^{53+}$, 2906.21 $[M + 52H]^{52+}$, 2962.08 $[M + 51H]^{51+}$, deconvolution of the ESI-MS, M = 153979 Da

Synthesis of ADC 4-12b. Prepared from **4-7b** (2.5 mg, 16 nmol, 1eq) and **2-9** (0.27 mg, 0.16 μmol, 10eq) with the method reported in Chapter 2 to yield antibody conjugate **4-12b** (2.1 mg, 82%). ESI-MS of Fc of **4-12b**: calcd. M = 28190 Da; found

(m/z),1880.37 $[M + 15H]^{15+}$, 2014.65 $[M + 14H]^{14+}$, 2169.49 $[M + 13H]^{13+}$, 2350.23 $[M + 12H]^{12+}$, deconvolution of the ESI-MS, M = 28191 Da

Synthesis of the M6P functionalized ADCs 4-13a. Prepared from **4-12a** (1.6 mg, 10 nmol, 1eq) and **4-11** (0.11 mg, 0.10 μmol, 10eq) with the method reported in Chapter 3 to yield antibody conjugate **4-13a** (1.5 mg, 92%). ESI-MS of intact **4-13a**: calcd. M = 156241 Da; found (m/z), 2949.05 $[M + 53H]^{53+}$, 3005.62 $[M + 52H]^{52+}$, 3064.49 $[M + 51H]^{51+}$, deconvolution of the ESI-MS, M = 156242 Da

Synthesis of the M6P functionalized ADCs 4-13b. Prepared from **4-12b** (1.6 mg, 10 nmol, 1eq) and **4-11** (0.11 mg, 0.10 μmol, 10eq) with the method reported in Chapter 3 to yield antibody conjugate **4-13b** (1.4 mg, 86%). ESI-MS of Fc of **4-13b**: M = 29322 Da; found (m/z),1955.93 $[M + 15H]^{15+}$, 2095.53 $[M + 14H]^{14+}$, 2256.72 $[M + 13H]^{13+}$, 2444.68 $[M + 12H]^{12+}$, deconvolution of the ESI-MS, M = 29323 Da

In Vitro Cytotoxicity Assay

BT474 cells (ATCC HTB-20) were cultured in HybriCare medium (ATCC 46-X) supplemented with 10% fetal bovine serum (FBS), 100 U/mL penicillin, and 100 μg/mL streptomycin in T-75 flasks (CELLTREAT). SK-BR-3 cells (ATCC HTB-30) were cultured in McCoy's 5A medium (ATCC 30-2007) supplemented with 10% fetal bovine serum (FBS), 100 U/mL penicillin, and 100 μg/mL streptomycin in T-75 flasks (CELLTREAT). T47D cells (ATCC HTB-133) were maintained in RPMI-1640

medium (ATCC 30-2001) containing FBS, 4 mg/L insulin, 100 U/mL penicillin, and 100 μg/mL streptomycin in T-75 flasks (CELLTREAT).

For the cytotoxicity assays, cells were seeded into 96-well plates with 10,000 cells per well and grown for 24 hours at 37 °C and 5% CO_2. The FBS containing media was removed. The serum free RPMI media with the antibody conjugates (starting at a concentration of 25 μg/mL for BT474, 25 μg/mL for SK-BR-3, and 10 μg/mL for T47D and serially diluted 1:3) was added. Each compound was assessed in triplicate wells, the cells without treatment served as control. After incubation for 72 hours, the antibody conjugates solution was removed before the incubation with RPMI media containing 10% cell counting kit-8 (Dojindo). The absorbance of formazan released by viable cells was measured at 450 nm using a spectrophotometer after incubation for 2−3 h at 37 °C and 5% CO_2. Finally, the cell viability curve and the EC50 values were calculated using GraphPad Prism software.

4.5 Supporting Information

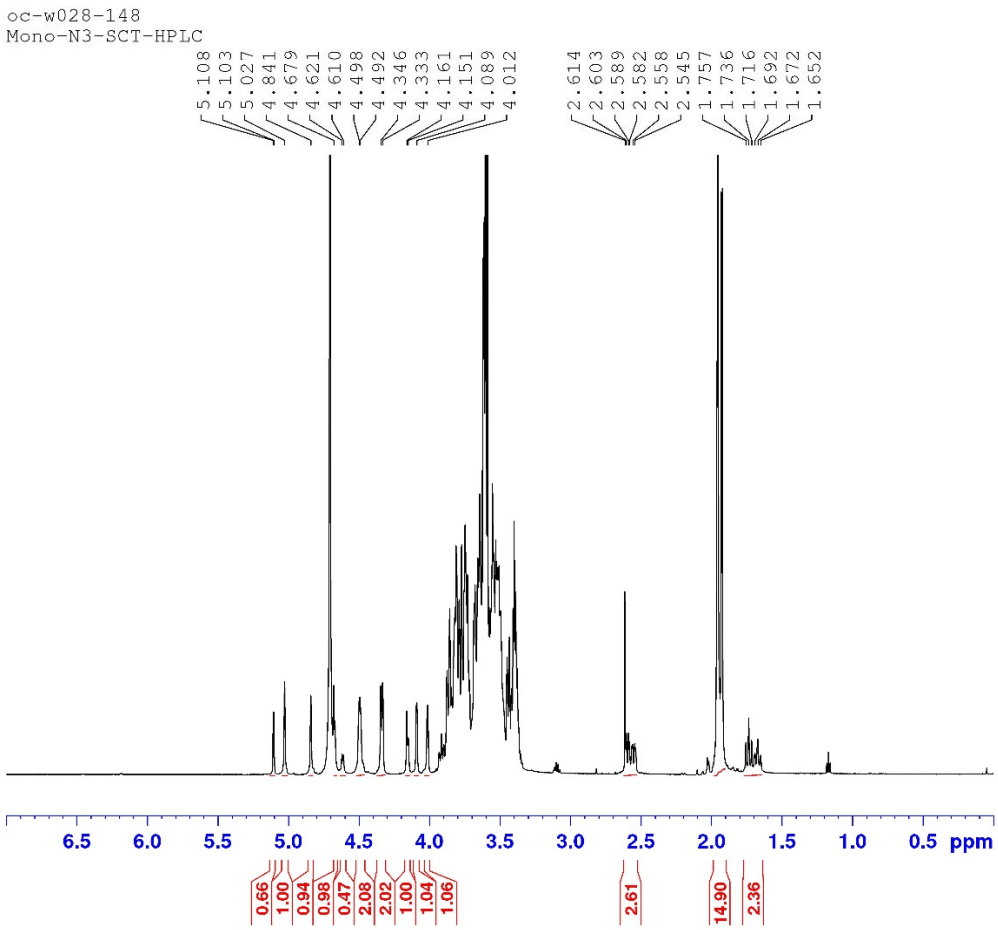

^{1}H NMR spectrum (600 MHz, D_2O): compound **4-2**

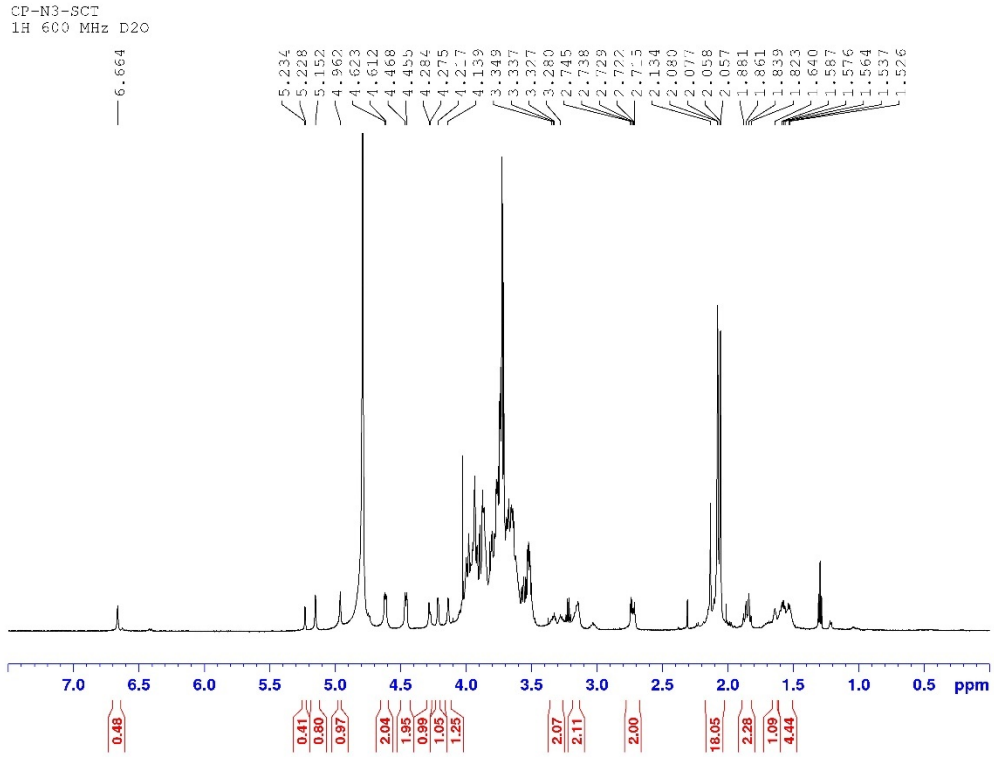

^{1}H NMR spectrum (600 MHz, D_2O): compound **4-3**

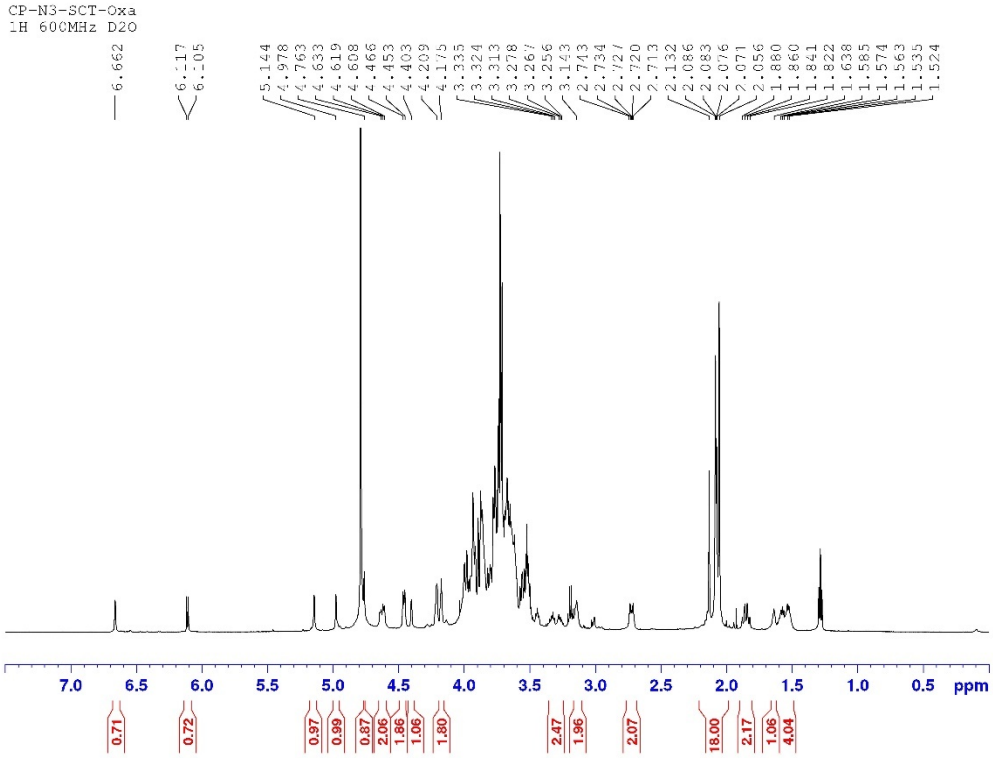

^{1}H NMR spectrum (600 MHz, D_2O): compound **4-4**

Chapter 5: Conclusions and Future Directions

The main focus of my thesis was to develop and optimize a general method for efficient antibody conjugation and functionalization based on the chemoenzymatic Fc remodeling method pioneered by the Wang group. In this method, the conserved Fc *N*-glycan on IgG antibodies was trimmed by the wild-type endoglycosidase, then the antibodies were functionalized with the endoglycosidase mutant and functionalized *N*-glycan oxazolines. The site-specific antibody conjugates could be generated by Click reactions for different purposes.

In Chapter 2, we reported the optimization of the reactions required for an efficient synthesis of the antibody conjugates. Firstly, the selectively modified glycan oxazolines were synthesized from free sialoglycan in a one-pot manner with high efficiency. And a highly efficient transglycosylation reaction based on an endoglycosidase mutant (Endo-S2 D184M) was optimized for transferring the tagged glycans to yield selectively tagged antibodies ready for Click drug conjugation. Thanks to the enhanced enzymatic activity of the Endo-S2 D184M mutant over the previously used Endo-S D233Q mutant, much less glycan oxazolines with much shorter reaction time was required to complete the enzymatic reaction, thus minimizing the potential non-enzymatic side reactions. This improved method was also flexible for introducing different bioorthogonal groups into an antibody, which allowed site-specific conjugation with different Click reactions to construct homogeneous antibody-drug conjugates. The homogeneous ADCs constructed by this method showed equally

excellent serum stability and demonstrated potent and selective cytotoxicity against Her2-overexpressing cancer cells.

In Chapter 3, we reported a highly efficient chemoenzymatic synthesis of homogeneous antibody-rhamnose cluster and antibody-αGal cluster conjugates based on the method we described in the previous chapter: the antibody conjugates were obtained by the chemoenzymatic Fc glycan remodeling followed by Click functionalization. Thanks to the broad substrate specificity of the Endo-S2 D184M, the antibody-rhamnose conjugate could also be achieved by direct Fc glycan remodeling with a rhamnose-preloaded glycan oxazoline. A side-by-side comparison study showed that the antibody-rhamnose cluster conjugates could recruit natural serum antibodies and complements for targeted cancer cell killing with much high potency than the corresponding antibody-αGal conjugates. These results suggested that antibody-rhamnose conjugates represented a promising strategy for augmenting the CDC activity for IgG antibodies by recruiting the more effective natural anti-Rha IgM antibodies.

In Chapter 4, we reported our preliminary research to enhance the therapeutic window and possibly broaden the scope for druggable tumor antigens by incorporating an internalizing factor onto the ADCs. With our improved *N*-glycan functionalization strategy, homogenous dual-functionalized antibody conjugates were generated with Fc glycan engineering. The antibody-drug conjugates incorporating a terminal mannose-6-phosphate (M6P) as an internalization ligand with orthogonal Click reactions. According to the SPR binding study, the resulting antibody conjugates showed strong binding to the M6P receptor. And cellular experiments suggested for the EGFR, a

slow-internalizing receptor, the antibody conjugate with M6P ligands demonstrated 2-3 fold increase in cytotoxicity compared to the conjugates with no M6P. While for the fast-internalizing receptors, like HER2, there was no significant difference. At the same time, the antibody conjugates remained their specificity against EGFR: non-specific toxicity was not observed up to 10 ug/mL for the antigen negative cell line (T47D).

For future studies, our group will continue to conduct the *in vitro* and *in vivo* evaluation of the ADCs generated in Chapter 2: we will do an *in vivo* efficacy study, based on mice xenograft model, to compare our ADCs to Kadcyla and Enhertu, the two commercially available ADCs against the HER2 over-expressing tumors; and a detailed pharmacokinetic study could be also conducted to compare the *in vivo* stability of the ADCs generated by different strategy. This conjugation method is also used by other lab members to generate antibody conjugates to degrade disease-associated protein target in serum. For example, a series of anti-PCSK9 antibody-galactose conjugates are generated to degrade the PCSK9 protein for reducing the blood cholesterol levels.

Also, as we discussed in Chapter 3, we will continue our research into the antibody-rhamnose conjugates with our collaborators specialized in MRSA. We will generate antibody-rhamnose conjugates targeting the MRSA-specific protein A. And we will conduct both *in vitro* and *in vivo* experiments to verify if they have therapeutic potential for the treatment of MRSA infections.

And for the antibodies with internalizing factors, as we discussed in Chapter 4, this work is a proof of concept that the ADCs with internalizing factors could improve

its cytotoxicity profile *in vitro*. For the next stage of this project, we will use cancer-specific ligands, such as folic acid as the internalization factors. In follow-up studies, the multivalent folate Clickable ligands could be synthesized with similar strategy that was reported in Chapter 3. We could use the double Click method to generate ADCs with two or eight folate residues per antibody. Then we could conduct *in vitro* and *in vivo* studies to evaluate their effectiveness as tumor specific internalizing factors.

Bibliography

1. Akkapeddi, P.; Azizi, S. A.; Freedy, A. M.; Cal, P.; Gois, P. M. P.; Bernardes, G. J. L., Construction of homogeneous antibody-drug conjugates using site-selective protein chemistry. *Chem Sci* **2016,** *7*, 2954-2963.
2. Sievers, E. L.; Senter, P. D., Antibody-drug conjugates in cancer therapy. *Annu Rev Med* **2013,** *64*, 15-29.
3. Lambert, J. M.; Berkenblit, A., Antibody-Drug Conjugates for Cancer Treatment. *Annu Rev Med* **2018,** *69*, 191-207.
4. Beck, A.; Goetsch, L.; Dumontet, C.; Corvaia, N., Strategies and challenges for the next generation of antibody-drug conjugates. *Nat Rev Drug Discov* **2017,** *16*, 315-337.
5. Chari, R. V.; Miller, M. L.; Widdison, W. C., Antibody-drug conjugates: an emerging concept in cancer therapy. *Angew Chem Int Ed* **2014,** *53*, 3796-3827.
6. Lehar, S. M.; Pillow, T.; Xu, M.; Staben, L.; Kajihara, K. K.; Vandlen, R.; DePalatis, L.; Raab, H.; Hazenbos, W. L.; Morisaki, J. H.; Kim, J.; Park, S.; Darwish, M.; Lee, B. C.; Hernandez, H.; Loyet, K. M.; Lupardus, P.; Fong, R.; Yan, D.; Chalouni, C.; Luis, E.; Khalfin, Y.; Plise, E.; Cheong, J.; Lyssikatos, J. P.; Strandh, M.; Koefoed, K.; Andersen, P. S.; Flygare, J. A.; Wah Tan, M.; Brown, E. J.; Mariathasan, S., Novel antibody-antibiotic conjugate eliminates intracellular S. aureus. *Nature* **2015,** *527*, 323-328.
7. Touti, F.; Lautrette, G.; Johnson, K. D.; Delaney, J. C.; Wollacott, A.; Tissire, H.; Viswanathan, K.; Shriver, Z.; Mong, S. K.; Mijalis, A. J.; Plante, O. J.; Pentelute, B. L., Antibody-Bactericidal Macrocyclic Peptide Conjugates To Target Gram-Negative Bacteria. *Chembiochem* **2018,** *19*, 2039-2044.
8.Tong, J. T. W.; Harris, P. W. R.; Brimble, M. A.; Kavianinia, I., An Insight into FDA Approved Antibody-Drug Conjugates for Cancer Therapy. *Molecules* **2021,** *26*, 5847.
9. Drago, J. Z.; Modi, S.; Chandarlapaty, S., Unlocking the potential of antibody-drug conjugates for cancer therapy. *Nat Rev Clin Oncol* **2021,** *18*, 327-344.
10. Rodrigues, T.; Bernardes, G. J. L., Development of Antibody-Directed Therapies: Quo Vadis? *Angew Chem Int Ed* **2018,** *57*, 2032-2034.
11. Jabbour, E.; Paul, S.; Kantarjian, H., The clinical development of antibody-drug conjugates - lessons from leukaemia. *Nat Rev Clin Oncol* **2021,** *18*, 418-433.
12. Agarwal, P.; Bertozzi, C. R., Site-specific antibody-drug conjugates: the nexus of bioorthogonal chemistry, protein engineering, and drug development. *Bioconjug Chem* **2015,** *26*, 176-192.
13. Strop, P.; Delaria, K.; Foletti, D.; Witt, J. M.; Hasa-Moreno, A.; Poulsen, K.; Casas, M. G.; Dorywalska, M.; Farias, S.; Pios, A.; Lui, V.; Dushin, R.; Zhou, D.; Navaratnam, T.; Tran, T. T.; Sutton, J.; Lindquist, K. C.; Han, B.; Liu, S. H.; Shelton, D. L.; Pons, J.; Rajpal, A., Site-specific conjugation improves therapeutic index of antibody drug conjugates with high drug loading. *Nat Biotechnol* **2015,** *33*, 694-696.
14. Chudasama, V.; Maruani, A.; Caddick, S., Recent advances in the construction of antibody-drug conjugates. *Nat Chem* **2016,** *8*, 114-119.
15. Junutula, J. R.; Raab, H.; Clark, S.; Bhakta, S.; Leipold, D. D.; Weir, S.; Chen, Y.; Simpson, M.; Tsai, S. P.; Dennis, M. S.; Lu, Y.; Meng, Y. G.; Ng, C.; Yang, J.; Lee, C. C.; Duenas, E.; Gorrell, J.; Katta, V.; Kim, A.; McDorman, K.; Flagella,

K.; Venook, R.; Ross, S.; Spencer, S. D.; Lee Wong, W.; Lowman, H. B.; Vandlen, R.; Sliwkowski, M. X.; Scheller, R. H.; Polakis, P.; Mallet, W., Site-specific conjugation of a cytotoxic drug to an antibody improves the therapeutic index. *Nat Biotechnol* **2008,** *26*, 925-932.
16. Strop, P.; Liu, S. H.; Dorywalska, M.; Delaria, K.; Dushin, R. G.; Tran, T. T.; Ho, W. H.; Farias, S.; Casas, M. G.; Abdiche, Y.; Zhou, D.; Chandrasekaran, R.; Samain, C.; Loo, C.; Rossi, A.; Rickert, M.; Krimm, S.; Wong, T.; Chin, S. M.; Yu, J.; Dilley, J.; Chaparro-Riggers, J.; Filzen, G. F.; O'Donnell, C. J.; Wang, F.; Myers, J. S.; Pons, J.; Shelton, D. L.; Rajpal, A., Location matters: site of conjugation modulates stability and pharmacokinetics of antibody drug conjugates. *Chem Biol* **2013,** *20*, 161-167.
17. Axup, J. Y.; Bajjuri, K. M.; Ritland, M.; Hutchins, B. M.; Kim, C. H.; Kazane, S. A.; Halder, R.; Forsyth, J. S.; Santidrian, A. F.; Stafin, K.; Lu, Y.; Tran, H.; Seller, A. J.; Biroc, S. L.; Szydlik, A.; Pinkstaff, J. K.; Tian, F.; Sinha, S. C.; Felding-Habermann, B.; Smider, V. V.; Schultz, P. G., Synthesis of site-specific antibody-drug conjugates using unnatural amino acids. *Proc Natl Acad Sci U S A* **2012,** *109*, 16101-16106.
18. Li, C.; Wang, L. X., Chemoenzymatic Methods for the Synthesis of Glycoproteins. *Chem Rev* **2018,** *118*, 8359-8413.
19. Wang, L. X.; Tong, X.; Li, C.; Giddens, J. P.; Li, T., Glycoengineering of Antibodies for Modulating Functions. *Annu Rev Biochem* **2019,** *88*, 433-459.
20. O'Shannessy, D. J.; Dobersen, M. J.; Quarles, R. H., A novel procedure for labeling immunoglobulins by conjugation to oligosaccharide moieties. *Immunol Lett* **1984,** *8*, 273-277.
21. Okeley, N. M.; Toki, B. E.; Zhang, X.; Jeffrey, S. C.; Burke, P. J.; Alley, S. C.; Senter, P. D., Metabolic engineering of monoclonal antibody carbohydrates for antibody-drug conjugation. *Bioconjug Chem* **2013,** *24*, 1650-1655.
22. Campbell, C. T.; Sampathkumar, S. G.; Yarema, K. J., Metabolic oligosaccharide engineering: perspectives, applications, and future directions. *Mol Biosyst* **2007,** *3*, 187-194.
23. Boeggeman, E.; Ramakrishnan, B.; Kilgore, C.; Khidekel, N.; Hsieh-Wilson, L. C.; Simpson, J. T.; Qasba, P. K., Direct identification of nonreducing GlcNAc residues on N-glycans of glycoproteins using a novel chemoenzymatic method. *Bioconjug Chem* **2007,** *18*, 806-814.
24. Li, X.; Fang, T.; Boons, G. J., Preparation of well-defined antibody-drug conjugates through glycan remodeling and strain-promoted azide-alkyne cycloadditions. *Angew Chem Int Ed* **2014,** *53*, 7179-7182.
25. van Geel, R.; Wijdeven, M. A.; Heesbeen, R.; Verkade, J. M.; Wasiel, A. A.; van Berkel, S. S.; van Delft, F. L., Chemoenzymatic Conjugation of Toxic Payloads to the Globally Conserved N-Glycan of Native mAbs Provides Homogeneous and Highly Efficacious Antibody-Drug Conjugates. *Bioconjug Chem* **2015,** *26*, 2233-2242.
26. Huang, W.; Giddens, J.; Fan, S. Q.; Toonstra, C.; Wang, L. X., Chemoenzymatic glycoengineering of intact IgG antibodies for gain of functions. *J Am Chem Soc* **2012,** *134*, 12308-12318.
27. Parsons, T. B.; Struwe, W. B.; Gault, J.; Yamamoto, K.; Taylor, T. A.; Raj, R.; Wals, K.; Mohammed, S.; Robinson, C. V.; Benesch, J. L.; Davis, B. G., Optimal

Synthetic Glycosylation of a Therapeutic Antibody. *Angew Chem Int Ed* **2016,** *55*, 2361-2367.
28. Tang, F.; Yang, Y.; Tang, Y.; Tang, S.; Yang, L.; Sun, B.; Jiang, B.; Dong, J.; Liu, H.; Huang, M.; Geng, M. Y.; Huang, W., One-pot N-glycosylation remodeling of IgG with non-natural sialylglycopeptides enables glycosite-specific and dual-payload antibody-drug conjugates. *Org Biomol Chem* **2016,** *14*, 9501-9518.
29. Iwamoto, M.; Yamaguchi, T.; Sekiguchi, Y.; Oishi, S.; Shiiki, T.; Soma, M.; Nakamura, K.; Yoshida, M.; Chaya, H.; Mori, Y.; Miyauchi, R.; Hasegawa, J.; Nagayama, T.; Honda, T., Pharmacokinetic and Pharmacodynamic Profiles of Glyco-Modified Atrial Natriuretic Peptide Derivatives Synthesized Using Chemo-enzymatic Synthesis Approaches. *Bioconjug Chem* **2018,** *29*, 2829-2837.
30. Manabe, S.; Yamaguchi, Y.; Matsumoto, K.; Fuchigami, H.; Kawase, T.; Hirose, K.; Mitani, A.; Sumiyoshi, W.; Kinoshita, T.; Abe, J.; Yasunaga, M.; Matsumura, Y.; Ito, Y., Characterization of Antibody Products Obtained through Enzymatic and Nonenzymatic Glycosylation Reactions with a Glycan Oxazoline and Preparation of a Homogeneous Antibody-Drug Conjugate via Fc N-Glycan. *Bioconjug Chem* **2019**, *30*, 1343-1355.
31. Faridoon, F.; Shi, W.; Qin, K.; Tang, Y.; Li, M.; Guan, D.; Tian, X.; Jiang, B.; Dong, J.; Tang, F.; Huang, W., New linker structures applied in glycosite-specific antibody drug conjugates. *Org Chem Front* **2019,** *6*, 3144-3149.
32. Xiao, H.; Chatterjee, A.; Choi, S. H.; Bajjuri, K. M.; Sinha, S. C.; Schultz, P. G., Genetic incorporation of multiple unnatural amino acids into proteins in mammalian cells. *Angew Chem Int Ed* **2013,** *52*, 14080-14083.
33. Bruins, J. J.; Blanco-Ania, D.; van der Doef, V.; van Delft, F. L.; Albada, B., Orthogonal, dual protein labelling by tandem cycloaddition of strained alkenes and alkynes to ortho-quinones and azides. *Chem Commun* **2018,** *54*, 7338-7341.
34. Adumeau, P.; Vivier, D.; Sharma, S. K.; Wang, J.; Zhang, T.; Chen, A.; Agnew, B. J.; Zeglis, B. M., Site-Specifically Labeled Antibody-Drug Conjugate for Simultaneous Therapy and ImmunoPET. *Mol Pharm* **2018,** *15*, 892-898.
35. Ilovich, O.; Qutaish, M.; Hesterman, J. Y.; Orcutt, K.; Hoppin, J.; Polyak, I.; Seaman, M.; Abu-Yousif, A. O.; Cvet, D.; Bradley, D. P., Dual-Isotope Cryoimaging Quantitative Autoradiography: Investigating Antibody-Drug Conjugate Distribution and Payload Delivery Through Imaging. *J Nucl Med* **2018,** *59*, 1461-1466.
36. Kang, J. C.; Sun, W.; Khare, P.; Karimi, M.; Wang, X.; Shen, Y.; Ober, R. J.; Ward, E. S., Engineering a HER2-specific antibody-drug conjugate to increase lysosomal delivery and therapeutic efficacy. *Nat Biotechnol* **2019,** *37*, 523-526.
37. Levengood, M. R.; Zhang, X.; Hunter, J. H.; Emmerton, K. K.; Miyamoto, J. B.; Lewis, T. S.; Senter, P. D., Orthogonal Cysteine Protection Enables Homogeneous Multi-Drug Antibody-Drug Conjugates. *Angew Chem Int Ed* **2017,** *56*, 733-737.
38. Yamazaki, C. M.; Yamaguchi, A.; Anami, Y.; Xiong, W.; Otani, Y.; Lee, J.; Ueno, N. T.; Zhang, N.; An, Z.; Tsuchikama, K., Antibody-drug conjugates with dual payloads for combating breast tumor heterogeneity and drug resistance. *Nat Commun* **2021,** *12*, 3528.
39. Shen, B. Q.; Xu, K.; Liu, L.; Raab, H.; Bhakta, S.; Kenrick, M.; Parsons-Reponte, K. L.; Tien, J.; Yu, S. F.; Mai, E.; Li, D.; Tibbitts, J.; Baudys, J.; Saad, O. M.; Scales, S. J.; McDonald, P. J.; Hass, P. E.; Eigenbrot, C.; Nguyen, T.; Solis, W. A.;

Fuji, R. N.; Flagella, K. M.; Patel, D.; Spencer, S. D.; Khawli, L. A.; Ebens, A.; Wong, W. L.; Vandlen, R.; Kaur, S.; Sliwkowski, M. X.; Scheller, R. H.; Polakis, P.; Junutula, J. R., Conjugation site modulates the in vivo stability and therapeutic activity of antibody-drug conjugates. *Nat Biotechnol* **2012,** *30*, 184-9.
40. Sellmann, C.; Doerner, A.; Knuehl, C.; Rasche, N.; Sood, V.; Krah, S.; Rhiel, L.; Messemer, A.; Wesolowski, J.; Schuette, M.; Becker, S.; Toleikis, L.; Kolmar, H.; Hock, B., Balancing Selectivity and Efficacy of Bispecific Epidermal Growth Factor Receptor (EGFR) x c-MET Antibodies and Antibody-Drug Conjugates. *J Biol Chem* **2016,** *291*, 25106-25119.
41. Li, J. Y.; Perry, S. R.; Muniz-Medina, V.; Wang, X.; Wetzel, L. K.; Rebelatto, M. C.; Hinrichs, M. J.; Bezabeh, B. Z.; Fleming, R. L.; Dimasi, N.; Feng, H.; Toader, D.; Yuan, A. Q.; Xu, L.; Lin, J.; Gao, C.; Wu, H.; Dixit, R.; Osbourn, J. K.; Coats, S. R., A Biparatopic HER2-Targeting Antibody-Drug Conjugate Induces Tumor Regression in Primary Models Refractory to or Ineligible for HER2-Targeted Therapy. *Cancer Cell* **2016,** *29*, 117-129.
42. DeVay, R. M.; Delaria, K.; Zhu, G.; Holz, C.; Foletti, D.; Sutton, J.; Bolton, G.; Dushin, R.; Bee, C.; Pons, J.; Rajpal, A.; Liang, H.; Shelton, D.; Liu, S. H.; Strop, P., Improved Lysosomal Trafficking Can Modulate the Potency of Antibody Drug Conjugates. *Bioconjug Chem* **2017,** *28*, 1102-1114.
43. Chari, R. V.; Miller, M. L.; Widdison, W. C., Antibody-drug conjugates: an emerging concept in cancer therapy. *Angew Chem Int Ed* **2014,** *53*, 3796-3827.
44. Walsh, S. J.; Bargh, J. D.; Dannheim, F. M.; Hanby, A. R.; Seki, H.; Counsell, A. J.; Ou, X.; Fowler, E.; Ashman, N.; Takada, Y.; Isidro-Llobet, A.; Parker, J. S.; Carroll, J. S.; Spring, D. R., Site-selective modification strategies in antibody-drug conjugates. *Chem Soc Rev* **2021,** *50*, 1305-1353.
45. do Pazo, C.; Nawaz, K.; Webster, R. M., The oncology market for antibody-drug conjugates. *Nat Rev Drug Discov* **2021,** *20,* 583.
46. VanBrunt, M. P.; Shanebeck, K.; Caldwell, Z.; Johnson, J.; Thompson, P.; Martin, T.; Dong, H.; Li, G.; Xu, H.; D'Hooge, F.; Masterson, L.; Bariola, P.; Tiberghien, A.; Ezeadi, E.; Williams, D. G.; Hartley, J. A.; Howard, P. W.; Grabstein, K. H.; Bowen, M. A.; Marelli, M., Genetically Encoded Azide Containing Amino Acid in Mammalian Cells Enables Site-Specific Antibody-Drug Conjugates Using Click Cycloaddition Chemistry. *Bioconjug Chem* **2015,** *26*, 2249-2260.
47. Nilchan, N.; Li, X.; Pedzisa, L.; Nanna, A. R.; Roush, W. R.; Rader, C., Dual-mechanistic antibody-drug conjugate via site-specific selenocysteine/cysteine conjugation. *Antibody therapeutics* **2019,** *2*, 71-78.
48. Shinmi, D.; Taguchi, E.; Iwano, J.; Yamaguchi, T.; Masuda, K.; Enokizono, J.; Shiraishi, Y., One-Step Conjugation Method for Site-Specific Antibody-Drug Conjugates through Reactive Cysteine-Engineered Antibodies. *Bioconjug Chem* **2016,** *27*, 1324-1331.
49. Dennler, P.; Chiotellis, A.; Fischer, E.; Bregeon, D.; Belmant, C.; Gauthier, L.; Lhospice, F.; Romagne, F.; Schibli, R., Transglutaminase-based chemo-enzymatic conjugation approach yields homogeneous antibody-drug conjugates. *Bioconjug Chem* **2014,** *25*, 569-578.
50. Anami, Y.; Xiong, W.; Gui, X.; Deng, M.; Zhang, C. C.; Zhang, N.; An, Z.; Tsuchikama, K., Enzymatic conjugation using branched linkers for constructing

homogeneous antibody-drug conjugates with high potency. *Org Biomol Chem* **2017,** *15*, 5635-5642.
51. Lin, S.; Yang, X.; Jia, S.; Weeks, A. M.; Hornsby, M.; Lee, P. S.; Nichiporuk, R. V.; Iavarone, A. T.; Wells, J. A.; Toste, F. D.; Chang, C. J., Redox-based reagents for chemoselective methionine bioconjugation. *Science* **2017,** *355*, 597-602.
52. Casi, G.; Huguenin-Dezot, N.; Zuberbühler, K.; Scheuermann, J.; Neri, D., Site-Specific Traceless Coupling of Potent Cytotoxic Drugs to Recombinant Antibodies for Pharmacodelivery. *J Am Chem Soc* **2012,** *134*, 5887-5892.
53. Zhang, C.; Dai, P.; Vinogradov, A. A.; Gates, Z. P.; Pentelute, B. L., Site-Selective Cysteine-Cyclooctyne Conjugation. *Angew Chem Int Ed* **2018,** *57*, 6459-6463.
54. Forte, N.; Chudasama, V.; Baker, J. R., Homogeneous antibody-drug conjugates via site-selective disulfide bridging. *Drug Discov Today: Technol* **2018,** *30*, 11-20.
55. Badescu, G.; Bryant, P.; Bird, M.; Henseleit, K.; Swierkosz, J.; Parekh, V.; Tommasi, R.; Pawlisz, E.; Jurlewicz, K.; Farys, M.; Camper, N.; Sheng, X.; Fisher, M.; Grygorash, R.; Kyle, A.; Abhilash, A.; Frigerio, M.; Edwards, J.; Godwin, A., Bridging disulfides for stable and defined antibody drug conjugates. *Bioconjug Chem* **2014,** *25*, 1124-1136.
56. Schneider, H.; Deweid, L.; Avrutina, O.; Kolmar, H., Recent progress in transglutaminase-mediated assembly of antibody-drug conjugates. *Anal Biochem* **2020,** *595*, 113615.
57. Manabe, S.; Yamaguchi, Y., Antibody Glycoengineering and Homogeneous Antibody-Drug Conjugate Preparation. *Chem Rec* **2021,** *21*, 1-11.
58. Stan, A. C.; Radu, D. L.; Casares, S.; Bona, C. A.; Brumeanu, T.-D., Antineoplastic Efficacy of Doxorubicin Enzymatically Assembled on Galactose Residues of a Monoclonal Antibody Specific for the Carcinoembryonic Antigen. *Cancer Res* **1999,** *59*, 115-121.
59. Zhou, Q.; Stefano, J. E.; Manning, C.; Kyazike, J.; Chen, B.; Gianolio, D. A.; Park, A.; Busch, M.; Bird, J.; Zheng, X.; Simonds-Mannes, H.; Kim, J.; Gregory, R. C.; Miller, R. J.; Brondyk, W. H.; Dhal, P. K.; Pan, C. Q., Site-specific antibody-drug conjugation through glycoengineering. *Bioconjug Chem* **2014,** *25*, 510-520.
60. Faridoon; Shi, W.; Qin, K.; Tang, Y.; Li, M.; Guan, D.; Tian, X.; Jiang, B.; Dong, J.; Tang, F.; Huang, W., New linker structures applied in glycosite-specific antibody drug conjugates. *Org Chem Front* **2019,** *6*, 3144-3149.
61. Zhu, Z.; Ramakrishnan, B.; Li, J.; Wang, Y.; Feng, Y.; Prabakaran, P.; Colantonio, S.; Dyba, M. A.; Qasba, P. K.; Dimitrov, D. S., Site-specific antibody-drug conjugation through an engineered glycotransferase and a chemically reactive sugar. *MAbs* **2014,** *6*, 1190-1200.
62. Li, X.; Fang, T.; Boons, G. J., Preparation of well-defined antibody-drug conjugates through glycan remodeling and strain-promoted azide-alkyne cycloadditions. *Angew Chem Int Ed* **2014,** *53*, 7179-7182.
63. Li, C.; Wang, L. X., Chemoenzymatic Methods for the Synthesis of Glycoproteins. *Chem Rev* **2018,** *118*, 8359-8413.
64. Fairbanks, A. J., The ENGases: versatile biocatalysts for the production of homogeneous N-linked glycopeptides and glycoproteins. *Chem Soc Rev* **2017,** *46*, 5128-5146.

65. Huang, W.; Giddens, J.; Fan, S. Q.; Toonstra, C.; Wang, L. X., Chemoenzymatic glycoengineering of intact IgG antibodies for gain of functions. *J Am Chem Soc* **2012,** *134*, 12308-12318.
66. Li, T.; Tong, X.; Yang, Q.; Giddens, J. P.; Wang, L. X., Glycosynthase Mutants of Endoglycosidase S2 Show Potent Transglycosylation Activity and Remarkably Relaxed Substrate Specificity for Antibody Glycosylation Remodeling. *J Biol Chem* **2016,** *291*, 16508-16518.
67. Li, T.; Li, C.; Quan, D. N.; Bentley, W. E.; Wang, L. X., Site-specific immobilization of endoglycosidases for streamlined chemoenzymatic glycan remodeling of antibodies. *Carbohydr Res* **2018,** *458-459*, 77-84.
68. Tang, F.; Wang, L. X.; Huang, W., Chemoenzymatic synthesis of glycoengineered IgG antibodies and glycosite-specific antibody-drug conjugates. *Nat Protoc* **2017,** *12*, 1702-1721.
69. Parsons, T. B.; Struwe, W. B.; Gault, J.; Yamamoto, K.; Taylor, T. A.; Raj, R.; Wals, K.; Mohammed, S.; Robinson, C. V.; Benesch, J. L.; Davis, B. G., Optimal Synthetic Glycosylation of a Therapeutic Antibody. *Angew Chem Int Ed* **2016,** *55*, 2361-2367.
70. Sianturi, J.; Manabe, Y.; Li, H. S.; Chiu, L. T.; Chang, T. C.; Tokunaga, K.; Kabayama, K.; Tanemura, M.; Takamatsu, S.; Miyoshi, E.; Hung, S. C.; Fukase, K., Development of alpha-Gal-Antibody Conjugates to Increase Immune Response by Recruiting Natural Antibodies. *Angew Chem Int Ed* **2019,** *58* (14), 4526-4530.
71. Manabe, S.; Abe, J.; Ito, Y., Amide bond formation of sialic acid in oligosaccharide without protecting group. *Heterocycles* **2018,** *97*, 1203-1209.
72. Noguchi, M.; Tanaka, T.; Gyakushi, H.; Kobayashi, A.; Shoda, S., Efficient synthesis of sugar oxazolines from unprotected N-acetyl-2-amino sugars by using chloroformamidinium reagent in water. *J Org Chem* **2009,** *74*, 2210-2.
73. Noguchi, M.; Nakamura, M.; Ohno, A.; Tanaka, T.; Kobayashi, A.; Ishihara, M.; Fujita, M.; Tsuchida, A.; Mizuno, M.; Shoda, S., A dimethoxytriazine type glycosyl donor enables a facile chemo-enzymatic route toward alpha-linked N-acetylglucosaminyl-galactose disaccharide unit from gastric mucin. *Chem Commun* **2012,** *48*, 5560-5562.
74. Manabe, S.; Yamaguchi, Y.; Matsumoto, K.; Fuchigami, H.; Kawase, T.; Hirose, K.; Mitani, A.; Sumiyoshi, W.; Kinoshita, T.; Abe, J.; Yasunaga, M.; Matsumura, Y.; Ito, Y., Characterization of Antibody Products Obtained through Enzymatic and Nonenzymatic Glycosylation Reactions with a Glycan Oxazoline and Preparation of a Homogeneous Antibody-Drug Conjugate via Fc N-Glycan. *Bioconjug Chem* **2019,** *30*, 1343-1355.
75. Li, T.; DiLillo, D. J.; Bournazos, S.; Giddens, J. P.; Ravetch, J. V.; Wang, L. X., Modulating IgG effector function by Fc glycan engineering. *Proc Natl Acad Sci U S A* **2017,** *114*, 3485-3490.
76. Iwamoto, M.; Sekiguchi, Y.; Nakamura, K.; Kawaguchi, Y.; Honda, T.; Hasegawa, J., Generation of efficient mutants of endoglycosidase from Streptococcus pyogenes and their application in a novel one-pot transglycosylation reaction for antibody modification. *PLoS One* **2018,** *13*, e0193534.
77. Loganzo, F.; Tan, X.; Sung, M.; Jin, G.; Myers, J. S.; Melamud, E.; Wang, F.; Diesl, V.; Follettie, M. T.; Musto, S.; Lam, M. H.; Hu, W.; Charati, M. B.; Khandke,

K.; Kim, K. S.; Cinque, M.; Lucas, J.; Graziani, E.; Maderna, A.; O'Donnell, C. J.; Arndt, K. T.; Gerber, H. P., Tumor cells chronically treated with a trastuzumab-maytansinoid antibody-drug conjugate develop varied resistance mechanisms but respond to alternate treatments. *Mol Cancer Ther* **2015,** *14*, 952-963.
78. Chio, T. I.; Gu, H.; Mukherjee, K.; Tumey, L. N.; Bane, S. L., Site-Specific Bioconjugation and Multi-Bioorthogonal Labeling via Rapid Formation of a Boron-Nitrogen Heterocycle. *Bioconjug Chem* **2019,** *30*, 1554-1564.
79. Oller-Salvia, B.; Kym, G.; Chin, J. W., Rapid and Efficient Generation of Stable Antibody-Drug Conjugates via an Encoded Cyclopropene and an Inverse-Electron-Demand Diels-Alder Reaction. *Angew Chem Int Ed* **2018,** *57*, 2831-2834.
80. Walker, J. A.; Bohn, J. J.; Ledesma, F.; Sorkin, M. R.; Kabaria, S. R.; Thornlow, D. N.; Alabi, C. A., Substrate Design Enables Heterobifunctional, Dual "Click" Antibody Modification via Microbial Transglutaminase. *Bioconjug Chem* **2019,** *30*, 2452-2457.
81. Doronina, S. O.; Toki, B. E.; Torgov, M. Y.; Mendelsohn, B. A.; Cerveny, C. G.; Chace, D. F.; DeBlanc, R. L.; Gearing, R. P.; Bovee, T. D.; Siegall, C. B.; Francisco, J. A.; Wahl, A. F.; Meyer, D. L.; Senter, P. D., Development of potent monoclonal antibody auristatin conjugates for cancer therapy. *Nat Biotechnol* **2003,** *21*, 778-84.
82. Ou, C.; Li, C.; Zhang, R.; Yang, Q.; Zong, G.; Dai, Y.; Francis, R. L.; Bournazos, S.; Ravetch, J. V.; Wang, L. X., One-Pot Conversion of Free Sialoglycans to Functionalized Glycan Oxazolines and Efficient Synthesis of Homogeneous Antibody-Drug Conjugates through Site-Specific Chemoenzymatic Glycan Remodeling. *Bioconjug Chem* **2021,** *32*, 1888-1897.
83. Liu, L.; Prudden, A. R.; Bosman, G. P.; Boons, G. J., Improved isolation and characterization procedure of sialylglycopeptide from egg yolk powder. *Carbohydr Res* **2017,** *452*, 122-128.
84. Li, T.; Tong, X.; Yang, Q.; Giddens, J. P.; Wang, L. X., Glycosynthase Mutants of Endoglycosidase S2 Show Potent Transglycosylation Activity and Remarkably Relaxed Substrate Specificity for Antibody Glycosylation Remodeling. *J Biol Chem* **2016,** *291*, 16508-16518.
85. Elliott, T. S.; Townsley, F. M.; Bianco, A.; Ernst, R. J.; Sachdeva, A.; Elsasser, S. J.; Davis, L.; Lang, K.; Pisa, R.; Greiss, S.; Lilley, K. S.; Chin, J. W., Proteome labeling and protein identification in specific tissues and at specific developmental stages in an animal. *Nat Biotechnol* **2014,** *32*, 465-472.
86. Dubowchik, G. M.; Firestone, R. A.; Padilla, L.; Willner, D.; Hofstead, S. J.; Mosure, K.; Knipe, J. O.; Lasch, S. J.; Trail, P. A., Cathepsin B-labile dipeptide linkers for lysosomal release of doxorubicin from internalizing immunoconjugates: model studies of enzymatic drug release and antigen-specific in vitro anticancer activity. *Bioconjug Chem* **2002,** *13*, 855-869.
87. Tsao, L. C.; Force, J.; Hartman, Z. C., Mechanisms of Therapeutic Antitumor Monoclonal Antibodies. *Cancer Res* **2021,** *81*, 4641-4651.
88. Owen, R. M.; Carlson, C. B.; Xu, J.; Mowery, P.; Fasella, E.; Kiessling, L. L., Bifunctional ligands that target cells displaying the alpha v beta3 integrin. *Chembiochem* **2007,** *8*, 68-82.

89. Sheridan, R. T.; Hudon, J.; Hank, J. A.; Sondel, P. M.; Kiessling, L. L., Rhamnose glycoconjugates for the recruitment of endogenous anti-carbohydrate antibodies to tumor cells. *Chembiochem* **2014,** *15*, 1393-1398.
90. Naicker, K. P.; Li, H.; Heredia, A.; Song, H.; Wang, L. X., Design and synthesis of alpha Gal-conjugated peptide T20 as novel antiviral agent for HIV-immunotargeting. *Org Biomol Chem* **2004,** *2*, 660-4.
91. Perdomo, M. F.; Levi, M.; Sallberg, M.; Vahlne, A., Neutralization of HIV-1 by redirection of natural antibodies. *Proc Natl Acad Sci U S A* **2008,** *105*, 12515-12520.
92. Li, X.; Rao, X.; Cai, L.; Liu, X.; Wang, H.; Wu, W.; Zhu, C.; Chen, M.; Wang, P. G.; Yi, W., Targeting Tumor Cells by Natural Anti-Carbohydrate Antibodies Using Rhamnose-Functionalized Liposomes. *ACS Chem Biol* **2016,** *11*, 1205-1209.
93. Galili, U.; Rachmilewitz, E. A.; Peleg, A.; Flechner, I., A unique natural human IgG antibody with anti-alpha-galactosyl specificity. *J Exp Med* **1984,** *160*, 1519-1531.
94. Galili, U.; Wang, L.; LaTemple, D. C.; Radic, M. Z., The natural anti-Gal antibody. *Subcell Biochem* **1999,** *32*, 79-106.
95. Parker, W.; Bruno, D.; Holzknecht, Z. E.; Platt, J. L., Characterization and affinity isolation of xenoreactive human natural antibodies. *J Immunol* **1994,** *153*, 3791-803.
96. Galili, U., Interaction of the natural anti-Gal antibody with alpha-galactosyl epitopes: a major obstacle for xenotransplantation in humans. *Immunol Today* **1993,** *14*, 480-2.
97. Oyelaran, O.; McShane, L. M.; Dodd, L.; Gildersleeve, J. C., Profiling human serum antibodies with a carbohydrate antigen microarray. *J Proteome Res* **2009,** *8*, 4301-4310.
98. Huflejt, M. E.; Vuskovic, M.; Vasiliu, D.; Xu, H.; Obukhova, P.; Shilova, N.; Tuzikov, A.; Galanina, O.; Arun, B.; Lu, K.; Bovin, N., Anti-carbohydrate antibodies of normal sera: findings, surprises and challenges. *Mol Immunol* **2009,** *46*, 3037-3049.
99. Hossain, M. K.; Vartak, A.; Karmakar, P.; Sucheck, S. J.; Wall, K. A., Augmenting Vaccine Immunogenicity through the Use of Natural Human Anti-rhamnose Antibodies. *ACS Chem Biol* **2018,** *13*, 2130-2142.
100. Jakobsche, C. E.; Parker, C. G.; Tao, R. N.; Kolesnikova, M. D.; Douglass, E. F., Jr.; Spiegel, D. A., Exploring binding and effector functions of natural human antibodies using synthetic immunomodulators. *ACS Chem Biol* **2013,** *8*, 2404-2411.
101. Chen, W.; Gu, L.; Zhang, W.; Motari, E.; Cai, L.; Styslinger, T. J.; Wang, P. G., L-rhamnose antigen: a promising alternative to alpha-gal for cancer immunotherapies. *ACS Chem Biol* **2011,** *6*, 185-191.
102. Sharp, T. H.; Boyle, A. L.; Diebolder, C. A.; Kros, A.; Koster, A. J.; Gros, P., Insights into IgM-mediated complement activation based on in situ structures of IgM-C1-C4b. *Proc Natl Acad Sci U S A* **2019,** *116*, 11900-11905.
103. Ugurlar, D.; Howes, S. C.; de Kreuk, B. J.; Koning, R. I.; de Jong, R. N.; Beurskens, F. J.; Schuurman, J.; Koster, A. J.; Sharp, T. H.; Parren, P.; Gros, P., Structures of C1-IgG1 provide insights into how danger pattern recognition activates complement. *Science* **2018,** *359*, 794-797.
104. Diebolder, C. A.; Beurskens, F. J.; de Jong, R. N.; Koning, R. I.; Strumane, K.; Lindorfer, M. A.; Voorhorst, M.; Ugurlar, D.; Rosati, S.; Heck, A. J.; van de Winkel, J. G.; Wilson, I. A.; Koster, A. J.; Taylor, R. P.; Saphire, E. O.; Burton, D. R.;

Schuurman, J.; Gros, P.; Parren, P. W., Complement is activated by IgG hexamers assembled at the cell surface. *Science* **2014,** *343*, 1260-1263.
105. Zhou, K.; Hong, H.; Lin, H.; Gong, L.; Li, D.; Shi, J.; Zhou, Z.; Xu, F.; Wu, Z., Chemical Synthesis of Antibody-Hapten Conjugates Capable of Recruiting the Endogenous Antibody to Magnify the Fc Effector Immunity of Antibody for Cancer Immunotherapy. *J Med Chem* **2022**, *65*, 323-332.
106. Ou, C.; Prabhu, S. K.; Zhang, X.; Zong, G.; Yang, Q.; Wang, L. X., Synthetic antibody-rhamnose cluster conjugates show potent complement-dependent cell killing by recruiting natural antibodies. *Chemistry* **2022,** *28*, e2022001.
107. Elgersma, R. C.; Coumans, R. G.; Huijbregts, T.; Menge, W. M.; Joosten, J. A.; Spijker, H. J.; de Groot, F. M.; van der Lee, M. M.; Ubink, R.; van den Dobbelsteen, D. J.; Egging, D. F.; Dokter, W. H.; Verheijden, G. F.; Lemmens, J. M.; Timmers, C. M.; Beusker, P. H., Design, Synthesis, and Evaluation of Linker-Duocarmycin Payloads: Toward Selection of HER2-Targeting Antibody-Drug Conjugate SYD985. *Mol Pharm* **2015,** *12*, 1813-1835.
108. Nicolaou, K. C.; Li, R.; Chen, Q.; Lu, Z.; Pitsinos, E. N.; Schammel, A.; Lin, B.; Gu, C.; Sarvaiya, H.; Tchelepi, R.; Valdiosera, A.; Clubb, J.; Barbour, N.; Sisodiya, V.; Sandoval, J.; Lee, C.; Aujay, M.; Gavrilyuk, J., Synthesis and Biological Evaluation of Shishijimicin A-Type Linker-Drugs and Antibody-Drug Conjugates. *J Am Chem Soc* **2020,** *142*, 12890-12899.
109. Zhang, W.; Wang, J.; Li, J.; Yu, L.; Wang, P. G., Large Scale Synthesis of A Derivative of An α-Galactosyl Trisaccharide Epitope Involved in the Hyperacute Rejection of Xenotransplantation. *J Carbohydr Chem* **2008,** *18*, 1009-1017.
110. Zhang, X.; Ou, C.; Liu, H.; Prabhu, S. K.; Li, C.; Yang, Q.; Wang, L. X., General and Robust Chemoenzymatic Method for Glycan-Mediated Site-Specific Labeling and Conjugation of Antibodies: Facile Synthesis of Homogeneous Antibody−Drug Conjugates. *ACS Chem Biol* **2021,** *16*, 2502-2514.
111. Noguchi, M.; Tanaka, T.; Gyakushi, H.; Kobayashi, A.; Shoda, S.-i., Efficient Synthesis of Sugar Oxazolines from Unprotected N-Acetyl-2-amino Sugars by Using Chloroformamidinium Reagent in Water. *J Org Chem* **2009,** *74*, 2210-2212.
112. Huang, W.; Yang, Q.; Umekawa, M.; Yamamoto, K.; Wang, L. X., Arthrobacter endo-beta-N-acetylglucosaminidase shows transglycosylation activity on complex-type N-glycan oxazolines: one-pot conversion of ribonuclease B to sialylated ribonuclease C. *ChemBioChem* **2010,** *11*, 1350-5.
113. Lin, H.; Hong, H.; Wang, J.; Li, C.; Zhou, Z.; Wu, Z., Rhamnose modified bovine serum albumin as a carrier protein promotes the immune response against sTn antigen. *Chem Commun* **2020,** *56*, 13959-13962.
114. Khongorzul, P.; Ling, C. J.; Khan, F. U.; Ihsan, A. U.; Zhang, J., Antibody-Drug Conjugates: A Comprehensive Review. *Mol Cancer Res* **2020,** *18*, 3-19.
115. Loganzo, F.; Sung, M.; Gerber, H. P., Mechanisms of Resistance to Antibody-Drug Conjugates. *Mol Cancer Ther* **2016,** *15*, 2825-2834.
116. Garcia-Alonso, S.; Ocana, A.; Pandiella, A., Resistance to Antibody-Drug Conjugates. *Cancer Res* **2018,** *78*, 2159-2165.
117. Oliveira, B. L.; Guo, Z.; Bernardes, G. J. L., Inverse electron demand Diels-Alder reactions in chemical biology. *Chem Soc Rev* **2017,** *46*, 4895-4950.

118. Oller-Salvia, B.; Kym, G.; Chin, J. W., Rapid and Efficient Generation of Stable Antibody-Drug Conjugates via an Encoded Cyclopropene and an Inverse-Electron-Demand Diels-Alder Reaction. *Angew Chem Int Ed* **2018,** *57*, 2831-2834.
119. Patterson, D. M.; Nazarova, L. A.; Xie, B.; Kamber, D. N.; Prescher, J. A., Functionalized cyclopropenes as bioorthogonal chemical reporters. *J Am Chem Soc* **2012,** *134*, 18638-43.
120. Plass, T.; Milles, S.; Koehler, C.; Szymanski, J.; Mueller, R.; Wiessler, M.; Schultz, C.; Lemke, E. A., Amino acids for Diels-Alder reactions in living cells. *Angew Chem Int Ed* **2012,** *51*, 4166-4170.
121. Speziale, P.; Rindi, S.; Pietrocola, G., Antibody-Based Agents in the Management of Antibiotic-Resistant Staphylococcus aureus Diseases. *Microorganisms* **2018,** *6*, 25.
122. Niederwieser, A.; Spate, A. K.; Nguyen, L. D.; Jungst, C.; Reutter, W.; Wittmann, V., Two-color glycan labeling of live cells by a combination of Diels-Alder and click chemistry. *Angew Chem Int Ed* **2013,** *52*, 4265-4268.
123. Liang, Y.; Mackey, J. L.; Lopez, S. A.; Liu, F.; Houk, K. N., Control and design of mutual orthogonality in bioorthogonal cycloadditions. *J Am Chem Soc* **2012,** *134*, 17904-17907.
124. Ghosh, P.; Dahms, N. M.; Kornfeld, S., Mannose 6-phosphate receptors: new twists in the tale. *Nat Rev Mol Cell Biol* **2003,** *4*, 202-212.
125. Coutinho, M. F.; Prata, M. J.; Alves, S., A shortcut to the lysosome: the mannose-6-phosphate-independent pathway. *Mol Genet Metab* **2012,** *107* (3), 257-66.
126. Banik, S. M.; Pedram, K.; Wisnovsky, S.; Ahn, G.; Riley, N. M.; Bertozzi, C. R., Lysosome-targeting chimaeras for degradation of extracellular proteins. *Nature* **2020,** *584*, 291-297.
127. Zhang, X.; Liu, H.; He, J.; Ou, C.; Donahue, T. C.; Muthana, M. M.; Su, L.; Wang, L. X., Site-Specific Chemoenzymatic Conjugation of High-Affinity M6P Glycan Ligands to Antibodies for Targeted Protein Degradation. *ACS Chem Biol* **2022.** doi: 10.1021/acschembio.1c00751.
128. Giddens, J. P.; Lomino, J. V.; DiLillo, D. J.; Ravetch, J. V.; Wang, L. X., Site-selective chemoenzymatic glycoengineering of Fab and Fc glycans of a therapeutic antibody. *Proc Natl Acad Sci U S A* **2018,** *115*, 12023-12027.
129. Yamaguchi, T.; Amin, M. N.; Toonstra, C.; Wang, L. X., Chemoenzymatic Synthesis and Receptor Binding of Mannose-6-Phosphate (M6P)-Containing Glycoprotein Ligands Reveal Unusual Structural Requirements for M6P Receptor Recognition. *J Am Chem Soc* **2016,** *138*, 12472-12485.
130. Zhang, X.; Liu, H.; Meena, N.; Li, C.; Zong, G.; Raben, N.; Puertollano, R.; Wang, L. X., Chemoenzymatic glycan-selective remodeling of a therapeutic lysosomal enzyme with high-affinity M6P-glycan ligands. Enzyme substrate specificity is the name of the game. *Chem Sci* **2021,** *12*, 12451-12462.